2015 Conference on Autonomous and Robotic Construction of Infrastructure

June 2-3 • Ames, IA

Iowa State University of Science and Technology

Proceedings of the 2015 Conference on Autonomous and Robotic Construction of Infrastructure

Edited by David J. White, Ahmad Alhasan, and Pavana Vennapusa

IOWA STATE UNIVERSITY
OF SCIENCE AND TECHNOLOGY

About CEER

The mission of the Center for Earthworks Engineering Research (CEER) at Iowa State University is to be the nation's premier institution for developing fundamental knowledge of earth mechanics, and creating innovative technologies, sensors, and systems to enable rapid, high quality, environmentally friendly, and economical construction of roadways, aviation runways, railroad embankments, dams, structural foundations, fortifications constructed from earth materials, and related geotechnical applications.

About MTC

The Midwest Transportation Center (MTC) is a regional University Transportation Center (UTC) sponsored by the U.S. Department of Transportation Office of the Assistant Secretary for Research and Technology (USDOT/OST-R). The mission of the UTC program is to advance U.S. technology and expertise in the many disciplines comprising transportation through the mechanisms of education, research, and technology transfer at university-based centers of excellence. Iowa State University, through its Institute for Transportation (InTrans), is the MTC lead institution.

About InTrans

The mission of the Institute for Transportation (InTrans) at Iowa State University is to develop and implement innovative methods, materials, and technologies for improving transportation efficiency, safety, reliability, and sustainability while improving the learning environment of students, faculty, and staff in transportation-related fields.

ISU Nondiscrimination Statement

Iowa State University does not discriminate on the basis of race, color, age, ethnicity, religion, national origin, pregnancy, sexual orientation, gender identity, genetic information, sex, marital status, disability, or status as a U.S. veteran. Inquiries regarding nondiscrimination policies may be directed to Office of Equal Opportunity, Title IX/ADA Coordinator, and Affirmative Action Officer, 3350 Beardshear Hall, Ames, Iowa 50011, 515-294-7612, email eooffice@iastate.edu.

Notice

The contents of this report reflect the views of the authors, who are responsible for the facts and the accuracy of the information presented herein. The opinions, findings and conclusions expressed in this publication are those of the authors and not necessarily those of the sponsors.

This document is disseminated under the sponsorship of the U.S. DOT UTC program in the interest of information exchange. The U.S. Government assumes no liability for the use of the information contained in this document. This report does not constitute a standard, specification, or regulation.

The U.S. Government does not endorse products or manufacturers. If trademarks or manufacturers' names appear in this report, it is only because they are considered essential to the objective of the document.

Quality Assurance Statement

The U.S. Department of Transportation (U.S. DOT) provides high-quality information to serve Government, industry, and the public in a manner that promotes public understanding. Standards and policies are used to ensure and maximize the quality, objectivity, utility, and integrity of its information. The U.S. DOT periodically reviews quality issues and adjusts its programs and processes to ensure continuous quality improvement.

Technical Report Documentation Page

1. Report No.	2. Government Accession No.	3. Recipient's Catalog No.
4. Title and Subtitle Proceedings of the 2015 Conference on Autonomous and Robotic Construction of Infrastructure		**5. Report Date** June 2015 **6. Performing Organization Code**
7. Author(s) Editors: David J. White, Ahmad Alhasan, and Pavana Vennapusa		**8. Performing Organization Report No.**
9. Performing Organization Name and Address Center for Earthworks Engineering Research Institute for Transportation Iowa State University Research Park 2711 S. Loop Drive, Suite 4700 Ames, IA 50010-8664		**10. Work Unit No. (TRAIS)** **11. Contract or Grant No.**
12. Sponsoring Organizations Midwest Transportation Center 2711 S. Loop Drive, Suite 4700 Ames, IA 50010-8664 Caterpillar, Inc. P.O. Box 1875 Peoria, IL 61656	U.S. Department of Transportation Office of the Assistant Secretary for Research and Technology 1200 New Jersey Avenue, SE Washington, DC 20590	**13. Type of Report and Period Covered** Proceedings **14. Sponsoring Agency Code** DTRT13-G-UTC37

15. Supplementary Notes

Visit www.intrans.iastate.edu and www.ceer.iastate.edu/carci/proceedings/ for pdfs of this and other publications.

16. Abstract

This is a proceedings of 21 papers presented at the 2015 Conference on Autonomous and Robotic Construction of Infrastructure at Iowa State University, Ames, Iowa, on June 2–3, 2015. The conference provided information on how autonomous robotics systems are being applied in practice, discussed emerging technologies, and described theories that will no doubt shape the future of this field. The papers cover a range of topics including mobile robotic operations, visual analysis, terrain modeling, simulations inspired by natural processes, multi-dimensional modeling, 3D printing, sensors, data processing, and new applications for construction technologies like photogrammetry. An underlying theme for many of the papers is data analytics—trying to make sense of and bring value to the deluge of data now being generated during construction operations (e.g., machine telematics, digital photos, weather data, sensors, etc.).

17. Key Words	18. Distribution Statement	
automated machine guidance—autonomous construction—earthworks engineering—robotic construction—transportation construction		
19. Security Classification (of this report) Unclassified.	**20. Security Classification (of this page)** Unclassified.	**21. No. of Pages** 269 / **22. Price** NA

Form DOT F 1700.7 (8-72) **Reproduction of completed page authorized**

Proceedings of the 2015 Conference on Autonomous and Robotic Construction of Infrastructure June 2015

Edited by

David J. White
Ahmad Alhasan
Pavana Vennapusa

Sponsors

Caterpillar, Inc.
Iowa Department of Transportation
Center for Industrial Research and Service, Iowa State University
Department of Civil, Construction, and Environmental Engineering, Iowa State University
Midwest Transportation Center, Iowa State University

IOWA STATE UNIVERSITY
Institute for Transportation

CENTER FOR
CEER
EARTHWORKS ENGINEERING
RESEARCH

MIDWEST
TRANSPORTATION
CENTER
MTC

IOWA STATE
UNIVERSITY
Department of Civil, Construction,
and Environmental Engineering

ciras

Proceedings of the 2015 Conference on Autonomous and Robotic Construction of Infrastructure

Library of Congress ISSN 2379-3597

ISBN: 978-0-9820144-3-1

An electronic version of the proceedings is available online,
http://www.ceer.iastate.edu/carci/proceedings/.

Marcia Brink, Production Editor
Institute for Transportation
Iowa State University
2711 S. Loop Drive, Suite 4700
Ames, IA 50010-8664

ACKNOWLEDGMENTS

The Center for Earthworks Engineering Research would like to thank the following organizations for sponsoring the 2015 Conference on Autonomous and Robotic Construction of Infrastructure and the related proceedings of papers:

Caterpillar, Inc.

Center for Industrial Research and Service, Iowa State University

Department of Civil, Construction, and Environmental Engineering, Iowa State University

Iowa Department of Transportation

Midwest Transportation Center, Iowa State University

U.S. Department of Transportation Office of the Assistant Secretary for Research and Technology

Contents

Foreword

By David J. White, Richard L. Handy Professor of Civil, Construction, and Environmental Engineering and Director, Center for Earthworks Engineering Research, Iowa State University of Science and Technology

Infusion of autonomous and robotic operations into infrastructure construction holds promise for significantly improving the quality, efficiency, and safety of building America's infrastructure. Due to the complex developments required in the areas of theory, data analytics, machine systems, operator training, specifications development, and sensors, it is envisioned that partnerships between academia, industry, and government agencies are needed to make strategic and efficient advancements in the near term to realize maximum benefit.

Although there are efforts focused on the topic of robotics for manufacturing, seemingly little attention has been given to the full spectrum of technologies, sensors, systems, specifications, training, visualization, and data analytics needed for automating the in situ manufacturing of our infrastructure. Robotics (including co-robotic operations) and autonomous equipment operations hold great potential for advancement. Even a small improvement in productivity could generate a significant return given the more than $100 billion annual investment in infrastructure construction. Unfortunately, infrastructure construction has only limited theory established for process control.

The 2015 Conference on Autonomous and Robotic Construction of Infrastructure at Iowa State University was organized to discuss application and theory for advancing autonomous and robotic-guided equipment to improve productivity, quality, reliability, and safety for civil infrastructure construction and maintenance. Unlike some conferences that focus on practice or theory and are dominated by one particular discipline, this conference provided information on how autonomous robotics systems are being applied in practice, discussed emerging technologies, and described theories that will no doubt shape the future of this field.

Focusing attention on this topic can be used to leverage needed investment in people and facilities to better anchor this area as a "core" national research focus. Given that this area of research and development covers a spectrum of needs, participants were invited to bridge the gaps within and between academia and industry.

Papers presented at the conference are collected in this proceedings. They cover a range of topics including mobile robotic operations, visual analysis, terrain modeling, simulations inspired by natural processes, multi-dimensional modeling, 3D printing, sensors, data processing, and new applications for construction technologies like photogrammetry. An underlying theme for many of the presentations was data analytics—trying to make sense of and bring value to the deluge of data now being generated during construction operations (e.g., machine telematics, digital photos, weather data, sensors, etc.). These papers show that there is tremendous interest in this topic and the future is bright.

When we look back 5, 10, and 20 years from now, I believe we will see that the participants in this conference continued their tremendous and exciting work to advance autonomous and robotics operations, that new collaborations were formed, and that new developments have indeed made significant contributions to improving human lives by betterment of the infrastructure construction processes.

Integrated Mobile Sensor-Based Activity Recognition of Construction Equipment and Human Crews

Reza Akhavian
Lianne Brito
Amir Behzadan
Department of Civil, Environmental, and Construction Engineering
University of Central Florida
12800 Pegasus Dr.
Orlando, FL 32816
reza@knights.ucf.edu
lianne.brito@ucf.edu
amir.behzadan@ucf.edu

ABSTRACT

Automated activity recognition of heavy construction equipment as well as human crews can contribute to correct and accurate measurement of a variety of construction and infrastructure project performance indicators. Productivity assessment through work sampling, safety and health monitoring using worker ergonomic analysis, and sustainability measurement through equipment activity cycle monitoring to eliminate ineffective and idle times thus reducing greenhouse gas emission (GHG), are some potential areas that can benefit from the integration of automated activity recognition and analysis techniques. Despite their proven performance and applications in other domains, few construction engineering and management (CEM) studies have so far employed non-vision sensing technologies for construction equipment and workers' activity recognition. The existence of a variety of sensors in ubiquitous smartphones with evolving computing, networking, and storage capabilities has created great opportunities for a variety of pervasive computing applications. In light of this, this paper describes the latest findings of an ongoing project that aims to design and validate a ubiquitous smartphone-based automated activity recognition framework using built-in accelerometer and gyroscope sensors. Collected data are segmented to overlapping windows to extract time- and frequency domain features. Since each sensor collected data in three axes (x, y, z), several features from all three axes are extracted to ensure device placement orientation independency. Finally, features are used as the input of supervised machine learning classifiers. The results of the experiments indicate that the trained models are able to classify construction workers and equipment activities with over 90% overall accuracy.

Key words: activity recognition—big data analytics—construction engineering—machine learning—mobile sensor

INTRODUCTION

With the ever-growing infrastructure projects, demands for information and automation technologies in the architecture, engineering, construction, and facility management (AEC/FM) industry is rapidly increasing. 3D printing in design and construction of affordable houses (Krassenstein 2015), drones for various applications in construction jobsites (Irizarry et al. 2012), and Micro-Electro-Mechanical Systems (MEMS) sensors for tracking and monitoring of construction resources (Akhavian and Behzadan 2015) are some of the examples of how latest

Proceedings of the 2015 Conference on Autonomous and Robotic Construction of Infrastructure, Ames, Iowa.

cutting-edge technology serves the AEC/FM industry. The latter, in particular, has ample unrivalled potentials for use in day-to-day operations due to the existence of various sensors in a major technology platform carried by almost everyone these days, the smartphone.

Ubiquity, affordability, small size, and computing power of mobile phones, equipped with a host of sensors have made them ideal choices for tracking and monitoring of construction resources. In particular, these built-in sensors can provide invaluable information regarding the performance, safety, and behavior of construction workers and equipment in the field. For example, activity analysis using inertial measurement unit (IMU) sensors including accelerometer and gyroscope can help evaluate the time spent on interconnected construction tasks. Such information results in better understanding and potential improvement of the processes involved. Moreover, effective and timey analysis and tracking of the construction resources can help in productivity measurement, progress evaluation, labor training programs, safety and health management, and greenhouse gas emission (GHG) and fuel consumption analysis in construction projects.

This paper presents the results of a smartphone sensors-based machine learning platform for accurate recognition and classification of activities performed by construction equipment and workers. Specifically, process data is collected using smartphone built-in accelerometer and gyroscope from construction equipment and human crews. Certain data pre-processing is then performed to prepare the data as the training input of supervised machine learning classifiers. The outputs of the classifiers are the labels of various activities carried out by the construction resources and detected using this framework.

LITERATURE REVIEW

Human Activity Recognition using Sensors

The initial efforts on human activity recognition date back to the late ’90s (Foerster et al. 1999). During the last 15-16 years, the use of MEMS sensors has increased tremendously for acquiring knowledge on humans’ activities. With the growing demand in activity recognition for different fields of research and practice, the cost of system implementation and prototyping has also decreased, which makes the technology more affordable and accessible to businesses and the industry. Most of the activity recognition research during the past decade has been conducted using wired or wireless accelerometers attached to different parts of a subject’s body. It has been proven that the accuracy of the recognition algorithm improves as sensors are attached to more than one part of the body, while a disadvantage of this approach is that the presence of multiple asynchronous sensors each communicating through a separate interface make the data collection process computationally inefficient and tedious, while ergonomically obtrusive and uncomfortable for the subject. In a study by Frank et al. (2010) MEMS-based IMUs attached to the performer’s waist were used to present four different algorithms and recognize daily activities such as standing, running, walking, and falling. Even though most of the activities were recognized with an accuracy of 93-100%, the rate of accuracy of detecting falling was 80%.

Activity recognition has been widely used in the medical field primarily for elderly patient monitoring. In a study by Gupta and Dallas (2014), waist-mounted triaxal accelerometer was used to classify gait events into six daily living activities including run, jump, walk, sit and transitional events including sit to stand and stand to kneel. While most of the previous studies measured the activities with accelerometer sensor, some studies added gyroscope sensor to improve the accuracy of classification. For instance, in a study aiming at accurate and fast fall

detection, Li et al. (2009) proved that using both accelerometer and gyroscope data for activity recognition yields in more accurate results than using accelerometer only. They reported specific improvement in classifying dynamic transitions rather than static postures and in determining whether the transitional movement was intentional. In another study, Frank et al. (2010) used MEMS-based IMU to train four different classification algorithms that recognized daily activities such as standing, sitting, walking, running, jumping, falling, and lying. In these and most other similar studies, the target activities for classification are daily routine tasks. However, activities in a construction jobsite are relatively more complex and involve interactions between multiple resources (human and equipment crews), which highlights the need for rigorous research in this area within the AEC/FM domain.

Design and development of a small-size, unobtrusive, and low-cost data collection scheme has been one of the most important challenges in improving the accuracy of activity recognition in a more affordable and robust manner (Lara and Labrador 2013). During the last decade and with the advancement of smartphones, a major paradigm shift occurred in the data collection scheme for human activity recognition. As mentioned before, nowadays smartphones include a wide variety of computationally powerful sensors. Many researchers seized this opportunity to build more pervasive human activity recognition systems. Kwapisz et al. (2011) conducted a study on 29 Android smartphone users that utilized accelerometer sensor to monitor daily activities such as walking, jogging, ascending stairs, descending stairs, sitting, and standing for a period of time. The most accurate classification results were achieved in two relatively straightforward activities: sitting and jogging (compared to walking, standing, and climbing up/down the stairs). Again, even though the target activities were recognized with 90% accuracy in most cases (except for climbing up/down the stairs), recognizing such daily and straightforward activities is relatively easier than those carried out in a construction site, for instance. Dernbach et al. (2012) published the results of their study aimed at measuring simple and more complex daily activities using built-in accelerometer and gyroscope sensors in smartphones. Simple activities included biking, climbing stairs, driving, lying, running, sitting, standing, and walking while complex activities included cleaning (i.e. wiping down the kitchen counter top and sink), cooking (i.e. heating a bowl of water in the microwave and pouring a glass of water from a pitcher in the fridge), medication (i.e. retrieving pills from the cupboard and sorted out a week's worth of doses), sweeping (i.e. sweeping the kitchen area), washing hands, and watering plants. Their results showed that while an accuracy of around 90% was achieved for simple activities, more complex activities were best classified with less than 50% accuracy. Moreover, in all activity types, adding gyroscope data to accelerometer data improved the results by 10-12%. Another research that used smartphone accelerometer and gyroscope sensors was conducted by Wu et al. (2012). In this research an iPod Touch was used for data collection measuring 13 different daily activities (e.g. stair climbing, jogging, sitting) from 16 human subjects. Using only the accelerometer data, the accuracy in recognizing these activities ranged between 50% to 100%, while adding the gyroscope data helped improve the results by another 3.1% to 13.4%.

Non-Human Subject Activity Recognition using Sensors

In addition to human activity recognition, classification of activities performed by construction equipment is investigated in this research. To the best of the authors' knowledge, very little research has been conducted aiming at non-human subject activity recognition since the application areas are rare and limited. For example, in transportation research and practice, the use of sensors for transportation mode detection, urban planning improvement, targeted advertising, and guidance systems has recently gained traction (Hemminki et al. 2013; Wang et al. 2010; Zheng et al. 2010). Although most of these studies primarily relied on global

positioning data (GPS) data for recognizing activities and in particular, transportation modes, some of them have used accelerometer data for more precision. In one study, Reddy et al. (2010) used GPS and accelerometer to classify stationary, walking, running, biking and motorized transportation. In their work, classification mainly relied on GPS speed for detecting motorized mode and no distinction was made between different motorized modalities. However, in another study aiming at improving this framework, Hemminki et al. (2013) used only accelerometer data to detect if the subject is stationary or on a motorized transportation and to classify the motorized transportation modalities into bus, train, metro, tram, or car. Using some improved algorithms for estimating the gravity component of the accelerometer measurements and feature extraction, they achieved higher precision and recall than the combined GPS and accelerometers approach while eliminating the high power consumption of the GPS sensor. In addition to transportation systems management and planning, a few construction engineering and management (CEM) research studies targeted non-human subject activity recognition that are summarized in the next Subsection.

Activity Recognition in Construction

Considering the dynamic and complex environment of most construction project sites, being able to control and measure the efficiency of construction resources is vital to the overall performance of the project in terms of time and financial resources. Moreover, by monitoring workers and equipment activities, catastrophes that include safety and health issues as well as many lawsuits could be prevented. Within the CEM research domain, vision-based systems are used in most existing object recognition and tracking frameworks. For example, Brilakis et al. (2011) proposed a framework for vision-based tracking of construction entities. Their methodology requires calibration of two cameras, recognition of construction resources and identification of the corresponding regions, matching the entities identified in different cameras, two-dimensional (2D) tracking of the matched entities, and finally calculating the 3D coordinates. This and similar vision-based approaches, although provide promising results for recognition and tracking of construction equipment, still require much computation in each one of the aforementioned steps. In another study, an image processing methodology was adopted for idle time quantification of hydraulic excavators (Zou and Kim 2007). The level of detail (LoD) of the framework, however, was limited to detection of only idle and busy states of a hydraulic excavator. For the purpose of learning and classification of labor and equipment actions, the concept of Bag-of-Video-Feature-Words model was extended into the construction domain (Gong et al. 2011). This technique uses unsupervised learning for classification, and only considers frequency of feature occurrence for classification. Another vision-based framework was proposed by Rezazadeh Azar and McCabe (2012) for dirt-loading cycles in earthmoving operations that depends on the location of equipment which requires the algorithm to be modified for every new jobsite.

Construction workers' activity recognition using vision-based systems has been also the subject of some other studies. For example, 3D range image cameras were used for tracking and surveillance of construction workers for safety and health monitoring (Gonsalves and Teizer 2009; Peddi et al. 2009). Gonsalves and Teizer (2009) indicated that if their proposed system is used in conjunction with artificial neural network (ANN), results would be more robust for prevention of fatal accidents and related health issues. In their study on construction workers' unsafe actions, Han and Lee (2013) developed a framework for 3D human skeleton extraction from video to detect unsafe predefined motion templates. All of these frameworks, although presented successful results in their target domain, require installation of multiple cameras (up to 8 in some cases), have short recognition distance (maximum of 4 meters for Kinect) and

require direct line of sight for implementation. Such shortcomings have served as a major motivation to investigate alternative solutions that can potentially alleviate these problems.

Non-vision-based (a.k.a. senor-based) worker activity analysis has recently gained popularity among CEM researchers. Cheng et al. (2013) used ultra-wide band (UWB) and Physiological Status Monitors (PSMs) for productivity assessment. However, the LoD in recognizing the activities was limited to identification of traveling, working, and idling states of workers and could not provide further insight into identified activities. In another set of research studies aiming at construction equipment activity analysis to support process visualization, remote monitoring and planning, queueing analysis, and knowledge-based simulation input modeling, the authors developed a framework by fusing data from ultra-wide band (UWB), payload, and orientation (angle) sensors to build a spatio-temporal taxonomy-based reasoning scheme for activity classification in heavy construction (Akhavian and Behzadan 2012, 2013, 2014).

As one of the first accelerometer-based activity recognition studies, Joshua and Varghese (2011) developed a work sampling framework for bricklayers. The scope of that study, however, was limited to only a single bricklayer in a controlled environment. Moreover, their proposed framework used accelerometer as the sole source of motion data. Also, the necessity of installing wired sensors on the worker's body may introduce a constraint on the worker's freedom of movement. In another study, Ahn et al. (2013) used accelerometers to classify an excavator operations into three modes of engine-off, idling, and working. Further decomposition of these activities, however, was not explored in their study.

METHODOLOGY

In this study, data are collected using mobile phone accelerometer and gyroscope sensors. Collected raw sensory data are segmented into windows containing certain number of data points. Next, key statistical features are calculated within each window. Furthermore, each segment is labeled based on the corresponding activity class performed at the time identified by the timestamp of the collected data. In order to train a predictive model, five classifiers of different types are used to recognize activities performed in the data collection experiments. Figure 1 depicts the steps from data collection to activity recognition.

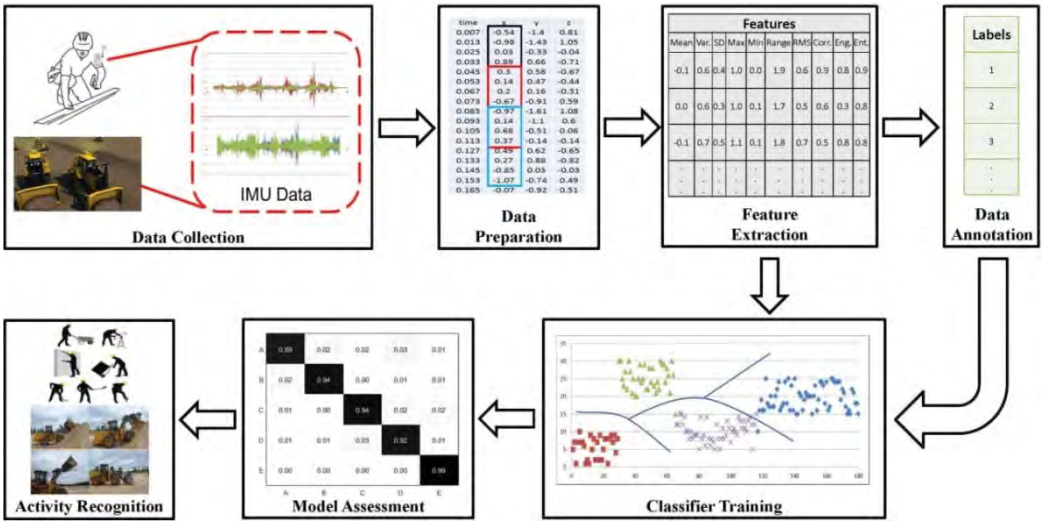

Figure 1. System architecture for activity recognition of construction resources using mobile phones

Data Collection

Data collection is performed using commercially available data logger applications for iOS and/or Android devices. Accelerometer sensors measure the acceleration of the device. The reading can be in one, two, or all three axes of x, y, and z. The raw data is represented as a set of vectors and returned together with a timestamp of the reading. Gyroscope is a sensor that measures the rotation rate of the device by detecting the roll, pitch, and yaw motions of the smartphone about the x, y, and z axes. Similar to accelerometer, readings are presented as time-stamped vectors. When the mobile device is attached to construction equipment or worker's body involved in different activities, these two sensors generate different (and distinct) patterns in their transmitted signals.

Data Preparation

A major step before transforming raw data into the input features for machine learning algorithms is removing noise and accounting for missing data. When collecting data for a long period of time, it is possible that the sensors temporarily freeze or fail to properly collect and store data for fractions of a second to a few seconds and in return, compensate for the missing data points by collecting data in a rate higher than the assigned frequency. In such cases, a preprocessing technique to fill in for missing data points and removing redundant ones can help insuring a continuous and orderly dataset. Also, since the raw data are often collected with a high sampling rate, segmentation of the data helps in data compression and prepares data for feature extraction (Khan et al. 2011). If segmentation is performed considering an overlap between adjacent windows, it reduces the error caused by the transition state noise (Su et al. 2014). The length of the window size depends on the sampling frequency and the nature of activities targeted for classification from which data is collected (Su et al. 2014).

Feature Extraction

Feature is an attribute of the raw data that should be calculated (Khan et al. 2011). In data analytics applications, statistical time- and frequency-domain features generated in each window are used as the input of the training process (Ravi et al. 2005). The ability to extract appropriate features depends on the application domain and can steer the process of retaining the relevant information. Most previous studies on activity recognition used almost the same set of features for training the models and classification of activities (Shoaib et al. 2015).

Data Annotation

Following data segmentation and feature extraction, the corresponding activity class labels should be assigned to each window. This serves as the ground truth for the learning algorithm and can be retrieved from the video recorded at the time of the experiment.

Supervised Learning

In supervised learning classification, class labels discussed in Data Annotation (above) are provided to the learning algorithms to generate a model or function that matches the input (i.e. features) to the output (i.e. activity classes) (Ravi et al. 2005). The goal is to infer a function using examples for which the class labels are known (i.e. training data). The performance of this function is evaluated by measuring the accuracy in predicting the class labels of unseen examples. Researchers have used different types of supervised classification methods for activity recognition (Kim et al. 2013; Reddy et al. 2010; Sun et al. 2010). Details of the supervised learning classification algorithms are discussed in the next Section.

Model Assessment

In order to determine the reliability of the trained model in detecting new examples of activity classes, part of the training dataset is used for testing the model. It is recommended that the test set is independent of the training set, meaning that the data that are used for testing have not been among the training data. For example, randomly chosen 10% of the training data can be left out so that the training is performed on the remaining 90% of the data. Assessment of the model provides an opportunity for its fine-tuning so that certain variables (e.g. regularization factor to prevent over-fitting in ANNs) in the algorithm can be revised to yield the best possible model.

Activity Recognition

Once the model is trained and its parameters are finalized, it can be used for recognizing activities for which it has been trained. While data is being collected to determine the activities according to a trained classifier, such data can be stored in a dataset repository and be added to the existing training data, so that the model is further trained with a richer training dataset.

DETAILS OF THE CLASSIFICATION ALGORITHMS

In the presented research, five different classification techniques are used in order to systematically evaluate their performance in accurately detecting construction activities. In particular, ANN, decision tree, K-nearest neighbor (KNN), logistic regression, and support vector machine (SVM) are employed for classification. Decision tree, KNN, and SVM have been previously used for activity recognition (Kose et al. 2012; Ravi et al. 2005; Yan et al. 2012) so they are selected in this study to evaluate their performance for classifying construction activities. However, ANN and logistic regression were examined to a much lesser extent (Staudenmayer et al. 2009).

Artificial Neural Network (ANN)

An ANN trained based on the experiments' data follows a simple pattern of one input, one hidden, and one output layer. The number of input layer units is set to the number of extracted features. The hidden layer consists of *p=25* units. The number of units for the output layer is equal to the number of activity classes, *n* in each case. Considering the large feature space and in order to prevent over-fitting, regularization was used. Using a regularization parameter, the magnitude of the model weights decreases, so that the model will not suffer from high variance to fail to generalize to the new unseen examples (Haykin et al. 2009). The activation function (i.e. hypothesis) used for minimizing the cost function in the training process is a Sigmoid function shown in Equation 1,

$$h_{\Phi}(x) = \frac{1}{1+e^{-\Phi x}} \quad (1)$$

in which $h(x)$ is the activation function (i.e. hypothesis), Φ is a matrix of model weights (i.e. parameters), and x is the features matrix. In this study, in order to minimize the cost function, the most commonly used ANN training method, namely feed-forward backpropagation is used. Considering a set of randomly chosen initial weights, the backpropagation algorithm calculates the error of the activation function in detecting the true classes and tries to minimize this error by taking subsequent partial derivatives of the cost function with respect to the model weights (Hassoun 1995).

Decision Tree

Decision tree is one of the most powerful yet simplest algorithms for classification (Bishop 2006). The decision tree method that is used in this research is classification and regression tree (CART). CART partitions the training examples in the feature space into rectangle regions (a.k.a. nodes) and assigns each class to a region. The process begins with all classes spread over the feature space and examines all possible binary splits on every feature (Bishop 2006). A split is selected if it has the best optimization criterion which is the Gini diversity index in this research, as shown in Equation 2,

$$I_G(f) = 1 - \sum_{i=1}^{k} f_i^2 \quad (2)$$

in which I_G is the Gini index, f_i is the fraction of items labeled with value i and k is the number of classes. The process of splitting is repeated iteratively for all nodes until they are *pure*. A node is considered *pure* if it contains only observations of one class, implying a Gini index of zero, or that there are fewer than 10 observations to split.

K-Nearest Neighbor (KNN)

Similar to the decision tree and unlike the ANN, KNN is a simple algorithm. Training examples identified by their labels are spread over the feature space. A new example is assigned to a class that is most common amongst its K nearest examples considering the Euclidean distance that is used as the metric in this research, and as appears in Equation 3,

$$D = \sqrt{(x_i^{(1)} - x_{new}^{(1)})^2 + (x_i^{(2)} - x_{new}^{(2)})^2 + \cdots + (x_i^{(d)} - x_{new}^{(d)})^2} \quad (3)$$

in which D is the Euclidean distance, x_i is an existing example data point which has the least distance with the new example, x_{new} is the new example to be classified, and d is the dimension of the feature space.

Logistic Regression

Logistic regression is a type of regression problems in which the output is discretized for classification (Hastie et al. 2009). Logistic regression seeks to form a hypothesis function that maps the input (i.e. training data) to the output (i.e. class labels) by estimating the conditional probability of an example belonging to class *k* given that the example actually belongs to the class *k*. This is accomplished by minimizing a cost function using a hypothesis function and correct classes to find the parameters of the mapping model (Hastie et al. 2009). The hypothesis function used in this research is the same as the activation function introduced in Equation 1 (the Sigmoid function) and thus the cost function to minimize is as shown in Equation 4,

$$J(\theta) = -\frac{1}{m}\left[\sum_{i=1}^{m} y^{(i)} \log h_\theta\left(x^{(i)}\right) + \left(1 - y^{(i)}\right) \log\left(1 - h_\theta\left(x^{(i)}\right)\right)\right] \quad (4)$$

in which $J(\theta)$ is the cost function, *m* is the number of training examples, $x^{(i)}$ is the *i*th training example, and $y^{(i)}$ is the corresponding correct label. Once the cost function is minimized using any mathematical method such as the Gradient Decent (Hastie et al. 2009) and parameters are found, the hypothesis will be formed. In multi-class classification, the one-versus-all method is

used to determine if a new example belongs to the class *k* (Hastie et al. 2009). Therefore, considering *k* classes, *k* hypothesis functions will be evaluated for each new example and the one that results in the maximum hypothesis is selected.

Support Vector Machine (SVM)

Compared to decision tree and KNN, SVM is considered as a more powerful classification algorithm. Although it has been widely used in vision-based pattern recognition and classification problems, some researchers (Bishop 2006) used it for classifying daily activities and thus its performance is also assessed in this research. In a nutshell, SVM tries to maximize the margin around hyperplanes that separate different classes from each other. SVM can benefit from a maximum margin hyperplane in a transformed feature space using kernel function to create non-linear classifiers. The kernel function used for non-linear classification in this research is Gaussian radial basis function (rbf) which has been successfully applied in the past to activity recognition problems (Ravi et al. 2005). Further description of SVM models are out of the scope of this study but can be found in (Bishop 2006).

VALIDATION EXPERIMENTS

In this Section, the description and details of two separate experiments conducted using construction equipment and workers in order to validate the designed activity recognition methods are provided.

Front-End Loader Activity Recognition

In this experiment, smartphones were placed inside the equipment cabin for data collection. At any time, two smartphones were simultaneously used to guarantee the uninterrupted storage of data. It must be noted that since data collection and feature extraction is done using tri-axial data, results do not depend on the placement orientation of the data collection device. Moreover, potential significant correlation between each pair of axes is reflected in three of the extracted features, thus guaranteeing capturing any distinguishable feature related to the placement orientation of the data collection devices. In order to fully automate the process of data collection, low-cost near field communication (NFC) RFID smart tags were also used (Want 2006). NFC tags were glued to the device holder (i.e. suction cup attached to the side window of the cabin) to automatically launch the data logger application once the smartphone was placed in the holder. A JOHN DEERE 744J front-end loader was employed for data collection. All experiment operations were fully videotaped for later activity annotation and labeling, and visual validation. Figure 2 shows how data collection devices were mounted and secured inside the target equipment cabin.

Figure 2. Smartphones mounted inside the front-end loader cabin

Data Collection

Data was collected using commercially available data logger applications for iOS and Android devices. The sampling frequency was set at 100 Hz. Among different modes of data collected in this study, it was observed that acceleration (i.e. vibration) values resulted from different equipment motions had the highest degree of volatility. Several sensor manufacturers have recommended that a bandwidth of 50 Hz be used for normal-speed vibration and tilt sensing applications. Therefore, in this research, and considering the Nyquist criterion in signal processing (Lyons et al. 2005), the sampling frequency was set at twice this value or 100 Hz. This bandwidth guaranteed that no significant motion was overlooked and at the same time, the volume of recorded data was not prohibitively large. Data was stored with comma separated value (CSV) format for processing in Microsoft Excel. The logger applications provided time-stamped data which facilitated the synchronization of data and video recordings. As mentioned earlier, GPS data was not directly used in data mining processes employed in this study and was only collected to demonstrate the potential of acquiring high accuracy positional data for such context-aware applications. Figure 3 shows snapshots of the collected accelerometer, gyroscope, and GPS data.

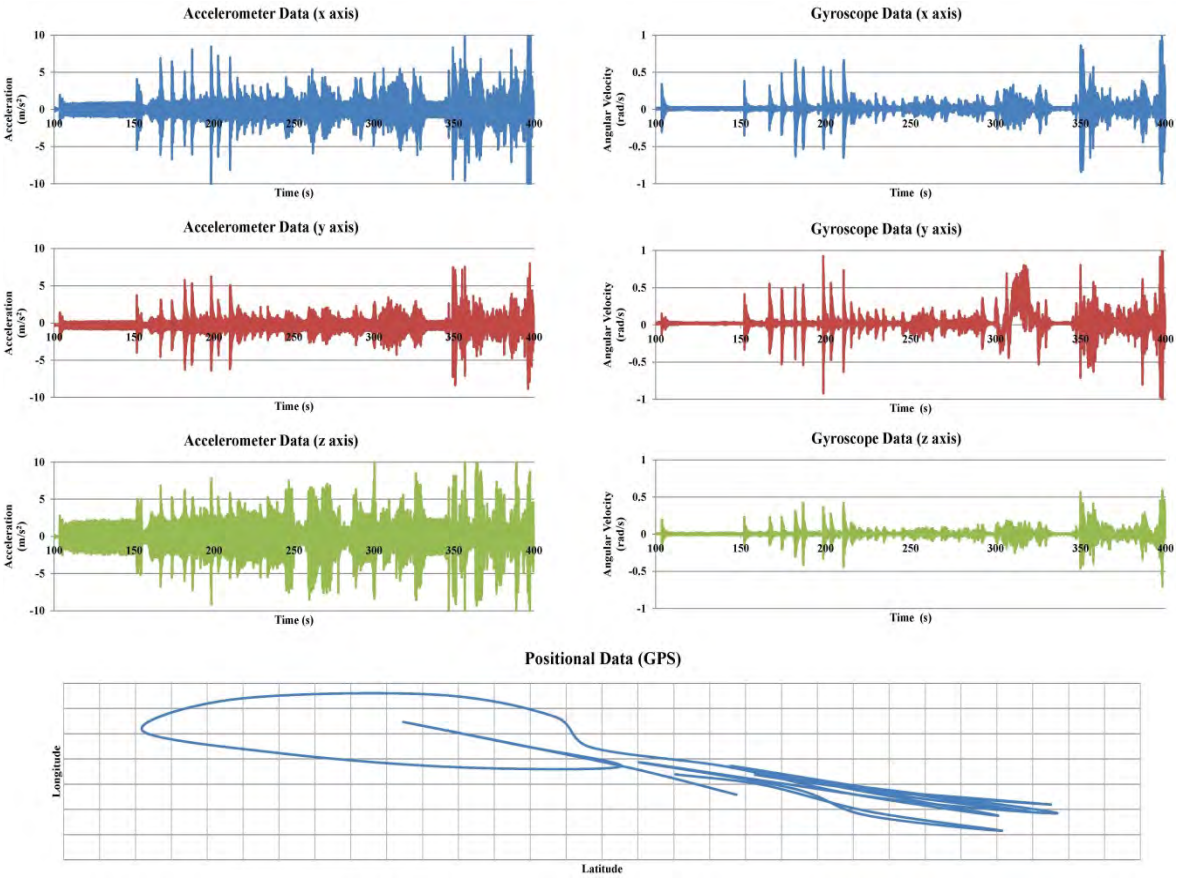

Figure 3. Snapshots of collected sensory data

Data Processing and Classification

Raw data must be first represented in terms of specific features over a window of certain data points. In this research, mean, variance, peak, interquartile range (IQR), correlation, and root

mean error (RMS) are the statistical time-domain features that were extracted from data. Moreover, signal energy was picked as the only frequency-domain feature since it had already shown positive discrimination results in previous studies (Figo et al. 2010; Khan et al. 2011) for context recognition using accelerometer data. These 7 features were extracted from both accelerometer and gyroscope data corresponding to each of the x, y, and z axis. Since both sensors return tri-axial values (x, y, z), a total of 42 (i.e. multiplication of 7 features from 2 sensors in 3 axes) features were extracted. The size of the window depends on the sampling frequency and thus, varies for different applications. However, it should be selected in such a way that no important action is missed. This can be achieved by overlapping consecutive windows. Previous studies using accelerometer for context recognition have suggested a 50% overlap between windows (Ahn et al. 2013; Darren Graham et al. 2005; DeVaul and Dunn 2001). Time-domain features can be extracted using statistical analysis. However, the frequency-domain feature (i.e. signal energy) should be extracted from the frequency spectrum which requires signal transformation. In this study, fast Fourier transform (FFT) was used to convert the time-domain signal to the frequency-domain. In order to be computationally efficient, FFT requires the number of data points in a window to be a power of 2. Data was initially segmented into windows of 128 data points with 50% overlap. Therefore, given a sampling frequency of 100 Hz, each window contained 1.28 seconds of the experiment data. A sensitivity analysis presented in Section 4.5 provides more detail about the process of selecting the proper window size. The entire data analysis process including feature extraction was performed in Matlab.

Among all extracted features, there are some that may not add to the accuracy of the classification. This might be due to the correlation that exists among the collected data and consequently extracted features, since many actions result in a similar pattern in different directions and/or different sensor types (i.e. accelerometer vs. gyroscope). Therefore, in order to reduce the computational cost and time of the classification process, and increase its accuracy, a subset of the discriminative features is selected by filtering out (removing) irrelevant or redundant features (Pirttikangas et al. 2006). In this study, two filtering approaches are used: ReliefF and Correlation-based Feature Selection (CFS). ReliefF is a weighting algorithm that assigns a weight to each feature and ranks them according to how well their values distinguish between the instances of the same and different classes that are near each other (Yu and Liu 2003). CFS is a subset search algorithm that applies a correlation measure to assess the goodness of feature subsets based on the selected features that are highly correlated to the class, yet uncorrelated to each other (Hall 1999).

Using CFS, irrelevant and redundant features were removed which yielded 12 features (out of 42). These features were than ranked by ReliefF using their weight factors. The first 12 features selected by ReliefF were compared to those selected by CFS and the 7 common features in both methods were ultimately chosen as the final feature space. Table 1 shows the selected features by each filter as well as their intersection.

A learning algorithm can be supervised or unsupervised depending on whether or not different classes are labeled for training. Although unsupervised methods can be employed for equipment action recognition (Gong et al. 2011), supervised learning algorithms provide better performance for this purpose (Golparvar-Fard et al. 2013). This is mainly due to the fact that action classes of a piece of equipment consist of some classes with limited number of instances. This creates an imbalanced set of classes (caused by large differences between the number of instances in some classes) that can very likely lead to over-fitting in unsupervised

learning classification. Among several supervised learning methods those that follow more complex algorithms may seem more accurate in classification.

Table 1. Selected features by CFS and ReliefF and their intersection (A: Accelerometer, G: Gyroscope)

Filter	Selected Features	Common Selected Features
CFS	A_mean_x, A_mean_y, A_mean_z, A_peak_x, A_iqr_y, A_iqr_z, A_correlation_z, A_rms_z, G_mean_x, G_mean_y, G_mean_z, G_variance_x	G_mean_z A_mean_x G_mean_x A_mean_y A_mean_z A_iqr_z A_peak_x
ReliefF	G_mean_z, A_mean_x, G_mean_x, A_peak_z, A_mean_y, A_correlation_y, A_correlation_x, A_mean_z, A_iqr_z, A_peak_x, A_peak_y, G_rms_z	

However, the choice of the learning algorithm is highly dependent on the characteristics and volume of data. As a result, a “single” best classifier does not generally exist and each case requires unique evaluation of the learning algorithm through cross validation (Goldberg 1989). Therefore, a number of learning algorithms are tested in this research to compare their performance in classifying actions using sensory data.

In this experiment, classification was performed by labeling the classes in different LoDs. The first set of training and classification algorithms is applied to three classes namely Engine Off, Idle, and Busy. Next, the Busy class is broken down into two subclasses of Moving and Scooping, and Moving and Dumping, and so on. As stated earlier, for action classification, five supervised learning methods were used: 1) Logistic Regression, 2) K-NN, 3) Decision Tree, 4) ANN (feed-forward backpropagation), and 5) SVM. Using different classifiers reduces the uncertainty of the results that might be related to the classification algorithm that each classifier uses.

Results of Equipment Activity Recognition

For each LoD, five classifiers were trained. Training and testing were performed through stratified 10-fold cross validations. In a *k*-fold cross validation the dataset is divided into *k* sets of equal sizes, and classifiers are trained *k* times, each time they are tested on one of the k folds and trained using the remaining $k - 1$ folds. Moreover, in the stratified *k*-fold cross validation, each fold contains almost the same proportions of classes as in the whole dataset. The mean accuracy is reported as the accuracy of each class. Result of the classification performance for each case (i.e. LoD) is presented in Table 2 in terms of overall classifier accuracy. As shown in Table 2, ANNs had the best relative overall accuracy among all five classifiers in all the LoDs. Moreover, although the 3-class level the accuracy gets to as high as 98.59%, the highest accuracy for the 4-classe level is 81.30% which is less than that of the 5-class level, which is 86.09%.

Table 2. Overall accuracy of classifiers for each LoD

	Classifier	Accuracy (%)
3 Classes	ANN	98.59
	DT	97.40
	KNN	97.65
	LR	96.93
	SVM	96.71
4 Classes	ANN	81.30
	DT	81.21
	KNN	80.51
	LR	77.58
	SVM	78.03
5 Classes	ANN	86.09
	DT	73.78
	KNN	84.20
	LR	84.42
	SVM	78.58

As stated earlier, construction equipment activity recognition has been previously explored through vision-based technologies. Gong et al. (2011) reported an overall accuracy of 86.33% for classification of three action classes of a backhoe. In a more recent study, Golparvar-Fard et al. (2013) achieved 86.33% and 76.0% average accuracy for three and four action classes of an excavator, respectively, and 98.33% average accuracy for three action classes of a dump truck. Although the target construction equipment are different in each case and action categories varies in these studies, the developed framework in this study that uses IMUs for the first time for construction equipment action recognition shows promising results when compared to existing vision-based systems that have been the subject of many research studies in the past few years.

Construction Workers' Activity Recognition

In a separate set of experiments, an outdoor construction workspace was created where different activities were performed by multiple workers. These activities included sawing, hammering, turning a wrench, loading sections into wheelbarrows, pushing loaded wheelbarrows, dumping sections from wheelbarrows, and returning with empty wheelbarrows. Activities were performed in 3 different categories in order to assess certain circumstances (as described later) in the outcome of classification. A Commercially available armband was used to secure a smartphone on the upper arm of the dominant hand of each worker. Recent research on the selection of accelerometer location on bricklayer's body for activity recognition has shown that according to the body movement of the worker while performing different bricklaying activities, among 15 potential locations for wearing an accelerometer, the lower left arm and the upper right arm are the two best locations that yield the highest information gain (Joshua and Varghese 2013). In this study, the lower arm was not selected for recognition of the activities of interest since it precludes convenient execution of some activities. Consequently, the selection of the upper arm was expected to provide accurate and consistent results compared to other locations on the body. Figure 4 shows some snapshots of the construction workers wearing

mobile phones on their upper arms while performing assigned activities in the experiments conducted in this research.

a b c

Figure 4. Snapshot of construction worker data collection experiments using mobile phones

Data Collection and Logging

Technical details of the data collection in terms of the mobile applications, sensors used (accelerometer and gyroscope), and sapling frequency (100 Hz) remained the same as the equipment data collection experiment described in the previous Section. Construction workers were asked to do their assigned activities for a certain period of time while waiting for a few seconds in between each instance of their assigned activities. Each activity was performed by two subjects for later user-independent evaluations. One subject performed only sawing. In this case, the goal of activity recognition was to differentiate between the time they were *sawing* and the time they were *not sawing*. Another subject performed hammering and turning a wrench. In this case, the activity recognition was intended to detect the time they were *hammering*, the time they were *turning the wrench*, and the time there were not doing any of the two activities. Finally, the last subject was responsible for pushing the wheelbarrow and loading/unloading the sections. Therefore, the activities to be recognized in this case were *loading* sections into a wheelbarrow, *pushing* a loaded wheelbarrow, *dumping* sections from a wheelbarrow, and *returning* with an empty wheelbarrow. Also, the entire experiment was videotaped for data annotation.

Data Processing and Classification

Classifications are conducted in 3 activity categories. Category 1 includes only one distinguishable activity, *sawing*, to assess the performance of the classifiers in detecting value-adding versus non-value-adding instances in a pool of accelerometer and gyroscope data. The result of classification in this category contributes to the overall performance of the developed activity recognition system when used for productivity measurement. In this category, *sawing* is categorized against *idling*. Category 2 includes instances of consecutive *hammering* and *turning a wrench* as two adjacent activities with almost similar corresponding movements of the worker's arm. These two activities are also classified against *idling* to assess the accuracy of the developed activity recognition system in differentiating between activities that produce similar physical body motions. Finally, in category 3, four activities that produce different distinguishable body movements are categorized. These activities include *loading sections into*

a wheelbarrow, *pushing a loaded wheelbarrow*, *dumping sections from a wheelbarrow*, and *returning an empty wheelbarrow*, that were also categorized against *idling*. Similar to the equipment experiments, 128 data points were segmented in one window and 50% overlap for the adjacent windows is considered. In this experiments, the extracted features are as follow: mean, maximum, minimum, variance, RMS, IQR, and correlation between each two pairs of axes comprised the seven time-domain features and spectral energy and entropy were the two frequency domain features. Considering data collection in three axes of the two sensors and nine independent features extracted per sensor per axis, a total of 54 features were extracted from all collected data.

Results of Workers' Activity Recognition

The performance of the classifiers is assessed in two ways. First, the training accuracy of each classifier was calculated. This means that all collected data points were used for both training and testing which provided an overall insight into the performance of a host of classification algorithms in recognizing construction worker activities using accelerometer and gyroscope data. Next, a more robust approach in evaluation of classifiers was adopted. In particular, 10-fold stratified cross validation was used and the results of the 10 replications of the training and testing were averaged out to report the overall accuracy.

The classification accuracies are reported for 3 activity categories listed in Table 3. The following activity codes are used in reporting the results: in the first category, activity *sawing (SW)* and *being idle (ID)* are classified. In the second category, activities *hammering (HM)*, *turning a wrench (TW)*, and *being idle (ID)* are classified. Finally, in the third category classification is performed on the activities *loading sections into wheelbarrow (LW)*, *pushing a loaded wheelbarrow (PW)*, *dumping sections from wheelbarrow (DS)*, *returning an empty wheelbarrow (RW),* and *being idle (ID)*. Table 3 shows the results of training and 10-fold cross validation classification accuracy the subject performing activities of category 1.

Table 3. Category 1 activities classification accuracy

Category 1	ANN	Decision Tree	KNN	Logistic Regression	SVM
Training	100.00	99.36	98.08	98.72	98.19
10-fold CV	96.77	96.06	95.95	96.05	96.91

According to Table 3, over 99% training accuracy was achieved in category 1 using ANN classifier. This confirms the hypothesis that IMU data pertaining to a single activity performed by different workers contain highly distinguishable patterns. However, training accuracy is not an appropriate measure to assess the ability of using such data for new instances of the same activity. Nevertheless, the stratified 10-fold cross validation results confirm that regardless of the nature of classification algorithm, a single activity can be recognized with over 96% accuracy using all five classifiers.

Since it is very likely that a construction worker performs more than one highly distinguishable activity at a time, activities performed in category 2 are designed such that they produce almost the same physical arm movement. Table 4 shows the training and 10-fold cross validation classification accuracy results of both subjects performing activities of category 2.

Table 4. Category 2 activities classification accuracy

Category 2	ANN	Decision Tree	KNN	Logistic Regression	SVM
Training	98.62	97.07	93.81	88.14	87.28
10-fold CV	93.19	85.83	87.80	86.42	85.34

Similar to category 1, the training accuracies are high particularly for the ANN classifier and the decision tree. While CART decision trees are not very stable and a small change in the training data can change the result drastically as appears in the outcome of the 10-fold cross validation, ANN presents an average of around 90% accuracy for both subjects. This is while all other classification methods performed almost the same with a slight superiority of KNN relative to the other algorithms. This result is particularly important considering the fact that the two activities in category 2 (i.e. *hammering* and *turning a wrench*) produce almost similar physical movements in a worker's arm.

In the third category, a mixture of different distinguishable activities performed by typical construction workers is included to evaluate the performance of the developed activity recognition system in recognizing them. Table 5 shows the training and 10-fold cross validation classification accuracy results of both subjects performing activities of category 3.

Table 5. Category 3 activities classification accuracy

Category 3	ANN	Decision Tree	KNN	Logistic Regression	SVM
Training	94.80	97.11	95.75	90.37	85.82
10-fold CV	92.01	87.95	90.75	90.75	84.42

According to Table 5, again decision tree gained a high accuracy in training while as expected; its performance is not the same in 10-fold cross validation evaluation. However, except for the decision tree and SVM, all other classifiers, namely ANN, KNN, and logistic regression resulted in around 90% average accuracy for both subjects. Similar to the other two categories, the feedforward back-propagation implementation of the ANN resulted in the highest accuracy among all.

SUMMARY AND CONCLUSIONS

The goal of the research presented in this paper was to investigate the prospect of using built-in smartphone sensors as ubiquitous multi-modal data collection and transmission nodes in order to detect detailed construction equipment activities. In spite of its importance, automated recognition of construction worker and equipment activities on the jobsite has not been given due attention in CEM literature. The discovered process-level knowledge can provide a solid basis for different applications such as productivity improvement, safety management, and fuel use and emission monitoring and control. In addition, this methodology can serve as a basis for activity duration extraction for the purpose of construction simulation input modeling.

In order to study construction equipment activity recognition, a case study of front-end loader was used to describe the methodology for action recognition and evaluate the performance of the developed system. In doing so, several important technical details such as selection of discriminating features to extract different LoDs for classification, and choice of classifier to be

trained were investigated. Results indicated that different equipment actions generate distinct data patterns (i.e. signatures) in accelerometer and gyroscope data. In the 3-class level a high accuracy of as 98.59% can be achieved using ANN. With the same choice of classifier, 81.30% and 86.09% accuracy was achieved for 4- and 5-class levels.

In case of workers' activity recognition, built-in sensors of ubiquitous smartphones have been employed to assess the potential of wearable systems for activity recognition. Smartphones were affixed to workers' upper arms using armbands, and accelerometer and gyroscope data were collected from multiple construction workers involved in different types of activities. The high levels of training accuracies achieved by testing several classification algorithms including ANN, decision tree, KNN, logistic regression, and SVM confirmed the hypothesis that different classification algorithms can detect patterns that exist within signals produced by IMUs while different construction tasks are performed. Through 10-fold stratified cross validation, algorithms were trained with 90% of the available data and the trained models were tested on the remaining 10%. In different categories of activities, around and over 90% accuracy was achieved. This promising result indicates that built-in smartphone sensors have high potential to be used as integrated data collection and activity recognition platforms in construction environments.

FUTURE WORK

A potential direction for future work in this research will be to explore whether the results achieved so far can be used for automatically extracting process knowledge such as activity durations and precedence logic for the purpose of ubiquitously updating and maintaining simulation models corresponding to field operations. In addition, another branch of future work rooted in the current research is automated identification of unsafe workers' postures in physically demanding construction activities. Work-related Musculoskeletal Disorder (WMSD), back, knee, and shoulders injuries are among the most common injuries that can be prevented or reduced by complying with Occupational Safety and Health Administration (OSHA) or the National Institute for Occupational Safety and Health (NIOSH) standards and rules (NIOSH 2015; OSHA 1990).

ACKNOWLEDGMENTS

The authors would like to acknowledge the help and support of Hubbard Construction, for providing access to active construction facilities for equipment data collection experiments. Any opinions, findings, conclusions, and recommendations expressed in this paper are those of the authors and do not necessarily reflect the views of Hubbard Construction. Also, the authors are grateful to the construction engineering research laboratory students who assisted in the data collection process.

REFERENCES

Ahn, C. R., S. Lee, and F. Peña-Mora. 2013. "The Application of Low-Cost Accelerometers for Measuring the Operational Efficiency of a Construction Equipment Fleet." *Journal of Computing in Civil Engineering*.

Akhavian, R., and A. H. Behzadan. 2012. "An Integrated Data Collection and Analysis Framework for Remote Monitoring and Planning of Construction Operations." *Advanced Engineering Informatics* 26 (4):749–761.

Akhavian, R., and A. H. Behzadan. 2013. "Knowledge-Based Simulation Modeling of Construction Fleet Operations Using Multimodal-Process Data Mining." *Journal of Construction Engineering and Management* 139 (11):04013021.
Akhavian, R., and A. H. Behzadan. 2014. "Evaluation of Queuing Systems for Knowledge-Based Simulation of Construction Processes." *Automation in Construction* 47:37-49.
Akhavian, R., and A. H. Behzadan. 2015. "Construction Equipment Activity Recognition for Simulation Input Modeling Using Mobile Sensors and Machine Learning Classifiers." *Advanced Engineering Informatics*.
Bishop, C. M. 2006. *Pattern Recognition and Machine Learning*. Vol. 4: springer New York
Brilakis, I., M. W. Park, and G. Jog. 2011. "Automated Vision Tracking of Project Related Entities." *Advanced Engineering Informatics* 25 (4):713-724.
Cheng, T., J. Teizer, G. C. Migliaccio, and U. C. Gatti. 2013. "Automated Task-Level Activity Analysis through Fusion of Real Time Location Sensors and Worker's Thoracic Posture Data." *Automation in Construction* 29:24-39.
Darren Graham, L., S. D. Smith, and P. Dunlop. 2005. "Lognormal Distribution Provides an Optimum Representation of the Concrete Delivery and Placement Process." *Journal of construction engineering and management* 131 (2):230-238.
Dernbach, S., B. Das, N. C. Krishnan, B. L. Thomas, and D. J. Cook. 2012. Simple and Complex Activity Recognition through Smart Phones. Intelligent Environments (IE), 2012 8th International Conference on.
DeVaul, R. W., and S. Dunn. 2001. "Real-Time Motion Classification for Wearable Computing Applications." *2001, project paper, http://www.media.mit.edu/wearables/mithril/realtime.pdf*.
Figo, D., P. C. Diniz, D. R. Ferreira, and J. M. Cardoso. 2010. "Preprocessing Techniques for Context Recognition from Accelerometer Data." *Personal and Ubiquitous Computing* 14 (7):645-662.
Foerster, F., M. Smeja, and J. Fahrenberg. 1999. "Detection of Posture and Motion by Accelerometry: A Validation Study in Ambulatory Monitoring." *Computers in Human Behavior* 15 (5):571-583.
Frank, K., M. J. V. Nadales, P. Robertson, and M. Angermann. 2010. Reliable Real-Time Recognition of Motion Related Human Activities Using Mems Inertial Sensors. Proceedings of the 23rd International Technical Meeting of the Satellite Division of the Institute of Navigation.
Goldberg, D. E. 1989. *Genetic Algorithms in Search, Optimization, and Machine Learning*. Vol. 412: Addison-wesley Reading Menlo Park
Golparvar-Fard, M., A. Heydarian, and J. C. Niebles. 2013. "Vision-Based Action Recognition of Earthmoving Equipment Using Spatio-Temporal Features and Support Vector Machine Classifiers." *Advanced Engineering Informatics* 27 (4):652-663.
Gong, J., C. H. Caldas, and C. Gordon. 2011. "Learning and Classifying Actions of Construction Workers and Equipment Using Bag-of-Video-Feature-Words and Bayesian Network Models." *Advanced Engineering Informatics* 25 (4):771-782.
Gonsalves, R., and J. Teizer. 2009. Human Motion Analysis Using 3d Range Imaging Technology. Proceedings of the 26th International Symposium on Automation and Robotics in Construction, at Austin, Texas.
Gupta, P., and T. Dallas. 2014. "Feature Selection and Activity Recognition System Using a Single Tri-Axial Accelerometer."
Hall, M. A. 1999. "Correlation-Based Feature Selection for Machine Learning." The University of Waikato.
Han, S., and S. Lee. 2013. "A Vision-Based Motion Capture and Recognition Framework for Behavior-Based Safety Management." *Automation in Construction* 35:131-141.
Hassoun, M. H. 1995. *Fundamentals of Artificial Neural Networks*: MIT press

Hastie, T., R. Tibshirani, J. Friedman, T. Hastie, J. Friedman, and R. Tibshirani. 2009. *The Elements of Statistical Learning*. Vol. 2: Springer
Haykin, S. S., S. S. Haykin, S. S. Haykin, and S. S. Haykin. 2009. *Neural Networks and Learning Machines*. Vol. 3: Pearson Education Upper Saddle River
Hemminki, S., P. Nurmi, and S. Tarkoma. 2013. Accelerometer-Based Transportation Mode Detection on Smartphones. Proceedings of the 11th ACM Conference on Embedded Networked Sensor Systems.
Irizarry, J., M. Gheisari, and B. N. Walker. 2012. "Usability Assessment of Drone Technology as Safety Inspection Tools." *Journal of Information Technology in Construction (ITcon)* 17:194-212.
Joshua, L., and K. Varghese. 2011. "Accelerometer-Based Activity Recognition in Construction." *Journal of Computing in Civil Engineering* 25 (5):370-379.
Joshua, L., and K. Varghese. 2013. "Selection of Accelerometer Location on Bricklayers Using Decision Trees." *Computer-Aided Civil and Infrastructure Engineering* 28 (5):372-388.
Khan, M., S. I. Ahamed, M. Rahman, and R. O. Smith. 2011. A Feature Extraction Method for Realtime Human Activity Recognition on Cell Phones. Proceedings of 3rd International Symposium on Quality of Life Technology (isQoLT 2011). Toronto, Canada.
Kim, T.-S., J.-H. Cho, and J. T. Kim. 2013. "Mobile Motion Sensor-Based Human Activity Recognition and Energy Expenditure Estimation in Building Environments." In *Sustainability in Energy and Buildings*, 987-993. Springer.
Kose, M., O. D. Incel, and C. Ersoy. 2012. Online Human Activity Recognition on Smart Phones. Workshop on Mobile Sensing: From Smartphones and Wearables to Big Data.
Krassenstein, E. 2015. "Renderings & Details Unveiled for Extraordinary 3d Printed Home in New York." http://3dprint.com/. Accessed May 8, 2015. http://3dprint.com/59753/d-shape-3d-printed-house-ny/.
Kwapisz, J. R., G. M. Weiss, and S. A. Moore. 2011. "Activity Recognition Using Cell Phone Accelerometers." *ACM SigKDD Explorations Newsletter* 12 (2):74-82.
Lara, O. D., and M. A. Labrador. 2013. "A Survey on Human Activity Recognition Using Wearable Sensors." *Communications Surveys & Tutorials, IEEE* 15 (3):1192-1209.
Li, Q., J. A. Stankovic, M. A. Hanson, A. T. Barth, J. Lach, and G. Zhou. 2009. Accurate, Fast Fall Detection Using Gyroscopes and Accelerometer-Derived Posture Information. Wearable and Implantable Body Sensor Networks, 2009. BSN 2009. Sixth International Workshop on.
Lyons, G., K. Culhane, D. Hilton, P. Grace, and D. Lyons. 2005. "A Description of an Accelerometer-Based Mobility Monitoring Technique." *Medical engineering & physics* 27 (6):497-504.
NIOSH. 2015. "Safety & Prevention." Accessed March 30, 2015. http://www.cdc.gov/niosh/topics/safety.html.
OSHA. 1990. "Excavation Final Rule." Safety and Health Administration,
Peddi, A., L. Huan, Y. Bai, and S. Kim. 2009. Development of Human Pose Analyzing Algorithms for the Determination of Construction Productivity in Real-Time. Construction Research Congress at Seattle, WA.
Pirttikangas, S., K. Fujinami, and T. Nakajima. 2006. "Feature Selection and Activity Recognition from Wearable Sensors." In *Ubiquitous Computing Systems*, 516-527. Springer.
Ravi, N., N. Dandekar, P. Mysore, and M. L. Littman. 2005. Activity Recognition from Accelerometer Data. AAAI.
Reddy, S., M. Mun, J. Burke, D. Estrin, M. Hansen, and M. Srivastava. 2010. "Using Mobile Phones to Determine Transportation Modes." *ACM Transactions on Sensor Networks (TOSN)* 6 (2):13.

Rezazadeh Azar, E., and B. McCabe. 2012. Vision-Based Recognition of Dirt Loading Cycles in Construction Sites.
Shoaib, M., S. Bosch, O. D. Incel, H. Scholten, and P. J. Havinga. 2015. "A Survey of Online Activity Recognition Using Mobile Phones." *Sensors* 15 (1):2059-2085.
Staudenmayer, J., D. Pober, S. Crouter, D. Bassett, and P. Freedson. 2009. "An Artificial Neural Network to Estimate Physical Activity Energy Expenditure and Identify Physical Activity Type from an Accelerometer." *Journal of Applied Physiology* 107 (4):1300-1307.
Su, X., H. Tong, and P. Ji. 2014. "Activity Recognition with Smartphone Sensors." *Tsinghua Science and Technology* 19 (3):235-249.
Sun, L., D. Zhang, B. Li, B. Guo, and S. Li. 2010. "Activity Recognition on an Accelerometer Embedded Mobile Phone with Varying Positions and Orientations." In *Ubiquitous Intelligence and Computing*, 548-562. Springer.
Wang, S., C. Chen, and J. Ma. 2010. Accelerometer Based Transportation Mode Recognition on Mobile Phones. Wearable Computing Systems (APWCS), 2010 Asia-Pacific Conference on.
Want, R. 2006. "An Introduction to Rfid Technology." *Pervasive Computing, IEEE* 5 (1):25-33.
Wu, W., S. Dasgupta, E. E. Ramirez, C. Peterson, and G. J. Norman. 2012. "Classification Accuracies of Physical Activities Using Smartphone Motion Sensors." *Journal of medical Internet research* 14 (5):e130.
Yan, Z., V. Subbaraju, D. Chakraborty, A. Misra, and K. Aberer. 2012. Energy-Efficient Continuous Activity Recognition on Mobile Phones: An Activity-Adaptive Approach. Wearable Computers (ISWC), 2012 16th International Symposium on.
Yu, L., and H. Liu. 2003. Feature Selection for High-Dimensional Data: A Fast Correlation-Based Filter Solution. ICML.
Zheng, Y., Y. Chen, Q. Li, X. Xie, and W.-Y. Ma. 2010. "Understanding Transportation Modes Based on Gps Data for Web Applications." *ACM Transactions on the Web (TWEB)* 4 (1):1.
Zou, J., and H. Kim. 2007. "Using Hue, Saturation, and Value Color Space for Hydraulic Excavator Idle Time Analysis." *Journal of computing in civil engineering* 21 (4):238-246.

Terrestrial Laser Scanning Roughness Assessments for Infrastructure

Ahmad Alhasan
Department of Civil, Construction and Environmental Engineering
Iowa State University
394 Town Engineering Building
Ames, IA 50011-3232
Email: aalhasan@iastate.edu

David J. White, Ph.D., P.E.
Department of Civil, Construction and Environmental Engineering
Iowa State University
422 Town Engineering Building
Ames, IA USA 50011-3232
Email: djwhite@iastate.edu

ABSTRACT

Road roughness is a key parameter for controlling pavement construction processes and for assessing ride quality of both paved and unpaved roads. This paper describes algorithms used in processing three-dimensional (3D) stationary terrestrial laser scanning (STLS) point clouds to obtain surface maps of point wise indices that characterize pavement roughness. The backbone of the analysis is a quarter-car model simulation over a spatial 3D mesh grid representing the pavement surface. Two case studies are presented, and results show high spatial variability in the roughness indices both longitudinally and transversely (i.e., different wheel path positions). It is proposed that road roughness characterization using a spatial framework provides more details on the severity and location of roughness features compared to the one-dimensional methods. This paper describes approaches that provide an algorithmic framework for others collecting similar STLS 3D spatial data to be used in advanced road roughness characterization.

Keywords: 3D laser Scanning—road roughness—algorithms

INTRODUCTION

Road surface roughness increases vehicle operation and travel delay costs (Gao and Zhang 2013; Ouyang and Madanat 2004); reduces vehicle durability (Bogsjö and Rychlik 2009; Oijer and Edlund 2004); and reduces ride quality and structural performance (Al-Omari and Darter 1994). Structural performance diminishes faster on rough roads because rough features increase dynamic stresses that accelerate structural deterioration (Lin et al. 2003). Accurate evaluation of pavement roughness levels and modes is a key factor in optimizing maintenance decisions (Chootinan et al. 2006; Kilpeläinen et al. 2011; Lamptey et al. 2008) and a leading indicator in construction quality assurance/quality control (QC/QA).

In 1986, the International Roughness Index (IRI) was introduced as a time stable pavement roughness measurement (Sayers et al. 1986; Sayers et al. 1986). Since then IRI has been widely used because it empirically correlates with ride quality and vehicle operating costs (Gao

Proceedings of the 2015 Conference on Autonomous and Robotic Construction of Infrastructure, Ames, Iowa.

and Zhang 2013; Ouyang and Madanat 2004; Tsunokawa and Schofer 1994). IRI is calculated by mathematically simulating the quarter-car dynamics and accumulating the quarter-car suspension response induced by variations in a vertical profile. Current teste method for measuring longitudinal profiles using an inertial profiler (ASTM E950 / E950M-09) is most suited for collecting data in one or two or even few profiles, however it is hard to synchronize these profiles to test the transverse variability in elevation at a specific point. Karamihas et al. (1999) investigated the variability in the IRI values for different profiles across the road, and reported that two profiles across the lane are not representative of the entire lane and that drivers typical wander laterally within a range of 50 cm (20 in).

Another limitation when reporting summary indices with fixed analysis interval, is the ability to detect localized features, Swan and Karamihas (2003) proposed reporting IRI continuously by applying a moving average to the suspension response. Studies have shown that local features affect rider comfort, pavement stresses, and cause most vehicle fatigue damage (Bogsjö and Rychlik 2009; Kuo et al. 2011; Oijer and Edlund 2004; Steinwolf et al. 2002).

Unlike paved roads, there is a lack of a common set of criteria to evaluate unpaved roads, many local agencies use visual inspection to estimate an IRI value (Archondo-Callao 1999; Namur and de Solminihac 2009; Walker et al. 2002). Some agencies combine visual inspection with direct measurement of defects (e.g., pothole depth, corrugation spacing) (Soria and Fontenele 2003; Woll et al. 2008). Several studies have pointed out the importance of precise assessment of unpaved road conditions using indirect data acquisition methods such as unmanned aerial vehicles (UAV), ground penetrating radar (GPR), and accelerometers to help transportation agencies decide whether to maintain or upgrade these roads (Berthelot et al. 2008; Brown et al. 2003; Zhang 2009; Zhang and Elaksher 2012).

Recent developments in laser scanning techniques and light detection and ranging (LIDAR) sensing have motivated researchers and practitioners to adopt these technologies due to the accurate and rich data measurements. Recent studies (Fu et al. 2013; Tsai et al. 2010; Zalama et al. 2011) have demonstrated the effectiveness of laser scanning and LIDAR in identifying geometrical features of interest (e.g., cracks, bumps). Also, recent studies have investigated the applicability of using stationary three dimensional (3D) laser scanning techniques in obtaining IRI by selectively extracting track profiles (Chang and Chang 2006) or by analyzing the surface to develop spatial roughness maps (Alhasan et al. 2015).

This study will introduce an overview of stationary laser scanning approach and the practical needs for applications in road roughness assessment. Also a discussion of a procedure and associated algorithms that can be used in processing 3D point clouds obtained for paved and unpaved sections, to obtain spatial surface maps of rectified slopes (RS) and IRI values across road sections. A brief review of frequency based analysis (i.e. Fast Fourier transform, FFT and Continues wavelet transform) will be introduced as well. Frequency based approaches can reveal the sources of road roughness. The backbone of the analysis approaches described herein is a quarter-car model.

DATA COLLECTION USING STATIONARY LASER SCANNER

LIDAR systems measure information (spatial coordinates and color) of a 3D space and store the information in a 3D point cloud. The term LIDAR is generic, and includes airborne laser scanning technologies, mobile scanners mounted on vehicles, and stationary laser scanners or stationary terrestrial laser scanners (STLS), where the laser scanner is fixed at a station with

known coordinates and based on the distance between the scanner and the detected points, a geospatially referenced 3D point cloud is constructed. Trimble CX 3D STLS system was used in two case studies to acquire 3D laser scans. The position accuracy of a single point is 4.5 mm at 30 m and drops to 7.3 mm at 50 m. The distance accuracy is 1.2 mm at 30 m and drops to 2 mm at 50 m. Figure 1 shows the scanner set-up.

Figure 1. Trimble CX 3D laser scanner set-up.

Scanning process starts by acquiring full scan that covers the 360° x 300° view. This scan produces a mother file that includes common targets (Figure 2) to be used for registration in the post processing. Area scans are then conducted to acquire denser point clouds for the areas of interest. The size of the targets affect the density of the full scan, where smaller targets require high density full scans to capture them. However, the density of the area scans can vary depending on the application. In the two case studies, criterion specified to analyze roads roughness from the point cloud was a maximum spacing of 100 mm in both spatial directions (longitudinal and transverse) between two consecutive points in the region of interest. By several trials it was found that a density of 35 mm at 100,000 mm for the area scans produced sufficiently dense clouds to satisfy the 100 mm spacing criterion.

Figure 2. Reference point (a) spherical targets and (b) flat black and white target.

After acquiring the data, the scan should be registered in a specialized software. Many activities can be performed using software packages, such as registration, fitting geometries. Registration of clouds is done by identifying common targets (spheres or flat targets as shown in Figure 2) appearing in the full scans of each consecutive station that share a common spatial domain with other stations. These targets are used as benchmarks to geospatially reference scans by matching the common target locations in each scan, and thus stitching the scans to produce a full 3D cloud. Figure 3 shows examples of the registered point clouds. The variation in color indicates the material reflectivity.

Figure 3. Registered point cloud.

After registration, the point clouds are cleaned of unnecessary data points, where the sections of interest should be separated from areas beyond the edges of the sections and noise from any passing vehicles that might appear in the scans. The final data points left after cleaning can be

exported in ASCII file format; these files contain the x, y, and z coordinates of the points in the section under consideration.

DATA PROCESSING

Visioning Algorithms

To use the road surface in simulations developed algorithms require a uniformly spaced grid the longitudinal direction. To achieve that a mesh grid is formed with grid elements that have a predefined *x* and *y* edge dimensions. The grid centre elevation is calculated as the average of all cloud points falling in that grid region. All points are rotated and translated to a local coordinate system corresponding to the longitudinal and transvers axes (Zalama et al. 2011). Transformation for processing along horizontal curves can be achieved by constructing a curvilinear local coordinate system; however, for simple geometries without curves the point cloud is rotated globally, where the x axis corresponds to the longitudinal direction and the y axis to the transverse direction. Vertical slopes are corrected by subtracting the z elevation along a quadratic fit from the *z* coordinate of the corresponding transformed points (Alhasan et al. 2015). Figure 4 shows a pavement section point cloud data after processing in the visioning algorithm.

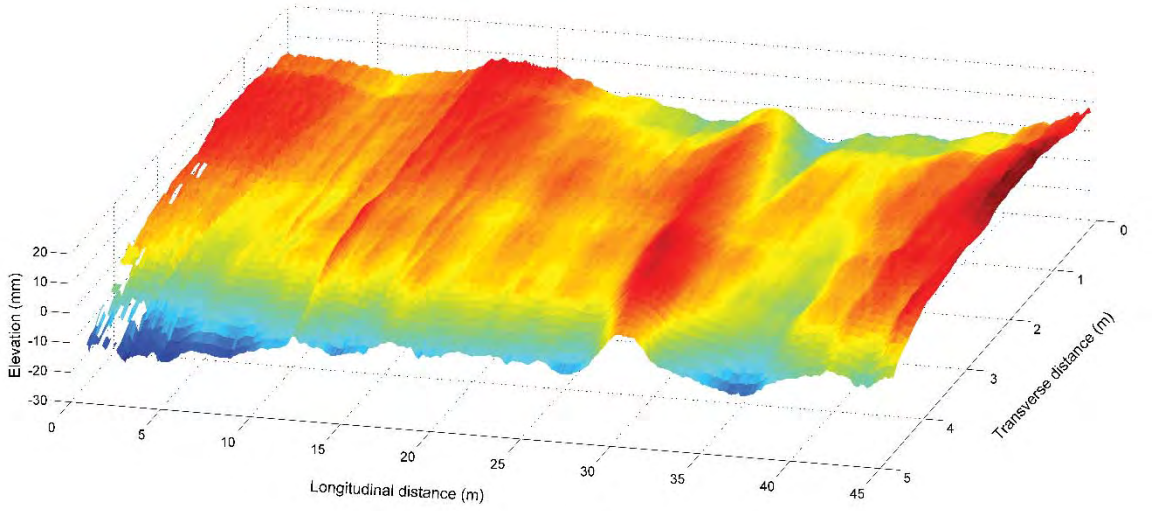

Figure 4. Point cloud data after processing in the visioning algorithm for a pavement section.

Roughness Evaluation Algorithms

Evaluation of roughness described herein is based on the responses of the quarter-car model described in (ASTM E1926-08). Figure 5 presents a schematic of the quarter-car model. Where M_s and M_u are the sprung and unsprung masses respectively, k_s and k_t are the suspension and tire spring coefficients respectively, and c_s is the suspension damping rate.

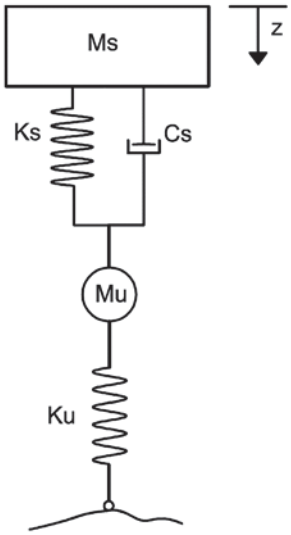

Figure 5. Quarter-car model.

The dynamics of the system can be described by four first-order differential equations presented in a matrix form (Sayers and Karamihas 1996) (Equations 1—4):

$$\dot{X} = AX + B\,h_{ps} \tag{1}$$

Where;

$$X = \begin{bmatrix} z_S & \dot{z}_S & z_u & \dot{z}_u \end{bmatrix}^T \tag{2}$$

$$A = \begin{bmatrix} 0 & 1 & 0 & 0 \\ -k_2 & -c & k_2 & c \\ 0 & 0 & 0 & 1 \\ \frac{k_2}{\mu} & \frac{c}{\mu} & -\frac{(k_1+k_2)}{\mu} & -\frac{c}{\mu} \end{bmatrix} \tag{3}$$

$$B = \begin{bmatrix} 0 & 0 & 0 & k1/\mu \end{bmatrix}^T \tag{4}$$

Where h_{ps} is the elevation of the profile after applying the moving average smoother; z_S and z_u are the elevations of sprung and unsprung masses; $\dot{z}_S$ and $\dot{z}_u$ are elevation time derivatives of sprung and unsprung masses; k_1 is the tire spring coefficient divided by the sprung mass, k_2 is

the suspension spring coefficient divided by the sprung mass, *c* is the suspension damping rate divided by the sprung mass, and μ is the ratio of unsprung to sprung mass. Two approaches can be followed to solve this system, a finite difference solution that solves the system in stepwise fashion and a frequency domain solution (Fourier analysis). The outcome of the solution is the rectified slope profile, which is the time rate at which the sprung mass is moving in the z direction relative to the unsprung mass. This index reflects the suspension rate for a quarter-car model.

Finite Difference Algorithms

The differential equation described in Equation 1 can be solved in state-space form as shown Equation 5 (Murray et al. 1994; Sayers and Karamihas 1996). FORTRAN code is provided in (ASTM E1926-08) to solve this system. The code can be translated to MATLAB code and used to simulate the quarter-car model over each longitudinal strip in the grid developed from the point cloud. A longitudinal strip is defined as a sequence of grid elements in the x direction having one y coordinate. The longitudinal strips are used as an input profile for simulations. This approach leads to a surface roughness map where the rectified slope is a function of the variable *x* and the fixed coordinate *y*. Because each profile is simulated independently, transverse effects such as rolling and pitch are not included.

$$X_i = S\,X_{i-1} + P\,h_{ps} \tag{5}$$

Where;

$$S = e^{A\Delta x/v}$$

$$P = A^{-1}(S - I)B \tag{6}$$

X, *A*, h_{ps}, and *B* are predefined in Equations 1—4, Δx is the spacing between profile points, *v* is the assumed speed of the model, and *I* is the identity matrix. The finite difference algorithm is implemented in many commercial packages and proved efficiency when used in analysing long profiles. However, the algorithm suffers from long memory effects, where the rectified slope at a point is affected by the elevation of previous points back to several meters, reaching 10 meters in some cases, and thus the starting point affects the results when analysing short profiles (Swan and Karamihas 2003). The critical length of the profile depends on several factors, the smoothness of the profile to be analysed and the sampling frequency of the data acquisition system.

Frequency domain algorithms

Frequency analysis is another approach to solve the described dynamic system. This approach namely depends on transforming the state equations from spatial to frequency or quasi-frequency domain. The analytical description of quarter-car model is best explained in terms of random signal analysis, where fast Fourier transformation (FFT) can be a helpful tool for such analysis. The basic assumption in this approach is that any profile can be decomposed into building sinusoids, for infinite precision the signal should be decomposed to an infinite number of sinusoids, however only finite number can be used to describe a signal. Results for the FFT analysis can be characterized by examining the height amplitude versus spatial frequency plots (Alhasan et al. 2015), or by applying a band-pass filter (Liu and Herman 1999) that characterizes the analytical solution of the quarter car model in frequency domain, this filter results in rectified slope profile.

Wavelet analysis techniques were developed independently in different fields (i.e., pure mathematics, physics, and engineering) to overcome the time-frequency resolution issue in Fourier analysis (Boggess and Narcowich 2009; Daubechies 1992). This issue results from the assumption that sines and cosines, which are infinitely periodic functions, are building blocks for any function. This assumption induces uncertainty in the analysis, where high resolution cannot be achieved simultaneously in both frequency and space domains. Wavelets, which can be thought of as wave pulses that translate in the spatial domain and can change size (i.e., dilate or shrink), are used as building blocks to overcome the time-frequency resolution issue. Wavelets come in families, and for each family there is a wavelet, the "mother wavelet," and a scaling function, a "father wavelet," although some families do not include scaling functions. Wavelet dispersion is controlled by a scale factor 'a', where larger scale factors correspond to dilated waves and smaller scale factors correspond to shrunken waves.

Wavelet transform projects (transforms) the profile on a wavelet function at different scales (layers of details) to result in wavelet coefficients describing the correlation between the signal and the wavelet function. This decomposition allows examining the location of features with certain frequency bands with known effect on vehicle response, and thus provides a valuable tool to determine localized features (Alhasan et al. 2015).

CASE STUDIES

Road roughness of two road sections was evaluated, the sections include a 55 m long rural unpaved road and a 58.8 m long HMA overlay over a jointed plain concrete pavement (JPCP) pavement. Figures 6a and 6b show the rectified slope map for rural road and the paved road respectively.

For the unpaved road the left lane extends between stations 0 and 3 in the transverse distance, and the right lane extends between stations 0 and -3. This map reveals great details, for instance the central region is unsystematically rough compared to the rest of the scan area, however a localized rough region appears in the left lane between stations 50 and 55, which corresponds to a loose pile of aggregate. The paved road surface map includes an approximately 3 m wide lane that extends between stations 0 and 4. The map shows the severity and location of the reflective cracks in the transvers direction.

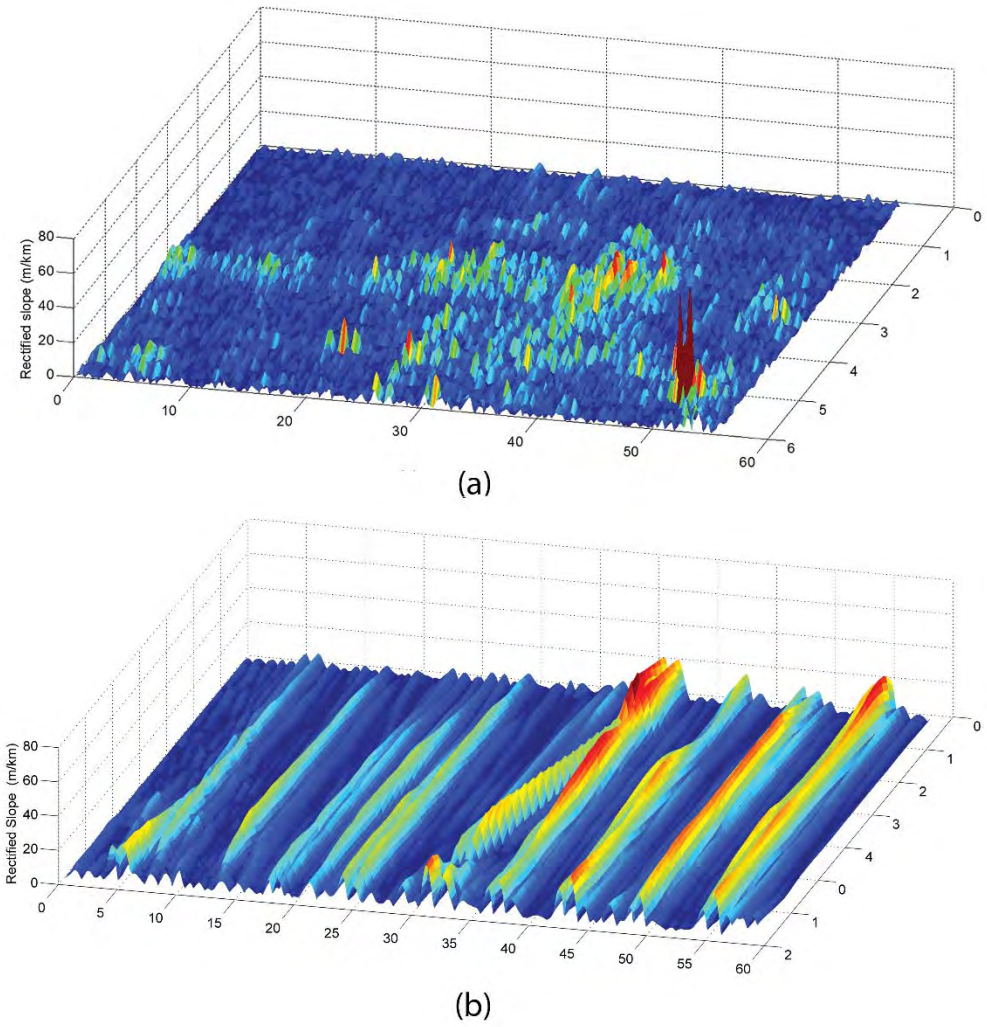

Figure 6. Absolute rectified slope surface maps for (a) unpaved and (b) paved roads.

The average of rectified slope values along each profile is defined as its IRI, since the map was generated by simulating a quarter-car model moving at a speed of 80 km/h. Figure 7 shows the IRI values versus width for both roads, it can be noticed that IRI values are highly variable. Due to the high variability in IRI values it is proposed to base the conclusions regarding surface roughness on the IRI versus width plots, and if a single summary index is needed median would be a more proper way to report overall IRI values than the average. The advantage of using the median is robustness to outliers.

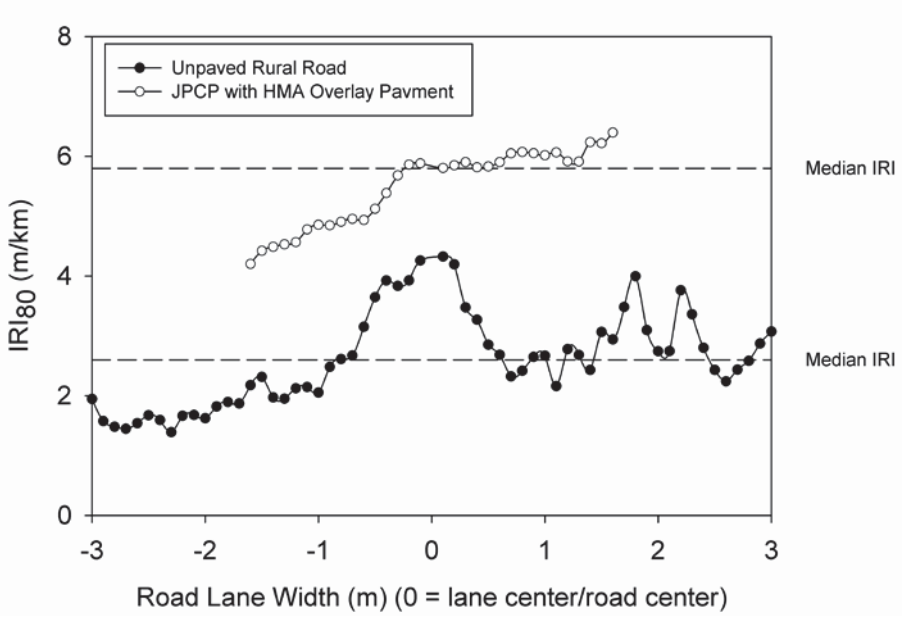

Figure 7. IRI versus width for both road sections included in the study.

To investigate the reason for low IRI values for the unpaved section, two profiles were transformed to frequency space, one profile corresponding to maximum IRI value and another profile corresponding to minimum IRI value. Each profile was decomposed into its constituent spectrum using the FFT (Figure 8). Presenting the results as height amplitude versus spatial frequency clearly shows different components of amplitude and frequency. The threshold for "smooth" was set at amplitude less than 0.4 mm. "Unsystematically rough" is defines as amplitude greater than 0.4 mm, but variable over a range of spatial frequencies. "Corrugation" is defined as amplitude with a central peak of greater than 0.7 mm and a spatial frequency of 1.5 to 2.5 (1/m). By examining the results this way, the source of roughness can be distinguished. And it can be seen that highest amplitudes are due to corrugations, however the quarter-car filter attenuates these frequencies, which results in substantially lower IRI values.

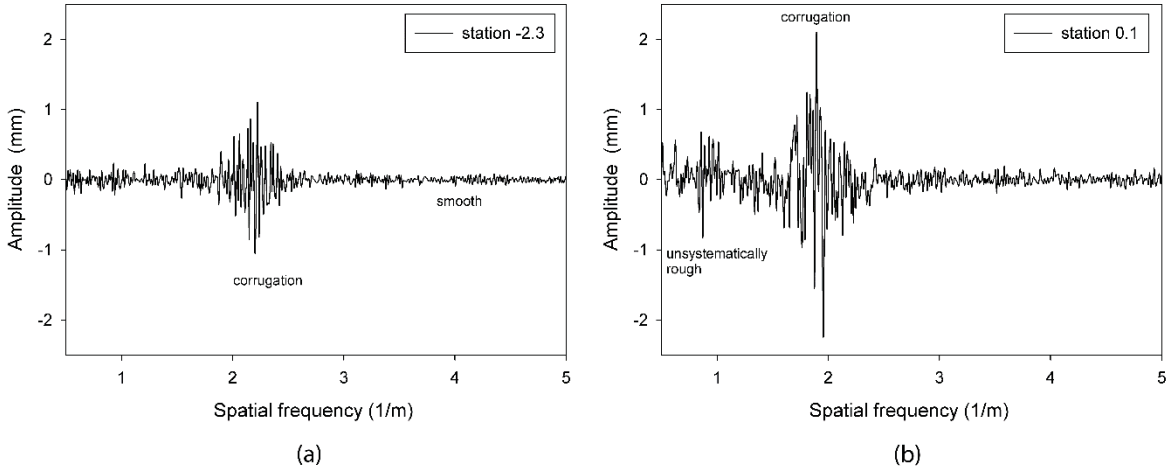

Figure 8. FFT for road profiles in (a) smooth surface with corrugations, (b) unsystematically rough surface with corrugations.

SUMMARY AND CONLUSIONS

This paper introduces the frame work of quantitative techniques for evaluating the surface roughness of paved and unpaved roads. Methods for evaluating the surface roughness can be set to two main categories, finite difference simulation and frequency domain analysis. The key findings from this research are:

- Terrestrial laser scanning is a promising technology to assess a range of surface conditions for unpaved roads.
- 2-D Surface roughness maps were developed using the information obtained from the laser scanner.
- Algorithms used in producing 2-D roughness maps are semi-automated, and further developments are expected to introduce fully automated algorithms that can process the data directly after scanning.
- IRI values are highly variable across the road section, thus it is hard to define the appropriate profile to be used as the representative profile.
- The proposed analysis technique can be used to identify localized rough features.
- Finite difference simulations are not suitable for short profiles.
- Filtering of the profiles in Fourier space as a tool to get the spatial roughness maps are more suitable compared to finite difference algorithms for analyzing short profiles, however wavelet analysis provide a more robust approach to analyze short profiles and identify localized features.
- At this stage, high resolution terrestrial laser scans are time consuming and require trained personnel; however, newer terrestrial laser scanners will be able to reduce the data acquisition time significantly due to faster scanning rates and longer ranges.

REFERENCES

ProVAL: Profile Viewing and Analysis Software, version 3.4 (2013),The Transtec Group, Inc. available from www.RoadProfile.com.

Al-Omari, B., and Darter, M. I. (1994). "Relationships between international roughness index and present serviceability rating." *Transportation Research Record*(1435).

Alhasan, A., White, D. J., and De Brabanter, K. (2015). "Continuous wavelet analysis of pavement profiles." *Automation in Construction*, Under review.

Alhasan, A., White, D. J., and De Brabanter, K. (2015). "Quantifying Unpaved Road Roughness from Terrestrial Laser Scanning." *2015 TRB 94th Annual Meeting*Washington, D.C.

Alhasan, A., White, D. J., and De Brabanter, K. (2015). "Spatial pavement roughness from stationary laser scanning." *International Journal of Pavement Engineering*, Under review.

Archondo-Callao, R. (1999). "Unpaved roads roughness estimation by subjective evaluation." *The World Bank*.

ASTM E950 / E950M-09 "Standard Test Method for Measuring the Longitudinal Profile of Traveled Surfaces with an Accelerometer Established Inertial Profiling Reference."ASTM International, West Conshohocken, PA, 2008, www.astm.org.

ASTM E1926-08 "Standard Practice for Computing International Roughness Index of Roads from Longitudinal Profile Measurements."ASTM International, West Conshohocken, PA, 2008, www.astm.org.

Berthelot, C. F., Podborochynski, D., Stuber, E., Prang, C., and Marjerison, B. (2008). "Saskatchewan Case Studies of Network and Project Level Applications of a Structural Asset Management System." *Proc., 7th International Conference on Managing Pavement Assets. TRB Committee AFD10 on Pavement Management Systems, Transportation Research Board, Washington, DC Retrieved October*, 2011.

Boggess, A., and Narcowich, F. J. (2009). *A first course in wavelets with Fourier analysis*, John Wiley & Sons.
Bogsjö, K., and Rychlik, I. (2009). "Vehicle fatigue damage caused by road irregularities." *Fatigue & Fracture of Engineering Materials & Structures*, 32(5), 391-402.
Brown, M., Mercier, S., and Provencher, Y. (2003). "Road maintenance with Opti-Grade®: Maintaining road networks to achieve the best value." *Transportation Research Record: Journal of the Transportation Research Board*, 1819(1), 282-286.
Chang, J.-R., and Chang, K.-T. (2006). "Application of 3 D laser scanning on measuring pavement roughness." *ASTM Journal of Testing and Evaluation*, 34(2), 83-91.
Chootinan, P., Chen, A., Horrocks, M. R., and Bolling, D. (2006). "A multi-year pavement maintenance program using a stochastic simulation-based genetic algorithm approach." *Transportation Research Part A: Policy and Practice*, 40(9), 725-743.
Daubechies, I. (1992). *Ten lectures on wavelets*, SIAM.
Fu, P., Lea, J. D., Lee, J. N., and Harvey, J. T. (2013). "Comprehensive evaluation of automated pavement condition survey service providers' technical competence." *International Journal of Pavement Engineering*, 14(1), 36-49.
Gao, H., and Zhang, X. (2013). "A Markov-Based Road Maintenance Optimization Model Considering User Costs." *Computer-Aided Civil and Infrastructure Engineering*, 28(6), 451-464.
Karamihas, S. M., Gillespie, T. D., Kohn, S. D., and Perera, R. W. (1999). "Guidelines for longitudinal pavement profile measurement: final report." 126p + appendices.
Kilpeläinen, P., Jaakkola, M., and Alanaatu, P. (2011). "Development of a control system for a multipurpose road repairing machine." *Automation in Construction*, 20(6), 662-668.
Kuo, C. M., Fu, C. R., and Chen, K. Y. (2011). "Effects of Pavement Roughness on Rigid Pavement Stress." *Journal of Mechanics*, 27(1), 1-8.
Lamptey, G., Labi, S., and Li, Z. (2008). "Decision support for optimal scheduling of highway pavement preventive maintenance within resurfacing cycle." *Decision Support Systems*, 46(1), 376-387.
Lin, J.-D., Yau, J.-T., and Hsiao, L.-H. (2003). "Correlation analysis between international roughness index (IRI) and pavement distress by neural network." *Proc., 82nd annual meeting in January, 2003*.
Liu, C., and Herman, R. (1999). "Road profile, vehicle dynamics, and ride quality rating." *Journal of transportation engineering*, 125(2), 123-128.
Murray, R. M., Li, Z., Sastry, S. S., and Sastry, S. S. (1994). *A mathematical introduction to robotic manipulation*, CRC press.
Namur, E., and de Solminihac, H. (2009). "Roughness of Unpaved Roads Estimation and Use as an Intervention Threshold." *Transp. Res. Record*(2101), 10-16.
Oijer, F., and Edlund, S. (2004). "Identification of transient road obstacle distributions and their impact on vehicle durability and driver comfort." *Vehicle System Dynamics*, 41, 744-753.
Ouyang, Y., and Madanat, S. (2004). "Optimal scheduling of rehabilitation activities for multiple pavement facilities: exact and approximate solutions." *Transportation Research Part A: Policy and Practice*, 38(5), 347-365.
Sayers, M. W., Gillespie, T. D., and Paterson, W. D. (1986). *Guidelines for conducting and calibrating road roughness measurements*.
Sayers, M. W., Gillespie, T. D., and Queiroz, A. (1986). "The international road roughness experiment. Establishing correlation and a calibration standard for measurements."
Sayers, M. W., and Karamihas, S. M. (1996). "Interpretation of road roughness profile data."
Sayers, M. W., and Karamihas, S. M. (1996). "Interpretation of road roughness profile data." University of Michigan Transportation Research Institute.

Soria, M., and Fontenele, E. (2003). "Field Evaluation of Method for Rating Unsurfaced Road Conditions." *Transportation Research Record: Journal of the Transportation Research Board*, 1819(-1), 267-272.

Steinwolf, A., Giacomin, J., and Staszewski, W. (2002). "On the need for bump event correction in vibration test profiles representing road excitations in automobiles." *Proceedings of the Institution of Mechanical Engineers, Part D: Journal of Automobile Engineering*, 216(4), 279-295.

Swan, M., and Karamihas, S. M. (2003). "Use of a ride quality index for construction quality control and acceptance specifications." *Transportation Research Record*(1861), p. 10-16.

Tsai, Y. J., Wu, J., Wang, Z., and Hu, Z. (2010). "Horizontal roadway curvature computation algorithm using vision technology." *Computer-Aided Civil and Infrastructure Engineering*, 25(2), 78-88.

Tsunokawa, K., and Schofer, J. L. (1994). "Trend curve optimal control model for highway pavement maintenance: Case study and evaluation." *Transportation Research Part A: Policy and Practice*, 28(2), 151-166.

Walker, D., Entine, L., and Kummer, S. (2002). "Gravel-Paser Manual: Pavement Surface Evaluation and Rating." Wisconsin Transportation Information Center.

Woll, J. H., Surdahl, R. W., Everett, R., and Andresen, R. (2008). "Road Stabilizer Product Performance: Seedskadee National Wildlife Refuge." Federal Highway Administration.

Zalama, E., Gómez-García-Bermejo, J., Llamas, J., and Medina, R. (2011). "An effective texture mapping approach for 3D models obtained from laser scanner data to building documentation." *Computer-Aided Civil and Infrastructure Engineering*, 26(5), 381-392.

Zhang, C. (2009). "Monitoring the Condition of Unpaved Roads with Remote Sensing and Other Technology." Geographic Information Science Center of Excellence, South Dakota State University.

Zhang, C., and Elaksher, A. (2012). "An Unmanned Aerial Vehicle-Based Imaging System for 3D Measurement of Unpaved Road Surface Distresses1." *Computer-Aided Civil and Infrastructure Engineering*, 27(2), 118-129.

Autonomous Construction of Separated Artifacts by Mobile Robots Using SLAM and Stigmergy

Hadi Ardiny, Stefan Witwicki, and Francesco Mondada
Robotic Systems Laboratory
École Polytechnique Fédérale de Lausanne
Lausanne 1015, Switzerland
Email: hadi.ardiny@epfl.ch, stefan.witwicki@epfl.ch, francesco.mondada@epfl.ch

ABSTRACT

Autonomous mobile robots equipped with arms have the potential to be used for automated construction of structures in various sizes and shapes, such as houses or other infrastructures. Existing construction processes, like many other additive manufacturing processes, are mostly based on precise positioning, which is achieved by machines that have a fixed mechanical link with the construction and therefore relying on absolute positioning. Mobile robots, by nature, do not have a fixed referential point, and their positioning systems are not as accurate as fixed-based systems. Therefore, mobile robots have to employ new technologies and/or methods to implement precise construction processes.

In contrast to the majority of prior work on autonomous construction that has relied only on external tracking systems (e.g., GPS) or exclusively on short-range relative localization (e.g., stigmergy), this paper explores localization methods based on a combination of long-range self-positioning and short-range relative localization for robots to construct precise, separated artifacts in particular situations, such as in outer space or in indoor environments, where external support is not an option.

Achieving both precision and autonomy in construction tasks requires understanding the environment and physically interacting with it. Consequently, we must evaluate the robot's key capabilities of navigation and manipulation for performing the construction in order to analyze the impact of these capabilities on a predefined construction. In this paper, we focus on the precision of autonomous construction of separated artifacts. This domain motivates us to combine two methods used for the construction: 1) a self-positioning system and 2) a short-distance relative localization. We evaluate our approach on a miniature mobile robot that autonomously maps an environment using a simultaneous localization and mapping (SLAM) algorithm; the robot's objective is then to manipulate blocks to build desired artifacts based on a plan given by a human. Our results illuminate practical issues for future applications that also need to integrate complex tasks under mobile robot constraints.

Keywords: autonomous construction—miniature mobile robot—self-positioning system—precise construction—unknown environments

Proceedings of the 2015 Conference on Autonomous and Robotic Construction of Infrastructure, Ames, Iowa.

I. INTRODUCTION

Construction automation is an interesting field focused on applying automating processes to reduce the cost of construction and/or to increase operational efficiency. Developments in robotics sciences have recently led to the use of various robotic platforms to achieve construction automation objectives, although fully automated construction is still a dream of civil engineers. Robotic developments have shown that robots could potentially perform construction tasks where human presence is impossible, undesirable, or intensively expensive, for instance, construction in hazardous areas after natural or man-made disasters such as earthquakes and nuclear accidents; construction under difficult physical conditions such as undersea or outer space locations; and construction where in area that are not readily accessible to humans or that require an initial structure to prepare the environment for human arrival. Robots can be used to build these structures for particular situations in the autonomous mode without explicit human intervention or with some levels of planning interaction conducted with a human supervisor.

Generally, a robot performing autonomous construction has to adapt itself to the sensed environment, make decisions regarding the execution of its task, and replan when its task is not executable. Mobile robots represent one type of robotic system that could be used for construction automation. Applying mobile robots to construction opens new approaches in this field. For instance, building large structures without being confined by dimensions is a challenge for current technologies; for example, we might need huge and expensive fixed-based fabricating systems (e.g., 3D printers) to build giant structures. Capabilities of mobile robots, however, allow them to create objects without fixed-base system constraints (e.g., size of the printer's frame constraint). Similar to social insects, such as ants, a group of mobile robots can work cooperatively, as a collective system, to efficiently build large-scale.

In contrast to these advantages, mobile robots, by nature, do not have a fixed referential point and their positioning systems are not as accurate as fixed-based systems. Existing construction processes, like many other additive manufacturing processes, are mostly based on precise positioning, which is achieved by machines that have a fixed mechanical link with the construction and rely on absolute positioning. Therefore, mobile robots have to compensate for this weakness with new technologies and/or methods to supply precision for construction processes. Although equipping robots with external tracking systems (e.g., GPS, camera) provides an accurate positioning system, but we aim to implement and study localization methods based on self-positioning system to autonomously handle construction tasks, especially where external tracking systems is are difficult to access and are expensive (e.g., undersea). On the other hand, the accuracy of self-positioning system is not sufficient to handle construction processes; therefore, we aim to combine it with short-range relative localization to provide the required precision for construction of structures spatially separated from one another, which we refer to here as separated artifacts.

In this paper, our goal is to develop a construction system by which robots are able to build separated artifacts. We evaluate our approach with a miniature autonomous mobile robot and simple blocks in unknown environments. The robot's objective is to build the artifacts using both the simultaneous localization and mapping algorithms (SLAM) and stigmergy based on a human-prescribed blueprint. In fact, it employs SLAM using the LIDAR scanner to autonomously map an environment and determine the current robot position. The robot's end effector is equipped to many IR-sensors that allow it to sense previously placed blocks in order to place subsequent blocks; this approach is commonly referred to as stigmergy [1].

In Section II, related work is discussed. The scenario and assumptions, robot hardware, and control are provided in Section III. The results and discussion are presented in Section IV. Finally, in Section V, we conclude for this study.

II. RELATED WORKS

In this section, we are primarily reviewing research that employs mobile robots for autonomous construction based on positioning systems, robot platforms, and materials. Obviously, precise positioning systems are necessary for most systems to support construction processes. At present, an external localization system could be employed to provide accurate systems for construction. In the research conducted at ETH Zurich, four quadcopters are exploited to construct a brick-like tower. They benefit from an external real-time camera system to guide robots to pick up and deposit objects according to the given blueprint [2]. Lindsey *et al.* [3] used a team of quadcopters to assemble the cubic structures with particular self-assembling rods . The VICON motion tracking system is used to estimate the position and orientation of the picked objects and aerial vehicles states. It provided position feedback at 150 Hz with marker position accuracy on the order of a millimeter. Moreover, VICON is used by ground robots to build roofed structures [4].

Another general external system is the GPS used by a robotic excavator with centimeter resolution allowing them to determine position accurately and then to control the motion of the robots [5]. In [6], the ROCCO robot was developed to assemble heavy blocks in industrial buildings with standardized layouts. It was equipped with digital angular encoders and an external global position sensor (telemeter) correct error. In [6], a method was demonstrated in simulation by which robots are able to build 2D structures of desired shapes by blocks. A robot acts as a stationary beacon to help other robots find its position. In [7], robot placed blocks of alternating color along a straight line starting with a pre-placed seed block located underneath a beacon. Although using external system improves the positioning system capability, many additional localization devices are required, which might be impossible or very expensive to provide, for example, in outer space or undersea construction. In contrast to these works, the robot is completely autonomous in our work and does not rely on any motion-capture systems or external localization systems.

However, some robots applied short-range relative localization for construction. Werfel *et al.* [8] present 3D collective construction in which enormous numbers of autonomous robots build large-scale structures. They employed a ground mobile robot that was inspired by activity of termites. Robots climb on the structure to drop passive solid blocks on top of it. They just use six active infrared (IR) sensors to recognize white stripes on the blocks and then determine their path and final destination. Novikov *et al.* [9] have built 3D shape structures by using deposition amorphous material with mobile heads. This method allows an object to be printed independent from its size of the object.

Stroupe *et al.* [10] present construction by two platform robots SRR and SRR2K in an outdoor environment. Each rover is holonomically equipped with a forward-facing stereo pair of cameras and a four degree-of-freedom arm. A triple-axis force-torque sensor on the gripper helps the rover maintain coordination for transporting and placing rods. This model provides high-precision manipulator placement by comparing the observed position of beam markers on the end effector with the obtained kinematics position of the end effector.

In some research, self-alignment methods have been used to tackle substance alignment and attachment restrictions. For instance, bricks are made from expanded foam, with physical features to achieve self-alignment and magnets for attachment [11]. In [12], self-alignment cubic modules are used to build structures. The special assembler robots manipulate and transport these modules. In [13], a novel robot used bidirectional geared rods and connectors to build a truss structure. In conclusion, using only the short-range relative localization limits construction to a local place because robots need to look at the local configuration of the building material to determine where to add additional materials.

Magnenat *et al.* [14] used a miniature autonomous robot with a magnetic manipulator to grasps ferromagnetic self-alignment blocks. This robot also has the LIDAR and camera on top. It used the odometry and laser data to perform SLAM and employed the front camera and proximity sensors to provide the required data for dropping blocks. The goal of this research was to use ten blocks to build a simple tower. We advance this research by studying the precision of using both a short-range relative localization and a self-positioning system for separated artifacts.

III. SYSTEM DESCRIPTION

A. Scenario and Assumptions

As overviewed in the Introduction, the goal of this experiment is to build separated artifacts based on a blueprint by a human in an unknown environment. We assume that the initial position of the robot is also the location of a block repository. We put a new block at the repository for each step of construction. The robot has to detect the block and align itself with respect to the block to able to pick up the block at the correct position of gripper.

The arena is a 200 cm × 100 cm rectangle with a flat surface that contains few obstacles. Note that the environment is unknown for the robot, and SLAM is used to inform the robot of its position and to map the environment for path planning as well. The artifacts, as illustrated later, are composed of simple polystyrene blocks with an attached stripe of ferromagnetic metal on the lower part of the body (Figure 1). Each block is 6 cm in length, 6 cm in width, and 18 cm in height, and it weighs approximately 20 g. The size and weight of the block are chosen to satisfy the requirements of the robot's gripper and the LIDAR.

After grasping the block, the robot moves toward the destination point. The path-planning algorithm determines the global path to the destination. It also sets the local path planning during its movements to avoid collision with dynamic obstacles and to correct the path based on the robot's improved position. The first block of the artifact will be dropped after the robot fine-tunes its position using the accurate movement behavior.[1] The robot returns and takes a new block from the repository. Now, the robot is ready to drop the second block of the artifact. The robot drops the second block beside the first block using stigmergy. In this section, we explained the construction scenario and assumptions. In the next sections, we first describe the robot hardware and then provide the details of the control system, including low-level behaviors and control architecture.

[1] See section 3-3-2

Figure 1. Polystyrene blocks are used for the experiments.

Figure 2. The MarXbot consists of the gripper, LIDAR, computer board, base modules.

B. Robot platform

For the experiment, we used a miniature and modular robot called marXbot [15] (Figure 2). The robot is 17 cm in diameter and 18 cm in height. It consists of four modules as follows:

Base: The non-holonomic base has 2 degrees of freedom (DOF), a 38Wh lithium polymer battery, and 24 proximity sensors.

Gripper: The 3 DOF magnetic manipulator consists of a magnetic switchable device to grasp ferromagnetic objects. This module has 20 proximity sensors for the alignment usage.

Computer board: This module includes the main computer based on a 533MHz Freescale i.MX31 with 128MB of RAM and running LINUX.

LIDAR: The 360° laser distance scanner (Neato LIDAR < $100) perceives walls and obstacles.

C. Control system

I) Control architecture

The control architecture, shown in Figure 3, consists of several layered modules. At the top, the *builder planner* serves to execute an overall construction of separated artifacts by generating a sequence of high-level sub-goals. These sub-goals either take the form of target poses for robot movement, which are delegated to the *navigation* block, or block manipulation sub-goals (such as *pickup* and *place*), which are delegated to the *middle planner*.

Navigation is implemented through a collection of ROS nodes, including navigation (Move_base[2]) and SLAM (Hector_mapping[3]) packages. The SLAM package receives the data from the LIDAR to map the environment and localize the robot. The navigation package obtains the map and positioning information from SLAM to direct and set the reliable paths for the mobile robot from the current position to the goal position. To physically move the robot, *navigation* in turn invokes low-level behaviors that have been pre-programmed using the ASEBA software architecture [16], which runs directly on the robot's microcontrollers.

The *middle planner,* implemented using state-of-the-art AI planning technologies [17], renders the robot fully autonomous in its manipulation of blocks in the environment. For each manipulation goal (pickup, drop, place-adjacent-to), the robot accesses a (pre-computed) conditional plan that iteratively selects among low-level task executions (e.g., approach-to-within-manipulation-distance, align-gripper-angle, grasp-block). Each of these low-level tasks is implemented as a finite state controller that, at 5Hz, senses using the gripper infrared and actuates the treel[4] and gripper motors. Due to sensory inaccuracies and environmental imperfections, the low-level tasks are not deterministic in their effects. For instance, a brief mis-measurement of infrared distances caused by fluctuations in ambient lighting could cause the align-gripper-angle controller to over-rotate the gripper such that the robot loses sight of the block that it is aligning with. When such unintended effects occur, the robot's conditional plan gracefully recovers by selecting the next appropriate task. In essence, the conditional plan composes a complex and dynamic sequences of tasks that is theoretically guaranteed [18] to eventually bring the robot to its manipulation goal.

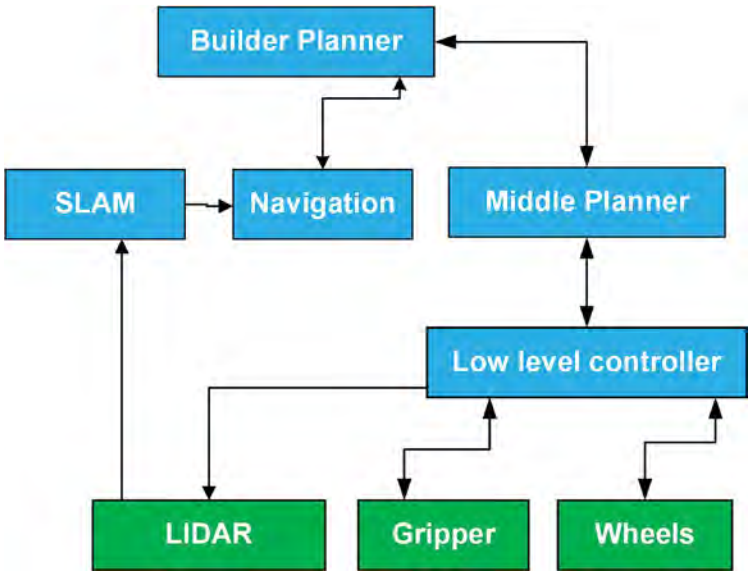

Figure 3. Control architecture in which green and blue boxes represent hardware and software layers, respectively.

[2] Move_base is a 2D navigation stack that receives information from sensors and a goal pose and then directs the mobile base by determining safe speed and reliable paths.

[3] Hector_mapping is a SLAM algorithm using LIDAR systems such as the Hokuyo UTM-30LX. The system has been used on unmanned ground robots, unmanned surface vehicles.

[4] Treel refers to a combination of a wheel and a track.

II) Low-level behaviors

Pick-up: The pick-up behavior has to accurately grasp blocks because a misaligned block will add errors to all subsequent operations. As illustrated in Figure 4, the middle planner generates a sequence of movements. At the beginning, the robot turns to face the repository. It uses both the ROS navigation and accurate movement behavior to align itself at the right angle; then it starts to find the nearest block (1). The robot then uses front infrared sensors of the gripper to tune the distance in respect to the blocks (2). Next, it rotates 90 degrees rightward, and the gripper rotates in the opposite direction (3), which situation helps the robot align itself laterally. Using the front infrared sensors of the magnetic gripper also helps the robots to align the block at the center of the gripper (4). When the block is centered, the robot performs a 90-degree leftward rotation while the gripper rotates in the opposite direction (5). It then moves forward and rotates a few degrees at a time to touch the block at the corner of the magnet position (6). When the robot touches the blocks, it grasps it and lifts up the gripper; this time the block is well aligned (7).

Traveling: This behavior consists of raising the gripper in order that the attached block and gripper do not interfere with the robot movements and SLAM.

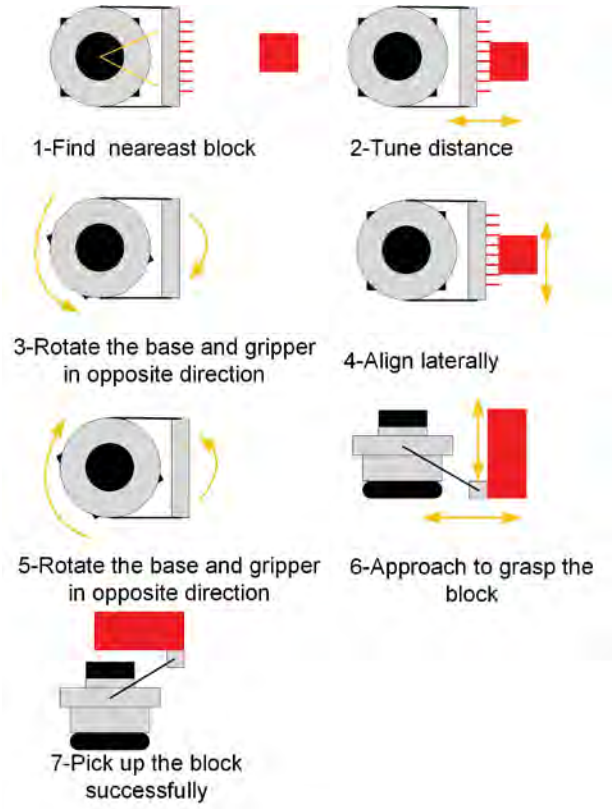

Figure 4. The movement sequence to pick up a block.

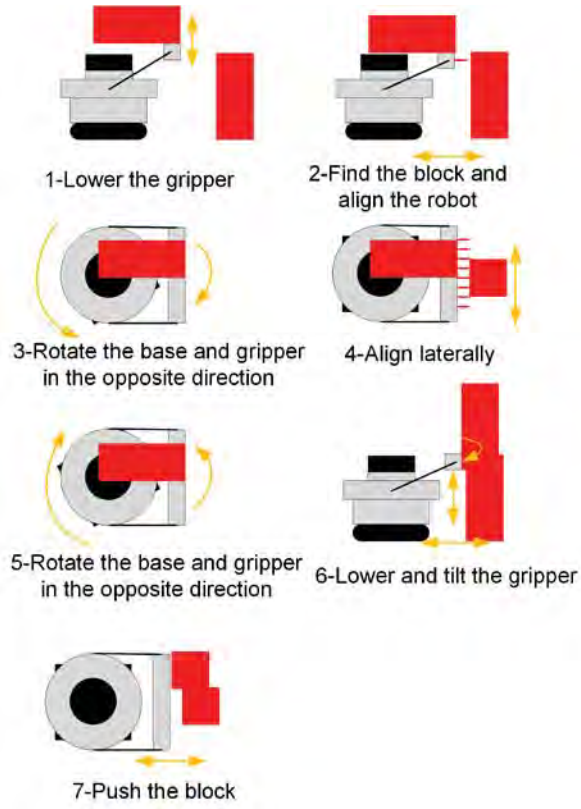

Figure 5. The movement sequence to drop a new block adjacent to a placed one.

Accurate movement: This behavior occurs in two modes to move the robot precisely. When the robot approaches a destination point, this behavior moves the robot to put it in the precise

position using a PID controller. In the first mode, it rotates and moves to correct its position in the X axis. The robot then rotates 90 degrees and moves to correct its position in the Y direction. Finally, it rotates to reach the goal yaw angle. In the second mode, the robot only rotates to correct its yaw angle. Depending on the situation in the planner request, the robot will use either the first or second mode.

Drop/Place-Adjacent-To: This behavior consists of dropping a block either in the first place of the artifact or directly adjacent to existent blocks. To build an artifact, the robot has to drop its first block. Thus, it simply lowers the gripper after finding the precise position and then disengages its magnetic switchable device. It then lifts its manipulator slightly and moves back for a short distance. For the remaining blocks of the artifact, the robot goes toward the artifact (1) and scans for it using the magnetic gripper's IR sensors. The robot computes the distance to the artifact and moves accordingly to tune its position (2). Then it rotates 90 degrees while it rotates the gripper in the reverse direction with the same angular speed. In this position (3), the robot aligns itself laterally and then finds the left edge of the placed block to drop the new one exactly beside it (4). The robot performs a 90-degrees leftward rotation while the gripper rotates in the opposite direction (5). It then moves forward, lower, and rotates the gripper by a few degrees at a time to avoid collision with the other blocks (6). It then lowers its gripper slightly and moves back a short distance. Finally, the robot tilts the gripper and moves forward to push and line up the block (7).

IV. RESULTS AND DISCUSSTION

We employed the marXbot for the two types of experiments. First, the robot places three blocks based on given positions to study the precision of SLAM. In the second type, we employed both stigmergy and SLAM to build several separated artifacts, each made up of composed by several blocks. Five trials were carried out for each type of experiment. Figure 6 illustrates the construction of artifacts through some snapshots at the different steps. After finishing artifact construction, we took a photo to measure construction performance. We extracted the red color through image-processing methods to compare the performance of each experiment with the ideal block arrangement. In the ideal block arrangement, we assumed SLAM and stigmergy were perfect, and artifacts were being built exactly based on the given map. Using this model, we can measure the translational and rotational errors of the blocks on the plane as illustrated in Figure 7. The graphs in Figure 9 and Figure 10 show these absolute errors for the two experiments. In the first experiment, the robot only drops blocks B1, B4, B8 (the first block of each artifact) using SLAM. The important error of placement based on SLAM, of one third of the block size, shows that we cannot use this positioning technique to build artifacts made of several blocks. If the robot employs only SLAM, the important positioning error will cause collisions among blocks or gaps between blocks of the artifacts. Nevertheless, the robot can find the approximate position of construction and then apply other methods (e.g., stigmergy) to successfully accomplish the construction.

For stigmergy, the robot uses infrared sensors to align itself with respect to the blocks that are already part of the artifact. Because the artifacts are not fixed to the ground, the dropping operation may cause a displacement of the existing blocks. As illustrated in Figure 10, the average errors of stigmergy for blocks B4 and B8 (first block of the second and third artifacts) are different from the errors measured after using only SLAM (see Figure 9). This shows that the sigmergy action moved these blocks. This means, for instance, that when the robot pushed the block to align it, it also pushed previously-placed blocks because of the errors in stigmergy positioning. Indeed, if the robot could apply a perfect stigmergy, we would expect to see the same precision for other blocks of the artifact as we saw for the first block.

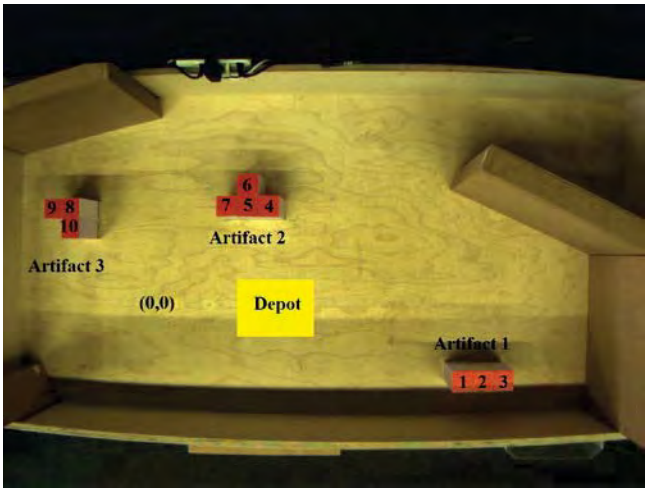

Figure 6. Ideal arrangement of the blocks is shown for the three artifacts. A comparison of built artifacts with this ideal arrangement provides the construction performance results. The robot starts from the (0,0) point to take a block from the repository. The numbers on the blocks point to the numerical order for the construction.

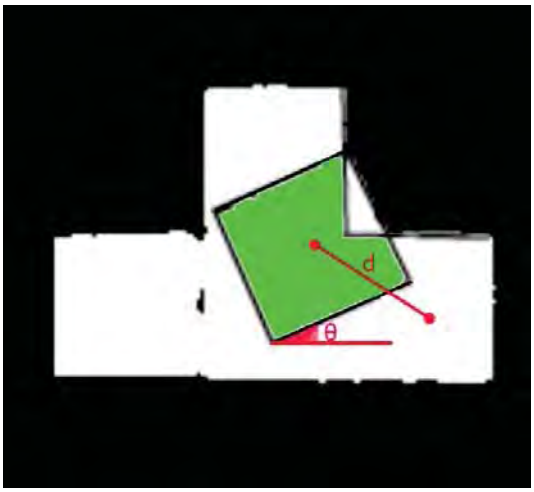

Figure 7. The processed image of the second artifact and measuring translational and rotational errors for the fourth block; *d* shows the distance between center of the squares, and *θ* shows the angle between the lower edges of the squares. Green color also depicts the overlap area between the fourth block and the second artifact.

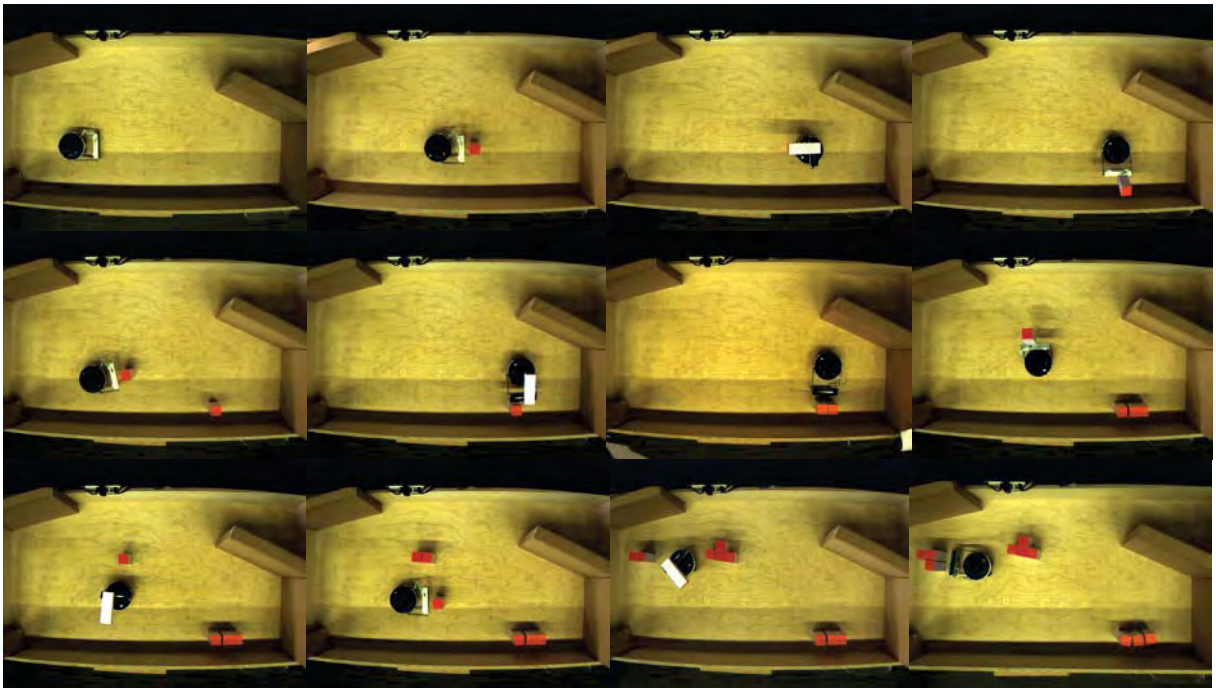

Figure 8. Image sequence of artifact construction

Overall, stigmergy could improve or weaken the precision. If the artifacts were fixed to the ground, the robots could be able to use force sensing to push the blocks without influencing the precision of the next dropping steps. Moreover, the minor difference of the translational and rotational blocks errors for each artifact shows that the building artifacts are not sensitive to the final shape or to the number of blocks used in these experiments.

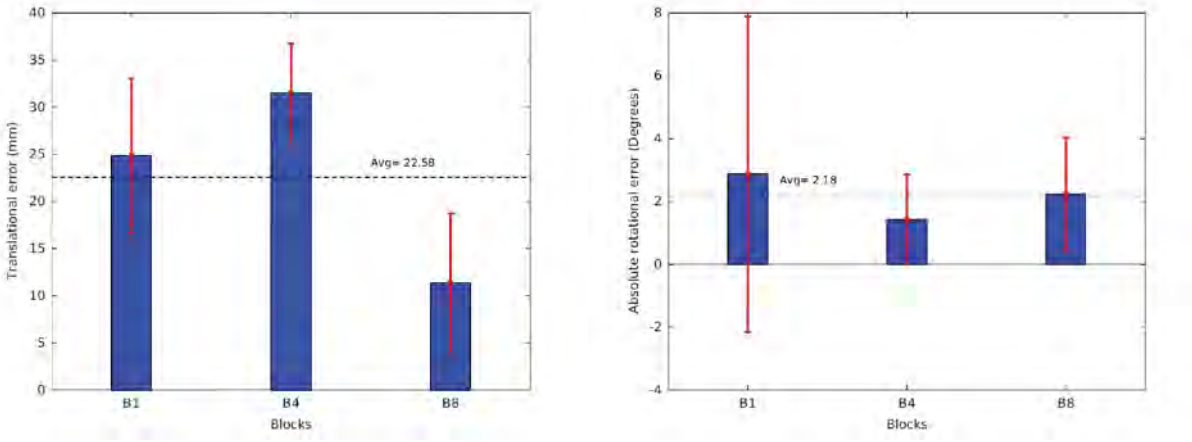

Figure 9. The left graph shows the translational error and the right graph shows the rotational error when the robot drops the first, fourth, and eighth blocks using just SLAM.

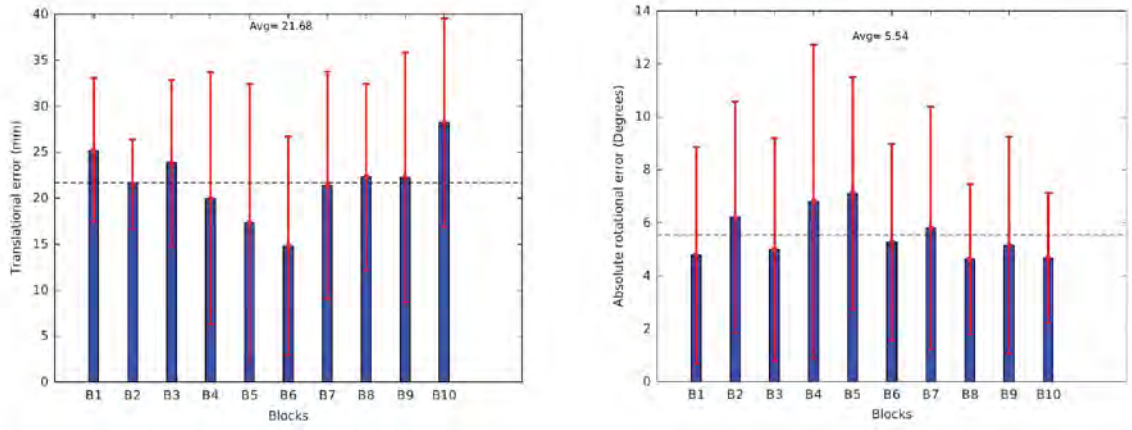

Figure 10. The left graph shows the translational error, and the right graph shows the rotational error when the robot is supposed to build the artifact with SLAM and stigmergy.

Finally, we measured the surface of each ideal artifact that is occupied by blocks placed by the robot. Ideally, the overlap percentage between the blocks and the given blueprint has to be a 100%. Figure 11 shows the overlap percentage for two construction types: single separated blocks or separated multiple-block artifacts. Note the average percent of the single-block construction is 57.88%, but it is 73.53% in artifact construction. This increase of performance does not mean that multiple-blocks artifacts are placed more precisely, because adjacent blocks can compensate for the positioning error for the global covering of the artifact surface. This

increase of performance only shows that stigmergy enables the construction of more coherent artifacts.

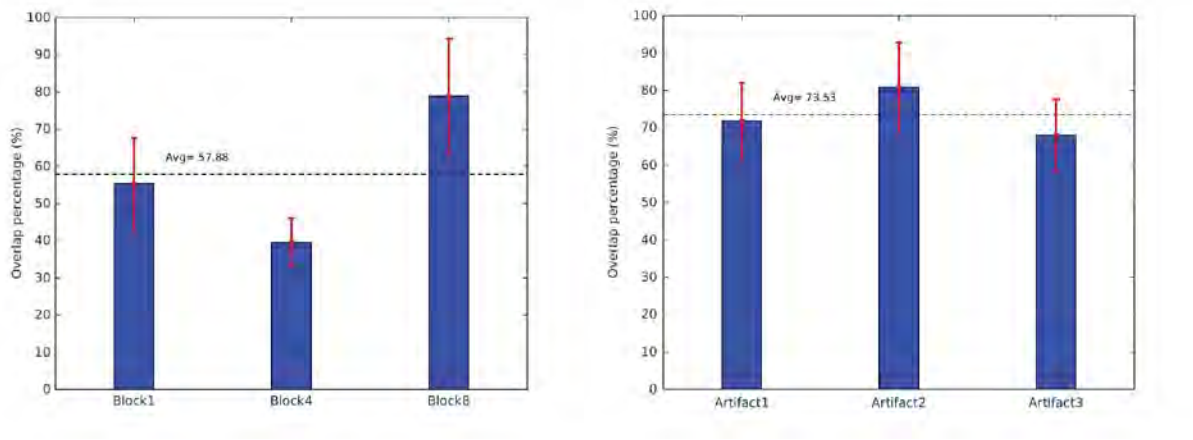

Figure 11. The left graph depicts the overlap percentage for dropping blocks based on the using SLAM, and the right graph depicts the overlap percentage for building the artifact based on using SLAM and stigmergy.

This section provided an analysis of the precision achieved by a mobile robot in building separated artifacts using SLAM and stigmergy. The SLAM algorithm was used as a localization and mapping method by a miniature mobile platform in an unknown environment. In our experiment, we have a translational error of about *21 mm* (one-hundredth of the diagonal of the environments) in a static environment using a miniature robot with a low-cost LIDAR. It is difficult to evaluate how this error will scale in a real environment because the SLAM accuracy depends on many factors; environment dimensions will clearly impact precision, as larger distances will generate larger measurement errors. The quality and quantity of landmarks also impacts the estimation of the position by the SLAM algorithm. A dynamic environment can also cause a loss of precision, as dynamic obstacles can hide interesting landmarks. Finally the quality of the sensor for distance measurement impacts the whole system directly. Obviously, there is a need to further develop the sensory system and SLAM algorithms for complex artifacts in real and large environments. Despite a lot of progress in the past decades in the SLAM field, high-precision applications are still challenging. For the time being, SLAM could help to find approximate construction sites and then the robot could use other methods to follow the construction, such as stigmergy as used in this research.

In this research, we applied stigmergy based on a pure IR-sensing system while the mechanical stigmergy can be more suitable to place the blocks. Today, companies are designing and manufacturing prefabricated components to increase construction speed and efficiency. New prefabricated components could be designed and made for robotic use in automated construction. For example, components with male–female connectors allow for automatic assembly in a more robust way [11]. Developing construction methods based on mechanical stigmergy or using force-sensing systems could provide a new way to place components in a more reliable and precise way.

Autonomous construction is also a complex application in which many failures can occur. These failures can propagate from one step to another, for instance, if the robot incorrectly grasps the

block, it could destroy the built structures. Thus, it is important to detect and correct faults. We performed fault detection for middle planner, which is responsible for the planning low-level behaviors (pick up, drop, place-adjacent-to); however, we need to improve the builder planner to take high-level decisions for failures caused during construction.

V. Conclusion

This paper presents an autonomous construction system for building separated artifacts with simple blocks. We used a miniature mobile robot that autonomously mapped an environment using a SLAM algorithm and then manipulated blocks to build desired and separated artifacts. Our approach was based on the combination of two methods: a self-positioning system (SLAM) to find the construction place in an unknown environment and stigmergy to build coherent artifacts. The control system allowed the robot to perceive and pick up the block, move toward the construction place in an unknown environment, and drop the block based on a human-prescribed blueprint. We observed that, even in an ideal environment, positioning using SLAM is not sufficiently precise. This task still requires improvement in sensing technology. We also observed that stigmergy allow the creation of coherent constructions. The process analyzed in this paper, based on mobile blocks and sensing stigmergy, could be improved by having blocks fixed when dropped and employing mechanical stigmergy.

As a result, in future works, we are focusing on developing robot hardware and improving the SLAM algorithm. We also plan to develop stigmergy and use force-sensing systems for mechanical stigmergy. Thanks to stigmergy and hardware development, robots could be used to build complex artifacts such as a multi-layer wall with prefabricated components.

REFERENCES

[1] G. Theraulaz and E. Bonabeau, “Coordination in distributed building,” *Science*, vol. 269, no. 5224, pp. 686–8, Aug. 1995.

[2] J. Willmann et al. “Aerial robotic construction towards a new field of architectural research,” *Int. J. Archit. Comput.*, vol. 10, no. 03, pp. 439–460, 2012.

[3] Q. Lindsey, D. Mellinger, and V. Kumar, “Construction of Cubic Structures with Quadrotor Teams,” in *Robotics: Science and Systems*, 2011.

[4] S. Wismer, G. Hitz, M. Bonani, A. Gribovskiy, and S. Magnenat, “Autonomous construction of a roofed structure: Synthesizing planning and stigmergy on a mobile robot,” in *IROS*, 2012, pp. 5436–5437.

[5] D. A. Bradley and D. W. Seward, “The Development, control and operation of an autonomous robotic rxcavator,” *Intell. Robot. Syst.*, no. 138257, pp. 73–97, 1998.

[6] E. Gambao, C. Balaguer, A. Barrientos, R. J. Saltarén, and E. A. Puente, “Robot assembly system for the construction process automation,” in *International Conference on Robotics and Autonomation*, April 1997, pp. 46–51.

[7] J. Wawerla, G. S. Sukhatme, and M. J. Mataric, “Collective construction with multiple robots,” in *International Conference on Intelligent Robots and Systems*, October 2002, pp. 2696–2701.

[8] J. Werfel, K. Petersen, and R. Nagpal, “Distributed multi-robot algorithms for the TERMES 3D collective construction system,” *RSJ Int. Conf. Intell. Robot. Syst. (IROS),*, 2011.

[9] P. Novikov, S. Maggs, D. Sadan, S. Jin, and C. Nan, “Robotic positioning device for three-dimensional printing,” *CoRR*, vol. abs/1406.3, pp. 1–14, 2014.

[10] A. Stroupe et al. “Sustainable cooperative robotic technologies for human and robotic outpost infrastructure construction and maintenance,” *Auton. Robot.*, vol. 20, no. 2, pp. 113–123, Apr. 2006.

[11] J. Werfel, K. Petersen, and R. Nagpal, “Designing collective behavior in a termite-inspired robot construction team,” *Science*, vol. 343, no. 6172, pp. 754–8, Mar. 2014.

[12] Y. Terada and S. Murata, “Automatic modular assembly system and its distributed control,” *I. J. Robot. Res.*, vol. 27, no. 3–4, pp. 445–462, Mar. 2008.

[13] F. Nigl, S. Li, J. Blum, and H. Lipson, “Structure-reconfiguring robots: autonomous truss reconfiguration and manipulation,” *IEEE Robot. Autom. Mag.*, vol. 20, no. 3, pp. 60–71, 2013.

[14] S. Magnenat, R. Philippsen, and F. Mondada, “Autonomous construction using scarce resources in unknown environments - Ingredients for an intelligent robotic interaction with the physical world.,” *Auton. Robot.*, vol. 33, no. 4, pp. 467–485, 2012.

[15] M. Bonani et al. “The marXbot, a miniature mobile robot opening new perspectives for the collective-robotic research,” in *2010 IEEE/RSJ International Conference on Intelligent Robots and Systems*, 2010, pp. 4187–4193.

[16] S. Magnenat and P. Rétornaz, “ASEBA: a modular architecture for event-based control of complex robots,” *IEEE/Asme Trans. mechatronics*, vol. 16, no. 2, pp. 321–329, 2011.

[17] S. Witwicki and F. Mondada, “Circumventing robots’ failures by embracing their faults: a practical approach to planning for autonomous construction,” in *The 29th AAAI Conference on Artificial Intelligence*, 2015, pp. 4298–4299.

[18] C. Muise, V. Belle, and S. A. McIlraith, “Computing contingent plans via fully observable non-deterministic planning,” in *The 28th AAAI Conference on Artificial Intelligence*, 2014, pp. 2322–2329.

A Comparison of Automated and Semi-Automated Compressed Earth Block Presses Using Natural and Stabilized Soils

Jedadiah F. Burroughs
Geotechnical and Structures Laboratory
US Army Engineer Research and Development Center
3909 Halls Ferry Road
Vicksburg, MS 39180
Jedadiah.F.Burroughs@usace.army.mil

Todd S. Rushing
Geotechnical and Structures Laboratory
US Army Engineer Research and Development Center
3909 Halls Ferry Road
Vicksburg, MS 39180
Todd.S.Rushing@usace.army.mil

C. Phillip Rusche
Geotechnical and Structures Laboratory
US Army Engineer Research and Development Center
3909 Halls Ferry Road
Vicksburg, MS 39180
Phillip.Rusche@usace.army.mil

ABSTRACT

This study compared the use of two compressed earth block press machines and the properties of compressed earth blocks made with natural and stabilized soils. The Vermeer BP714 Block Press uses a hydraulically driven, two-stage compression process to produce compressed earth blocks with consistent density and dimensions similar in shape to concrete masonry units. The AECT Impact 2001A uses a hydraulically driven, fully automated single stage compression process to produce modular compressed earth blocks with simple prismatic geometries at a rate of 240 blocks per hour. This study focused on the advantages and disadvantages of using each press, as well as the compressive strength development of compressed earth blocks made with selected soils and soil stabilizers. Recommendations for the suitability of each machine for different soil conditions are given.

Key words: adobe—compressed earth block—construction materials—hydraulic press—soil stabilization

PROBLEM STATEMENT

It is estimated that one third of the world's population lives in earthen structures. For many centuries, adobe blocks have been used as the main earthen construction element. The process for making adobe blocks is a time-consuming and inefficient process that can last in excess of three weeks (Dominguez 2011). In an effort to more efficiently study this traditional

Proceedings of the 2015 Conference on Autonomous and Robotic Construction of Infrastructure, Ames, Iowa.

construction material, the US Army Engineer Research and Development Center has used compressed earth blocks (CEBs) as surrogates for adobe blocks.

Compressed earth blocks are earthen construction elements produced using a mechanized hydraulic ram to compact soil into a mold. The soil is molded in a relatively dry state (generally less than 10% moisture content) resulting in blocks that are strong and weather resistant. Since CEBs have very consistent geometry, they can be readily stacked to form walls of structures. Doors, windows, fixtures, and utilities can all be incorporated in similar ways to masonry construction. Earthen structures made using CEBs are inexpensive, versatile, and energy efficient. For these reasons, CEBs have become a popular construction technique in disadvantaged areas. CEB machines are commercially available to produce blocks in a range of sizes and shapes.

One example is the AECT Impact 2001A. This automated machine produces CEBs at a rate of four blocks per minute that are 12-inches long, 6-inches wide, and between 2-inches and 4.5-inches tall. Each block weighs approximately 15 to 20 lbs depending on soil type, block thickness, moisture content, etc. Soil is loaded into a hopper situated above a single stage compression ram. All soil particles must be finer than ½ inch to pass the screen covering the hopper. Soil is manually loaded into the hopper by means of buckets, shovels, etc. A full hopper will produce between eight and nine blocks. Once soil is loaded, the diesel engine is started and block production is initiated by pressing the start button. Soil is dropped from the hopper into a rectangular cavity that sets the length and width dimensions at 12-inches and 6-inches respectively. The depth of the cavity is determined by the position of a hydraulic ram and is set by the user. Once soil has been loaded, the cavity is covered by an automatically sliding tray and pressed by a vertical ram. The end of the compression stage is selected by the operator, and can be either a set dimension or a maximum forming pressure. For the AECT Impact 2001A, the maximum hydraulic pressure that is applied is 3000 psi. If the maximum pressure is reached prior to reaching the required thickness, compression is stopped. The block is then pressed out of the mold vertically and pushed out of the machine. Because the compressive force is limited, blocks of varying thickness can be produced from a single run of material. Variability in moisture throughout a soil can cause changes in the amount of soil that fills the cavity and thus influence final block dimensions. Blocks can be produced with initial soil moisture contents from approximately 5% to 20%. In general, wetter soil produces thinner blocks. Block production continues as long as there is adequate soil filling the hopper. The AECT Impact 2001A and example blocks are shown in Figure 1. This trailer mounted system can either be towed with a standard two inch ball hitch or moved easily on site by hand.

Another commercially available CEB machine is the Vermeer BP714. This semi-automated machine produces blocks of uniform size, approximately 14-inches long, 7-inches wide, and 4-inches tall, with interlocking geometric features and through-holes at a rate of three blocks per minute. With the through-holes, the Vermeer BP714 produces CEBs that are reminiscent of concrete masonry units (CMUs). Each block weighs approximately 20 lbs, which varies depending on soil type, moisture content, and additives. The through-holes align when stacked and can be fitted with reinforcing steel or conduit and/or filled with mortar or grout for further strengthening. Similar to the AECT Impact 2001A, soil is loaded into a screened hopper. The hopper on the Vermeer BP714 holds enough soil to produce approximately 14 blocks. Rather than being fully automated, the Vermeer BP714 is controlled by three control levers and functions in a semi-automated fashion. One lever controls a vertical ram used for filling the soil cavity and compressing to a fixed thickness. One lever controls a horizontal ram used to maneuver the dirt tray to move soil from the hopper to the compression cavity. The third lever

controls two tapered, vertical pins, nominally three inches in diameter, that push through the block from beneath to form the through-holes and compresses the block to consistent forming pressures. After the block is formed, the vertical ram presses the block out of the mold, and the horizontal ram pushes the block out of the machine. The Vermeer BP714 is shown in Figure 2. This press is affixed to skids and can be easily moved with a forklift or pallet jack of sufficient capacity.

Figure 1. AECT Impact 2001A machine and example blocks

Figure 2. Vermeer BP714 and example blocks

Since compressed soil is susceptible to erosion by water, CEBs are usually produced using soil that has been mixed with a stabilizer to increase durability. Soil stabilization techniques are well known for a variety of engineering purposes, and known techniques can be applied to CEBs. Portland cement added at about 6% to 8% by volume is a common soil stabilizer that undergoes a hydraulic reaction that binds soil particles. Many other additives are used for soil stabilization including polymers, petroleum byproducts, microorganisms and their secretions, enzymes, fibers, minerals, pozzolans, and industrial waste products such as fly ash.

RESEARCH OBJECTIVES

The objective of this study was to compare the functionality of both the Impact 2001A and Vermeer BP714 using identical soil and stabilizers. By using similar soils and stabilizers, the effects of the CEB presses themselves could be directly studied. Recommendations for the use of each machine and its suitability with different soil types were also developed. The effects of each machine and block geometry on the compressive strength development of the blocks were also studied.

RESEARCH METHODOLOGY

For the purposes of this study, a clayey sand (SC) from central Louisiana was chosen for use. Soil classification data is given in Table 1. This soil was chosen due to its sand and clay contents. Previous studies had shown that soils with greater than 50% sand content and at least 10% clay performed better than lower sand or clay soils (Dominguez 2011). Also, the plasticity index is given as 20 indicating low plasticity clay particles. High plasticity clays tend to be more highly expansive when exposed to moisture, which can negatively affect the performance of compressed earth blocks. Also given in Table 1 is soil characterization data on three other soil types for reference. SM Blend is very similar to what is found in most arid climates. NP designates that the soil is non-plastic. Non-plastic soils have little to no natural cohesion, so binders are required to produce even low quality CEBs. Buckshot clay is a high plasticity, very expansive clay. While soils such as this tend to produce CEBs with satisfactory green properties, the CEBs tend to lose structure and stability due to changes in humidity. Agricultural loam is representative soil for most agricultural fields. While materials such as this do exhibit some natural cohesion, the high silt content leads to low strength CEBs. For stabilized soils, Type I portland cement was chosen as the stabilizing agent. The addition of portland cement at 6-8% by volume is a common stabilizer of soils because it undergoes a hydraulic reaction to bind soil particles together. Various forms of portland cement are also available in most areas throughout the world, so studying its use in CEBs can have wide-reaching implications.

Table 1. Soil characterization data

Soil	Sand (%)	Silt (%)	Clay (%)	PI
Louisiana clay	54	24	22	20
SM Blend	60	38	2	NP
Buckshot clay	3	18	79	64
Agricultural loam	15	63	22	11

Soil was excavated approximately one week prior to production of CEBs. The soil was stored in a climate controlled area to minimize moisture content changes. The soil was used at its in-situ moisture content. As it was field excavated, the soil contained many large clumps that were much too large to pass the screens on either machine's hopper. In an effort to eliminate the majority of the clumps and to better homogenize the material, the soil was tilled and placed in a paddle mixer prior to use. The soil after being removed from the paddle mixer is shown in Figure 3. Even after tilling and mixing with the paddle mixer, the soil still has some large clumps. Many of these large clumps were broken down by hand prior to adding the material to the CEB machines. The paddle mixer used in this study is shown in Figure 4. For stabilized blocks, portland cement was added at a rate of 7% by volume while the material was mixing in the paddle mixer. The addition of dry powdered portland cement helped to remove moisture from the soil and allow the mixing action to eliminate more clumps. Soil before and after the addition of portland cement is shown in Figure 5. The soil after the addition of portland cement is much more uniform than the soil without binders.

Figure 3. Louisiana clay prior to CEB production

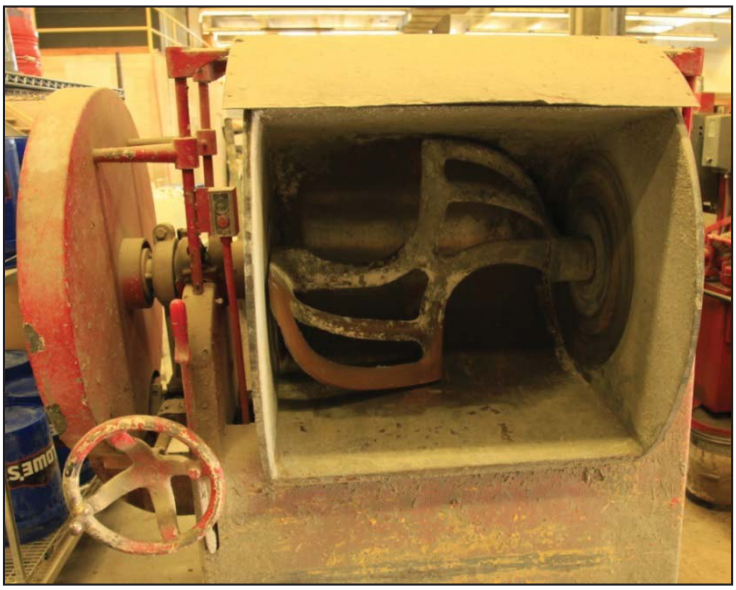

Figure 4. Paddle mixer

The first part of the study focused on the production of blocks with natural soil. Approximately 35 blocks were made using each machine and stored in a climate controlled area exposed to the ambient atmosphere. The second part of the study focused on the production of blocks with soil stabilized with portland cement. Approximately 35 blocks were produced with stabilized soil and wrapped in plastic and stored in a climate controlled area. These blocks were wrapped to minimize the loss of moisture needed to react with the added portland cement.

Figure 5. Louisiana clay before (right) and after (left) adding 7% portland cement by vol.

After blocks had been allowed to dry/cure for a specified time, the full CEBs were tested using a 400-kip hydraulic press. Full blocks were tested per the recommendations of the machine manufacturers. Due to the irregular surface profile of CEBs produced with the Vermeer BP714, custom compression plates were used to evenly transfer the load across the cross-section. At least 10 blocks were tested for each soil or soil-cement combination at seven, 14, and 28 days to help increase statistical accuracy and reliability. These ages are standard testing ages for cementitious materials and can be used to show strength development over time.

KEY FINDINGS

The production of blocks varied dramatically between machines and soils. The AECT Impact 2001A press is much more user friendly for first time users. After cranking the diesel engine, all that was necessary to produce blocks was the addition of soil to the hopper and pressing the start button. First time users of the Vermeer BP714 have to learn the correct operation of the hydraulic levers to produce blocks. Incorrect sequencing of the control levers can lead to poor block consolidation or repetitive compression. As a result, initial block production is a much slower process. Periodically, as soil continues to be compacted with the Vermeer BP714, the compression pins need to be cleaned to function properly. Once a consistent operating procedure is learned, the larger hopper on the Vermeer BP714 allows for more blocks to be made before additional soil is needed.

For natural soil, the production of blocks was much easier with the AECT Impact 2001A. The soil was very sticky in its natural condition and did not readily fall from the hopper when using the Vermeer BP714. This caused problems in block production because too little material was filling the press cavity. To alleviate some of these issues, soil was manually added to the cavity and rodded to aid in consolidation. No such problems arose using the AECT Impact 2001A. Once portland cement was added, both machines functioned at much higher efficiency. With less clumps being present and the soil being drier overall, the material much more readily filled the compression cavities of both machines. The manual addition and rodding of soil with the Vermeer BP714 was not needed with stabilized soil.

Table 2-Table 4 below show the compressive strength data for each material/machine combination at each of the three ages.

Table 2. 7-day compressive strength data

Soil/Machine	7-day Compressive Strength			
	Samples	Avg. (psi)	St. Dev. (psi)	COV (%)
AECT Impact 2001A Natural Soil	12	549	80	14.6
Vermeer BP714 Natural Soil	11	258	84	32.4
AECT Impact 2001A Stabilized Soil	12	709	80	11.3
Vermeer BP714 Stabilized Soil	12	790	128	16.2

At seven days, the AECT Impact 2001A CEBs with natural soil are over twice as strong as the same blocks made in the Vermeer BP714. This is partly because of the production difficulties when using the Vermeer machine with natural soil. The CEBs were most likely not compacted as well as ideal. The stabilized soil tested with nearly identical strength regardless of machine. This is indicative of the consistency of the soil after the addition of portland cement.

Table 3. 14-day compressive strength data

Soil/Machine	14-day Compressive Strength			
	Samples	Avg. (psi)	St. Dev. (psi)	COV (%)
AECT Impact 2001A Natural Soil	12	612	136	22.2
Vermeer BP714 Natural Soil	12	368	97	26.5
AECT Impact 2001A Stabilized Soil	12	972	204	21.0
Vermeer BP714 Stabilized Soil	12	773	154	19.9

After 14 days, once again the AECT Impact 2001A CEBs with natural soil exhibited much greater compressive strength than the blocks made with the Vermeer BP714. Blocks made with stabilized soil in the AECT Impact 2001A showed a nearly 300 psi increase over the seven days since the previous test age. The blocks made with stabilized soil in the Vermeer BP714 showed no strength increase between seven and 14 days. This was an unexpected result attributed to the moisture retained in the different block types. The Vermeer blocks were much wetter in appearance and feel at 14 days than were blocks made with the AECT machine.

Table 4. 28-day compressive strength data

Soil/Machine	28-day Compressive Strength			
	Samples	Avg. (psi)	St. Dev. (psi)	COV (%)
AECT Impact 2001A Natural Soil	12	746	49	6.6
Vermeer BP714 Natural Soil	12	415	43	10.3
AECT Impact 2001A Stabilized Soil	12	1251	193	15.5
Vermeer BP714 Stabilized Soil	15	1603	218	13.6

Minimal strength increase was seen between 14 and 28 days with natural soil CEBs. The maximum average compressive strength of the Vermeer natural soil blocks was lower than the

initial average compressive strength of the AECT natural soil blocks. This further showed the difference in quality of the blocks made with natural soil. The CEBs made with stabilized soil in the Vermeer BP714 showed a significant strength increase between 14 and 28 days. As previously mentioned, this is attributed to the rate of drying of the blocks. The significant strength final strength difference of 352 psi between the stabilized soil blocks showed the value of having a two stage compression process. The additional compression stage allowed for more thorough compression of the blocks than the single stage compression used by the AECT Impact 2001A. The AECT stabilized soil CEBs also showed a strength increase between 14 and 28 days, albeit at a much lower rate than the Vermeer BP714 stabilized soil blocks. Figure 6 shows the compressive strength development of each soil and machine combination versus time.

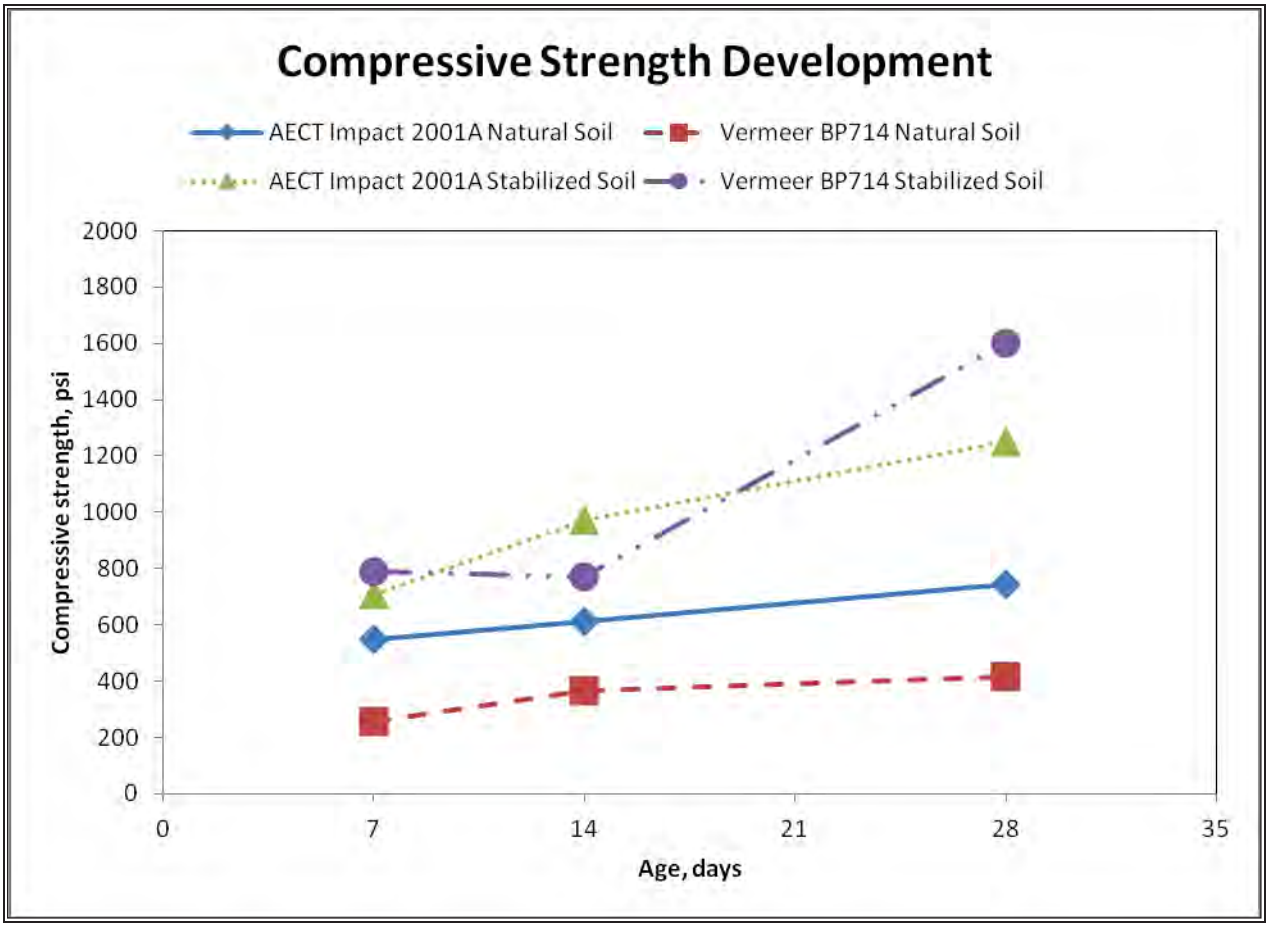

Figure 6. Mean compressive strength development versus time

CONCLUSIONS

The data recorded from the natural soil blocks indicated that the AECT Impact 2001A can be used to produce blocks with significant quality advantages over blocks made with Vermeer BP714 when the soil used may be in less than desirable conditions. The data recorded from the stabilized soil blocks showed that, for more uniform and free flowing soil, the Vermeer BP714 produced higher quality blocks than the AECT Impact 2001A. The Vermeer BP714 has a two-stage compression process that allows for more uniformly consolidated blocks, rather than the one-stage compressive action of the AECT Impact 2001A. However, the AECT Impact 2001A is

much more forgiving of imperfect soil conditions due to the solid rectangular construction of the blocks. Because blocks produced with the Vermeer machine have through-holes, the soil must readily be able to fill around the large pins in the mold. No such problems arise with the AECT machine, so more clumpy soils are more easily used. As a result of the AECT machine being more automated than the Vermeer machine, less training time is needed prior to block production. The through-holes produced by the Vermeer machine allow for construction advantages and easier handling of the blocks. While the waste can be recycled, there is much less of it in the production of blocks with the AECT Impact 2001A. Figure 7 shows blocks as they exit the two machines. Note all of the excess loose soil that is on the top of the Vermeer block and along the exit chute. This loose material is not present on the AECT block. The AECT blocks are ready-made for stacking, whereas the Vermeer blocks must be brushed off prior to stacking. Periodically, this loose material can be added back to the hopper, provided it has not be contaminated with foreign material, extra water, etc. In conclusion, the AECT Impact 2001A is a more user-friendly machine that produces perfectly functional CEBs with a wider variety of soils. The Vermeer BP714 requires more preprocessing of the soil and slightly more operating effort than the AECT Impact 2001A. However, these added efforts allow the Vermeer BP714 to produce more robust and consistent CEBs.

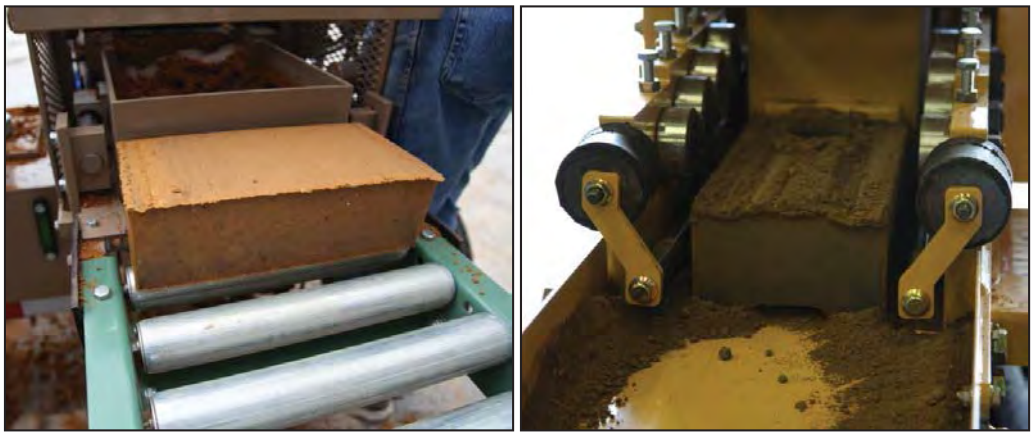

Figure 7. Blocks exiting the AECT Impact 2001A (left) and Vermeer BP714 (right).

ACKNOWLEDGEMENTS

The authors would like to acknowledge the Transatlantic Division of the US Army Corps of Engineers for funding this research study. Additionally, we could not have completed this study without the help of our many technicians who worked tirelessly to assure that blocks were produced and cured in the manner prescribed. Special thanks are given to Mr. Lawrence Jetter and Mr. Jimmy Allen for their help with the AECT Impact 2001A press and to Mr. Adam de Jong for his help with the Vermeer BP714 press. Permission to publish is granted by the Director, Geotechnical and Structures Laboratory.

REFERENCES

Dominguez, T. (2011). *Guide G-521: ABCs of Making Adobe Bricks.* New Mexico State University, College of Agricultural, Consumer and Environmental Sciences. Las Cruces, NM: New Mexico State University.

Virtual Operator Modeling Approach for Construction Machinery

Yu Du
Industrial and Manufacturing Systems Engineering Department
Iowa State University
0068 Black Engineering Building
Ames, Iowa 50011
yudu@iastate.edu

Michael C. Dorneich
Industrial and Manufacturing Systems Engineering Department
Iowa State University
3028 Black Engineering Building
Ames, Iowa 50011
dorneich@iastate.edu

Brian L. Steward
Agricultural and Biosystems Engineering Department
Iowa State University
2325 Elings Hall
Ames, Iowa 50011
bsteward@iastate.edu

Eric R. Anderson
C&F Dynamics Systems Modeling
Deere & Company
18600 S John Deere Rd
Dubuque, Iowa 52001
AndersonEricR@johndeere.com

Lawrence F. Kane
A&T Dynamic System Modeling
Deere & Company
1100 13th Ave
East Moline, Illinois 61244
KaneLawrenceF@johndeere.com

Brian J. Gilmore
Advanced Systems Engineering
Deere & Company
One John Deere Place
Moline, Illinois 61265
GilmoreBrianJ@johndeere.com

Proceedings of the 2015 Conference on Autonomous and Robotic Construction of Infrastructure, Ames, Iowa.

ABSTRACT

Greater understanding of how highly skilled operators achieve high machine performance and productivity can inform the development of automation technology for construction machinery. Current human operator models, however, have limited fidelity and may not be useful for machinery automation. In addition, while physical modeling and simulation is widely employed in product development, current operator simulation models may be a limiting factor in assessing the performance envelope of virtual prototypes. A virtual operator modelling approach for construction machinery was developed. Challenges to the development of human operator models include determining what cues and triggers human operators use, how human operators make decisions, and how to account for the diversity of human operator responses. Operator interviews were conducted to understand and build a framework of tasks, strategies, cues, and triggers that operators commonly use while controlling a machine through a repeating work cycle. In particular, a set of operation data were collected during an excavator trenching operation and were analyzed to classify tasks and strategies. A rule base was derived from interview and data analyses. Common nomenclature was defined and is explained. Standard tasks were derived from operator interviews, which led to the development of task classification rules and algorithm. Task transitions were detected with fuzzy transition detection classifiers.

Key words: human operator modeling—construction machinery—excavator trenching—machinery operations

INTRODUCTION

Introducing new product features can impact machine performance goals such as higher productivity or fuel economy. Virtual design, the process by which new features are modeled and tested in a simulation environment, is typically conducted early in the design process where it is less expensive to make changes. While machines have been modeled with a fidelity that enables robust testing, approaches to operator modelling technology are limited, which in-turn limits the ability of engineers to make solid comparisons in the virtual prototyping stage between different design alternatives. Given the tightly coupled, non-linear nature of the sub-system dynamics in off-road vehicles, combined with a strong human-in-the-loop involvement of operators, dynamic simulation of the complete vehicle system must include the operator, environment, and working tasks (Filla et al., 2005).

Expert human operators display several characteristics: humans can adapt quickly to context using prior experience and training; humans have the ability to integrate contextual cues and strategies; and expert operators can often outperform automated functions. As human operators gain experience, their operations progress from a primarily knowledge-based behavior, to rule-based behavior, and finally to skill-based behavior (Rasmussen, 1983). Knowledge-based behavior depends on explicitly formulated goals and plans. With more practice, operators become rule-based, where sequences of action become rules to follow. Eventually, the expert exhibits skill-based behavior, where much of the action takes place without conscious control (Rasmussen, 1983). These human characteristics are quite different from those of automated machine systems.

An automated system can significantly improve consistency of repeated tasks in a stable, controlled environment which does not have much variation. In the research area of autonomous vehicles, optimal operation methods were identified, which were used to control the vehicle autonomously for situations without much variation (Bradley, 1998; Wu, 2003). However,

when the operating environment or conditions change within which an automated system operates, higher-level machine intelligence technologies, beyond closed-loop control, must be in place for the autonomous system to adapt to these changes. Developing these types of behavioral responses for autonomous systems is challenging. A robust automation system with perception of external cues and use of internal goals, may be able to exhibit adaptive behavior. For this behavior, expert human operator behavior and decision making process may have great utility. A virtual operator model aims to capture key behaviors of human operators, enabling autonomous system to adapt to external environment changes.

A virtual operator model is designed explicitly to be independent of the vehicle model. Without this independence, operator models that are highly tuned for particular vehicle models must be retuned when vehicle designs are changed. To avoid the cumbersome nature of this tight dependency, an operator model should adapt to changes in vehicle capabilities such as available power or mechanical linkage constraints.

The objective of this work was to develop an approach to virtual operator modeling (VOM). The VOM is an encapsulated model independent from the machine model with a well-defined interface. The outputs of the VOM are the control inputs to the construction machine model. The VOM should simulate human operators' behavior and decision making to generate appropriate control inputs for vehicle model simulation. The initial phase of this work is described in this paper.

The methodology used to inform the VOM design included expert operator interviews, machine data analysis, and task-based state modelling. The ability to have adaptive VOM will enable enhanced performance analysis including fuel efficiency, productivity, and component loading and strategies for robust automation technology development.

RELATED WORK

Preliminary studies of operator modeling found in autonomous vehicle research helps to develop an understanding of how a virtual operator model can be used to improve autonomous control systems. Data collection, task analysis and human behavior study techniques can be combined to gather, organize, and represent how human operators perform certain operations, supported by their strategies, situation awareness, knowledge, and decision making process.

Operator Modeling Approaches

Two virtual operator modeling approaches, task-oriented and reference-oriented, for construction equipment, were found in the literature. Task-oriented approaches simulated machine operations that go through a repeated sequence of tasks to accomplish a high-level goal. Operation modelling was based on a finite state machine and combination of a finite state machine and controllers for generating machine control inputs for each task making up the operation (Filla, 2005; Elezaby, 2011). Generally, a decision making module and a command conditioning module are needed for virtual operator modeling. The decision-making module perceives and classifies information. The command conditioning module generates appropriate control inputs. Validation was limited to the comparison of simulated paths with experimental paths for different vehicle components (Filla, 2005). By contrast, a reference-oriented approach simulates machines navigating along predefined paths to accomplish some type of operational goal. For example, a steering controller was developed for vehicles by compensating path tracking errors (Norris, 2003).

Operator modeling attempts can be also found in research investigating approaches to enabling the autonomous operation of construction equipment. Operator strategies and behavior were studied and used to develop the control module for autonomous trenching activities. For example, adaptation to different obstacles was realized by using different strategies from discovered through operator behavior studies. It was determine, for example, that human operators penetrate and drag the bucket for dense soil, while they penetrate and rotate the bucket for loose soil (Bradley, 1998). Additionally Wu (2003) developed an approach to automatic adaptation to different materials for a wheel loader dig cycle by using neural network and fuzzy logic approaches.

Task Modeling Approaches

Data collection and task analysis are human factors methods, which are commonly used for human subject-related research. Data collection is normally the first step to start the project, which collects specific information about the tasks, the system, and operation information of human operators including communication and controls. Common data collection methods include interviews, questionnaires, and observations (Stanton & Walker, 2005). Task analysis methods result in hierarchical task analysis, which decomposes the higher level task into subtasks with detailed information needed to perform the task. In general, task analysis can be classified as knowledge-based and entity-relationship-based analysis: knowledge-based analysis focuses on the knowledge in term of objects to the task; entity-relationship-based analysis focuses on finding the connection between actions and objects (Dix, Finley, Abowd & Beale, 2004).

Autonomous Control

Autonomy in semi-controlled environments like those associated with construction or agricultural application requires specification and generation of human-like behavior. Han et al. (2015) presented a multi-layered design framework for behavior-based autonomous or intelligent systems. Intelligent systems have the ability to perceive cues from the environment and machine and plan processes for adapting to different situations. Blackmore et al. (2007) proposed a behavior-based approach to agricultural field robotics with the capability to perform operations in unknown field conditions, which includes integrated human-like adaptation ability with intelligence for perception, and decision making in robotics.

MODELING METHODS

For this project, the excavator trenching operation was selected as the target construction machine operation for virtual operator development. Excavator trenching is a very common construction operation, which contains multiple tasks and deals with multiple situations. During the operation, an operator needs to make a trench at a predetermined location and orientation with defined dimensions, and dump the material either in a defined area or into a truck. Operators tend to work at their maximum ability to finish trenching as soon as possible. To automate the trenching operation, an autonomous system must mimic human operator behavior to adapt to different situations or disturbances during the operation.

To develop a virtual operator model that replicates human operator behavior, operator interviews were first conducted to understand the approach of operators and to collect information about their behavior. The modeling structure described in Figure 1 describes the elements of the VOM.

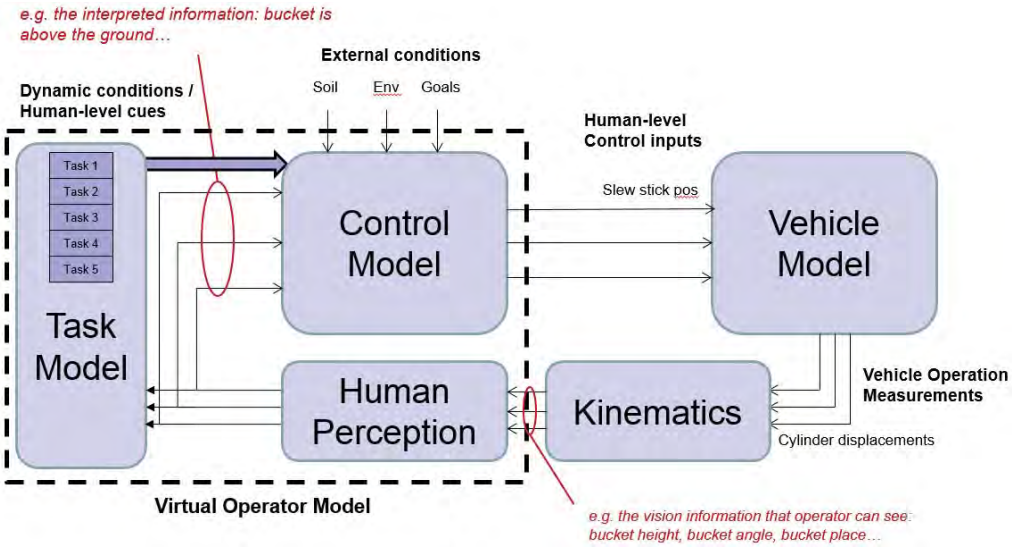

Figure 1. The virtual operator model interacts with the vehicle model through a well-defined interface.

The vehicle model provides machine signals like cylinder extension length and velocity. Vehicle data can be translated into the absolute position and orientation of machine implement elements such as buckets and booms through a kinematic model of the machine. These dynamic variables are closely related to the visual cues that the human operator uses for decision making during the work cycle. The signal flow in this operator model and vehicle model structure forms a closed loop for simulation.

The virtual operator model consists of three modules: the human perception module, the task model module, and the control model module. The human perception module is responsible for acquiring the vehicle model measurements and transforming them into information at the human perception level that human operators use for decision making. The vehicle model produces measurements such as cylinder displacements. However, humans perceive the vehicle in terms of position and location, such as bucket height. A kinematic model translates raw vehicle data into human-level perceptual cues. The human perception model triggers transitions between tasks by interpreting these visual cues and sounds to trigger transitions between tasks. The task model module uses the results from the human perception module to determine the sequence and status of tasks. The control model module uses task goals, modified by external conditions like soil condition, environmental condition, to generate control inputs for the vehicle model.

Three steps were followed to develop a modeling approach for virtual operator modeling. The first step was to interview operators, observe the operation, and acquire machine data. Secondly, the operation was analyzed to define the tasks and relate machine data to those tasks. The third step developed the transition detection classifier to identify transitions between tasks, which led to a state sequence model.

Data Collection

Operator interviews were conducted to gain a deeper understanding of the information needed and operator behaviors during the trenching operation. An interview protocol was developed to determine an operator's operating experience, behavior, strategies, and possible problems

during operation. Three participants with different backgrounds and skill levels participated in the interviews. With experience from a wide range of different machines, the interviews provided general information about the trenching operation in general and was not limited to specific types of machines. The interview protocol was used to guide the interviews, and written notes as well as audio records were collected from the interviews. In addition, operators reviewed recorded videos of themselves operating the machinery. They reviewed their operation and walked through the video in a think-aloud technique (Lewis, 1982; Ericsson & Simon, 1993) with verbal identification of tasks, needs, goals, strategies, and behavior. This work collected both descriptive data as well as quantitative data, which enabled a combination of knowledge based and entity relationship based analysis for accurate task analysis.

Machine data recorded during predefined excavator trenching operations were used for analysis of operator's operational behavior. An excavator was equipped with cameras inside the cab and outside the cab, which captured both video and audio, an eye tracking sensor to record and track the real-time view field of the operators, and sensors were used to log data produced from the machinery itself. Machine operation data were collected during the operation with signal channels of operator inputs, cylinder positions, and relative speed and direction.

Task and Data Analysis

Task analysis was used to represent the trenching operation and to support a detailed understanding of trenching. Tasks were identified and described based on operator interviews and operation observations. Perception of cues, selection of strategies, and subtasks was summarized in detail.

Machine data were analyzed and related to the task analysis, which described the tasks identified for trenching and specified control input information related to each task. Data analysis was performed on the machine data to identify different tasks defined from task analysis, which represents the actual operation information about the sequence, timing information, and control inputs of the tasks.

Task and data analysis resulted in a qualitative task analysis and a quantitative data-based task classification, which provided an accurate description of the trenching operation. A task model was established to represent the trenching operation with detailed information about human operator behavior, strategies, and control input for each task.

Fuzzy Transition Detection Classifiers

By classifying numerical signals into human perceivable information used for reasoning, fuzzy transition detection classifiers were developed for successful detection of transitions between tasks. Transition detection classifiers predicted the transitions between tasks, which can inform the virtual operator model when to generate control inputs for the next task. Based on machine data, the dynamic state of excavator implement elements were determined through a kinematic model, which can be translated to human perceivable descriptive information using fuzzy transition detection classifiers. Fuzzy transition detection classifiers were used to identify the transition between tasks based on some of these common cues and triggers that operators use. To develop the fuzzy transition detection classifier, membership functions were determined to describe each of signals required for rules, which were classified into different levels with descriptive language similar to how human operators perceive the signals. A set of rules were derived based on the classified human perceivable signals to identify transitions between tasks, which serve as reasoning statements in the fuzzy transition detection classifiers. The outputs

from the fuzzy transition detection classifiers represent the transitions between the tasks. By successfully identifying the transitions between tasks, the state model was completed, which represents the current state of the operation and the start of the next state.

MODELING RESULTS

Task and Data Analysis Results

The tasks and sub-tasks of the trenching operation were identified from the operator interviews and are summarized in a nominal task timeline (see Figure 2). Five main tasks were identified within the trenching operation: bucket filling, bucket lifting, swing to dump, dumping, and swing back to trench. The timing of the start and end of each task was estimated through review and analysis of video of a trenching operation for one of the participants. It was noted in both interviews and video analysis that the tasks overlap. Task overlap was a consistent theme among all participants – one participant said that the more expert the operator, the more he or she can overlap tasks to increase efficiency and reduce cycle time. While the video analysis of timing provided a qualitative estimation of task overlap, vehicle data analysis (described later in this section) was used to obtain more precise estimates of task timing.

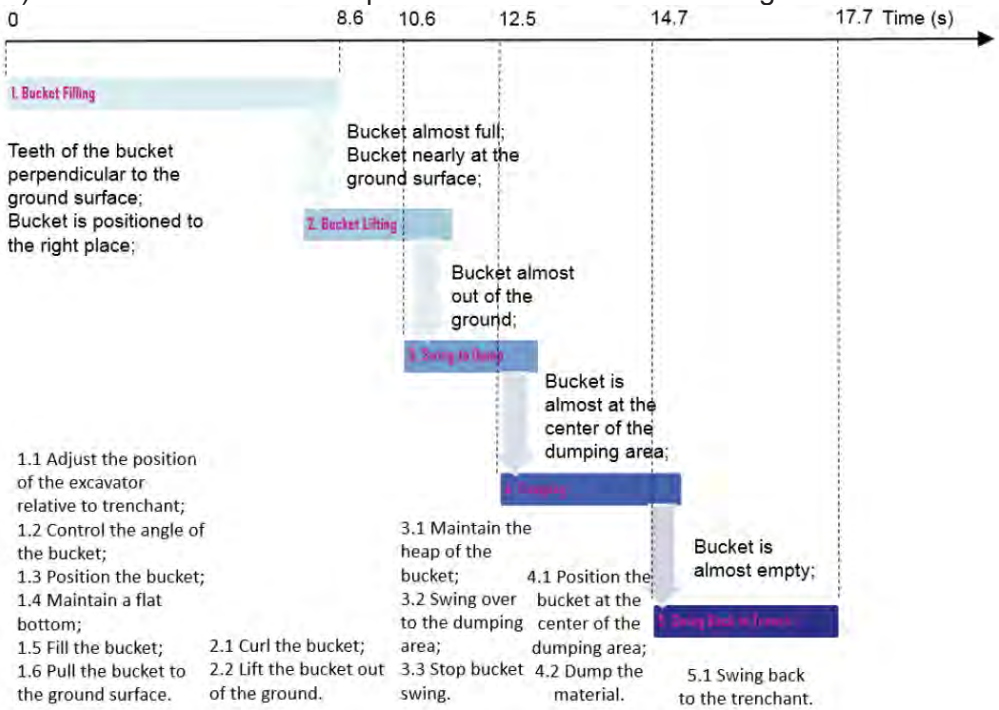

Figure 2. Task timeline based on human operator interviews. Task start and end times were calculated based on analysis of videos of trenching operations.

The durations of specific tasks were overlaid on traces of the machine cylinder extension lengths, swing speed, and operator inputs (see Figure 3). The topmost graph of Figure 3 shows the cylinder extension positions for the Boom, Arm, and Bucket. The remaining graphs show operator control inputs for Swing, Boom, Arm, and Bucket. All these signals were used to identify the five tasks: Bucket Filling, Bucket Lifting, Swing to Dump, Dumping, and Swing to Trench within two work cycles. Rectanglar bars with different colors were used to show the start time point and end time point of tasks with task names on them. Timing information of tasks could be directly read from the diagram.

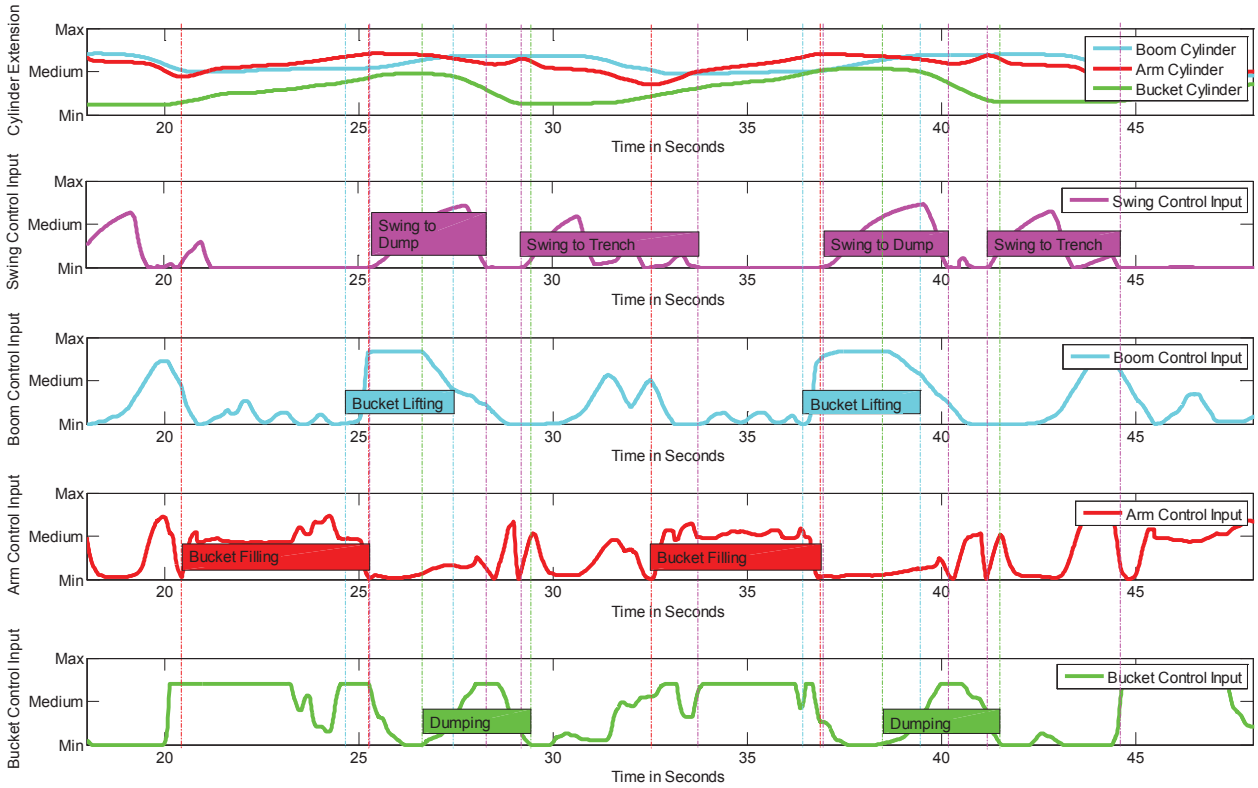

Figure 3. Data Characterization with Task Timing Overlaid on Traces of the Operator Inputs and Machine Configurations.

Transition Detection

Task transition identification aims to predict when the operator transitions attention from one task to another based on vehicle state. Measured vehicle signals were classified into human perceivable descriptive information, which enabled human-like reasoning rules. For example, by comparing the bucket height to the ground surface, three levels were defined for states BelowSurface, NearSurface, and AboveSurface.

INALTable 1 contains the example of rules used in the fuzzy transition detection classifiers to detect the transition between Swing to Trench and Bucket Filling.

With this information, the operator model transitions through the task model and provides correct reference inputs to the controller and task model. Figure 1 represents the transition identification result between Swing back to Trench and Bucket Filling. The green line represents the fuzzy classification result for the transition detection. The blue line represents the ground truth task for Bucket Filling, which describes when Bucket Filling starts and ends. By comparison of the traces, the correct detection happens when the green line starts to rise slightly ahead of blue line, since the goal of the classifier is to predict a transition between tasks. If the green line raises later than the blue line, the transition is detected late.

INALTable 1. Transition Rules to detect the transition between the Swing and Bucket Filling tasks.

From Swing to Trench to Bucket Filling:
1. If (BucketHeight is BelowSurface) and (SwingAngle is NearTrench) and (ExtensionDistance is Extended) then (BucketFillTransition is BucketFill)
2. If (BucketHeight is BelowSurface) and (SwingAngle is NearTrench) and (ExtensionDistance is MidRange) then (BucketFillTransition is BucketFill)
3. If (BucketHeight is BelowSurface) and (SwingAngle is NearTrench) and (ExtensionDistance is Retracted) then (BucketFillTransition is BucketFill)
4. If (BucketHeight is AboveSurface) then (BucketFillTransition is Swing2Dig)
5. If (BucketHeight is NearSurface) and (SwingAngle is NearTrench) and (ExtensionDistance is Extended) then (BucketFillTransition is Swing2Dig)

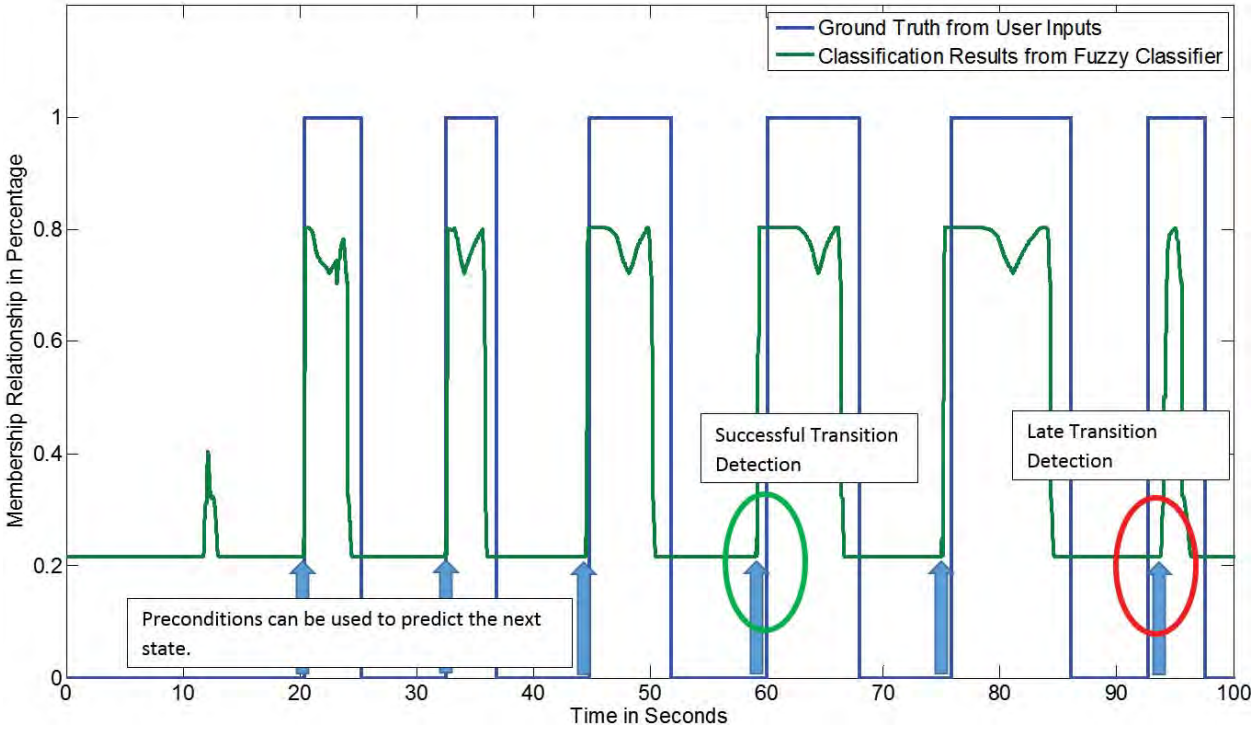

Figure 4. Transition Detection Results between Swing back to Trench and Bucket Filling

By combining of all identified transitions within the trenching operation, the sequence of tasks and current state of the operation can be represented. Figure 5 visualizes the sequence of the tasks with information about when each task starts, which can be considered as a state sequence model. An accurate task sequence is important timing and state information for control signal generation.

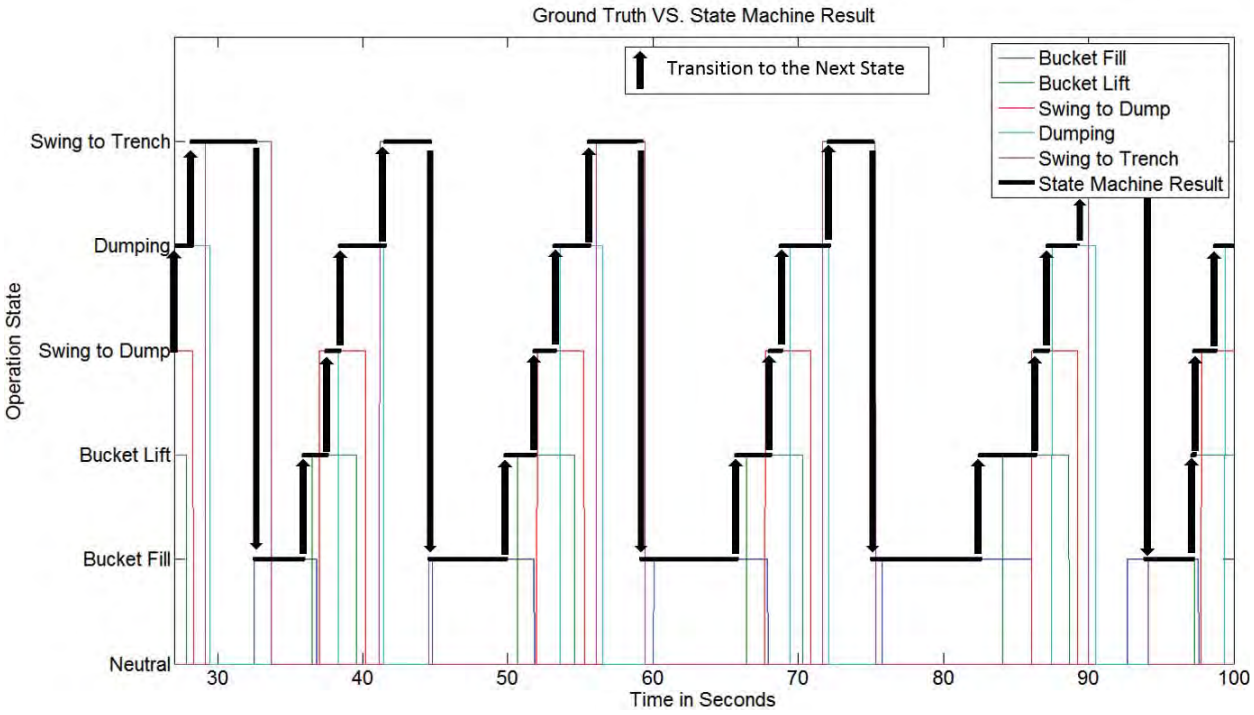

Figure 5. State Sequence derived from Fuzzy Transition Detection Classifiers to Represent the Transition Time to each Task

DISCUSSION AND CONCLUSION

Virtual operator modelling based on studies of human operator perception, decision making, and behaviors can be used to improve development of autonomous and robotics systems and improve evaluation methods in virtual environments. It has a direct benefit for automating construction activities. Initial work focused on construction vehicle operation; future work will expand the application area to agricultural operations, using similar approaches. The main challenges of developing virtual operator models are understanding the ability of human operators to adapt, modeling operator perception, and modeling operator decision making. This paper introduced methods used to collect data and identify information needed to start modelling. A fuzzy logic task transition model has shown promising performance in correctly identifying transitions between tasks. Expert behavior has in part been identified as the ability of operators to overlap tasks within an operation. Future work will include developing methods for identifying overlapping tasks, modeling overlap, and generating control inputs.

ACKNOWLEDGEMENTS

This work was funded by Deere & Company. The opinions expressed herein are those of the authors and do not necessarily reflect the views of Deere & Company.

REFERENCES

Dix, A., Finley, J., Abowd, G. & Beale, G. (2004). Human-computer interaction. England: Pearson Education Limited.

Bradley, D., & Seward, D., (1998). The Development, Control and Operation of An Autonomous Robotic Excavator. Journal of Intelligent and Robotic Systems 21: 73-97, 1998.

Elezaby, A. A. (2011). Virtual Autonomous Operator Model for Construction Equipment Applications. Dissertation, University of Illinois – Chicago, Chicago, Illinois.

Filla. R. (2005). Operator and Machine Models for Dynamic Simulation of Construction Machinery. Thesis No. 1189. Linkopings University, Linkoping, Sweden.

Filla, R., Ericsson, A., & Palmberg, J.-O. (2005). Dynamic Simulation of Construction Machinery: Towards an Operator Model. International Fluid Power Exhibition 2005 Technical Conference, Las Vegas, (NV), USA, pp. 429-438.

Han, S., Steward, B. L., and L. Tang. (2015). Intelligent Agricultural Machinery and Field Robots. In Precision Agriculture Technology for Crop Farming, ed. Zhang, Q. CRC Press.

Norris, W. R. (2001). A Design Framework for Qualitative Human-in-the-Loop System Development. Dissertation, University of Illinois at Urbana Champaign, Champaign, Illinois.

Rasmussen, J. (1983). Skills, rules, and knowledge; signals, signs, and symbols, and other distinctions in human performance models. Systems, Man and Cybernetics, IEEE Transactions, (3), 257-266.

Stanton, N. A., & Walker, G. H. (2013). Human factors methods: a practical guide for engineering and design. Ashgate Publishing, Ltd.

Wu, L., (2003). A Study on Automatic Control of Wheel Loaders in Rock/Soil Loading. Ph.D. thesis, University of Arizona.

Vision-Based Machine Pose Estimation for Excavation Monitoring and Guidance

Chen Feng
Kurt M. Lundeen
Suyang Dong
Vineet R. Kamat
Department of Civil and Environmental Engineering
University of Michigan
2350 Hayward Street, 2340 G.G. Brown Building
Ann Arbor, MI 48109-2125
cforrest@umich.edu

ABSTRACT

The ability to automatically estimate the pose of an articulated machine's base (e.g., tracks or wheels) and its articulated components (e.g., stick and bucket) is crucial for technical innovations aimed at improving both safety and productivity in several construction tasks. Vision-based pose estimation, in which optical cameras monitor fiducial markers to determine their three dimensional relative pose (i.e., position and orientation), offers a promising low cost alternative to currently available sensor packages that are non-ubiquitous and cost prohibitive. This paper presents an overview of the design and implementation of this technique. A computer vision based solution using a network of cameras and markers is proposed to enable a three-dimensional pose tracking capability for articulated machines. First, markers are installed on both the machine's components and the jobsite. The site markers are installed and surveyed so their poses are known in a project coordinate frame. Cameras then observe the markers to measure their relative transformations, and calculate the machine components' poses in the project frame. Several prototypes have been developed to evaluate the system's performance on an articulated excavator. Through extensive sets of uncertainty analyses and field experiments, the proposed method has been shown to achieve centimeter level depth tracking accuracy at a 15m range with only two ordinary cameras and multiple markers, providing a flexible and cost-efficient alternative to other commercial products that use infrastructure dependent sensors like GPS. A working prototype has been tested on several active construction sites with positive feedback from excavator operators confirming the solution's effectiveness.

Key words: camera—excavator—guidance—marker—pose

INTRODUCTION

The construction industry has long been affected by high rates of workplace injuries and fatalities. According to the Census of Fatal Occupational Injuries (CFOI) report (Bureau of Labor Statistics, 2013), the construction industry had the largest number of fatal occupational injuries, and in terms of rate ranked the fourth highest among all industries.

In addition to the safety concerns, there are also increasing concerns of relatively stagnant productivity rates and skilled labor shortage in the construction industry. For example, recently the construction sector in the United Kingdom is reported to be in urgent need of 20% more skilled

Proceedings of the 2015 Conference on Autonomous and Robotic Construction of Infrastructure, Ames, Iowa.

workers and thus 50% more training provision by 2017, to deliver projects in planning (LCCI/KPMG, 2014).

Excavation is a typical construction activity affected by the safety and productivity concerns mentioned above. Excavator operators face two major challenges during excavation operations, described as follows:

First is *how to maintain precise grade control*. Currently, grade control is provided by employing grade-checkers to accompany excavators during appropriate operations. Grade-checkers specialize in surveying and frequently monitor the evolving grade profile. The evolving grade profile is compared to the target grade profile and this information is communicated by the grade-checker to the excavator operator. The operator reconciles this information and adjusts the digging strokes accordingly. This process is repeated until the target profiles are achieved. Employing grade-checkers is not only dangerous but also results in a significant loss in excavation productivity due to frequent interruptions required for surveying the evolving profile.

Second is *how to avoid collisions* to either human workers, buried utilities, or other facilities, especially when excavator operators cannot perceive the digging machine's position relative to hidden obstructions (i.e., workers or utilities) that it must avoid. According to the aforementioned CFOI report, among all the causes for the 796 fatal injuries in the U.S. construction industry in 2013, the cause of striking by object or equipment comprised 10 percent. This percentage is even higher in other industries such as agriculture (19%), forestry (63%), and mining (23%). Besides directly causing fatal injuries on jobsites, construction machines can also inadvertently strike buried utilities, thus disrupting life and commerce, and pose physical danger to workers, bystanders, and building occupants. Such underground strikes happen with an average frequency of about once every six minutes in the U.S. by the nation's leading organization focused on excavation safety (Common Ground Alliance, 2015). More specifically, excavation damage is the third biggest cause of breakdowns in U.S. pipeline systems, accounting for about 17% of all incidents, leading to over 25 million annual utility interruptions (US DOT PHMSA, 2015).

Automation and robotics in construction (ARC) has been extensively promoted in the literature as a means of improving construction safety, productivity and mitigating skilled labor shortage, since it has the potential to relieve human workers from either repetitive or dangerous tasks and enable a safer collaboration and cooperation between construction machines and the surrounding human workers. In order to apply ARC and increase intelligence of construction machines to improve either safety or productivity for excavation and many other activities on construction jobsites, one of the fundamental requirements is the ability to automatically and accurately estimate the pose of an articulated machine (e.g., excavator or backhoe). The pose here includes the position and orientation of not only the machine base (e.g., tracks or wheels), but also each of its major articulated components (e.g., stick and bucket).

When a construction machine can continuously track its end-effector's pose on the jobsites, such information can be combined together with the digital design of a task, either to assist human operators to complete the task faster and more efficiently, or to eventually finish the task autonomously. For example, an intelligent excavator being able to track the pose of its bucket can guide its operator to dig trenches or backfill according to designed profiles more easily and accurately with automatic grade-check. This can eventually lead to fully autonomous construction machines. When construction machines becomes more intelligent, it can be expected to save time in training operators and thus to mitigate skilled labor shortage and also improve productivity.

On the other hand, when construction machines are aware of the poses of their components at any time and location on jobsites, combined with other abilities such as the recognition of human workers' poses and actions, such machines will be able to make decisions to avoid striking human workers, for example by sending alerts to their operators or even temporarily taking over the controls to prevent accidents. Thus it will help to decrease the possibilities of those injuries and fatalities and improve the safety on construction jobsites. Similarly, with continuous tracking of the pose of its end-effector (e.g., a bucket of an excavator), an intelligent excavator could perform collision detection with an existing map of underground utilities and issue its operator a warning if the end-effector's distance to any buried utilities exceeds some predefined threshold.

Thus, from a safety, productivity, and economic perspective, it is critical for such construction machines to be able to automatically and accurately estimate poses of any of their articulated components of interest. In this paper, a computer vision based solution using planar markers is proposed to enable such capability for a broad set of articulated machines that currently exist, but cannot track their own pose. A working prototype (Figure 1) is implemented and shown to enable centimeter level excavator bucket depth tracking.

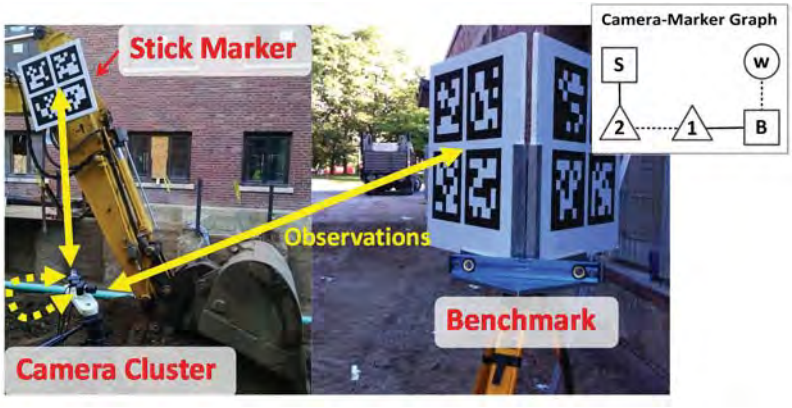

Figure 1. Overview of the SmartDig prototype

The remainder of the paper is organized as follows: Related work is reviewed first. The authors' technical approach is then discussed in detail. The experimental results are presented afterwards. Finally, the conclusions are drawn and the authors' future work is summarized.

PREVIOUS WORK

The majority of the construction machines on the market do not have the ability to track their poses relative to some project coordinate frames of interest. To track and estimate the pose of an articulated machine, there are mainly four groups of methods.

First are the 2D video analysis methods, stimulated by the improvement in computer vision on object recognition and tracking. Static surveillance cameras were used to track the motion of a tower crane in (Yang, Vela, Teizer, & Shi, 2011) for activity understanding. Similarly in (Rezazadeh Azar & McCabe, 2012) part based model was used to recognize excavators for productivity analysis. This type of methods generally require no retrofitting on the machine, but suffers from both possibilities of false or missed detection due to complex visual appearance on jobsites and the relative slow processing speed. Although real-time methods exist as in (Memarzadeh, Heydarian, Golparvar-Fard, & Niebles, 2012; Brookshire, 2014), they either cannot

provide accurate 6D pose estimation, or require additional information such as a detailed 3D model of the machine.

Second are stereo vision based methods. A detailed 3D model of the articulated object was required in (Hel-Or & Werman, 1994) in addition to stereo vision. A stereo camera was installed on the boom of a mining shovel to estimate pose of haul trucks in (Borthwick, Lawrence, & Hall, 2009), yet the shovel's own pose was unknown. In (Lin, Lawrence, & Hall, 2013) the shovel's swing rotation was recovered using stereo vision SLAM, yet the pose of its buckets was not estimated. This type of methods can be infrastructure independent if with SLAM, yet some problems (sensitivity to lighting changes or texture-less regions) remain to be resolved for more robust applications.

Third are laser based methods, e.g., (Duff, 2006; Kashani, Owen, Himmelman, Lawrence, & Hall, 2010; Cho & Gai, 2014), which rooted from the extensive use of laser point clouds in robotics. This type of methods can yield good pose estimation accuracy if highly accurate dense 3D point clouds of the machine are observed using expensive and heavy laser scanners. Otherwise with low quality 2D scanners, only decimeter level accuracy was achieved [9] (Kashani, Owen, Himmelman, Lawrence, & Hall, 2010).

Finally are angular sensor based methods, such as (Ghassemi, Tafazoli, Lawrence, & Hashtrudi-Zaad, 2002; Cheng & Oelmann, 2010; Lee, Kang, Shin, & Han, 2012). They are usually infrastructure independent and light-weight, but the resulting pose estimation is either not accurate enough or sensitive to changes of magnetic environment which is not uncommon in construction sites and can lead to large variations in the final estimation of the object poses. Moreover this type of methods only estimate the articulated machine's pose relative to the machine base itself, if without the help of sensors dependent on infrastructure that consume power and need careful maintenance like GPS. However the use of GPS brings several technical challenges. For example, construction sites in a lot of cases do not have good GPS signals to provide accurate position estimation when these sites are located in urban regions or occluded by other civil infrastructure such as under bridges. Sometimes GPS signals could even be blocked by surrounding buildings on jobsites and thus fail to provide any position estimation (Cui & Ge, 2003). In addition, since the GPS only provides 3D position estimation, to get the 3D orientation estimation one needs at least two GPS receivers at different locations of a rigid object. When the object is small, such as a mini-excavator's bucket, the estimated 3D orientation's uncertainty will be high.

TECHNICAL APPROACH

In this section, different versions of the proposed articulated machine pose estimation system design are explained first. Then, the process to calibrate this system is described. Finally, uncertainty analysis is explored for the system with some important observations of the relationship between the system configuration and its stability, i.e., uncertainty of the estimated pose.

System Design

As mentioned previously, this computer vision based articulated machine pose estimation solution relies on a method called marker based pose estimation. Generally, marker based pose estimation firstly finds a set of 2D geometry features (e.g., points or lines) on an image captured by a calibrated camera, then establishes correspondences between another set of 2D or 3D geometry features on a marker whose pose is known with respect to a certain coordinate frame

of interest, and finally estimates the pose of the camera in that coordinate system. If 2D-2D correspondences are used, the pose is typically estimated by homography decomposition. If 2D-3D, the pose is typically estimated by solving the perspective-n-point (PnP) problem. Two typical marker-based pose estimation methods are AprilTag (Olson, 2011) and KEG (Feng & Kamat, 2012) algorithms.

There are two ways of applying marker based pose estimation for poses of general objects of interest. As shown in Figure 2, one way is to install the calibrated camera 1 rigidly on the object of interest (in this case, the cabin of the excavator), and pre-survey the marker 1's pose in the project coordinate frame. The other way is to install the marker 2 rigidly on the object (in this case, the stick of the excavator), and pre-calibrate the camera 2's pose in the project coordinate frame. As long as the camera 2 (or the marker 1) stays static in the project coordinate frame, the pose of the excavator's stick (or the cabin) can be estimated in real-time.

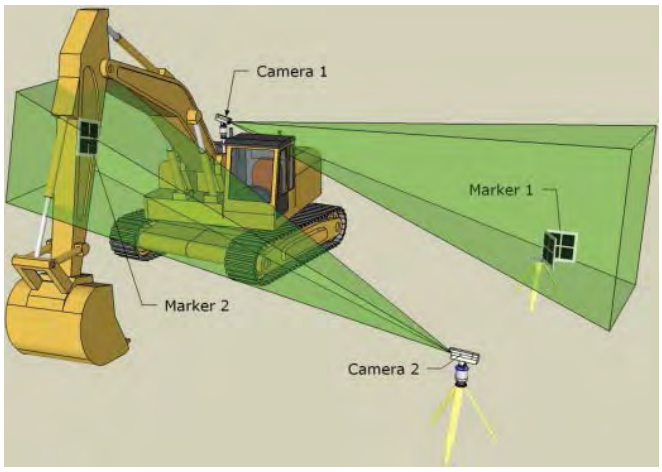

Figure 2. Two examples of basic camera marker configuration

However, these basic configurations don't always satisfy application requirements. For example, if only the camera 1 and the marker 1 are used, the excavator's stick pose cannot be estimated. On the other hand when only the camera 2 and the marker 2 are used, once the stick leaves the field of view (FOV) of the camera 2, the stick's pose becomes unavailable as well. Thus it is necessary to take a camera's FOV into consideration when designing an articulated machine pose estimation system. This understanding leads to the camera marker network design proposed as follows.

Camera Marker Network

A camera marker network is an observation system containing multiple cameras or markers for estimating poses of objects embedded in this system. It can be abstracted as a graph with three types of nodes and two types of edges (e.g., Figure 3). A node denotes an object pose (i.e. the local coordinate frame of that object), which can be a camera, a marker, or the world coordinate frame. An edge denotes the relative relationship between two objects connected by this edge, which can be either image point observations for the previously mentioned marker based pose estimation, or a known pose constraint (e.g., through calibration).

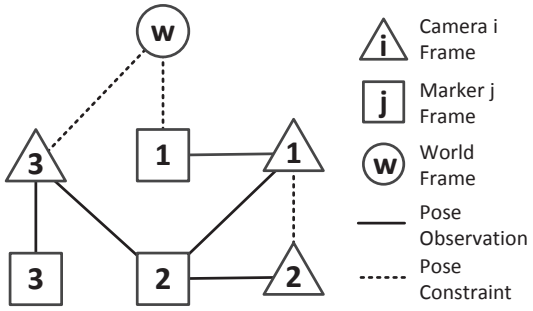

Figure 3. An example graph of a camera marker network

Thus, if at least one path exists between any two nodes in such a graph, the relative pose between them can be estimated. In addition, any loop in the graph means a constraint of poses that can be used to improve the pose estimation. For example, in Figure 3, marker 2's pose in the world frame can be found via a path through camera 3 whose own pose in the world frame is pre-calibrated. The marker 2's pose can also be better estimated when observed by the rigidly connected camera 1 and 2 whose relative pose is pre-calibrated, since a loop is created.

Applying this concept to articulated machine pose estimation results in numerous possible designs. One of the possible camera marker networks is shown in Figure 4, camera 1 observes the benchmark while camera 2 observes the stick marker, and the rigid transformation between the two cameras is pre-calibrated. Thus as long as the two markers stay inside the two cameras' FOV respectively, the stick's pose in the world frame can be estimated. It is worth noting that this only illustrate a simple configuration. With more cameras and markers in the network, there are more chances of creating loops and thus improving pose estimation, especially considering that surveillance cameras are becoming popular in construction jobsites whose poses can be pre-calibrated and thus act as the camera 3 in Figure 3.

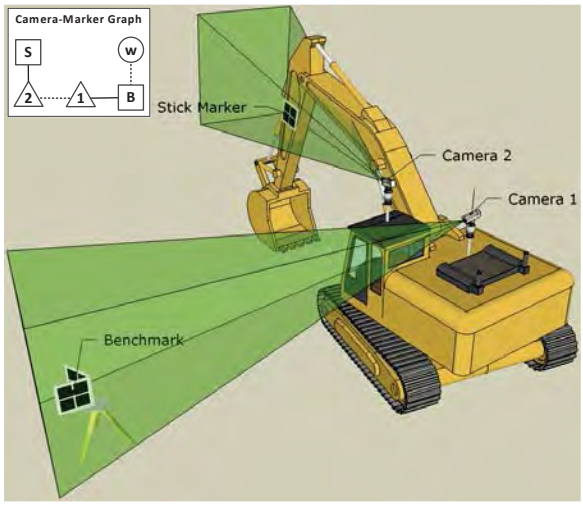

Figure 4. Multiple-camera multiple-marker configuration

Prototypes

Multiple prototypes have been implemented to realize the above described camera marker network designs. Figure 5 demonstrates one of the early prototypes implementing a single-camera multiple marker configuration. A mechanical device driven by a synchronous belt was

adopted to map the relative rotation between the excavator bucket and the stick to the relative rotation between the stick marker and the rotary marker. This implementation enables pose tracking of the excavator bucket.

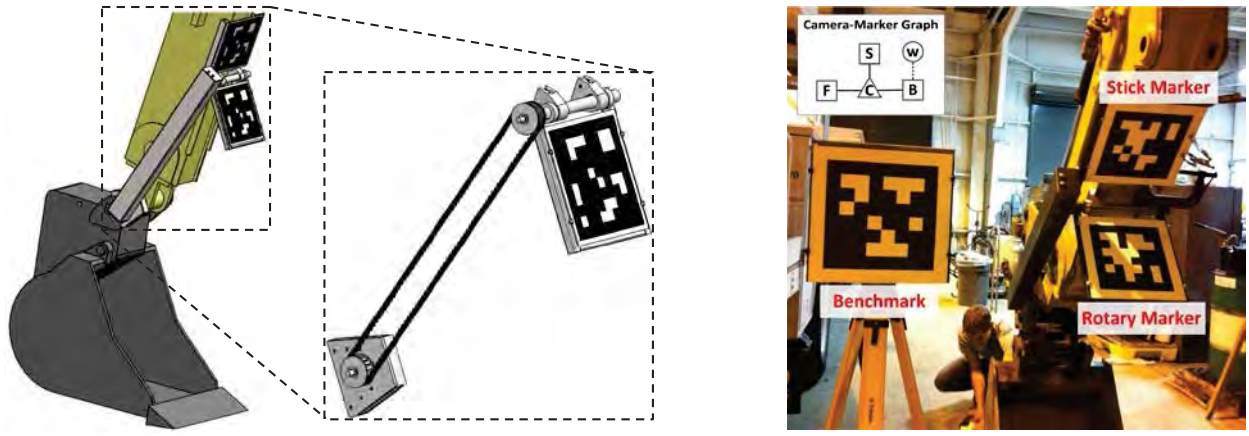

Figure 5. Synchronous belt prototype design

The prototype functions by means of two markers. The first marker, termed stick marker, is rigidly attached to the stick with a known relationship to the bucket's axis of rotation. The second marker, termed rotary marker, is attached at a location removed from the vicinity of the bucket. The rotary marker is constrained with one degree of rotational freedom and a known angular relationship to the bucket. If the bucket's geometry is also known, or measured onsite, then all necessary information is available to deduce tooth pose, as shown in Figure 6.

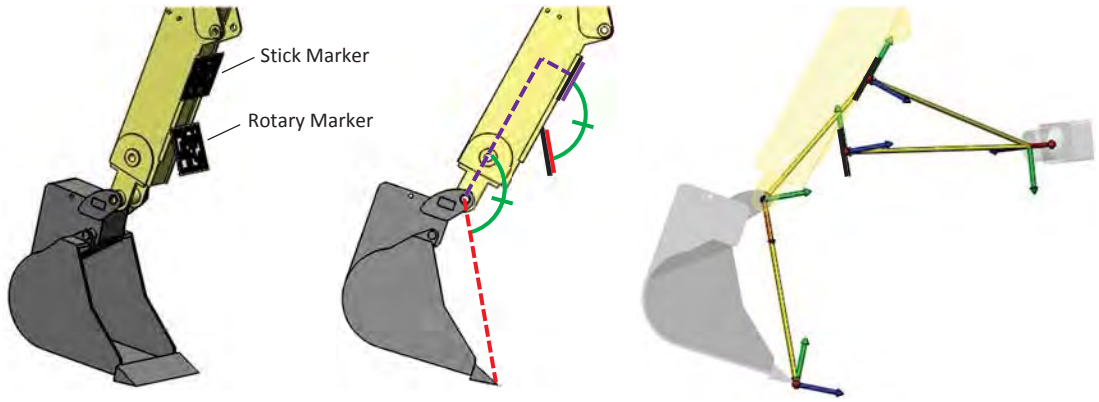

Figure 6. Bucket tooth pose calculation in the synchronous belt prototype

Due to the potential interference of the rotary marker and any obstructions during excavation, the above synchronous belt prototype was slightly modified and evolved to the current prototype as shown in Figure 7. The newer working prototype implements the multiple-camera multiple-marker configuration similar to Figure 5. Two cameras are rigidly mounted forming a camera cluster. A cable potentiometer is installed on the bucket's hydraulic cylinder to track the relative motion of the excavator bucket and the stick even if the bucket is deep inside the earth. In addition to possessing a cable potentiometer for measuring linear displacement, the device contains a

microcontroller for signal conversion, a radio for wireless transmission, and a battery for power, all of which are mounted inside an enclosure for protection.

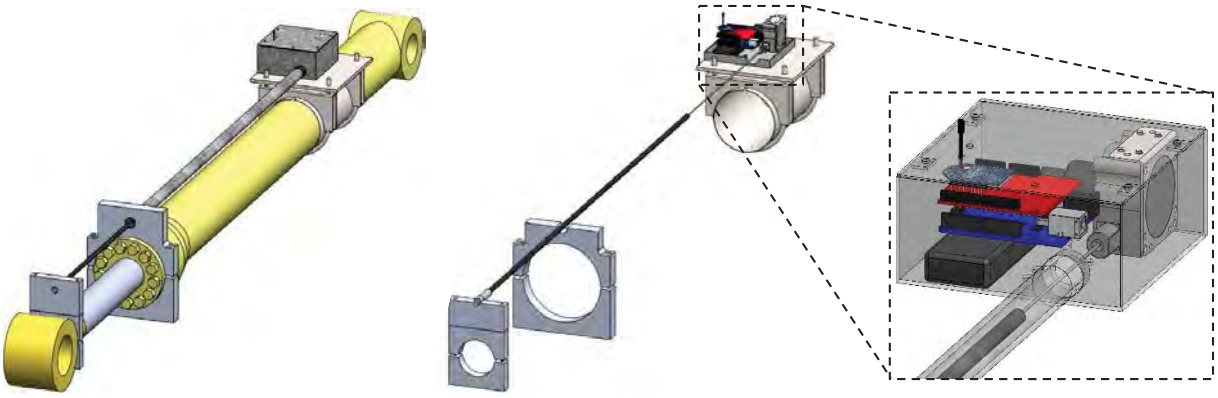

Figure 7. Cable potentiometer prototype

System Calibration

Three types of calibration are necessary for an articulated machine pose estimation system implementing the above camera marker network design.

The first type is intrinsic calibration which determines internal parameters (e.g., focal length) of all cameras in the system. This is done using same methods as in (Feng, Xiao, Willette, McGee, & Kamat, 2014).

The second type is extrinsic calibration which determines relative poses (e.g. dotted edges in the graph) designed to be calibrated before system operation. There are two kinds of such poses: 1) poses of static markers in the world frame, and 2) poses between rigidly connected cameras. The first kind of poses can be calibrated by traditional surveying methods using a total station. The second kind of poses, however, cannot be directly surveyed physically since a camera frame's origin and principal directions usually cannot be found or marked tangibly on that camera. Thus to calibrate a set of m rigidly connected cameras, a camera marker graph needs to be constructed as denoted in Figure 8. A set of n markers' poses need to be surveyed in the world frame. Then when the m cameras observe these n calibration markers, the graph is formed to estimate each camera's pose in the world frame and thus their relative poses between each other (i.e., edges with question mark) are calibrated. It is suggested to ensure that multiple loops exist in this graph to improve the accuracy of the poses to be calibrated. Such loop exists as long as at least two markers are observed by a same camera simultaneously. It is also worth noting that with enough many calibration markers, each camera's intrinsic parameters can be further optimized together with their extrinsic parameters.

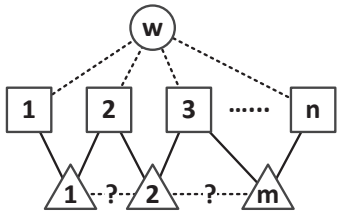

Figure 8. A camera marker graph for extrinsic calibration

The third and final type of calibration involves mapping a relationship between the cable potentiometer output and the pose of the excavator's bucket. The calibration process requires a marker to be attached to the side of the bucket for the duration of the calibration process. The system is then calibrated by moving the bucket through its range of motion and mapping the potentiometer output to the relative transformation between the stick marker and bucket teeth. After the calibration process, the marker is removed from the bucket. The system then functions by measuring stick marker pose and cylinder stroke length, and mapping such measurements to bucket tooth pose.

Uncertainty Analysis

It is not sufficient to only estimate the pose of an articulated machine. The uncertainty of the estimated pose is critical for the following reasons. Firstly the uncertainty provides a measure of the confidence level of the estimated pose, which is necessary for many downstream applications (e.g., deciding buffer size for collision avoidance). Secondly it serves as a tool for evaluating the stability of the pose estimation system under different configurations, and thus further guiding to avoid critical configurations that lead to unstable pose estimation.

To perform uncertainty analysis on the proposed camera marker network pose estimation system, the system is firstly abstracted as the following state space model:

$$\mathbf{Z} = \mathbf{F}(\mathbf{X}; \mathbf{Y}, \mathbf{C}) \tag{1}$$

where **X** is the state vector of the network (usually encodes the poses of nodes in the graph), **Z** is the predicted measurement vector containing image coordinates of all the points projected from markers, **Y** is the known parameters (usually contains marker points' local coordinates), **C** is the calibrated parameters (usually encodes all cameras' intrinsic parameters and all calibrated poses), and **F** is the system's observation function parameterized by **Y** and **C**, i.e., the camera perspective projection function.

For example, for a network of a single camera and a single marker, **X** is a 6×1 vector that encodes the marker's orientation and position in the camera frame; **Y** is a $3n \times 1$ vector containing *n* marker points' coordinates from surveying; **C** is a vector of the camera intrinsic parameters. If another marker is added to this network, **Y** should be extended with points on the new marker.

Uncertainty Propagation

No matter how complex such a network is and what method is used to get an initial estimate of **X** (either PnP or homograph decomposition), the optimized state $\hat{\mathbf{X}}$ can be calculated by the following least square optimization, i.e., bundle adjustment:

$$\hat{\mathbf{X}} = \arg\min_{\mathbf{X}} \left\| \hat{\mathbf{Z}} - \mathbf{F}(\mathbf{X}; \mathbf{Y}, \mathbf{C}) \right\|^2_{\mathbf{P}_{\hat{\mathbf{Z}}}} \tag{2}$$

where $\mathbf{P}_{\hat{\mathbf{Z}}}$ is the a priori covariance matrix of the actual measurements $\hat{\mathbf{Z}}$, typically assumed as $\sigma_u^2 \mathbf{I}$ when image coordinates are measured with a standard deviation of σ_u.

To backward propagate the measurement uncertainty $\mathbf{P}_{\hat{\mathbf{Z}}}$ to the uncertainty of the optimized state $\hat{\mathbf{X}}$ requires linearization of **F** around $\hat{\mathbf{X}}$. Since the error is assumed to come from only the measurements (the uncertainty in calibrated parameters **C** can be included in future work, but is assumed to be negligible in this paper), one can directly apply the results in (Hartley & Zisserman, 2000) to calculate the uncertainty of the optimized states:

$$\mathbf{P}_{\hat{\mathbf{X}}} = (\mathbf{J}^{\mathrm{T}}\mathbf{P}_{\hat{\mathbf{Z}}}^{-1}\mathbf{J})^{-1} = \sigma_u{}^2(\mathbf{J}^{\mathrm{T}}\mathbf{J})^{-1} \tag{3}$$

where $\mathbf{J} = \left.\frac{\partial \mathrm{F}}{\partial \mathbf{X}}\right|_{\hat{\mathbf{X}}}$ is the Jacobian matrix of **F** evaluated at $\hat{\mathbf{X}}$.

Uncertainty and Configuration

Equation (3) not only provides a means of evaluating uncertainty of the optimized pose estimation of a camera marker network, but also provides a tool to predict the system stability at any given system configuration **X** before even making any measurements. This is done by evaluating the Jacobian matrix **J** of F at that **X**, and then applying equation (3) to predict the covariance matrix. It is based on the fact that the aforementioned backward propagation of measurement uncertainty does not directly rely on specific measurements. In fact it directly relies on the system configuration **X** around which the linearization is performed. Thus, when evaluating Jacobian matrix **J** at a configuration **X**, equation (3) yields the theoretically best/smallest pose estimation uncertainty one can expect at that configuration, which denotes the system stability at that configuration.

Using this method, some important empirical conclusions on the basic single-camera single-marker system are found about relationships between system stability and configuration, based on numerical experiments, which are useful for more complex system design and are listed as follows. Similar analysis will be performed to multiple-camera or multiple-marker system in future work.

1. *The marker's origin/position in the camera frame, ${}^c\mathbf{t}_m$, has the largest uncertainty along a direction nearly parallel to the camera's line of sight to the marker*, i.e., ${}^c\mathbf{t}_m$ itself. Figure 9 exemplifies this observation at two randomly generated poses between the camera and the marker.

2. *The largest uncertainty of marker's position in the camera frame increases approximately quadratic to the marker's distance to the camera; compared to which the two smallest uncertainty's increases are almost negligible*. Figure 10 shows a typical example.

3. *The largest uncertainty of marker's position in the camera frame increases approximately linear to the camera focal length; compared to which the two smallest uncertainty's increases are almost negligible*. Figure 11 shows a typical example.

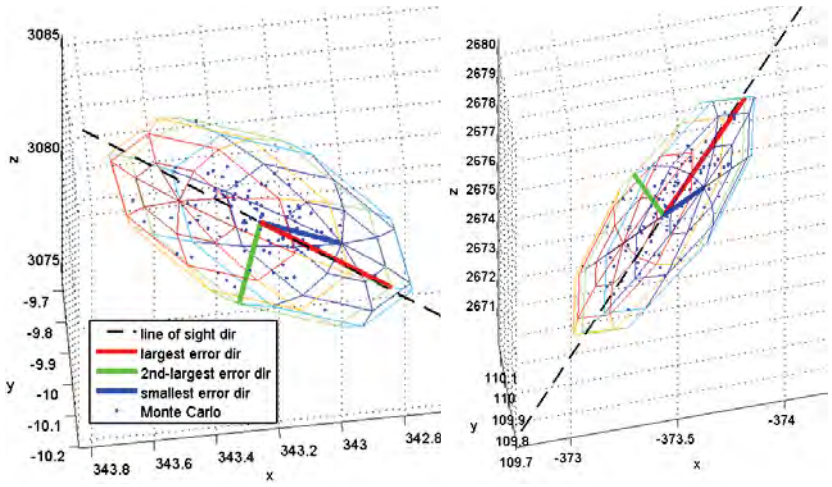

Figure 9. Largest position error direction

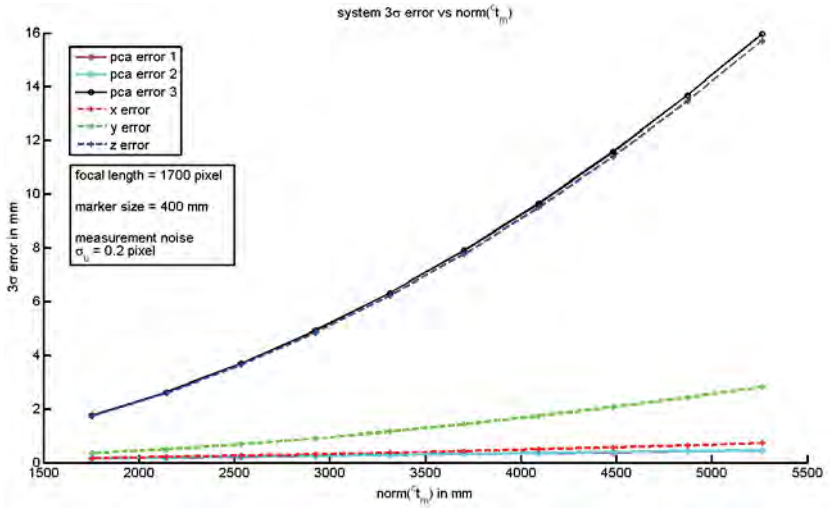

Figure 10. Position error vs marker distance

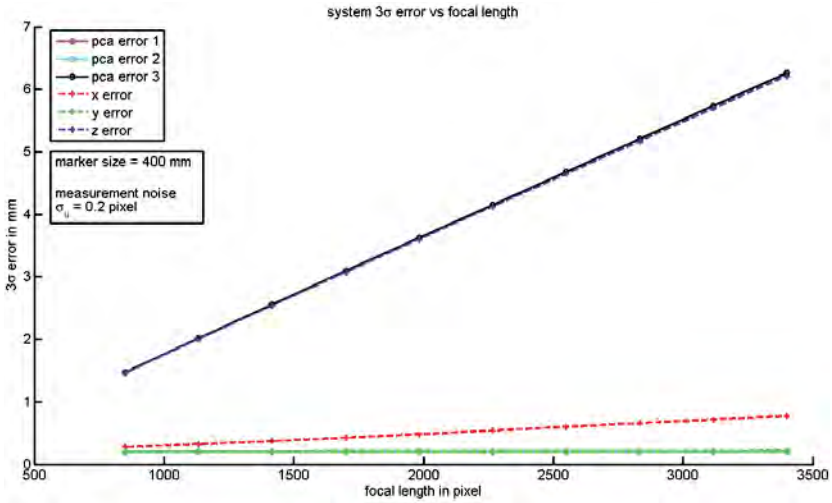

Figure 11. Position error vs focal length

EXPERIMENTAL RESULTS

Feasibility Experiments

Before implementing the pose estimation system prototypes, a set of experiments were performed to test the feasibility of marker based pose estimation in different indoor/outdoor construction environments. In all the experiments, AprilTag (Olson, 2011) was chosen as the basic marker detection and tracking algorithm.

Firstly, the outdoor detectability of markers was tested. A marker's detectability is a function of many factors including the marker size, the distance between the marker and the camera, included angle between the camera viewing direction and the marker plane's normal direction, and also image resolution. Since the distance between the marker and the camera is the most critical factor affecting the method's feasibility in real applications, this experiment is performed by fixing other factors and then gradually increasing the distance of the marker in front of the camera, until the algorithm fails to detect the marker, and recording the distance. Varying other factors and repeating this process results in Table 1. One can consult this table to decide how large the marker should be to fit application need.

Table 1. Outdoor detectability of AprilTag

Max Detectable Distance (m)		Marker Angle (degree)			
		0	45	0	45
Marker Size (m^2)	0.2 x 0.2	6.10	4.88	11.28	8.84
	0.3 x 0.3	8.23	7.01	14.94	11.58
	0.46 x 0.46	13.41	11.28	25.91	21.64
	0.6 x 0.6	19.51	16.46	34.44	30.48
Image Resolution		640 x 480		1280 x 960	
Focal Length		850 pixels		1731 pixels	
Processing Rate		20 Hz		5 Hz	

Secondly, illumination is a critical factor affecting performance of many computer vision algorithms. The AprilTag algorithm was thus tested under various illumination conditions to examine its robustness for construction applications. Figure 12 shows successful marker detection under different indoor/outdoor lighting conditions. These experiments and following extensive prototype tests proved AprilTag based marker detection method's robustness to illumination changes.

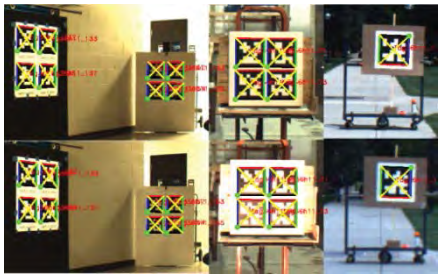

Figure 12. Marker detection vs illumination

Finally, for uncertainty propagation, one needs to have a prior estimation of the image measurement noise's standard deviation σ_u. This is achieved by collecting multiple images under a static camera marker pose. Repeating this process for different poses and collecting

corresponding image measurement statistics lead to an image measurement covariance matrix $\boldsymbol{\Sigma}_u$, which can be further relaxed to $\sigma_u^2\mathbf{I}$ to include all the data points. Figure 13 shows that $\sigma_u = 0.2$ pixel is reasonable.

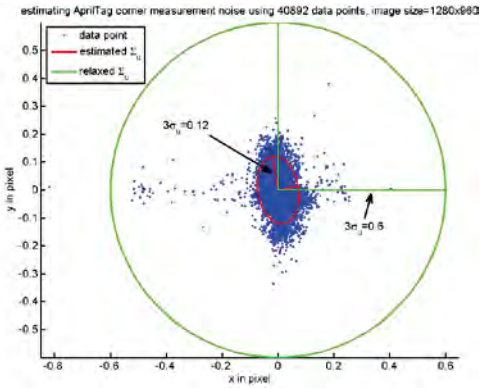

Figure 13. Image measurement noise estimation

Mockup Experiments

As previously mentioned, a multiple-camera multiple-marker articulated machine pose estimation prototype has been implemented with the application of estimating an excavator's bucket depth in a project frame, which could be used for automatic excavation guidance and grade control.

The top row of Figure 14(a) shows the camera cluster of the prototype in Figure 1, and different experiment configurations to test the depth estimate's accuracy. The experiments were setup by observing the two markers in the bottom row of Figure 14(a) using the two cameras in the cluster respectively. Then the depth difference between the two markers was estimated using the proposed method, while the ground truth depth difference between the two marker centers was measured by a total station with 1 mm accuracy. Figure 14(b) illustrates the configurations of different sets of such experiments, for comprehensive tests of the method's accuracy under several system and design variations. The first set varies one of the marker's pitch angle (top row of the figure). The second set varies its height (bottom-left). The third set varies its distance to the camera (bottom-middle). And the fourth set varies the number of tags used in that marker (bottom-right).

(a) Setup

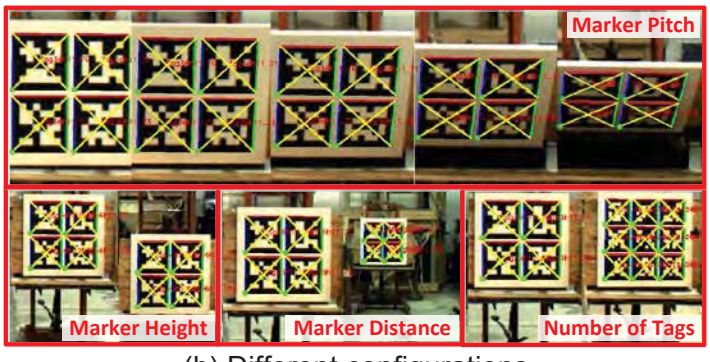

(b) Different configurations

Figure 14. Mockup experiment setup

Figure 15 shows the absolute depth errors comparing the ground truths with the results from camera marker network pose estimation, in the above mentioned different sets of prototype experiments, using the box quartile plot. Note that **all errors are less than 2.54 cm, even when observed from more than 10 meters away**. Further experiments showed that the system worked up to 15 meters.

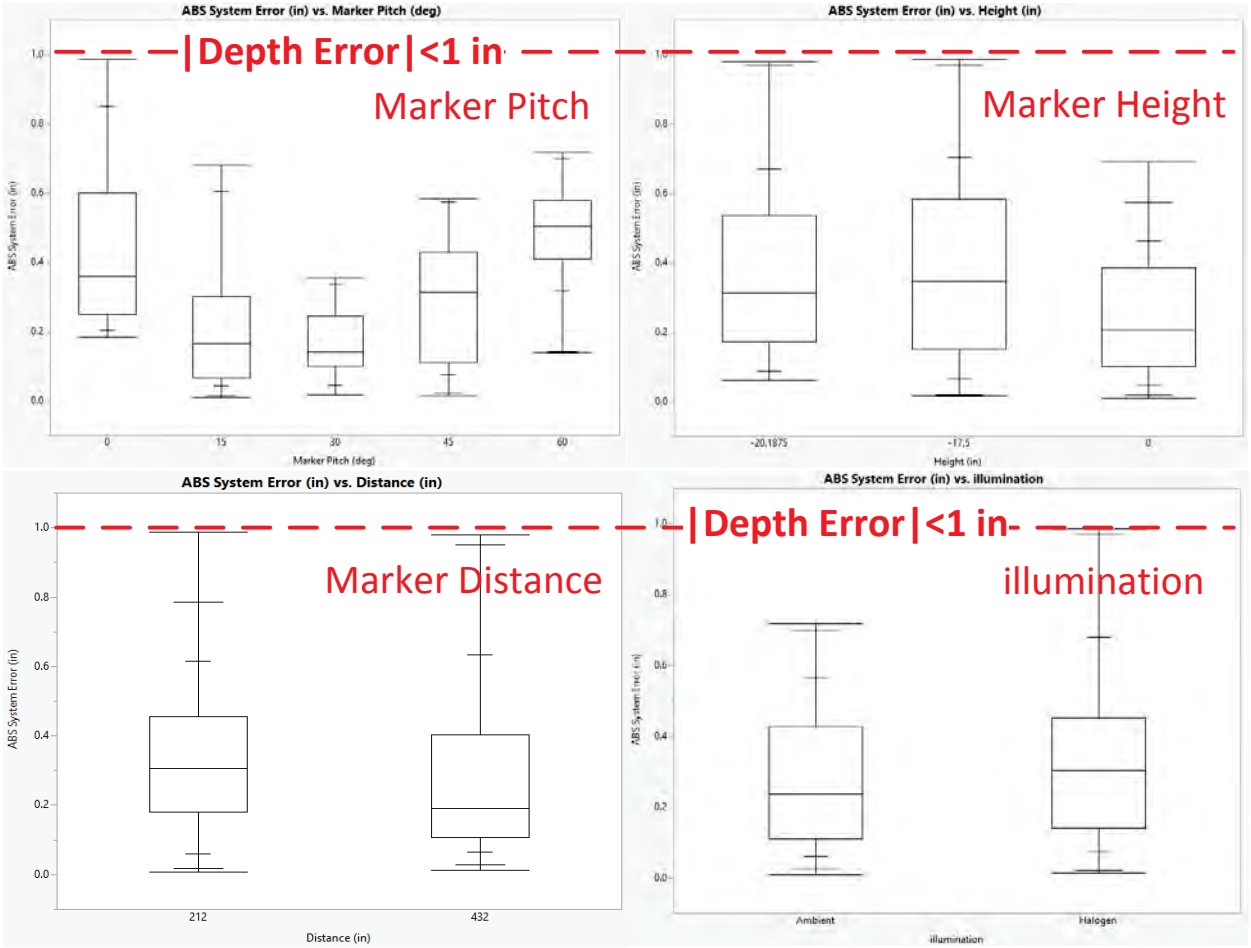

Figure 15. Error vs. configuration

Prototype Experiments

Another experiment was conducted to characterize the performance of the cable potentiometer prototype. The prototype was installed and tested on a Caterpillar 430E IT Backhoe Loader, as shown in Figure 16. The experiment involved calibrating the sensor system, placing the backhoe in random poses, using the sensors to estimate bucket tooth height, and comparing estimates with ground truth measurements obtained using a total station. The experiment's pass/fail criterion was set at 2.5 centimeters (1 inch) of absolute error.

Figure 16. Calibration of cable potentiometer prototype installed on a backhoe

A total of eight trials were conducted. For each trial, three components of tooth position (*x*, *y*, and *z*, where *y* corresponds to the zenith direction) were measured and compared with ground truth measurements, as shown in Figure 17. Of the twenty-four data points collected, only three points exceeded the pass/fail criterion of 2.5 centimeters (1 inch) of absolute error. Though the system's ability to estimate *x*-position only marginally met the pass criterion, the system's performance as a whole was deemed satisfactory, especially considering that accuracy along the zenith direction is more important in many excavation applications.

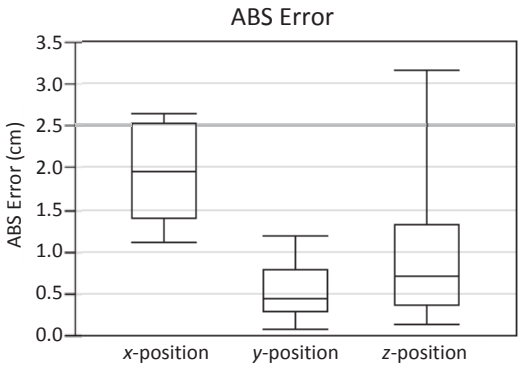

Figure 17. Cable potentiometer experimental results

The cable potentiometer prototype was also tested on an active construction site, as shown in Figure 1 and Figure 18. The system was used to assist the operator in trenching operations. A computer screen was mounted in the operator's cabin, providing a display of bucket height relative to a desired trench grade specified by the job plans.

Figure 18. Cable potentiometer prototype installed on excavator

Shown in Figure 19 is a short section of trench in which the operator conducted a side-by-side comparison of traditional grading versus grading guided by the sensor system. The resulting trench depth differences between the manual grade and the guided grade (by the prototype) were less than 1 inch, which fulfils the need of many construction applications.

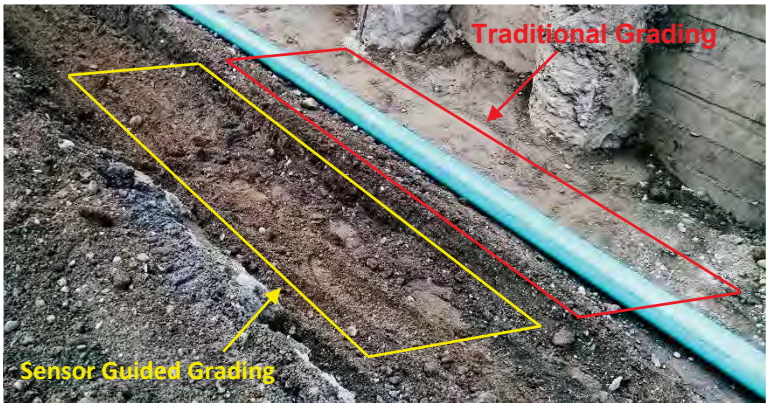

Figure 19. Comparison of sensor guided grading versus traditional grading

CONCLUSIONS AND FUTURE WORK

This paper proposed a vision based pose estimation solution for articulated machines using a camera marker network. The uncertainty of the network pose estimation is analyzed through backward propagation of measurement covariance matrix. Based on this, an efficient approach of evaluating such a pose estimation system's uncertainty at any given state is introduced and applied to the basic single-camera single-marker system to find some important relationships between system states and corresponding system uncertainty, which is useful to guide more complex design. The conducted experiments and a working prototype proved the proposed solution's feasibility, robustness, and accuracy for real world construction applications.

The authors' current and planned work in this research direction is focused on continuously improving the estimation accuracy such as taking the uncertainty of calibrated parameters **C** into

consideration, and also analyzing uncertainty versus system configuration for more complex camera marker networks.

ACKNOWLEDGMENTS

This research was funded by the United States National Science Foundation (NSF) via Grants CMMI-1160937, CMMI-1265733, and IIP-1343124. The authors gratefully acknowledge NSF's support. The authors also thank Walbridge Construction Company, Eagle Excavation Company, and the University of Michigan Architecture, Engineering and Construction (AEC) division for their support in providing access to construction equipment and job sites for experimentation and validation. The authors would also like to thank Dr. Manu Akula, Dr. Ehsan Rezazadeh Azar, and Mr. Nicholas Fredricks for their invaluable help during experiments. Any opinions, findings, conclusions, and recommendations expressed in this paper are those of the authors and do not necessarily reflect the views of the NSF, Walbridge, Eagle Excavation, or the University of Michigan. Suyang Dong and Vineet R. Kamat have a significant financial and leadership interest in a start-up company named Perception Analytics & Robotics LLC (PeARL), and are the inventors of technology (proposed to be licensed by PeARL) involved in or enhanced by its use in this research project.

REFERENCES

Borthwick, J., Lawrence, P., & Hall, R. (2009). Mining haul truck localization using stereo vision. *Proceedings of the Robotics and Applications Conference*, *664*, p. 9.

Brookshire, J. (2014). *Articulated pose estimation via over-parametrization and noise projection.* Cambridge: MIT.

Bureau of Labor Statistics. (2013). *Census of Fatal Occupational Injuries (CFOI) - Current and Revised Data.* Retrieved February 3, 2015, from http://www.bls.gov/iif/oshcfoi1.htm

Cheng, P., & Oelmann, B. (2010). Joint-angle measurement using accelerometers and gyroscopes—A survey. *IEEE Transactions on Instrumentation and Measurement, 59*(2), 404--414.

Cho, Y., & Gai, M. (2014). Projection-Recognition-Projection Method for Automatic Object Recognition and Registration for Dynamic Heavy Equipment Operations. *Journal of Computing in Civil Engineering, 28*(5), A4014002.

Common Ground Alliance. (2015, March 03). *Survey finds that nearly half of homeowners who plan to dig this year will put themselves and others at risk by not calling 811 before starting*. Retrieved May 18, 2015, from http://commongroundalliance.com/media-reports/press-releases/survey-finds-nearly-half-homeowners-who-plan-dig-year-will-put

Cui, Y., & Ge, S. (2003). Autonomous vehicle positioning with GPS in urban canyon environments. *IEEE Transactions on Robotics and Automation, 19*(1), 15--25.

Duff, E. (2006). Tracking a vehicle from a rotating platform with a scanning range laser. *Proceedings of the Australian Conference on Robotics and Automation*, *12.*

Feng, C., & Kamat, V. R. (2012). Plane Registration Leveraged by Global Constraints for Context-Aware AEC Applications. *Computer-Aided Civil and Infrastructure Engineering, 28*(5), 325-343.

Feng, C., Xiao, Y., Willette, A., McGee, W., & Kamat, V. R. (2014). Towards Autonomous Robotic In-Situ Assembly on Unstructured Construction Sites Using Monocular Vision. *Proceedings of the 31th International Symposium on Automation and Robotics in Construction*, (pp. 163-170). Sydney, Australia.

Ghassemi, F., Tafazoli, S., Lawrence, P., & Hashtrudi-Zaad, K. (2002). An accelerometer-based joint angle sensor for heavy-duty manipulators. *Proceedings of IEEE International Conference on Robotics and Automation*, *2*, pp. 1771--1776.

Hartley, R., & Zisserman, A. (2000). *Multiple view geometry in computer vision.* Cambridge University Press.

Hel-Or, Y., & Werman, M. (1994). Model based pose estimation of articulated and constrained objects. *ECCV* (pp. 262--273). Springer.

Kashani, A., Owen, W., Himmelman, N., Lawrence, P., & Hall, R. (2010). Laser Scanner-based End-effector Tracking and Joint Variable Extraction for Heavy Machinery. *The International Journal of Robotics Research, 29*(10), 1338-1352.

LCCI/KPMG. (2014). *Skills to Build: LCCI/KPMG Construction Skills Index 2014.* Retrieved February 6, 2015, from http://www.kpmg.com/uk/en/issuesandinsights/articlespublications/pages/construction-skills-index-2014.aspx

Lee, S., Kang, M.-S., Shin, D.-S., & Han, C.-S. (2012). Estimation with applications to dynamic status of an excavator without renovation. *Gerontechnology, 11*(2), 414.

Lin, L.-H., Lawrence, P., & Hall, R. (2013). Robust outdoor stereo vision SLAM for heavy machine rotation sensing. *Machine vision and applications, 24*(1), 205--226.

Memarzadeh, M., Heydarian, A., Golparvar-Fard, M., & Niebles, J. (2012). Real-time and automated recognition and 2D tracking of Construction workers and equipment from Site video streams. *Int. Workshop on Computing in Civil Engineering.*

Olson, E. (2011). AprilTag: A robust and flexible visual fiducial system. *Proceedings of the 2011 IEEE International Conference on Robotics and Automation*, (pp. 3400-3407).

Rezazadeh Azar, E., & McCabe, B. (2012). Part based model and spatial--temporal reasoning to recognize hydraulic excavators in construction images and videos. *Automation in construction, 24*, 194--202.

US DOT PHMSA. (2015). *Pipeline Incident 20 Year Trends.* Retrieved February 4, 2015, from http://www.phmsa.dot.gov/pipeline/library/datastatistics/pipelineincidenttrends

Yang, J., Vela, P., Teizer, J., & Shi, Z. (2011). Vision-based crane tracking for understanding construction activity. *Proc. ASCE IWCCE*, 258--265.

A User-centered Approach to Investigate Unmanned Aerial System (UAS) Requirements for a Department of Transportation Applications

Masoud Gheisari
Building Construction Science Program
Mississippi State University
823 Collegeview St. 132C Howell Building
Mississippi State MS 39762;
mgheisari@caad.msstate.edu

Javier Irizarry
School of Building Construction
Georgia Institute of Technology
245 4th Street, NW, Rm 138
Atlanta, GA 30332
javier.irizarry@caad.gatech.edu

ABSTRACT

This user-centered study explored the usability of Unmanned Aerial Systems (UASs) in Georgia Department of Transportation (GDOT) operations. The research team conducted a series of semi-structured interviews with subject matter experts in GDOT divisions. Interviews focused on (1) the basic goals of the operators, (2) their major decisions for accomplishing those goals, and (3) the information requirements for each decision. Following an interview validation process, a set of UASs design characteristics that fulfill user requirements of each previously identified division was developed. And ultimately five reference systems were proposed using a house-of-quality viewgraph to illustrate the relationships between GDOT tasks and potential UASs aiding those operations. Each of these five reference systems (Flying Camera, Flying Total Station, Perching Camera, Medium Altitude & Long Endurance (MALE), and Complex Manipulation) was then discussed in terms of its Airframe, Payload, Control Station, and System capabilities. These technical requirements determined would aid in more rapid development of test UASs for GDOT use as well as advance GDOT's implementation of UASs to help accomplish the Department's goals.

Key words: human-centered technology—unmanned aerial system (UAS)—house of quality (HoQ)

Proceedings of the 2015 Conference on Autonomous and Robotic Construction of Infrastructure, Ames, Iowa.

INTRODUCTION

Innovative applications of Unmanned Aerial System (UAS) for improved mapping operations take advantage of several inherent characteristics of UAV systems. For instance, aerial video, collected by visible or infrared video cameras deployed on UAV platforms, is rapidly emerging as a low cost, widely used source of imagery for response to time-critical disaster applications (Wu and Zhou 2006) or for the purpose of fire surveillance (Wu et al. 2007).

During the past decade, UASs have been applied in a wide range of traffic management, transportation and construction disciplines related to Departments of Transportation (DOTs), including traffic surveillance *(1,2)*, traffic simulation *(3,4)*, monitoring of structures *(5,6),* avalanche control *(7)*, aerial assessment of road surface condition *(8)*, bridge inspection *(9)*, and safety inspection on jobsite *(10)*. States such as Virginia *(11)*, Florida *(12)*, Ohio and Washington *(1),* Utah *(13)* were leading UAS application and implementation within their DOTs. This chapter introduces a wide variety of UAS applications in traffic management, transportation and construction disciplines related to DOTs. One of the very recent UAS-based projects supported by a DOT was in the State of Georgia in which a group of researchers from the Georgia Institute of Technology explored the feasibility of using this leading edge technology in several divisions and offices within GDOT *(14, 15, 16)*. The goal of this study was aligned with the Federal Aviation Administration (FAA) goals of efficient integration of UASs into the nation's airspace for civilian and public applications. Integrating UAS into GDOT practices might seem very beneficial at first glance, but the most important issue that was investigated at the first step in that GDOT-supported project was to see how usable this technology could be within GDOT divisions and offices.

RESEARCH METHODOLOGY

Having the UAS might seem very useful for most GDOT practices but the very first issue that should be resolved is whether this technology would be usable for different applications within GDOT divisions and offices. A usable UAS should be designed firstly by investigating the user requirements across all divisions and offices of GDOT and then identifying and developing a set of design characteristics for the UAS based on the previously identified user requirements. Even when a real UAS is designed based on user requirements; it should be tested using real users of the system to evaluate its applicability and usability. The work plan of this research has been illustrated in Figure 1.

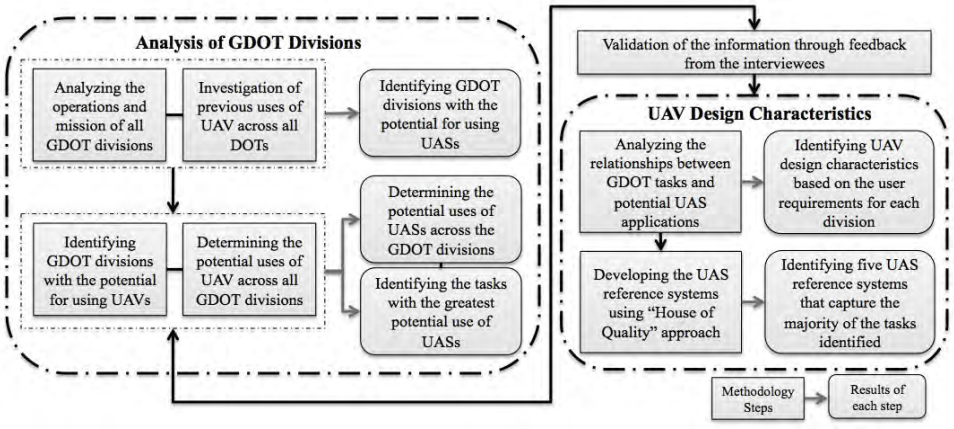

Figure 1. Project Methodology

The research team first studied all GDOT divisions and offices to identify those that were expected to have a potential for using UASs. This analysis was performed by investigating the

operations, mission and sets of responsibilities that each division and their internal offices have. At the same time, previous uses of UASs across all DOTs as well as the current status of different civilian applications of UASs were investigated. This step resulted in the identification of four divisions (of the twelve overall divisions of GDOT) with the highest potential for benefitting from UAS technology; construction, engineering, intermodal, permits and operation. Semi-structured interviews were conducted with subject matter experts in each identified division to identify the basic goals of the operators and the information requirements for each decision. Once the potential uses of UASs across the GDOT divisions were determined, more than 40 tasks were identified and selected as the tasks with the greatest potential use of UAV in the near term. The majority of the tasks are centered around collecting data, providing information, and decision making based on the data. Currently most of the related data are collected through field personnel. All of the information was validated through feedback from the interviewees. Finally, this step resulted in the identification of 19 main tasks as well as their duration, frequency, and environment. Following the interview validation process, a set of UASs design characteristics that fulfill user requirements of each previously identified division was developed. The following sections provide more details on the analysis of GDOT divisions and technical and operational requirements of UASs.

ANALYSIS OF GDOT DIVISIONS

All divisions and offices of the GDOT were studied to identify the divisions with the highest potential for benefitting from UAV technology. The GDOT consists of 8 divisions; each relating to a major area of transportation concern as follows: administration, construction, engineering, finance, intermodal, local grants and field services, program delivery, and permits and operations.

This analysis is performed by investigating the operations, mission and sets of responsibilities that each division and their internal offices might have. Having a clear understating of what other DOTs have done and determining the current status of civilian application of UAVs were utilized to identify different divisions of GDOT with potential of applying UAVs. Of the twelve overall divisions of GDOT, four divisions with the highest potential for benefitting from UAV technology were selected for further investigation (construction, engineering, intermodal, permits and operation). Figure 2 shows some of the tasks and responsibilities associated with each of the selected GDOT divisions. Through a series of interviews with employees at the division and office level, the user requirements of each identified division/office were investigated.

The Construction Division is responsible for construction contract administration and overseeing construction projects and permitting in the State of Georgia. It conducts general construction oversight and also oversees project advertising, letting and awards, and testing of materials. Furthermore, it inspects and monitors contractual field work, specifies material requirements, and provides geotechnical services. Interviews were conducted with eight engineers at management and operational levels. Its goal is to provide the resources necessary to insure the quality of construction projects by improving decisions made in the field, making information available for training and to maintain statewide consistency.

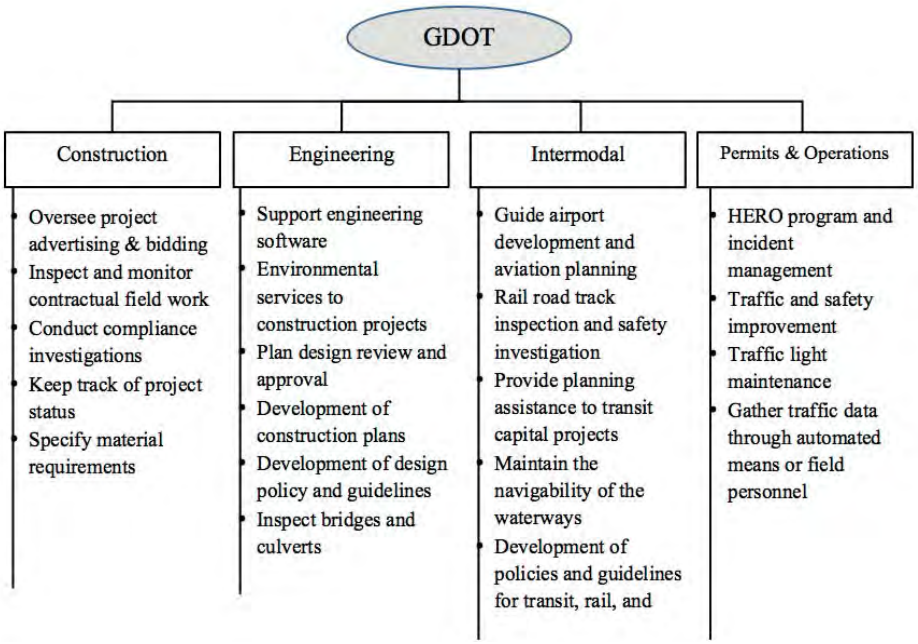

Figure 2. GDOT divisions with the highest potential for benefitting from UAV technology

The Engineering Division develops environmental studies, right-of-way plans, construction plans and bid documents through a cooperative effort that results in project design and implementation. Moreover, the division is responsible for supporting and maintaining all engineering software, engineering document management, and state wide mapping. Four interviews were conducted with persons in charge of activities conducted by the engineering division.

The main responsibility of the Intermodal Division is to support and facilitate the development and implementation of intermodal policies, planning, and projects in the highway program and organize all major statewide non-highway programs for the development of a comprehensive transportation system. The intermodal division consists of four main programs: (1) aviation programs is tasked to guide airport development and to assure a safe and well-maintained system of public-use airports; (2) transit programs provide transit capital and operating assistance to the urban and all metropolitan planning organizations in Georgia; (3) rail programs include track inspection and safety investigation for the Georgia rail system in cooperation with the Federal Railroad Administration; (4) waterways programs maintain the navigability of the Atlantic Intracoastal waterway and Georgia's deep water ports in Savannah and Brunswick. Consequently, five interviews were conducted with members from the intermodal division, including at least one interviewee from each of the above programs.

The Permits and Operations Division ensures a safe and efficient transportation system by collecting traffic data, addressing maintenance needs (e.g. related to traffic lights) and regulating the proper use of the state highway system. In order to improve traffic flow and coordinate traffic engineering, traffic safety, and incident management statewide, the division collects traffic data (e.g. flow, speed, counts) using a wide range of devices (e.g. video cameras, microwave sensors, and computer applications pertaining to traffic services). This division consists of four offices: Transportation Data, Utilities, Traffic Operations, and Maintenance. Interviews were conducted with seven engineers at management, district and area office levels.

IDENTIFICATION OF OPERATIONAL REQUIREMENTS

In order to determine the operational requirements for UAS usage for a specific division that could benefit from such technology, a user-centered top-down approach was chosen. In this user focused approach, the overall tasks and user requirements are categorized into various functions and components, enabling a comprehensive understanding of users' goals, their working environment, and decision-making processes.

The data sample comprised of 24 GDOT employees in the major fields of construction, engineering, intermodal and traffic operations who volunteered to participate in the study. Prior to the interview, all participants were required to give informed consent that explains to an individual who volunteers to participate in the study, the goals, processes, and risks involved. Therefore, each participant was presented with an Informed Consent Form for him or her to read in agreement to participate in the study. The university's Institutional Review Board (IRB) evaluated and approved the study protocol.

Semi-structured interviews were conducted with subject matter experts in each identified division to identify the basic goals of the operators and the information requirements for each decision. Once the potential uses of UASs across the GDOT divisions were determined, more than 40 tasks were identified and selected as the tasks with the greatest potential use of UAV in the near term. The majority of the tasks are centered around collecting data, providing information, and decision making based on the data. Currently most of the related data are collected through field personnel. All of the information was validated through feedback from the interviewees. Finally, this step resulted in the identification of 19 main tasks as well as their duration, frequency, and environment. An example is shown in Figure 3, in which "Construction Site Measurement (Task 04)" is identified as an outdoor, mobile task in the range of 0.5 to 10 miles, and with an approximate duration of 2-3 hours. The information for this frequent task (frequency is hourly and/or daily) is based upon the validated data resulting from the interview process. Of the 7 validated data for construction-related tasks, 71% (5 of 7) of the respondents believed that the task is performed locally. A local task occurs at one location or a job site that can be best described by the length and width of the area. However, a distributed task occurs along a road, a river, or a railway. More details about the tasks and responsibilities associated with each of the selected GDOT divisions can be found in *(14)*.

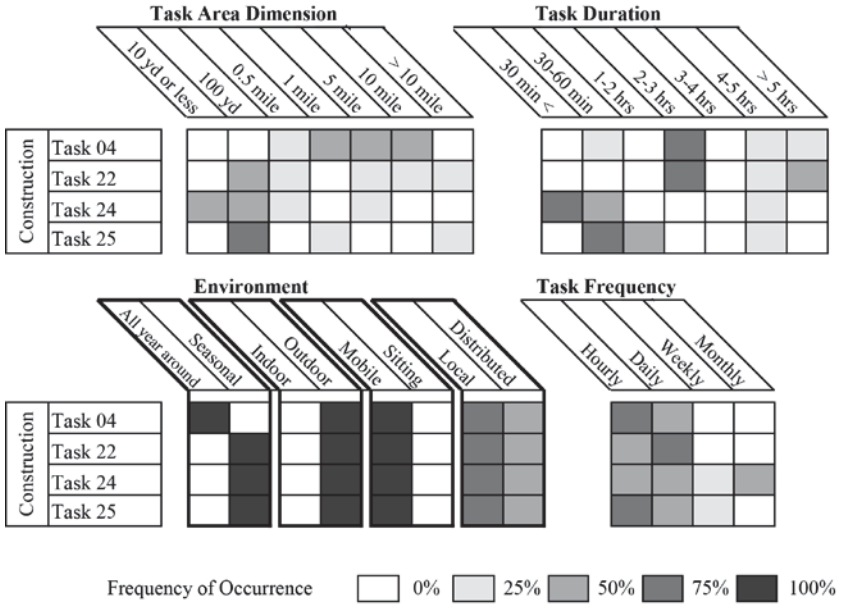

Figure 3. Construction Division Task Requirement Matrix

Based on the records and interviews, the study team created a list of tools used while performing the identified tasks. The tools (and technology) used by the GDOT personnel can be classified under eight categories: Measuring equipment are used in various linear, areas, and counting measurements. Examples include measuring wheel and tape, distance meter, air meters, scoops, and thermometer. Surveying equipment (e.g. theodolite, total station, GPS devices, etc.) are used to produce accurate maps and dimensions of the site. Engineering software tools are used to collect and process observation data from the workplace. The most important example is “Site Manager” software that is used by construction office. Computer hardware, specialized software, and communication devices are used together to collect, analyze, and transmit data collection and communication processes. Basic hand tools and digital cameras are frequently used by GDOT employees traveling out-of-office. Finally, many of the tasks performed by the division of permits and traffic operations require vehicle detection and mobile application tools. Examples include traffic counter, radar gun, range finder, and turning movement counter.

Figure 4 shows the result operational requirement matrix that includes each division’s operation, user characteristics, working environment, and technology use. The frequency of occurrence is calculated based upon the number of tasks performed in each division. To identify missing information and errors in the matrix and validate its outcomes, this matrix was then taken back to the subject matter experts who were interviewed. All of the information was validated through feedback of the interviewees.

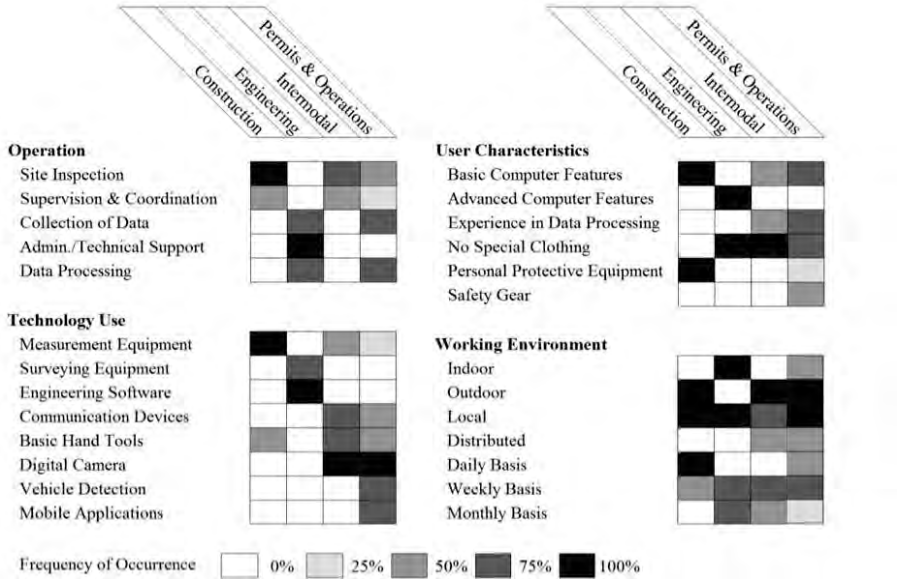

Figure 4. Operational Requirement Matrix

Figure 5 shows the created UAV requirement matrix for the identified divisions within GDOT; the left part is pertaining to the notion of UAV classes, while the right part shows the sensor suites. Based upon the task classification of being either local or distributed, the related primary descriptor (a length or an area, respectively), and the task attributes duration and frequency, the identified tasks can be binned.

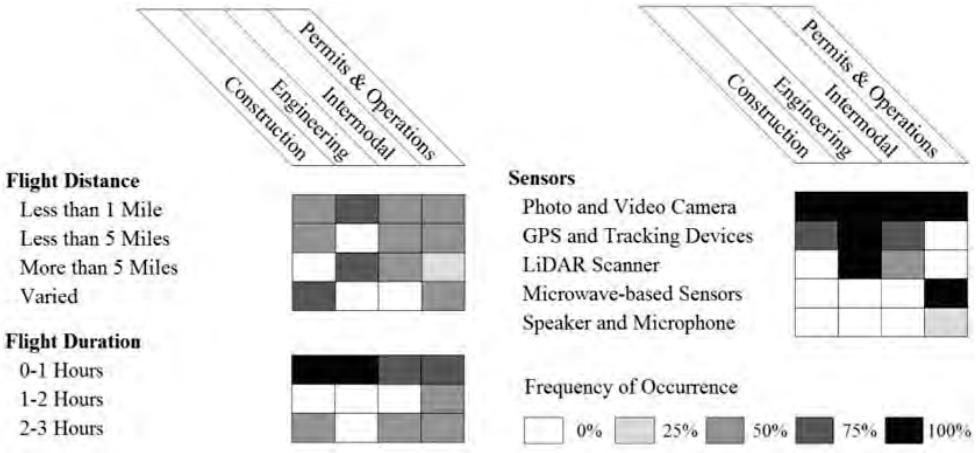

Figure 5. Technical Requirement Matrix

TECHNICAL AND OPERATOR REQUIREMENTS

For the technical analysis, a UAS is broken into three components: Vehicle, Control Station, and System. The Vehicle section groups requirements for the UAV, which are mainly airframe hardware related requirements (Table 1).

Table1. Technical Requirements; Vehicle

Vehicle Requirements	Description
Airframe Ruggedness	tries to capture the overall “sturdiness” of the UAV
Airframe Availability	is one major factor in the overall availability of the UAV, which in essence consists of the airframe, the avionics (the “autopilot”), and the payload (i.e. sensors)
Endurance	is an abstract high-level requirement that tries to capture the technical aspects of available operational time and is mainly driven by the chosen aircraft category (for example, a rotary or fixed wing vehicle) and the size
Actuated Video Camera	requires a video sensor of the airframe to be moveable in any or all of the three axes of motion, roll, pitch, and yaw
Actuated Non-Video Sensor Package	package captures the need to steer other payload sensors, potentially independent of the video source
Telepresence	establishes communication with people in the vicinity of the aircraft usually through a voice and/or video communication feature
Manipulator and/or Effector	usually ranges from simple grappling hooks to fully articulate and very dexterous robotic arms.

The Control Station groups requirements for hard- and software for the control station utilized by the UAS operator, however, the software considered is related to the graphical user interface (GUI) of the interface and does not include specific guidance, navigation, and control (GNC) aspects. The details of these requirements are discussed in the following table (Table 2). Guidance, navigation, and control (GNC) requirements are grouped into the System section, which mainly contains capability features of the reference systems (Table 3)

Table2. Technical Requirements; Control Station

Control Station Requirements	Description
Interactive Object Selection & Identification	relates to the GUI of the control station and requests a simple interface to directly interact with video coming from the UAV
Ruggedness	relates to the capability of control station to be capable of being used outdoors, potentially in harsh conditions
Portability	covers the requirement to easily transport the control station

Table3. Technical Requirements; System Requirements

Control Station Requirements	Description
Sense and Avoid	allows a UAS to detect cooperative as well as non-cooperative traffic in the vicinity of the aircraft and conduct evasive maneuvers if a collision might be imminent
Waypoint Navigation	allows a UAS to follow a flight plan through the means to waypoints
Kinematically Constrained Operations	restricts the possible motion through physical means (e.g. a flexible cable or a rigid connector)
Unattended Deployment and Return	imposes the requirement for automatic take-off and landing without the need of an external pilot
High-precision Navigation	poses the requirement to achieve a navigation solution that is comparable to the accuracy achievable through the use of ground surveying methods (e.g. total station equipment)
Simultaneous Location and Mapping (SLAM)	describes the capability of a system to navigate through a priori unknown environment while building a map of that environment
Advanced Data-link and Networking	captures the need for Radio Frequency (R/F) communication capabilities beyond a simple point-to-point link between the UAV and its control station
Sensor Data Abstraction and Reduction	captures the need for the system to automatically process raw sensor data and only provide the (abstract) result to the operator
Vision Based Data Extraction	captures the request for any kind of computer vision based algorithm like pattern recognition, optical flow, or feature point based processes

The result of the user-centered approach summarized in Figure 2 is a list of operator's requirements. The list is further refined by the subject matter experts who were interviewed. The result of this step was a list of 22 operator requirements (see Table 4).

Table 4. Operator Requirements

#	Requirement	#	Requirement
1	First-Person Video (FPV) Operation	**12**	Precise navigation
2	Non-FPV Operation	**13**	Provides survey-quality data
3	Pilot-independent sensor package control	**14**	Correlate sensor data to plans/drawings
4	Use at construction site	**15**	"Line-of-sight" clearance measurements
5	Use at traffic signal site	**16**	Collect floating traffic samples
6	Metro-area range/coverage	**17**	Allows triggering a "reset"
7	Get point coordinates	**18**	Interact with inspected element
8	Measure site dimensions	**19**	Establish contact to people
9	Estimate volumes	**20**	Eliminate need for human task execution
10	Create digital elevation model	**21**	Conduct traffic counts
11	Count/track/detect items	**22**	Data on demand

REFERENCE SYSTEMS

Based upon the validated data resulting from the interview process, the researchers used their expertise to group tasks based upon a “best fit” to potential UAS and created a set of five reference systems.

System A – Flying Camera

The air unit of System A, the Flying Camera, provides the most basic functionality of placing a (video) camera anywhere in the accessible space and streaming live video to the operator (see Figure 6). This system has been discussed in more details at *(16)*

Usage Scenario: The Flying Camera could be used in any situation where a video or picture is all that is needed as a data input. The operator would simply start the system, use FPV to frame the picture or video needed, record the images and finish the task at hand. The data post processing could be as simple as storing the resulting still photo or video sequence or interacting with the live video feed from the UAV.

Airframe: The airframe for System A would need to be VTOL capable, fairly robust, and safe to be used around people, for example a small scale quad rotor with shrouded propellers. The benefit of a quad rotor over a conventional helicopter would be the reduced mechanical complexity and hopefully a resulting increase in robustness.

Payload: System A would most likely not carry any special payload beside a video camera. Actuating the camera could improve the performance, so, in order to maintain a high level of robustness, a virtual camera tilting could be implemented through several small scale cameras. The setup could provide a low resolution feed and, upon operator request, high(er) definition onboard video recording or still photography.

Control Station: The control station would be primarily focused on ruggedness and portability. A first implementation could be a based on a tablet computer, utilizing on-screen virtual controls, with the potential to expand the setup with a dedicated game pad style controller or a pair of video goggles for improved FPV operation. If goggles are used, the GUI interface of the tablet based control station software would need to be adapted to be compatible to the utilized controller.

Required Infrastructure: No special infrastructure is necessary to operate System A. However, there is the need for training, maintenance, and recharging, which needs to be organized. As the system presumably would be small enough to be transported in a protective case in a car’s trunk or pickup bed, no special transport equipment should be needed.

Capabilities: The systems capabilities would mainly rely on computer vision based algorithms performed off board (i.e. with a transmission time delay) and only with the limited computational power available in a tablet.

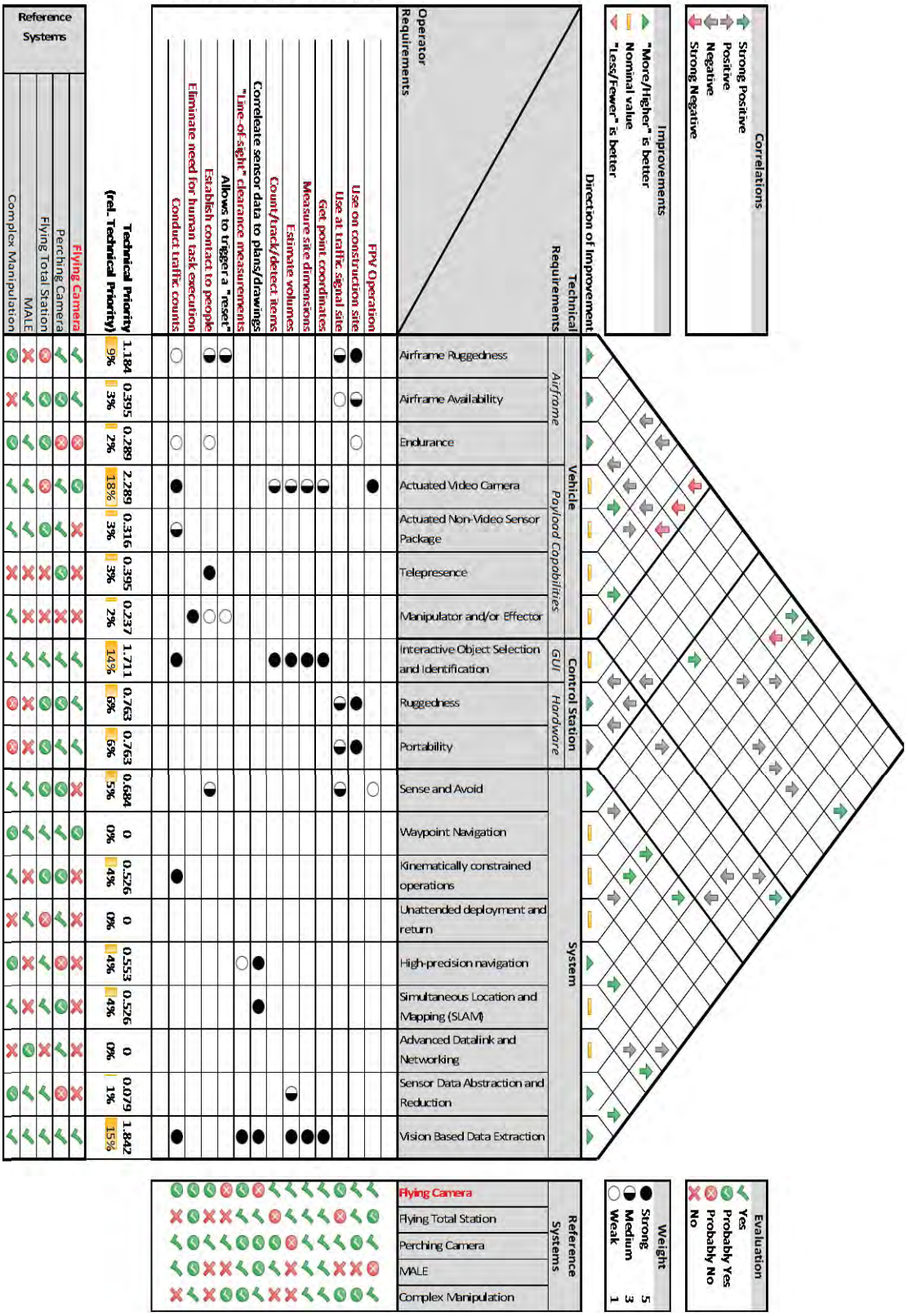

Figure 6. House of Quality for System A (Flying Camera)

System B – Flying Total Station

System B expands upon System A by providing higher quality measurements of the environment. The main focus of the system is to act as a flying total station, i.e. perform tasks similar to the ones done by a survey crew, but faster, especially in otherwise unprepared environments. As the systems' expected operational radius is limited, the UAV could be tethered to a power outlet at the control station site (see Figure 7).

Usage Scenario: The flying total station could be used anytime survey data or location data of survey quality is needed. The system could be brought on scene, maneuvered to the area to be surveyed (either through FPV video or conventional third person flying), and the survey could be started. Post processing would presumably be similar to post-processing regular total station data.

Airframe: System B would need an airframe that is capable of prolonged hover operations, precise positioning, and a certain level of failure tolerance to protect against the loss of potentially expensive sensors. These requirements would point towards a multi copter which is designed for redundancy. This could be a hexa- or octocopter which is sized so that not all rotors are needed to stay airborne. As people, both cooperative as well as non-cooperative, would presumably negatively impact the survey process by blocking line of sight, it can be assumed that the system would be operated in the presence of relatively few cooperative people, as such reducing the requirements for safety through shrouds, etc.

Payload: The system would presumably carry LiDAR equipment to replicate a total station. Additionally, altimeter, for example sonar or laser based, could be used to establish a correct above ground altitude and in reverse determine the elevation of the terrain. Additional onboard computational power might be required to process the LiDAR data.

Control Station: The control station for System B would most likely be comprised of a powerful ruggedized laptop as well as a GNSS reference station to establish a differential correction for the navigation solution.

Required Infrastructure: System B would not need any special communications landing site infrastructure to be operated. However, due to the size of the UAV as well as the additional antennas for the control station, the system most likely would be comprised of some larger crates (to be transportable by pickup or SUV). An alternative would be a dedicated trailer or van. (For more details on dedicated vehicles, see Section 5.2.6, the infrastructure requirements for System E.)

Capabilities: The increased computation power both on- as well as offboard would allow the system to not only utilize vision to detect and identify objects, but also to process video data in combination with the LiDAR data to perform SLAM-based high precision navigation. Furthermore, the system should be able to allow working with digital plans and drawings, for example to check the correct location of construction features, roadway markings, or property boundaries.

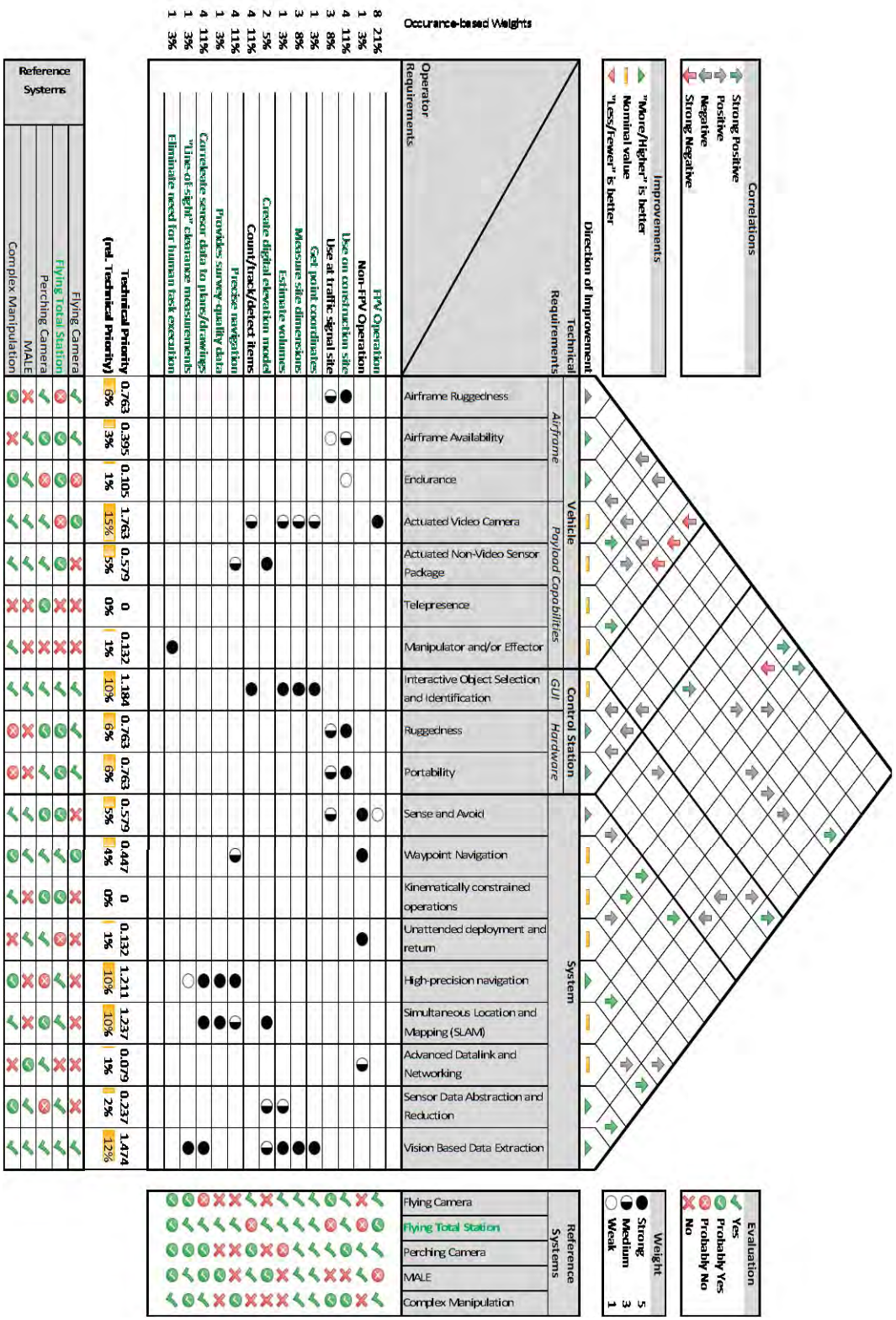

Figure 7. House of Quality for System B (Flying Total Station)

System C – Perching Camera

System C is also expands upon System A, but mainly focusing on a prolonged capturing of the environment. Based upon that, operational endurance is a main application goal of System B. This could either be achieved through highly efficient flight, which might be hard to achieve given that a considerable amount of that flight time could be hover or hover-like operations, or it could be achieved through perching (see Figure 8).

Usage Scenario: Due to the pertinent standby capability perching provides, System C could mainly be used in two modes: as an ad-hoc deployed UAS for local, on-site inspection or measurement tasks, or as a deployed-on-demand system. The former usage is comparable to that of System A. The later usage would imply that System C UAVs have strategically located fixed “base stations,” which would serve as recharging stations and potentially as communication towers. A user requiring services provided by System C would use a control station, request a UAV, and be given control over the closes available air unit. Once the operator doesn’t need the services any longer, the UAV would be released and return to a base station.

Airframe: As a result from the perching requirement, the airframe is required to be relatively small to be able to get to potential perching locations as well as being robust to inadvertent collisions close to the selected perching location. Furthermore, the airframe needs to be equipped with a landing gear of sorts to facilitate perching on poles, or traffic signal installations. These requirements could be realized with a smaller scale hexa-copter or potentially a small electric conventional helicopter.

Required Infrastructure: The perching capability recommends System C for an extended dual use: one the one hand as a mobile UAS with the described capabilities, on the other hand as a static continuously operating camera. A potential scenario could be the deployment of several dedicated perching locations which could double as a charging or refueling station. If the System C units then provide a MANET capability, System C units could, for example, replace the conventional Navigator cameras installed throughout the Atlanta metro area. Resulting from that, a set of permanent perching locations are needed. These base stations would provide recharging capabilities, allow easy access for maintenance, and could also double as R/F communication outlets spanning the MANET utilized by System C.

Payload: Given that perching could limit the achievable attitudes while landed, actuated video and non-video sensor packages are presumably necessary to compensate for that. Given the use cases for System C, it seems likely that the system would also provide telepresence equipment as well as advanced networking capabilities.

Control Station: The control stations for System C could be of several types. Given the potential use cases, operators should be able to use control stations tailored to them and their particular needs: HERO personnel, for example, could utilize a rugged tablet computer based system comparable to a unit used to control System A; GDOT employees working in the Traffic Control Center could use a software that operates on their desktop computers; traffic engineering and traffic management personnel could use a laptop. The control station would provide a FPV interface and a graphical tool for waypoint navigation as well as indicating measurement areas or regions of interest.

Capabilities: System C would mainly provide vision based capabilities, potentially making use of dedicated external computation centers to support limited computation power available in tablet based control stations. The system would expand upon the capabilities of System A, especially toward traffic related tasks.

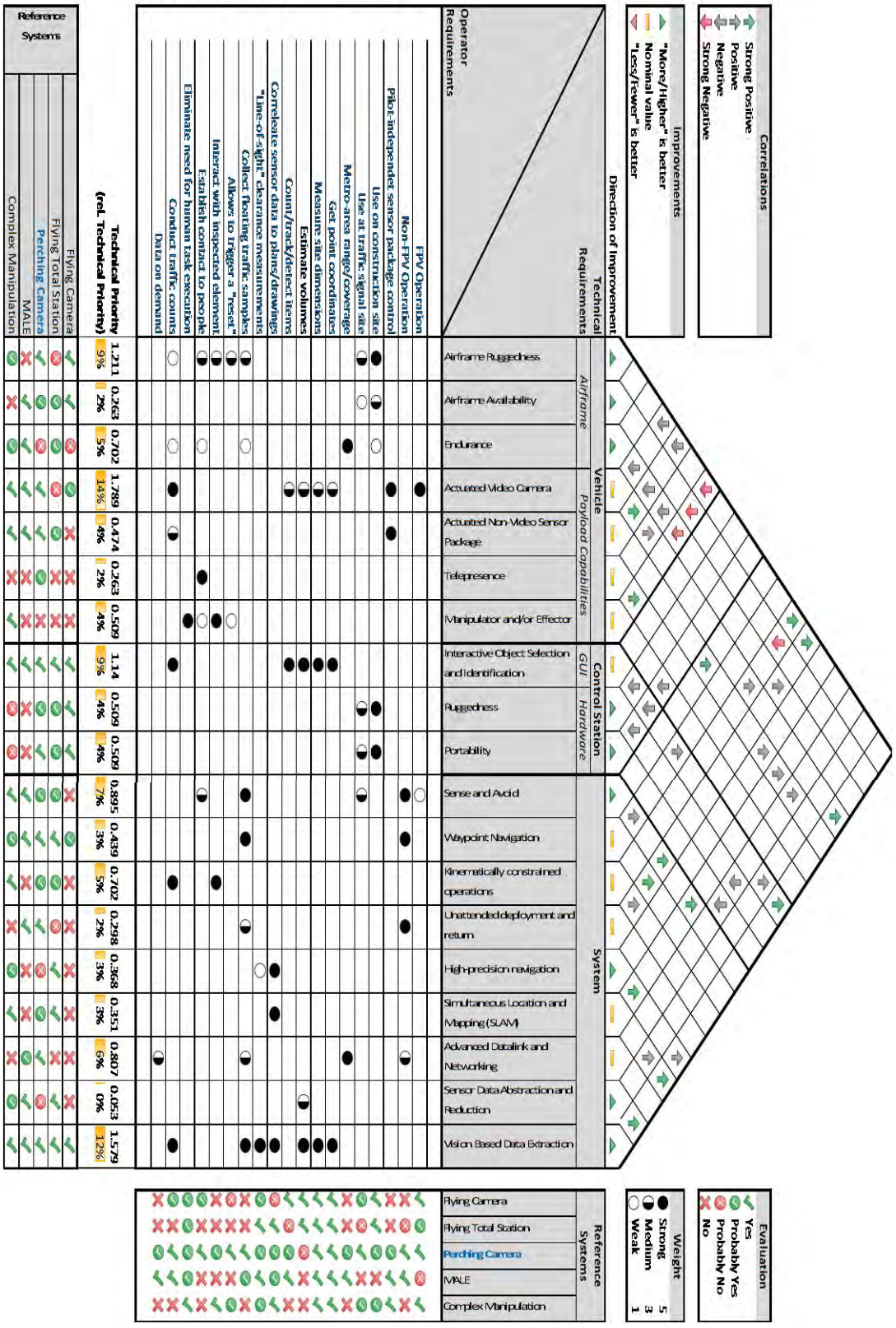

Figure 8. House of Quality for System C (Perching Camera)

System D – Medium Altitude, Long Endurance (MALE)

Whereas the proposed Systems A through C could be classified as having a local operational area, System D is designed to expand this to a regional scale. The UAV would allow long operational usage throughout a county-sized area. The system separates the piloting tasks from the payload operation and data acquisition tasks, allowing for a very high level of operator interaction (see Figure 9).

Usage Scenario: System D could operate in two ways, comparable to System C. In the ad-hoc mode, the UAV would be stationed at an airfield and would get airborne as soon as an operator requests control over a system. In the data-on-demand scenario, the air unit(s) of System C would loiter over a dedicated operational area in a low energy standby mode. Once an operator requests data, the system would relocate to the specific area requested and start to operate its payload sensors.

Airframe: The airframe of choice for System D would most likely be a fixed wing aircraft design, sized somewhere in the 2 m to 6 m wingspan regimen. The airframe would provide all mandated general aviation equipment, for example, aviation band radios, a transponder, and most likely an Automatic dependent surveillance-broadcast (ADS-B) transceiver, as the system would have to operate within the (controlled) national airspace, among other general aviation traffic.

Payload: The system would primarily provide a calibrated pan/tilt/zoom video sensor to provide high quality aerial photography. The system could augment this with ground scanning LiDAR systems and directional antennas for advanced networking features. Further sensor equipment could include microwave based systems to detect traffic movements or near and far infrared systems to aid in the localization of stranded motorists at night or the detection of wild fires. Further optional payload capabilities could include R/F relay stations for first responder disaster response communication systems.

Control Station: The control station for System D would most likely be consisting of several independent units. One of them would be the payload focused unit available to the payload focused operators. Related to that would be a highly portable data display unit, available to first responders on site, which could be used to access the data provided from the system. Separate from that would be a control station for an external pilot which would aid the system during taxi, take-off, and landing operations as well as serve as a voice relay when conversing with ATC.

Required Infrastructure: System D would require an airstrip for take-off and landing. Given that the system should need much smaller take-off and landing distanced, operation out of a general aviation (GA) airport is not necessary and a dedicated airstrip might mitigate a lot of integration into GA ground operations. If a dedicated airstrip is chosen, external pilots for take-off and landing aiding could also have better access to the runway strip. As the system should provide longer range operations, ground communication stations with dedicated directional antennas might be necessary and could also be located at the utilized airstrip. Furthermore, maintenance and refueling opportunities need to be provided.

Capabilities: System D would primarily provide aerial photographic and video data, which would satisfy the quality requirements of photogrammetric applications. The payload operator could also make live feeds of the video data available to first responders or HERO units. System D could also be used as a disaster response communication relay station in case conventional ground based infrastructure would not be available. System D could also provide Navigator like traffic sensing capabilities, which could allow temporary traffic data capturing during larger events outside the conventionally covered areas.

Figure 9. House of Quality for System D (MALE)

System E – Complex Manipulation

An example for this category: This most likely would be a custom made multi-rotor with 8 or more rotors or an even more special “inverted” helicopter, where the main rotor sits below most of the airframe. The multi-rotor configuration or the low main rotor configuration would most likely be necessary to allow an tele-robotics style manipulator to act above the rotor disc(s), as this most likely would be safest for working under bridges. The system would be transported in a dedicated van/truck and could potentially be tethered to allow for prolonged operations in hover and/or while powering the manipulator. The system would most likely have an external (safety) pilot as we well as a remote operator (in the van/truck) (see Figure 10).

System E allows its operators to completely perform a task through telepresence and tele-robotics in areas that are either complicated or dangerous to access for humans. As such the focus of the system shifts from a primarily sensing oriented operation to tasks which include also portions in which previously inspected elements need to be manipulated.

Usage Scenario: System E is specifically slanted to be used for bridge or other structural inspection activities. As such the system would be relocated to the current site under inspection and the operated on site for the duration of the inspection. The main motivation behind System E is to replace special access equipment needed during complex inspection tasks in order to get the human inspector(s) to the inspection site. The system would presumable be used by at least two operators: a dedicated external pilot, primarily responsible for piloting the UAV and maneuvering the unit to the inspection site and a dedicated payload operator who would focus on using the manipulator and effectors to conduct the actual inspection task. As the later presumably would need a feedback device to control the manipulator, the payload operator is assumed to work out of a dedicated control station vehicle, while the pilot operator is located at a vantage point that provides good situational awareness of the situation the UAV operates in. Both operators would have voice communication equipment to coordinate their efforts.

Airframe: The airframe of System E most likely would have to be a custom designed system. As the system’s tasks include object manipulation, the airframe has to support a manipulator or effector of sorts which raises the question of the general geometry of the system. The airframe would have to be able to hover and provide VTOL capabilities, which would mean rotors, but also provide a large operational range for the manipulator. A possible solution could be a large scale multi-rotor where the manipulator is mounted above the main rotor disk, which allows using the system to be used, for example, under bridges. Multirotor configurations are preferable for such arrangements as it is easier ti build airframe structure through the non-rotor occupied center. However, fixing this arrangement would limit the system to tasks in which the manipulator wouldn’t have to be used below the main rotor discs of the multirotor setup. Switching this to a conventional helicopter setup with a rotor head configuration that allows for highly negative pitch angles could, in combination with advanced GNC algorithms, be used to allow such a system to continuously operate in both orientations: manipulator above the main rotor as well as below. The airframe furthermore would have to be strong enough to support not only the manipulator, but also all the forces applied through it. Additionally several thrusters could be needed to provide pushing or pulling forces without major changes in the vehicle attitude.

Payload: The primary payload of System E would be the manipulator or effector and the supporting telepresence and situational awareness sensors. These could include a stereo vision rig, a time-of-flight camera or some similar close range 3D sensor, and LiDAR systems. Additionally the system potentially would have to carry a selection of grappling interfaces and probing tools.

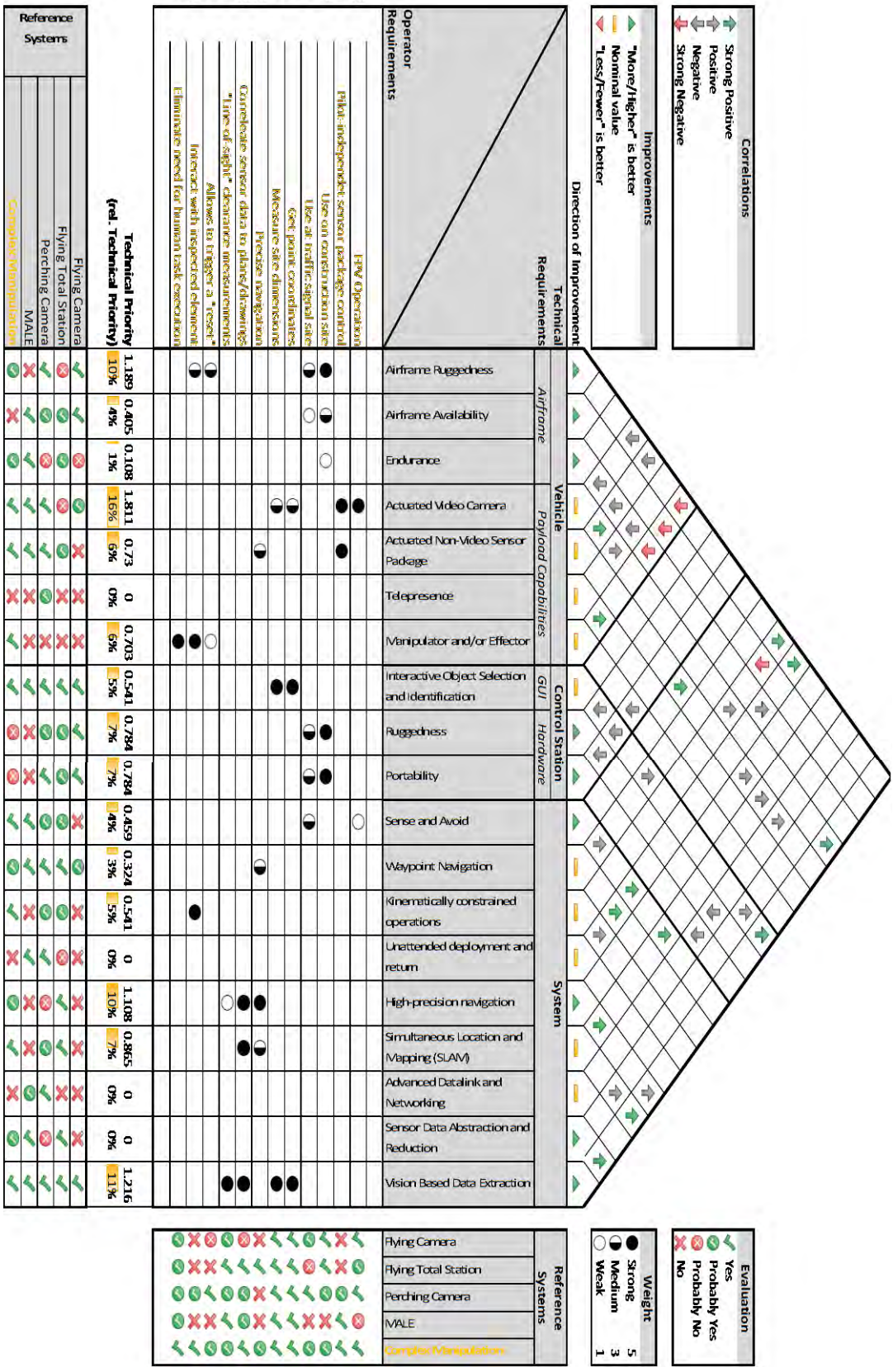

Figure 10. House of Quality for System E (Complex Manipulation)

Control Station: The control station most likely would also be split into two parts, one more tailored towards the needs of an external safety pilot, and more tailored towards the needs of the main payload operator. The former would need to focus on providing the external pilot with a good situational awareness of the surroundings of the vehicle, later would need to include a device to control the installed manipulator and request necessary manipulating forces in addition to the forces needed to maintain flight.

Required Infrastructure: System E would need a dedicated vehicle. This vehicle would on the one side serve as the transport vehicle to get the system to the different inspection sites and on the other side double as the control station once the system is unloaded. The vehicle would provide a source of power, an indoor workstation for the payload operator, and the required computer systems. Additionally it would also carry all the other required elements for the inspection tasks, i.e. any potentially necessary specialized sensors, etc. The vehicle furthermore would carry traffic control devices to setup and secure the operations.

Capabilities: The system would mainly provide capabilities comparable to a trained human worker operating out of a bucket truck or a similar reach extending device. To maintain prolonged operations, the system could be tethered to an external power source and would need to provide the ability to operate under kinematic constraints, not only from the tether, but also and especially when latchet onto other objects.

CONCLUSION

After conducting interviews with 24 individual in the four selected GDOT divisions, the research team identified tasks that could benefit from the use of UAS technology. The majority of the tasks in GDOT divisions with the highest potential for benefitting from UAS technology are centered around collecting data, providing information, and decision making based on the data. Each task is also characterized by particular attributes (e.g. location where the tasks are performed and the time required to complete a given task) that yield a better understanding of the environmental conditions. Thus, UAS technical requirements that embed the operational and technical requirements for development of a potential UAS have been investigated. The result of this investigation was the identification of five potential systems. Given the issues with cost related data collection in this study, it is recognized that additional research is needed to obtain a clearer idea of the economic and intangible benefits of the use UASs for GDOT operations. A possible departure point would be the selection of construction related tasks. It would be possible to perform a detailed tasks analysis for a construction jobsite inspection task to set the base for UAS operator system interface needs. The analysis would include a detailed assessment of the current practice and shadowing of personnel performing the task. In that way an estimate of the time and cost of performance could be developed. Based on this analysis, a potential UAS flight path through a jobsite could be established. Using a staff mounted sensor suite as a UAS mock-up or an off-the –shelf UAS, sensor data including video would be collected along the established flight paths. Then, a software replica of the site would be developed, using the collected data. The system developed would be used in a staged field test in an access-controlled construction site to validate the simulation results. This activity (and preparations for it) would include direct coordination with the FAA. The technical requirements determined would also aid in more rapid development of test UASs for GDOT use as well as advance GDOT's implementation of UAS(s) to help accomplish the Department's goals.

ACKNOWLEDGMENTS

The authors gratefully acknowledge the support provided for this research by GDOT under grant 12-38. The views and opinions presented in this paper are those of the authors do not necessarily reflect the views, opinions or policy of GDOT.

REFERENCES

[1] Coifman, B., M. McCord, R. G. Mishalani, and K. Redmill. Surface transportation surveillance from unmanned aerial vehicles. Presented at Proc. of the 83rd Annual Meeting of the Transportation Research Board, Washington, D.C., 2004.

[2] Srinivasan, S., H. Latchman, J. Shea, T. Wong, and J. McNair. Airborne traffic surveillance systems: video surveillance of highway traffic. Presented at ACM 2nd international workshop on Video surveillance & sensor networks, New York, NY, 2004.

[3] Puri, A., K. Valavanis, and M. Kontitsis. Generating traffic statistical profiles using unmanned helicopter-based video data. Presented at International Conference on Robotics and Automation. , Roma, Italy, 2007.

[4] Coifman, B., M. McCord, R. Mishalani, M. Iswalt, and Y. Ji. Roadway traffic monitoring from an unmanned aerial vehicle. Presented at Intelligent Transport Systems, 2006.

[5] Rathinam, S., Z. W. Kim, and R. Sengupta. Vision-Based Monitoring of Locally Linear Structures Using an Unmanned Aerial Vehicle 1. Journal of Infrastructure Systems, Vol. 14, No. 1, 2008, pp. 52-63.

[6] Frew, E., T. McGee, Z. Kim, X. Xiao, S. Jackson, M. Morimoto, S. Rathinam, J. Padial, and R. Sengupta. Vision-based road-following using a small autonomous aircraft. Presented at Aerospace Conference, 2004.

[7] McCormack, E. D., and T. Trepanier. The use of small unmanned aircraft by the Washington State Department of Transportation.In, Washington State Department of Transportation, 2008.

[8] Zhang, C., and A. Elaksher. An Unmanned Aerial Vehicle-Based Imaging System for 3D Measurement of Unpaved Road Surface Distresses1. Computer-Aided Civil and Infrastructure Engineering, Vol. 27, No. 2, 2012, pp. 118-129.

[9] Metni, N., and T. Hamel. A UAV for bridge inspection: Visual servoing control law with orientation limits. Automation in Construction, Vol. 17, No. 1, 2007, pp. 3-10.

[10] Irizarry, J., M. Gheisari, and B. N. Walker. Usability assessment of drone technology as safety inspection tools. Journal of Information Technology in Construction (itcon), Vol. 17, 2012, pp. 194-212.

[11] Carroll, E. A., and D. B. Rathbone. Using an Unmanned Airborne Data Acquisition System (ADAS) for Traffic Surveillance, Monitoring, and Management. Presented at ASME 2002 International Mechanical Engineering Congress and Exposition, New Orleans, LA, 2002.

[12] Werner, J. FDOT explores the viability of using unmanned aerial vehicles (UAVs) for traffic surveillance. Newsletter of the ITS Cooperative Deployment Network [online], 2003.

[13] Barfuss, S. L., A. Jensen, and S. Clemens. Evaluation and Development of Unmanned Aircraft (UAV) for UDOT Needs.In, UDOT, Utah Department of Transportation, 2012.

[14] Irizarry, J., and E. N. Johnson. Feasibility Study to Determine the Economic and Operational Benefits of Utilizing Unmanned Aerial Vehicles (UAVs).In, GDOT, Georgia Department of Transportation, 2014.

[15] Karan, E. P., C. Christmann, M. Gheisari, J. Irizarry, and E. N. Johnson. A Comprehensive Matrix of Unmanned Aerial Systems Requirements for Potential Applications within a Department of Transportation. Presented at Construction Research Congress 2014: Construction in a Global Network, Atlanta, GA, 2014.

[16] Gheisari, M., Karan, E. P., Christmann, H. C., Irizarry, J., & Johnson, E. N. (2015). Investigating Unmanned Aerial System (UAS) Application Requirements within a Department of Transportation. In *Transportation Research Board 94th Annual Meeting* (No. 15-1430).

Simulation of Biologically-Inspired Control Algorithms for Teams of Ground Vehicles

Christopher Goodin, Zachary Prevost
Geotechnical and Structures Laboratory
U.S. Army Engineer Research and Development Center
3909 Halls Ferry Road
Vicksburg, MS 39180
christopher.t.goodin@usace.army.mil, zachary.t.prevost@usace.army.mil

Bertrand Lemasson
Environmental Laboratory
U.S. Army Engineer Research and Development Center
3909 Halls Ferry Road
Vicksburg, MS 39180

ABSTRACT

While the software controlling autonomous systems has grown more complex, controlling systems of robots with multiple autonomous agents remains a challenging research area. Assigning tasks or roles to each individual agent in the group is time consuming and may restrict collaborative behaviors. One possible solution to this problem is to enable individual autonomous agents with relatively simple interactive logic that allows more complex group behaviors to emerge. We have tested the validity of this method by applying simple social models derived from collective animal behavior to autonomous unmanned ground vehicles. We have evaluated the results of this approach using high-fidelity simulations in the Virtual Autonomous Navigation Environment (VANE). Our initial findings demonstrate the potential of biologically inspired control algorithms for enabling navigation in groups of autonomous ground vehicles.

Key words: autonomy—social navigation—HMMWV

INTRODUCTION

The potential for autonomous navigation by unmanned ground vehicles (UGV) holds great promise for military applications. However, unlike autonomous navigation of civilian vehicles, which can be operated on previously mapped road networks, military vehicles may require off-road navigation with little previously known information about the state of the terrain. In addition, without the benefit of well-marked lanes, road signs, and rules of the road, autonomous navigation in off-road environments must work in a dynamic, unconstrained environment.

Many of the complexities of autonomous operation in an off-road environment can be avoided by having the autonomous vehicle simply follow a lead-vehicle driven by human. If the autonomous vehicle can maintain close contact with the lead vehicle, then high-level autonomous decision-making, and the problems associated with it, can be avoided. However, in situations where the ratio of unmanned (follower) to manned (leader) vehicles becomes large, simple follower behaviors will not produce optimal results for the group.

Proceedings of the 2015 Conference on Autonomous and Robotic Construction of Infrastructure, Ames, Iowa.

In this work we will demonstrate the feasibility of using biologically inspired control algorithms for UGV operating in teams with manned ground vehicles. These algorithms work by having each robot compare its own state to the state of the vehicles (both manned and unmanned) around it. We use high-fidelity simulations from the Virtual Autonomous Navigation Environment (VANE) [1] to show that these biologically-inspired algorithms give rise to group behaviors in teams of manned and unmanned UGV that depend on the ratio of manned to unmanned vehicles.

BACKGROUND

Biologically inspired control

We implemented biologically inspired algorithms for controlling the robotic vehicles. In this work, the inverse distance weights how individuals perceive one another; closer vehicles are given more importance than those farther away. While there are additional mechanisms used by animals to process information, such as selective attention to salient features [2,3], our goal was to begin by integrating cognitive effects at the simplest level (sensory perception) to explore their impact on the collective motion of realistically simulated ground vehicles.

In the algorithm used in this work, the robots desired velocity was determined by comparing its own velocity with all the other vehicles, and weighting the averaged results by the inverse of the distance calculates velocity. So for vehicle i with velocity $\vec{v}_i$ the desired velocity $\vec{v}_i'$ is given by

$$\vec{v}_i' = \frac{1}{w} \sum_{j=1, i \neq j}^{n} w_{ij} (\vec{v}_j - \vec{v}_i) \quad (1)$$

where n is the total number of vehicles and the weights are given by

$$w_{ij} = \left\| \vec{r}_i - \vec{r}_j \right\| \quad (2)$$

and the total weight factor w is given by

$$w = \sum_j w_{ij} \, . \quad (3)$$

The Virtual Autonomous Navigation Environment

The VANE is a high fidelity, physics-based robotics simulator that features realistic models for vehicle dynamics, vehicle-terrain interaction, environment, and sensors. Vehicle dynamics is simulated using the Chrono::Vehicle multi-body dynamics library [4]. Chrono::Vehicle features detailed models of the suspension element, chassis inertial properties and running gear. In our simulations, Chrono::Vehicle was coupled to the Ground Contact Element (GCE) tire-terrain interaction model [5]. The GCE features a nodal-based radial spring tire model coupled to empirically derived soil models, resulting in realistic torque calculations for the tire in a wide variety of terrain conditions. Terrains are represented as highly attributed triangular meshes.

Sensor models in the VANE use detailed ray tracing to simulate the reflection of visible and infrared wavelengths in the environment. This includes environmental light for camera sensors and active sources such as the lasers in LADAR systems. The VANE also features a detailed GPS model that accounts for multipath reflections, satellite occlusion, dilution-of-precision, and atmospheric effects [6].

EXPERIMENT DETAILS

The VANE simulation used a HMMWV as the test vehicle. The HMMWV was modeled in Chrono::Vehicle with the double-wishbone suspension in the standard HMMWV configuration. In order to focus on the interactional aspects of navigation, the terrain was flat and there were no obstacles. A simulated visualization of the formation of HMMWV is shown in Figure 1.

Figure 1. Visualization of the group of 7 HMMWV

We performed experiments with groups of 4, 7, and 10 vehicles. For each group of vehicles, we varied the number of vehicles that were autonomous. In the experiments, the autonomous vehicles were not equipped with any sensing capability, but all the vehicles communicated their state (position and velocity) to a common server to which all other vehicles subscribed. This was the only information that the vehicles shared.

The initial configuration of the vehicles was a staggered column, as depicted in Figure 1, with an average longitudinal spacing of 10 meters and an average lateral spacing of five meters. The initial position of each vehicle was randomly varied by up to 2.5 meters in any direction, and the initial orientation was randomly varied by 25 degrees. These ranges were chosen to give the maximum possible variation to the simulations while ensuring the vehicles did not collide with each other.

In the experiment, the driven vehicles abruptly changed course after five seconds to simulate an avoidance maneuver. In the maneuver, the manned vehicles quickly turned to the left while maintaining formation. Ten trials were run for each combination of manned and unmanned vehicles shown in Table 1, and the average alignment at 15 seconds was calculated for each configuration.

To quantify leader-follower coordination between manned and unmanned vehicles we measured the alignment of the unmanned vehicles with the manned vehicles after 15 seconds, 10 seconds after the turn maneuver was initiated. For manned vehicles, denoted subscript m, and unmanned vehicles, denoted subscript u, the alignment, α, of the system is given by

$$\alpha = \frac{1}{2n_m n_u} \sum_m \sum_u \frac{\vec{v}_m \bullet \vec{v}_u}{\|\vec{v}_m\| \|\vec{v}_u\|} \qquad (4)$$

where n_m and n_u are the numbers of manned, and unmanned vehicles respectively, and the factor of 2 is to account for double counting of pairs.

The alignment defined by Equation 4 would have a theoretical minimum of -1 (unmanned vehicles perfectly anti-aligned with manned vehicles) and a maximum of 1 (all vehicles perfectly aligned). The alignment of a randomly oriented system of vehicles will be close to 0. Because the vehicles were nearly aligned in the initial configuration, the system started with $\alpha \approx 1$, and the alignment typically improved steadily until the abrupt movement event, at which point the alignment decreased. Figure 2 shows the alignment of a group of ten robots, with one driven as a function of time.

Table 1. Experiment Matrix

Number of Vehicles	Number Driven	Ratio	Alignment	Std Error
4	1	25.0%	0.880	0.001
4	2	50.0%	0.933	0.005
4	3	75.0%	0.948	0.002
7	1	14.3%	0.864	0.004
7	2	28.6%	0.901	0.004
7	3	42.9%	0.931	0.003
7	4	57.1%	0.952	0.002
10	1	10.0%	0.852	0.003
10	2	20.0%	0.878	0.004
10	4	40.0%	0.927	0.003
10	5	50.0%	0.956	0.003

RESULTS AND DISCUSSION

The results of the experiment are shown in Table 1. In general, groups with a higher fraction of manned vehicles had better alignment after the maneuver than those groups with fewer manned vehicles, as would be expected. Figure 2 compares the average over all ten trials for the alignments of ten robots with either five or one driven configuration. Note that the maneuver event occurred at five seconds, and the final alignment was measured at 15 seconds. This plot demonstrates how the alignment of the group tended to diverge over time in groups with smaller numbers of manned vehicles.

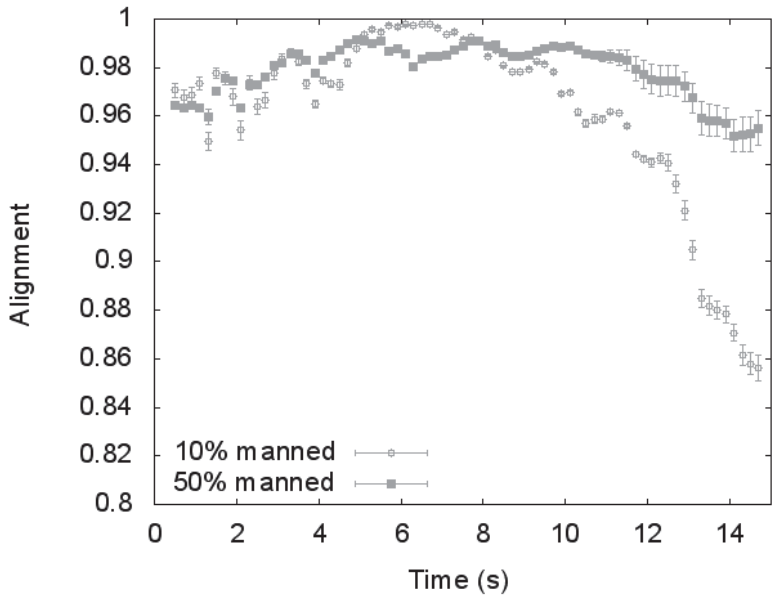

Figure 2. Alignment of a group of 10 robots, with one manned. Data points are sampled every 0.3 s. and represent means ± 1 standard error.

In Figure 3, we show the paths of vehicles from one of the simulations with seven vehicles. In the left figure, only one vehicle was manned, while in the right figure, four vehicles were manned. The manned vehicles are denoted with a thick red line, while the unmanned vehicles are denoted with a thin gray line. The results depicted in Figure 3 show the typical result that after the maneuver initiated at five seconds, the unmanned systems tended to move as a group, and that group was influenced by the number and proximity of manned vehicles. Systems with greater than 50% manned vehicles tended to recover alignment after the maneuver, while systems with less than 50% recovered with proportionally varying degrees of success.

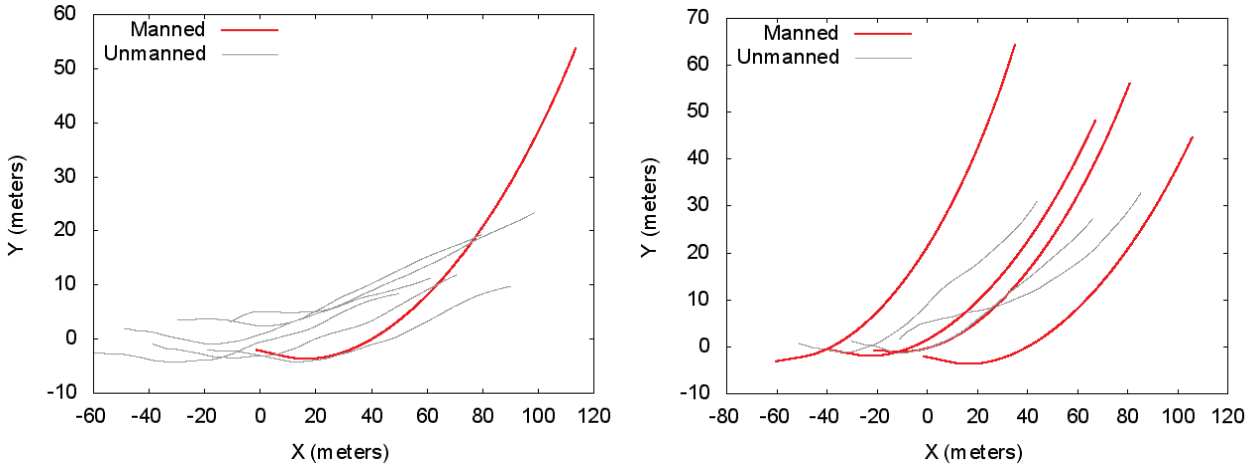

Figure 3. Comparison of the paths taken by a group of 7 vehicles with six unmanned systems (left) and 3 unmanned systems (right)

Figure 4 shows another summary of the data. In this figure, the average alignment of the system after 15 seconds is plotted against the percentage of manned vehicles. The alignment of the system increases linearly with increasing percentage of manned vehicles up to 50%, above 50% the increase in alignment levels off. The black line is a fit to the points below 50% manned with the form

$$\alpha = 0.244 P_m + 0.828 \quad (5)$$

where P_m is the percentage of manned vehicles. The fit has a coefficient of determination of R^2=0.982.

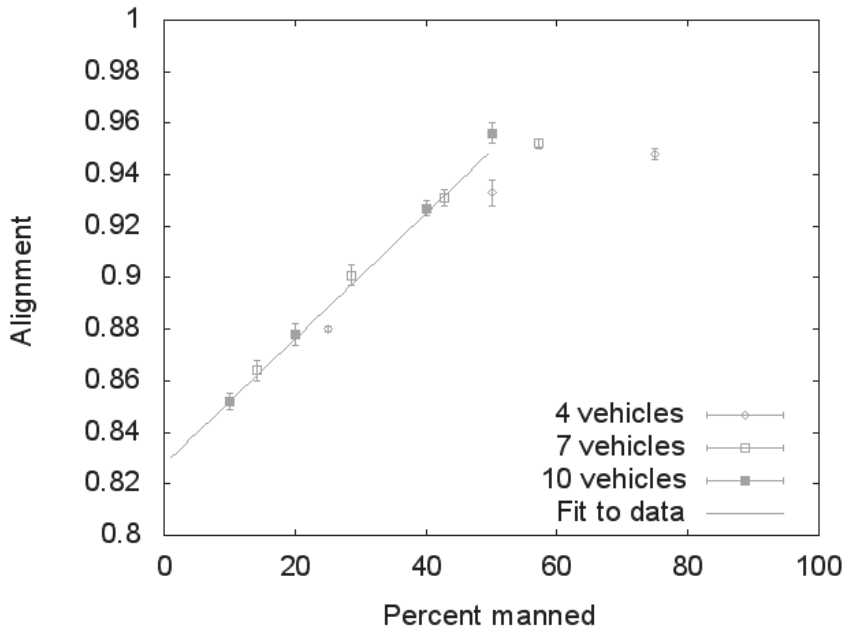

Figure 4. Alignment of the vehicles as a percentage of manned systems. Data points represent means ± 1 standard error.

CONCLUSIONS AND FUTURE WORK

In this work we showed how simple control algorithms inspired by biological systems can be used to control mixed groups of manned and unmanned vehicles. We demonstrated a method for determining the influence of the percentage of unmanned systems that used high-fidelity simulations of the dynamics of wheeled vehicles and were able to determine a clear trend and threshold for optimizing performance.

The current dynamics agree with theoretical and empirical work on the influence of majority-minority interactions in the collective movement decisions of groups. When individuals are unaware of who is in charge, and pool all social cues indiscriminately, followers will either adopt a new course that is a compromise (Fig. 3, left), or else follow the majority (Fig. 3, right) [7.8]. In future work we will explore how selective attention to particular features can shift these dynamics across groups of increasing size [3]. In addition, we will parameterize those algorithms to allow optimization of the control algorithms for a particular task such as navigation

or obstacle avoidance. Finally, we will expand the analysis to include heterogeneous groups of vehicles consisting of trucks of various sizes.

REFERENCES

[1] Goodin, C., George, T. R., Cummins, C. L., Durst, P. J., Gates, B. Q., & McKinley, G. B. (2012). The Virtual Autonomous Navigation Environment: High Fidelity Simulations of Sensor, Environment, and Terramechanics for Robotics. In *Earth and Space 2012* (pp. 1441-1447).

[2] Ballerini, M., Cabibbo, N., Candelier, R., Cavagna, A., Cisbani, E., Giardina, I., Lecomte, V., Orlandi, A., Parisi, G., Procaccini, A., Viale, M., & Zdravkovic, V. (2008) Interaction ruling animal collective behavior depends on topological rather than metric distance: evidence from a field study. *Proceedings of the National Academy of Sciences, U.S.A.,*105(4), 1232-1237.

[3] Lemasson, B. H., Anderson, J. J., & Goodwin, R. A. (2013). Motion-guided attention promotes adaptive communications during social navigation. *Proceedings of the Royal Society B: Biological Sciences*, *280*(1754), 20122003.

[4] Tasora, A., & Anitescu, M. (2009). A fast NCP solver for large rigid-body problems with contacts, friction, and joints. In *Multibody Dynamics* (pp. 45-55). Springer Netherlands.

[5] Creighton, D. C., McKinley, G. B., Jones, R. A., & Ahlvin, R. B. (2009). *Terrain Mechanics and Modeling Research Program: Enhanced Vehicle Dynamics Module* (No. ERDC/GSL-TR-09-8). Engineer Research and Development Center, Geotechnical and Structures Laboratory.

[6] Goodin, C., Durst, P. J., Gates, B., Cummins, C., & Priddy, J. (2010). High fidelity sensor simulations for the virtual autonomous navigation environment. In *Simulation, Modeling, and Programming for Autonomous Robots* (pp. 75-86). Springer Berlin Heidelberg.

[7] Couzin, I. D., Krause, J., Franks, N. R., & Levin, S. A. (2005). Effective leadership and decision-making in animal groups on the move. *Nature*,*433*(7025), 513-516.

[8] Biro, D., Sumpter, D. J., Meade, J., & Guilford, T. (2006). From compromise to leadership in pigeon homing. *Current Biology*, *16*(21), 2123-2128.

Case Study on 3D Modeling and AMG Practices

Fangyu Guo
Department of Civil, Construction, and Environmental Engineering
Iowa State University
136 Town Engineering Building
Ames, IA, 50011
Email: fangyu@iastate.edu

Yelda Turkan
Department of Civil, Construction, and Environmental Engineering
Iowa State University
428 Town Engineering Building
Ames, IA, 50011
Email: yturkan@iastate.edu

Charles T. Jahren
Department of Civil, Construction, and Environmental Engineering
Iowa State University
456 Town Engineering Building
Ames, IA, 50011
Email: cjahren@iastate.edu

ABSTRACT

The adoption of 3D modeling and automatic machine guidance (AMG) are becoming more popular in the transportation industry. With a 3D model uploaded to an on-board computer within a piece of heavy construction equipment, operators can easily monitor machine operations with respect to grad and location or engage the machine to produce the proper grade automatically. Thus, it provides great convenience and improved productivity for field workers.

AMG and 3D modeling have been identified as enabling technologies for a Civil Integrated Management (CIM) system. When CIM is implemented, an entire transportation agency and stakeholder partners share in the use and development of a common data pool that is accessible to authorized users involved with all phases of a transportation facility life cycle (such as planning, design, construction, maintenance and rehabilitation) and all departments in the agency (Administration, finance, operation and others). The concept of CIM was developed and promoted by the United States Federal Highway Administration in 2013 and was established to make better use of accurate data and information that results from the utilization of advanced technologies and/or tools thus to facilitate more effective decision making for transportation projects.

Using the CIM concept and framework, technologies such as 3D modeling and AMG could be more efficiently adopted within the full life cycle of a transportation facility. More importantly, data could be collected and managed systematically in the early phases of a project life cycle so they could be useful for later phases of the facility lifecycle. The purpose of this study is to investigate how CIM system could support autonomous construction and vice versa. During a domestic scan effort, seven state agencies and their contractors collaborated to present their extensive experiences on certain CIM related practices and tools. In particular, the experiences

Proceedings of the 2015 Conference on Autonomous and Robotic Construction of Infrastructure, Ames, Iowa.

of the agencies that were under investigation regarding 3D modeling and AMG will be addressed in this paper. In addition, the benefits and challenges of using 3D modeling and AMG will also be discussed.

Keywords: civil integrated management (CIM)—3D modeling—automatic machine guidance (AMG)

PROBLEM STATEMENT

Productivity, quality, and safety are important aspects of any transportation project and are used as measures of project success. Various technologies and tools have been used to achieve better productivity, quality, and safety. Adoption of 3D engineered models in the transportation industry is relatively behind the adoption of Building Information Modeling (BIM) in the building industry. However, this is now changing; the transportation industry is adopting 3D engineered models at an increasing rate. In 2010, the adoption rate of 3D engineered models for transportation projects was 27%, which was increased to 46% in 2012 (McGraw-Hill 2012). The successful implementation of BIM in the building industry is a good example. It is critical for transportation industry to investigate the lessons learned from the building industry and start implementing 3D engineered models and other supporting technologies such as Automatic Machine Guidance (AMG) in their projects. The implementation of 3D engineered models is expected to bring benefits such as less rework and change orders (Parve 2013), more effective communications (Olde and Hartmann 2012), reduced time and costs, and improved quality and productivity (Myllymaa and Sireeni 2013; Cylwik and Dwyer 2012). Similarly, the major benefits of using AMG include increased quality and productivity, and reduced time and costs on job sites (Peyret 2000).

For an agency planning to implement a new technology, it is important to investigate the best practices and lessons learned from other agencies that already have extensive experiences with that particular technology. Since Iowa DOT was identified as one of the leading state DOTs for 3D modeling implementation (EDC 2013), this paper presents a case study on Iowa DOT's best practices and lessons learned from the use of 3D modeling and AMG.

RESEARCH OBJECTIVES

The objectives of this study are presented as follows:

- Learn Iowa DOT's progress on the use of 3D engineered models and AMG;
- Study how the agency transitioned from the traditional processes to the new processes of implementing 3D engineered models and AMG;
- Identify the benefits and challenges of using 3D engineered models and AMG within the agency;
- Conclude lessons learned from the adoption of 3D engineered models and AMG for the agency.

RESEARCH METHODOLOGY

The results presented in this paper are obtained from the National Cooperative Highway Research Program (NCHRP) Domestic Scan project 13-02 - Advances in CIM. The scan project investigated the current practices related to Civil Integrated Management (CIM) adopted by various state DOTs. During the project, 3D engineered models and AMG were identified as two of the enabling technologies for CIM implementation. The scan panel members were composed of various state DOTs and the Federal Highway Administration (FHWA) personnel, and a

subject matter expert (SME). The third author of this paper served as the SME, and the other two authors assisted the SME during this project. The scan team conducted an initial survey, called desk scan, to obtain knowledge on CIM and CIM-related technologies and tools. The amplifying questions were prepared by the scan team and sent to target agencies. The scan team then spent two weeks in total visiting seven leading state DOTs who had extensive experiences in CIM-related practices. All day workshops and presentations were provided by the host agencies and their contractors. It is also important to note here that there were also intensive interactions during these meetings between the host agencies and the scan team members. Detailed notes were taken during the meetings for further analysis. The data related to the implementation of 3D engineered models and AMG by Iowa DOT were extracted and analyzed in this paper. The results obtained from the coding strategies (Maxwell 2013) are presented in the following section.

KEY FINDINGS

Progress on 3D Engineered Models and 3D Renderings

Transitioning from 2D to 3D design is one of the main goals of Iowa DOT. Iowa DOT uses 3D renderings extensively to communicate with public, which allows the public to have a better understanding about the project and its impact on the surrounding environment. Great amount of details can be added to 3D renderings, although it might be challenging to add paint lines on roads. Furthermore, these renderings can be used as a starting point for 3D design. Currently, they are modeling all their highway projects in 3D using Bentley Corridor Modeler software package. Newly hired personnel are given proper training on 3D modeling knowledge and skills. When Iowa DOT first started 3D modeling, 2D cross sections would be developed and used to build a 3D model. This has been improved over the years. Today, 3D models are developed first and cross sections are extracted from the 3D models. Model development process has been standardized within the agency to ensure designers use the same approach to build the model, so that the same type of information can be obtained from a 3D model. Iowa DOT also adjusted the proportion of in-house modeling development effort over time. They used to develop all 3D models in-house, which consumed great amount of their time since they wanted to ensure the resulting products fit contractors' needs. Currently, 70% of the 3D models are developed in-house, and the rest 30% are developed by their consultants. The standardized tools and templates, which were developed by Iowa DOT, are shared with their consultants. With this adjustment, time and effort for in-house modeling development is reduced while maintaining the same model quality. The completed models are typically provided to the contractors before the bidding process, since design-bid-build is the dominant project delivery method for their projects. Overall, it can be concluded that 3D models and 3D renderings help improve communications between Iowa DOT and their contractors and with the public respectively.

Some of the challenges experienced by Iowa DOT in implementing 3D modeling are as follows. First, copyright issues can be quite challenging. It is hard to determine who can change or modify which information. Iowa DOT has a copyright policy and the state of Iowa has a copyright law in place. However, this is not yet included in the consultant contracts. Second, the entire model development process has to be changed. Attribute data should properly be assigned to each 3D object in 3D models. In the future, Iowa DOT plans to develop 4D (3D+ time (schedule)) animations for their projects. Having 4D models is expected to give public a better idea about how the project will look like once it is completed.

Progress on AMG

In the past, contractors who wanted to implement AMG would take 2D project plans to their consultants and have them build 3D models based on the 2D plans, so that they could use the

3D models on their equipment for AMG. This was changed after Iowa DOT started to develop 3D models and provide them for AMG use. Before Iowa DOT start implementing 3D modeling for machine control, they met with Trimble, Leica, CAT, and other manufacturers to learn about the current status and discuss the future direction for construction equipment. Based on the discussions during those meetings, they decided to do a pilot project where they made it mandatory to use 3D models and AMG. Based on the benefits observed, they continued using these technologies for other projects. This pushed their grading contractors transition from traditional equipment to AMG in order to stay in business. Construction equipment is continuously improved, and it is becoming easier for contractors to use. Operators can easily adjust the location and movement of certain parts of equipment (such as blade or bucket) based on the guidance provided by GPS. Construction equipment with a GPS device installed can be either purchased or rent from dealers. Most contractors in Iowa prefer purchasing equipment to renting, as most jobs require the use of AMG to some extent.

Based on Iowa DOT's experiences, stringless paving technology helped increase the quality of paving greatly. Stakes only need to be placed every 1000 feet when using stringless paving, which greatly improves the safety in the field. Competition among contractors became more intense with little changes in bid prices. Although setting up the machine control in the field increased the upfront project costs, the overall project cost did not change much compared to traditional process of not using AMG.

From contractor's perspective, the following benefits were observed when AMG was used:

- Productivity and accuracy are greatly improved with the adoption of AMG
- Owners tend to be more satisfied with the product delivered with AMG.
- Design changes could be integrated easier and faster.
- Problems could be detected early in the process via 3D models that are intended to be used for AMG.
- Field safety is greatly improved since less people are needed on the job site for AMG-implemented projects.

Lessons Learned from the Model Centric Design

Iowa DOT learned the following lessons from implementing 3D modeling and AMG for highway projects.

- Before implementing a new technology or a new approach, it is important to set the goals first, and then determine how to achieve them.
- It is beneficial to consult with industry practitioners to better understand their needs. Iowa DOT started to use standard data exchange format (LandXML), naming convention, color paper, and others based on the feedback they received from their contractors and consultants.
- It is beneficial to set up some rules to standardize the process and keep those rules consistent. For example, color plans were adopted about five or six years ago within the agency. The same color coding system was used for all projects to maintain the consistency, so that there were no confusions about the color codes.
- It is critical to organize the data or documents (naming convention, file format, etc.) well. Better organized documents help people perform better when searching and sorting information.
- It would be beneficial to maintain continuous communication with industry associations. For example, discussions with the associated general contractors of America (AGC) helped Iowa DOT determine a future direction that matches the direction of AGC. Also,

annual meetings with AGC keep Iowa DOT up to date with the development and utilization of the most recent technologies and tools in the industry.

- How the agency approaches training is a key to success. In-time and periodical training is proven to be the most efficient.

CONCLUSIONS

This paper focused on the implementation of 3D engineered models and AMG by Iowa DOT, which was identified as one of the leading state DOTs in this area. A brief introduction was provided on how the agency transitioned from traditional design and construction processes to new processes where 3D models and AMG are used. Benefits, challenges, and lessons learned from using these technologies were also discussed. The findings of this study would be beneficial to the agencies that are planning to implement these technologies within their organization. Before implementing a new technology, it is important for agencies to consult other agencies and/or companies with extensive experiences using a particular technology and discuss it with software or hardware vendors to set up a clear goal and select the best way to start. Lessons learned from pilot projects can be great guidance for future projects. Benefits and challenges should also be clearly identified. This may help motivate employees to use the technologies and tools. Finally, as agencies become more experienced with new technologies and tools, proper standards should be put in place to improve the overall work efficiency.

ACKNOWLEDGMENTS

The material presented in this paper is based on the presentations and documents obtained during the Scan 13-02 project - Advances in Civil Engineering Management (CIM), which was supported by the National Cooperative Highway Research Program (NCHRP) 20-68A US Domestic Scan Program. Scan team members included John Adam of Iowa DOT, Katherine Petros and Brian Cawley of the US Federal Highway Administration, Rebecca Burns of Pennsylvania, Duane Brautigam of Florida DOT, Julie Kliewer of Arizona DOT, John Lobbestael of Michigan DOT, Stan Burns and Randall R. Park of Utah DOT, David Jeong of Iowa State University. The scan team was supported by Harry Capers, Jake Almborg, and Melissa Jiang of Aurora and Associates, P.C.. Their assistance in analyzing the data collected during the site visits is gratefully acknowledged. We would also like to convey our sincere thanks to Iowa DOT for their continuous support during this project.

REFERENCES

Cylwik, E. and Dwyer, K. (2012). “Virtual Design and Construction in Horizontal Infrastructure Projects.” *Engineering News-Record*, <http://enr.construction.com/engineering/pdf/News/Virtual%20Design%20and%20Construction%20in%20Horizontal%20Construction-05-03-12.pdf> (May 02, 2015)

Every Day Counts (EDC). (2013). “”3D Engineered Models for Construction Implementation Plan.” Federal Highway Administration. 1-20.

Maxwell, J.A. (2013). *Qualitative Research Design (3rd ed.)*. Thousands Oaks, CA: SAGE Publications, Inc.

McGraw Hill Construction. (2012). “The Business Value of BIM.” *SmartMarket Report*, New York.

Myllymaa, J., and Sireeni, J. (2013). “Cost Savings by Using Advanced VDC Tools and Processes, Case Studies from Europe,” Presentation at the 2013 Florida Department of Transportation Design Training Expo, June 12-14, 2013. http://www.dot.state.fl.us/structures/designexpo2013/2013ExpoPresentations.shtm (May 02, 2015)

Olde Scholtenhuis, L. L., & Hartmann, T. (2012). “An object model to support visualizations and simulations of subsurface utility construction activities.” In Proceedings of 14th International Conference on Computing in Civil and Building Engineering.
Parve L. (2013), “Redesigning a complex, critical freeway: Building information modeling helps deliver cost avoidance and savings for Wisconsin's Mitchell Interchange Project.” <http://www.rebuildingamericasinfrastructure.com/print-magazinearticle-redesigning_a_complex__critica-9018.html> (May 02, 2015)
Peyret, F. et al. (2000). “The Computer Integrated Road Construction Project.” *Automation in Construction*, 9, 447-461.

A Formalism for Utilization of Autonomous Vision-Based Systems and Integrated Project Models for Construction Progress Monitoring

Kevin K. Han
Department of Civil and Environmental Engineering
University of Illinois at Urbana-Champaign
205 N. Matthews Ave
Urbana, IL 61874
kookhan2@illinois.edu

Jacob J. Lin
Department of Civil and Environmental Engineering
University of Illinois at Urbana-Champaign
205 N. Matthews Ave
Urbana, IL 61874
jlin67@illinois.edu

Mani Golparvar-Fard
Department of Civil and Environmental Engineering & Computer Science
University of Illinois at Urbana-Champaign
205 N. Matthews Ave
Urbana, IL 61874
mgolpar@illinois.edu

ABSTRACT

Actual and potential progress deviations during construction are costly and preventable. However, today's monitoring programs cannot easily and quickly detect and manage performance deviations. This is because (1) the current methods are based on manual observations made at specific locations and times; and (2) the captured progress information is not integrated with "as-planned" 4D Building Information Models (BIM). To facilitate this process, construction companies have focused on collecting as-built visual data through hand-held cameras and video recorders. They have also assigned field engineers to filter, annotate, organize, and present the collected data in comparison to 4D BIM. However, cost and complexity associated with collecting, analyzing and reporting operations still result in sparse and infrequent monitoring and therefore a portion of the gains in efficiency is consumed by monitoring costs. To address current limitations, this paper outlines a formal process for automating construction progress monitoring using visual data captured via camera-equipped Unmanned Aerial Vehicles (UAVs) and 4D BIM. More specifically, for data collection, formal methods are proposed to identify monitoring goals for the UAVs using 4D BIM and autonomously acquiring and updating the necessary visual data. For analytics, several methods are proposed to generate 3D and 4D as-built point cloud models using the collected visual data, to integrate them with BIM, and to automatically conduct appearance-based and geometrical reasoning about progress deviations. For reporting, a method is proposed to characterize the analyzed and identified progress deviations using performance metrics such as the Earned

Proceedings of the 2015 Conference on Autonomous and Robotic Construction of Infrastructure, Ames, Iowa.

Value Analysis (EVA) or Last Planner System (LPS) concepts. These metrics are then visualized via color-coding the BIM elements in integrated project models, presented to project personnel via a scalable and interactive web-based environment. The validation of this formalism is discussed based on several real-world case studies.

Key words: progress monitoring—vision-based system—unmanned aerial vehicles—BIM

INTRODUCTION

Actual and potential progress deviations during construction of buildings and infrastructure systems are costly but are preventable. To capture construction performance deviations accurately and to make effective and prompt decisions based on the captured performance deviations, frequent and accurate methods are needed for tracking construction progress. If implemented on a daily basis, such methods can effectively bridge the gap in information sharing between daily work execution and weekly work planning/coordination, ultimately leading to improved project efficiencies (Bosché et al. 2014; Yang et al. 2015).

Today's construction progress tracking methods, however, do not provide the accuracy and frequency necessary for effective project controls. This is in large due to the labor intensive processes involved with as-built data collection and analysis (Bae et al. 2014). It is common for field engineers and superintendents to walk around the site, take photos, and document the progress of ongoing operations, nevertheless this process is time consuming as it needs to be conducted per daily task and for all associated construction elements. The ability to perform monitoring and photographic documentation is also restricted by hard-to-reach areas. This constraint negatively impacts the completeness of the data collection process. Once this data is collected (whether it is complete or not), the field engineers filter, annotate, organize, and present the collected data in comparison to 4D BIM. However, the cost and complexity associated with the analysis and reporting operations result in sparse and infrequent monitoring (Bae et al. 2013). Therefore through these activities for project controls, a portion of the gains in efficiency is consumed by monitoring costs.

Over the past few years, research has focused on addressing current limitations through (1) automatically generating 3D point cloud models from unstructured images and video sequences (Brilakis et al. 2011; Golparvar-Fard et al. 2009), (2) aligning the resulting 3D point cloud models with 4D BIM (Golparvar-Fard et al. 2011), and then (3) methods that can automatically infer the status of work tasks and their relevant elements using geometry information (Golparvar-Fard et al. 2012), appearance information (Han and Golparvar-Fard 2015), and via leveraging formalized construction sequencing knowledge and reasoning mechanisms (Han and Golparvar-Fard 2014a). While significant progress is achieved, yet many areas in research are still open which require further investigation.

This paper presents a formal process for automating construction progress monitoring via images taken with camera-equipped Unmanned Aerial Vehicles (UAVs) and 4D BIM. To address the current limitations in accuracy and completeness of the data collection, we propose to build on the emerging practice of using camera-equipped UAVs for collecting close-range site imagery. Different from these practices, we propose to use 4D BIM to identify monitoring goals for visual data collection, path planning, and autonomous navigation of the UAV through both exterior and interior construction scenes. We also present a method that leverages BIM (1) to improve accuracy and completeness of the 3D image-based point cloud modeling via UAV captured images, and (2) for a better alignment of the images and the resulting point cloud

models with the 4D BIM. For analytics, methods are presented to leverage geometry, appearance, and inter-dependency information among elements together with formalized construction sequencing knowledge to document progress for work tasks that have corresponding physical elements. A new system architecture is also proposed for visualizing the collected images, produced 3D point cloud models, and 4D BIM in a scalable web-based environment. This environment allows user interactions which is particularly important for collecting inputs on task constraints and those tasks that do not necessarily have physical element correspondences. As shown in Figure 1, the resulting integrated project models can be used to minimize the gap in information communication between work task coordination and daily task execution. It can also support the identification and removal of work constraints and root-cause analysis in construction coordination meetings.

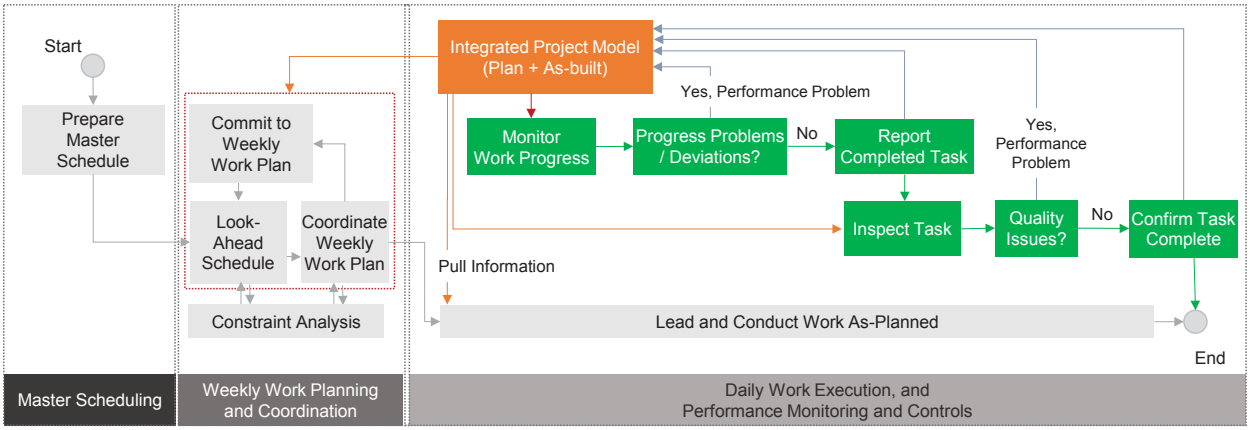

Figure 1. The planning, execution and monitoring of weekly work plans and how integrated project models generated via images taken from camera-equipped UAVs and BIM can improve current work flows.

In the following, we provide an overview on the state of the practice and research on using camera-equipped UAVs and BIM for progress monitoring. Next, we propose a formalized procedure for leveraging 4D BIM for enhanced data collection, analytics, and communication of construction progress deviations. A discussion is also provided on how the proposed procedure and its associated tools can improve current information sharing and enhance construction coordination processes.

STATE OF PRACTICE AND RESEARCH ON USING CAMERA-EQUIPPED UAVS AND BIM FOR CONSTRUCTION PROGRESS MONITORING

Data collection

Over the past two years, the application of camera-equipped UAVs for comprehensive visual documentation of work-in-progress on construction sites has gained significant popularity among the Architecture/Engineering/Construction and Facility Management (AEC/ FM) practitioners. Many construction and owner companies have procured their own UAV platforms for frequent data collection. Several companies have also emerged that provide close range aerial image data collection as a service. Ideally these UAVs should operate on sites on a daily basis such that an accurate and complete visual documentation of work in progress can be achieved.

To operate autonomously, the UAV operators manually place waypoints on 2D maps and leverage GPS coordinates for path planning and navigation purposes. The reliance on GPS for navigation limits autonomous data collection to outdoors and causes major difficulties in dense urban areas. Also the presence of steel components on sites affect the accuracy of the magnetometers used on these platforms for navigation purposes, potentially causing safety issues on construction sites. Placing waypoints manually can also create potential safety hazards as the 2D maps used for navigation do not reflect the most updated status of the resources on site, and leave the UAV operators to approximate the 2D location and height of the new construction and resources such as mobile cranes.

Because the locations where construction progress is expected on project sites are not known in advance, current best practices require the UAVs to cover the entirety of a site. Since current batteries are limited to 15-35min operations, covering the entirety of a project site needs multiple flights and manual supervision by the UAV operators. With the number of images increasing, the computation time necessary for processing these images, generating 3D point cloud models, and analyzing work-in-progress also exponentially grows.

While research (Lin et al. 2015a; Siebert and Teizer 2014; Zollmann et al. 2014) has focuses on leveraging UAV-based images for progress monitoring, the aforementioned challenges are still remained unexplored. Figure 2 (a) shows a camera-equipped UAV flying onsite, (b) an operator using the controller to navigate the UAV for data collection and (c) a commercially available application (DJI Ground Station 2015) for setting the waypoints for UAV navigation.

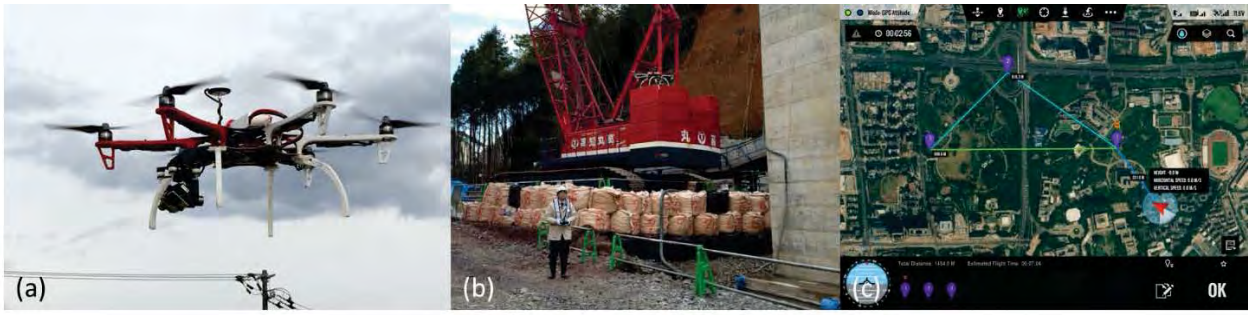

Figure 2. (a) camera-equipped UAV (b) operator executing data collection task on the construction site, (c) waypoints setting in commercially available application (DJI Ground Station 2015).

Visual Analytics for Progress Tracking

Today, there are two dominant practices for leveraging images collected from camera-equipped UAVs for tracking work in progress:

(1) Generating large panoramic images of the site and superimposing these large-scale high resolution images over existing maps– While these images provide excellent visuals to ongoing operation, they lack 3D information to assist with area-based and volumetric-based measurements necessary for progress monitoring. Also none of the current commercially available platforms provide a mechanism to communicate *who* is working on *which* tasks at *what* location.

(2) Producing 3D point cloud models– Over the past decade, the state-of-the-art in image-based 3D modeling methods from computer vision domain has significantly advanced. These

developments have led to several commercially available platforms that can automatically produce 3D point cloud models from collections of overlapping images. Several AEC/FM firms have started to leverage these platforms to produce as-built 3D point cloud models of their project sites via images taken from camera-equipped UAVs. Nevertheless, today's practices are mainly limited to measuring excavation work and stockpiles. This is because highly overlaying images taken with a top-down view can produce high quality 3D models of these operations. However creating complete 3D point cloud models for building and infrastructure systems also requires the UAVs to fly around the structure to capture work in progress. Because there is not automated mechanism for identifying most informative viewpoints, often the produced 3D point cloud models are incomplete. Also the state of the art Structure from Motion (SfM) techniques for image-based 3D reconstruction –as used in (Golparvar-Fard et al. 2012; Golparvar-Fard et al. 2011) - may distort angles and distances in generated point cloud models. Figure 3 shows an example of a point cloud model that was generate via highly overlapping images taken around the perimeter of a construction site. The reconstructed 3D point cloud is up-to-scale and exhibits problems in completeness and accuracy.

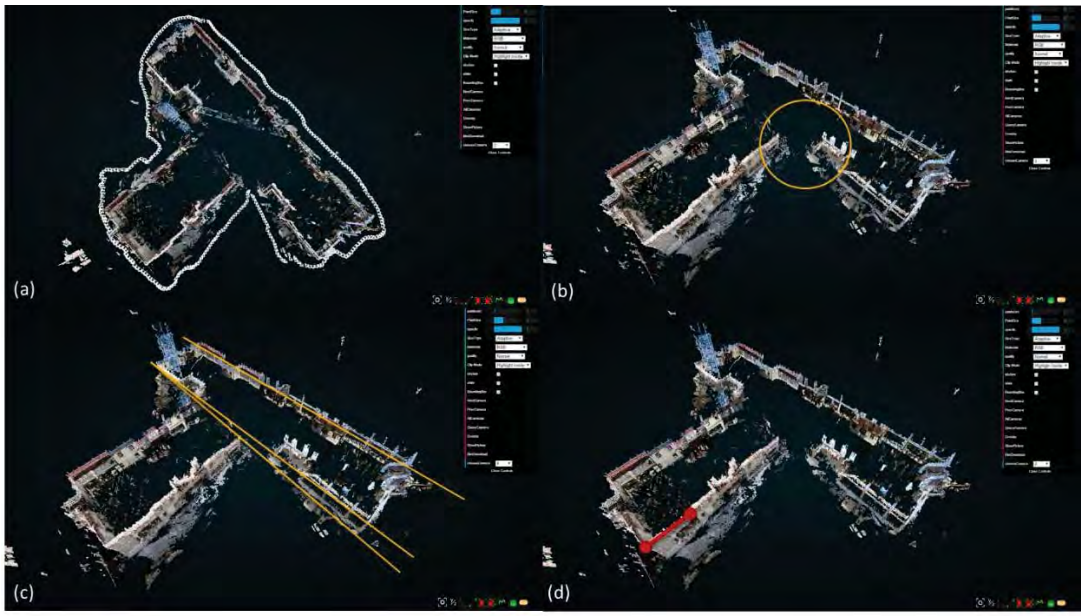

Figure 3. Typical challenges in using Standard SfM techniques for image-based 3D reconstruction: (a) the UAV's flight path around the project site for data collection. Here the location and orientation of the images taken are shown with small pyramids; (b) the produced 3D point cloud model is incomplete; (c) distortions in angle and distance, and (d) the reconstructed 3D point cloud is up to scale and is unit less.

Comparing Image-based 3D Point Clouds and BIM

Once the as-built 3D point cloud models are generated and are integrated with as-planned BIM, the resulting integrated project models can be used to identify progress deviations. The state-of-the-art methods for identifying these deviations mainly falls into two categories:

(1) *Analyzing the physical occupancy of the as-built models*: Research on occupancy based assessment methods use 3D point cloud models and BIM to monitor whether or not structural elements, Mechanical/Electrical/plumbing (MEP) components, or temporary resources such as formwork and shoring are physically present in the as-built point cloud model. These methods

are still challenged with the lack of enough details in (1) BIM and (2) work breakdown structure of the schedule. The 4D BIM may not have a physical representation for all elements, particularly for the temporary resources. Hence model-driven monitoring is not possible for all elements. The lack of formalized construction sequencing knowledge such as steps in placement of concrete elements (i.e. forming, reinforcing, placing, and stripping) in 4D BIM also adds to the complexity of the assessments, since without knowing exactly when each element is expected to be placed, identifying the most updated progress status is not possible.

(2) *Analyzing the appearance of the changes of the as-built models*: The latest research on appearance-based assessment of the as-built models superimposes the BIM with the 3D point cloud models and then back-projects the BIM elements to the images used to generating the point cloud model. From these back projections, several squared shape image patches are sampled and used to analyze the observed construction material. The most observed material from these image patches is then used to infer the most updated status of progress for each element in 4D BIM (Han and Golparvar-Fard 2015).

While significant advancement in research has been made, still applying these methods to a full-scale projects requires (1) accounting for the lack of details in 4D BIM, (2) addressing as-built visibility issues, (3) creating large-scale libraries of construction materials that could be used for appearance-based monitoring purposes; and (4) methods that can jointly leverage geometry, appearance, and interdependency information in BIM for monitoring purposes.

Visualization and Information Communication

Today's platforms for visualizing and communicating work in progress can produce 2D panoramas and 3D point cloud models (with or without BIM) for highlighting the work in progress and deviations from plan. The current 2D interfaces build on panoramic images and present a top-down view of project sites and ongoing operations. These project controls interfaces also provide tools for annotating the imagery for monitoring work in progress and field reporting purposes. However the provided functions are not sufficient for practical progress monitoring and information communication. For example, none of the current interfaces envision any workflow as to how the visuals can facilitate information sharing and communication.

The 3D interfaces also have a number of challenges that currently prevent their wide spread application. These interfaces either show the BIM or the 3D point cloud models. Hence it is difficult to differentiate and highlight the changes between isolated as-planned and as-built models. Also, the measurement tools in these interfaces are only capable of basic interactive operations such as 3D volumetric measurements from point cloud models. To facilitate information sharing and communication, the integrated project models – produced by superimposing BIM and the 3D point cloud models– should remain accessible by all onsite and offsite practitioners. Without having access to scalable and interactive web-based systems that can support such functionalities, it will be difficult to use the integrated project models to support smooth flow of information among project participants.

Overall, there is a lack of an end-to-end formalized procedure that can take account for visual as-built data collection, progress monitoring analytics, and visualization. In the following, a formal procedure is presented that can address current limitations. The opportunities for further research in each step of the procedure are discussed as well.

FORMAL METHODS FOR AUTONOMOUS MONITORING OF CONSTRUCTION PROGRESS

This section proposes a procedure for autonomous vision-based monitoring of construction progress, which consists of 1) data collection using camera-equipped UAVs, 2) vision-based analytics and comparison with 4D BIM for reasoning about progress deviations, and 3) performance analysis and visualization. Figure 4 illustrates these steps in detail.

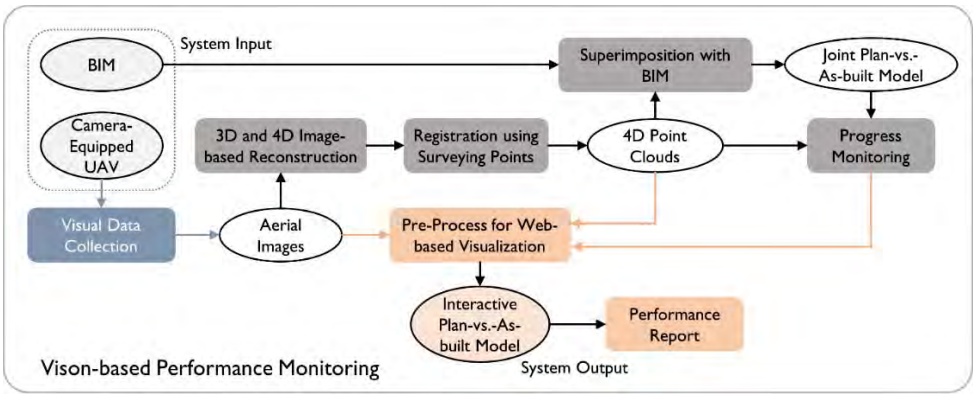

Figure 4. A procedure for autonomous vision-based monitoring of construction progress

Data collection

Figure 5 shows two different procedures for collecting visual data using UAVs for construction progress monitoring. In the first procedure, the images are directly used to produce 3D and 4D point cloud models. In the procedure shown in Figure 5b, the 4D BIM is used to assist with the data collection process. Since the 4D BIM entails information about where changes are expected to happen on a construction site, it can serve as a great basis for identifying scanning goals, path planning and navigation. This strategy can also potentially address the current limitations associated with path planning and navigation of the UAVs in interior spaces and dense urban areas. This is particularly important as current methods primarily rely on GPS for UAV control purposes while at indoor scenes or dense urban areas, reliable GPS is not accessible.

To support a complete and accurate image-based reconstruction – whether BIM is used for data collection or not– images should be taken with an overlap of 60-70%+. This rule of thumb guarantees detection of sufficient number of visual features in each image, which is typically required for standard Structure form Motion procedures. Taking images with such overlaps require adjusting and controlling the flight path and speed of the UAV. BIM guided data collection process as discussed in (Lin et al. 2015b) will certainly require less number of images and can more intelligently assist with choosing informative views necessary for progress monitoring purposes.

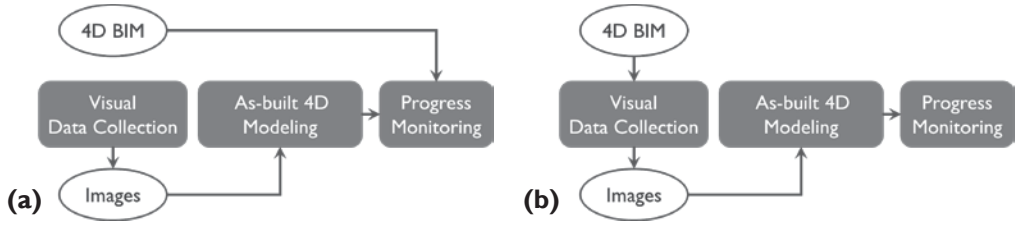

Figure 5. Two different alternatives for progress monitoring data collection

Data analytics

Alignment of image and BIM is the first step in vision-based analytics for construction progress monitoring. In early research (Golparvar-Fard et al. 2012), a pipeline of image-based reconstruction procedures consisting of Structure from Motion and Multi View Stereo algorithms were used to generate point clouds and then transform them into the BIM coordinate system. However, the 3D point cloud models generated through these standard procedures are up to scale. To recover the scale, a user-driven process is required to select at least three correspondences between the BIM and the point cloud. Utilizing these correspondences between the 3D point cloud model and BIM, the least square registration problem can be solved for the 7 degrees-of-freedom (3 rotation, 3 translation, 1 uniform scale) to transform and scale the point cloud to the BIM coordinate system. This manual process can be improved by leveraging BIM as a priori and adopting a constrained-based procedure for image-based 3D reconstruction which is shown in Figure 6 (Karsch et al. 2014). The results from preliminary experiments in (Karsch et al. 2014) show that the accuracy and completeness of the image-based 3D point clouds can be significantly improved with using BIM as a priori (Figure 7).

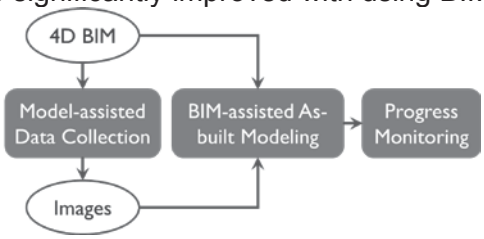

Figure 6. Leveraging BIM as *a priori* for as-built modeling purposes

Figure 7. BIM-assisted SfM: enhanced accuracy of overlaying BIM on site images.

Geometry and appearance-based progress monitoring analysis is the next step of data analytics. As discussed in section 2 current practices are suffering from challenges of geometry and appearance-based progress monitoring methods. To formalize the utilization of integrated project models for progress monitoring purposes and facilitating information flows, the following practical challenges that should be addressed first:

(1) *Lack of detail in as-planned models*- For accurate progress monitoring analytics, the as-planned model should contain a BIM with level of development of 400/450. It should also reflect daily operational details within the work break down structure (WBS) of the schedule which is to be integrated with BIM. Nevertheless, in today's practice of project controls, daily operation-level tasks are not often reflected in the WBS. Their corresponding elements such as scaffolding and shoring are also not typically represented in BIM. Hence with using these models, it is not easy to identify "who does which work at what location", especially for works related to temporary structures and for detecting both geometry and appearance based changes. Formalizing knowledge of construction sequencing and then enhancing the BIM with relevant reasoning mechanism, can enhance current progress monitoring methods. Figure 8 illustrates an example of this issue. As can be seen in the figure, the rebars and formwork should have been present in the as-planned models for accurate assessment of work-in-progress on placement a concrete foundation wall.

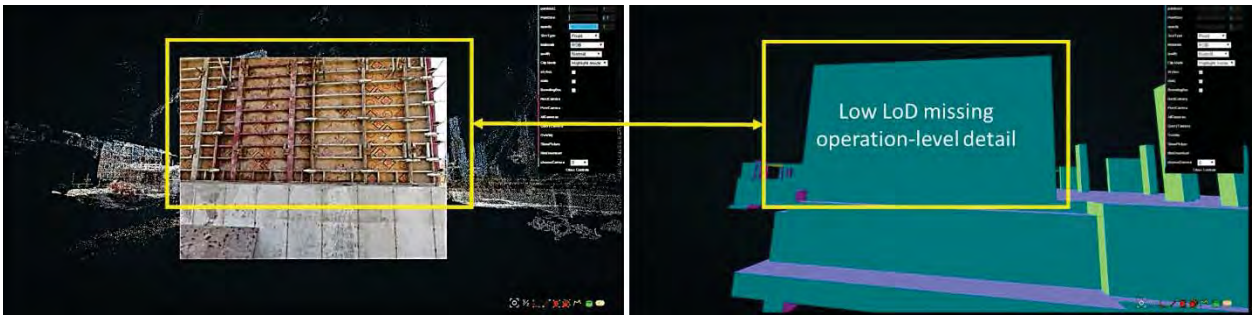

Figure 8. The necessary LoD in BIM that can enable comparison between as-built and as-planned for progress monitoring (Han et al. 2015)

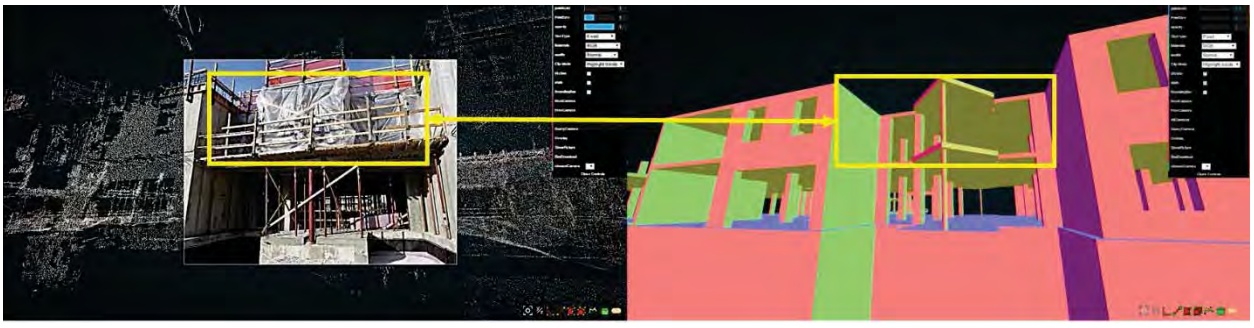

Figure 9. An example on how formalized knowledge of construction sequencing can resolve limited visibility issues

(2) *Limited visibility*- Although taking images from different viewpoints – assisted by the UAVs– may reduce the challenges associated with no visibility to construction elements, yet any progress monitoring method should still be able to account for progress reasoning based on

partial element visibilities. Formalizing knowledge of construction sequencing and integrating that into BIM through a reasoning mechanism can address this issue to some degree. The preliminary study conducted in (Han and Golparvar-Fard 2014b) shows that such formalized knowledge can enhance the performance of vision-based progress monitoring methods by five to seven percent. Figure 9 illustrates a case with a visibility issue that can be resolved by this reasoning mechanism.

Visualization and Information Communication

Developing a scalable and interactive web-based platform for visualizing images, point cloud models, BIM, together with analytical tools– particularly considering the limited memory and bandwidth on commodity smartphones and tablets– is challenging. The main requirements are:

(1) Interaction, presentation, and manipulation of large-scale point cloud models,
(2) Displaying integrated point cloud model with 4D BIM, and
(3) Offering quick and easy to use analytical and communication tools.

As a first step towards addressing these challenges, (Lin et al. 2015a) introduces a new web platform that can visualize as-built vs as-planned models. This new platform allows users to access integrated project models on smartphones and tablets. To present large-scale point cloud models in a convenient and scalable manner considering the limited memory available in commodity smartphones and tablets, the point cloud models are structured in form of nested octrees similar to (Scheiblauer et al. 2015). Figure 10 shows the developed web platform for visualizing as-built point clouds generated by camera-equipped UAV and as-planned BIM. Figure 10b in particular shows an example of the nested octree.

This data structure subsamples the point cloud and only shows relevant points depending on the user viewpoint. Also the number of points projected to the same pixel on the screen will be reduced according to the level of details chosen by the user. Loading a point cloud with density of 10 million points takes only approximate to 2 seconds on a standard commodity smartphone. The manipulation method can also be adjusted to first person or third person view controls. The platform is built with BIMServer (Beetz et al. 2010) to integrate 4D BIM (Figure.10 g-h) for visualization and information retrieval purposes. The semantic information necessary for progress monitoring (e.g. expected construction materials and element inter-dependency information) can be queried from BIM and presented through the integrated platform. To assist with documenting work in progress for those tasks that do not have any geometrical representation, several new tools are also created that allow the point cloud model to be directly color coded and semantics such as “who does which work at what location” to be accounted for based on various locations. This location-based method allows the issues associated with level of detail in BIM to be also addressed, since now the users can push and pull information from any user-annotated location (with or without a BIM representation). Integrating various workflows such as quality control as shown in Figure 1 is part of ongoing research.

DISCUSSION

The integrated project model presented in the previous section can bridge the gap in information sharing between the downstream feedback (onsite activities) and the short-term planning (coordination meeting). By providing a near real-time visualization of ongoing work, particularly *who does which work at what location*, it allows the most updated status of work in progress to be communicated among all parties on and offsite. The platform shows potential in supporting easy and quick identification of potential performance problems. It can also support root-cause analysis discussions in coordination meetings, ultimately leading to a more smooth flow of production in construction. Instead of measuring and communicating retrospective progress

metrics such as the EVA or Percentage Plan Complete (PPC) metrics, intuitive and data-driven communication of work in progress can allow for measuring progress based on more informative metrics such as task maturity or Task Anticipated (TA) and Tasks-Made-Ready (TMR) (Hamzeh et al. 2015).

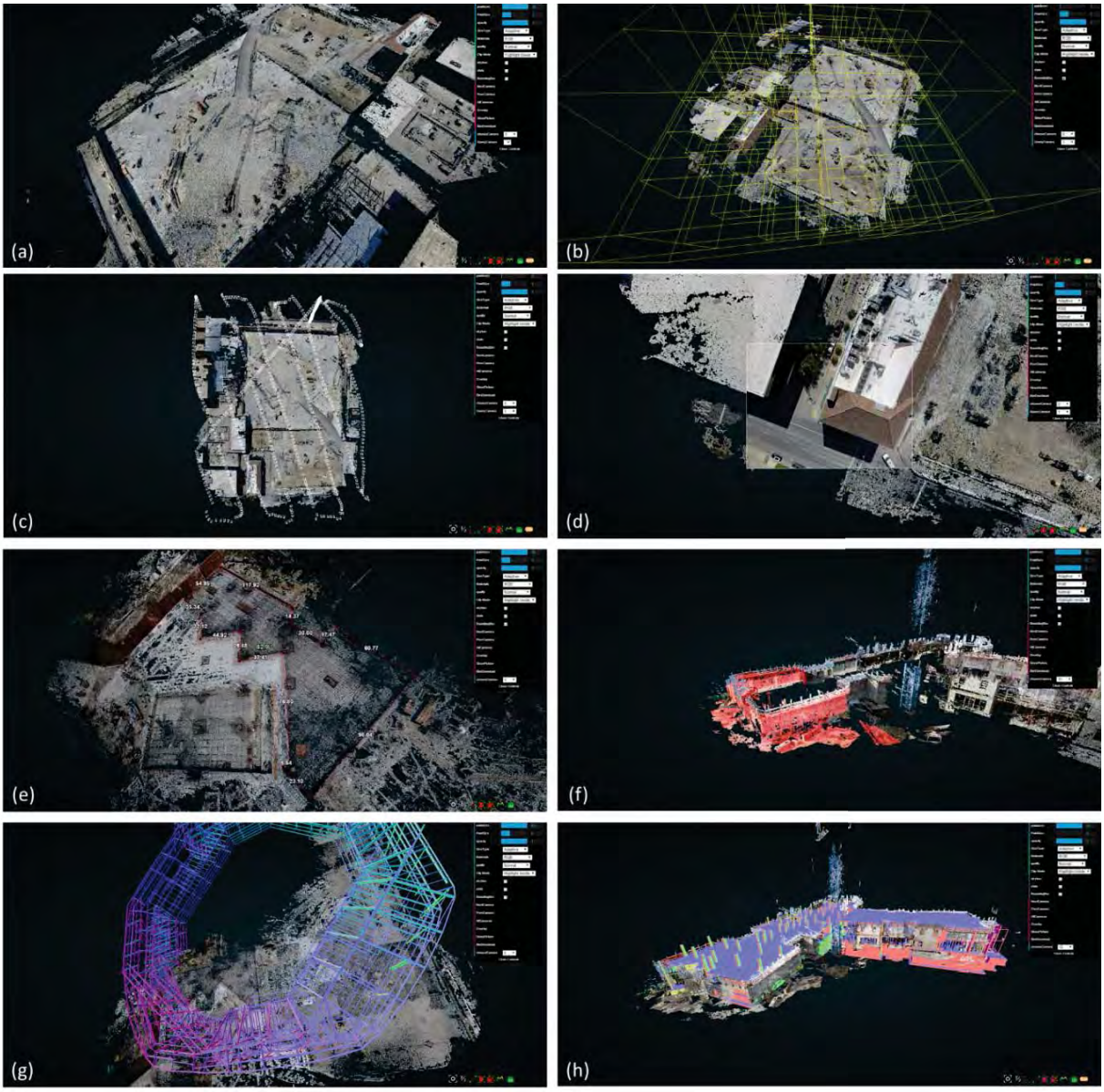

Figure 10. Web platform for visualizing as-built point clouds generated by camera-equipped UAV and as-planned BIM. (a) as-built point cloud; (b) the nested octree for pre-processing and visualizing point cloud in a scalable manner; (c) the location and orientation of the UAV-mounted camera when images were taken derived from the Structure from Motion algorithm; (d) viewing the point cloud models through one of the camera view points and texture mapping the frontal face of the camera frustum; (e) area measurement tool which directly operated on the as-built point cloud; (f) color coding part of the as-built point cloud for communicating who does which work at what location; (g) and (h) integrated visualization of the as-built point cloud and the as-planned BIM for two different construction projects.

CONCLUSION AND FUTURE WORK

This paper presents a formalized procedure via utilizing images taken by camera-equipped UAVs and BIM for generating integrated project models for construction progress monitoring purposes. The various aspects of data collection, analysis, and communication as it pertains to these integrated project models were discussed. These integrated project models have potential for enhanced information flow and improving situational awareness on construction projects. They can also support identifying and removing work constraints in coordination meetings, and measuring proactive metrics such as task maturity, Task Anticipated (TA), or Tasks-Made-Ready (TMR). The current limitations in data collection and analysis were discussed as well. Ongoing research is focused on addressing these limitations as well as conducting pilot projects on using the proposed procedures for creating integrated project models and validating their potential in smoothening information flow and improving situational awareness on construction projects.

ACKNOWLEDGMENTS

This research is financially supported by the National Science Foundation (NSF) Grant CPS #1446765. Any opinions, findings, and conclusions or recommendations expressed in this material are those of the authors and do not necessarily reflect the views of the National Science Foundation. The technical support of the industry partners in providing access to their sites for data collection and assisting with progress monitoring analytics is also appreciated.

REFERENCES

Bae, H., Golparvar-Fard, M., and White, J. (2013). “High-precision vision-based mobile augmented reality system for context-aware architectural, engineering, construction and facility management (AEC/FM) applications.” *Visualization in Eng*, Springer, 1(1), 1-13.

Bae, H., Golparvar-Fard, M., and White, J. (2014). “Image-Based Localization and Content Authoring in Structure-from-Motion Point Cloud Models for Real-Time Field Reporting Applications.” *Journal of Computing in Civil Engineering, DOI: 1023 .1061/(ASCE)CP.1943-5487.0000392*, B4014008, 637–644.

Beetz, J., van Berlo, L., de Laat, R., and van den Helm, P. (2010). “bimserver. org–An Open Source IFC Model Server.” *Proceedings of the CIB W78 2010: 27th International Conference–Cairo, Egypt*, (Weise 2006), 16–18.

Bosché, F., Ahmed, M., Turkan, Y., Haas, C. T., and Haas, R. (2014). “The value of integrating Scan-to-BIM and Scan-vs-BIM techniques for construction monitoring using laser scanning and BIM: The case of cylindrical MEP components.” *Automation in Construction*, 49, 201-213, Elsevier.

Brilakis, I., Fathi, H., and Rashidi, A. (2011). “Progressive 3D reconstruction of infrastructure with videogrammetry.” *Automation in Construction*, Elsevier, 20(7), 884–895.

DJI Ground Station (2015). http://www.dji.com/info/releases/dji-released-2-4g-bluetooth-datalink-ipad-ground-station, last accessed 5/18/2015.

Golparvar-Fard, M., Pena-Mora, F., and Savarese, S. (2009). “D4AR- A 4-Dimensional Augmented Reality model for automating construction progress data collection, processing and communication.” *Journal of ITCON*, 14(1), 129–153.

Golparvar-Fard, M., Peña-Mora, F., and Savarese, S. (2011). “Integrated Sequential As-Built and As-Planned Representation with Tools in Support of Decision-Making Tasks in the AEC/FM Industry.” *Journal of Construction Engineering and Management*. 137(12), 1-21.

Golparvar-Fard, M., Peña-Mora, F., and Savarese, S. (2012). “Automated Progress Monitoring Using Unordered Daily Construction Photographs and IFC-Based Building Information Models.” *Journal of Computing in Civil Engineering*, 10.1061/(ASCE)CP.1943–5487.0000205.

Hamzeh, F. R., Saab, I., Tommelein, I. D., and Ballard, G. (2015). “Understanding the role of ‘tasks anticipated’ in lookahead planning through simulation.” *Automation in Construction*, 49, Part A(0), 18–26.

Han, K., and Golparvar-Fard, M. (2014a). “Multi-Sample Image-Based Material Recognition and Formalized Sequencing Knowledge for Operation-Level Construction Progress Monitoring.” *Computing in Civil and Building Engineering*, I. Raymond and I. Flood, eds., American Society of Civil Engineers, 364–372.

Han, K., and Golparvar-Fard, M. (2014b). “Multi-Sample Image-Based Material Recognition and Formalized Sequencing Knowledge for Operation-Level Construction Progress Monitoring.” *International Conference on Computing in Civil and Building Engineering, 2014*, 364–372.

Han, K., and Golparvar-Fard, M. (2015). “Appearance-based material classification for monitoring of operation-level construction progress using 4D BIM and site photologs.” *Automation in Construction*, Elsevier, 53, 44–57.

Han, K., Lin, J., and Golparvar-Fard, M. (2015). “Model-driven Collection of Visual Data using UAVs for Automated Construction Progress Monitoring.” *Int’l Conference for Computing in Civil and Building Engineering 2015, Austin, TX June 21-23*.

Karsch, K., Golparvar-Fard, M., and Forsyth, D. (2014). “ConstructAide: analyzing and visualizing construction sites through photographs and building models.” *ACM Transactions on Graphics (TOG)*, ACM, 33(6), 176.

Lin, J., Han, K., Fukuchi, Y., Eda, M., and Golparvar-Fard, M. (2015b). “Model-Based Monitoring of Work-in-Progress via Images Taken by Camera-Equipped UAV and BIM.” *2nd International Conference on Civil and Building Engineering Informatics*, Tokyo, Japan.

M. Golparvar-Fard, Pena-Mora, F., Savarese, S., Golparvar-Fard, M., Pena-Mora, F., and Savarese, S. (2011). “Monitoring changes of 3D building elements from unordered photo collections.” *Computer Vision Workshops (ICCV Workshops), 2011 IEEE International Conference on*, 249–256.

Scheiblauer, C., Zimmermann, N., and Wimmer, M. (2015). “Workflow for Creating and Rendering Huge Point Models.” *Fundamentals of Virtual Archaeology: Theory and Practice*, A K Peters/CRC Press.

Siebert, S., and Teizer, J. (2014). “Mobile 3D mapping for surveying earthwork projects using an Unmanned Aerial Vehicle (UAV) system.” *Automation in Construction*, Elsevier, 41, 1–14.

Yang, J., Park, M.-W., Vela, P. A., and Golparvar-Fard, M. (2015). “Construction performance monitoring via still images, time-lapse photos, and video streams: Now, tomorrow, and the future.” *Advanced Engineering Informatics*, Elsevier. 29 (2), 211–224.

Zollmann, S., Hoppe, C., Kluckner, S., Poglitsch, C., Bischof, H., and Reitmayr, G. (2014). “Augmented Reality for Construction Site Monitoring and Documentation.” *Proceedings of the IEEE*, IEEE, 102(2), 137–154.

Exploratory Study on Factors Influencing UAS Performance on Highway Construction Projects: as the Case of Safety Monitoring Systems

Author [1] Sungjin Kim, [2] Javier Irizarry
School of Building Construction, College of Architecture
Georgia Institute of Technology
280 Ferst Drive, 1st Floor
Atlanta, GA, 30318
Email: sungjinkim@gatech.edu, javier.irizarry@coa.gatech.edu

ABSTRACT

Highways are one of the most important infrastructure systems that support our society. Infrastructure construction projects, particularly highway projects, have become increasingly large and complex. It is critical that project managers protect workers from accidents by providing a safe work environment. Therefore, safety managers should frequently monitor the worksite conditions and prevent accidents on construction sites. Unmanned Aerial Systems (UASs) have a great potential to fly and monitor highway construction sites, since the horizontal layout of these jobsites has few obstacles that disturb the operation of UASs. Comprehensive literature reviews aim to refine factors influencing the performance of UAS as safety monitoring systems on the jobsite. A questionnaire survey was developed to analyze UAS implications on highway projects and critical factors based on the derived potential 29 factors and 17 benefits that can be performance measure attributes. As a beginning step of understanding UAS in construction environments, this exploratory research contributes to defining critical factors influencing the performance of UAS on highway construction environments.

Key words: critical factor analysis—highway construction project—performance measurement—safety monitoring system—unmanned aerial system (UAS)

INTRODUCTION

Infrastructure construction projects require a significant amount of time, capital and human resources during the project life cycle. It has also required more advanced construction management systems to assists project managers with the significant challenges faced in continuously evolving worksites. One of the most momentous challenges in infrastructure sites is construction workers' safety. Even with the progress made in site safety, the laborers are still exposed to hazardous conditions. The Occupational Safety and Health Administration (OSHA) in the United States requires that project owners and contractors have a duty to prevent workers from having fatal accidents on worksites. According to the U.S. Bureau of Labor Statistics, 796 construction-related fatal injuries were occurred in 2013 (BLS 2015). This statistic indicated the fatality ratio in construction industry is a big concern in the United States.

One of the safety managers' main responsibilities is to observe workers' behavior, work sequencing and the jobsite conditions to prevent workers from having construction-related accidents. For the last few years, many researchers have developed advanced Information Technology (IT) based safety monitoring systems to reduce accidents on construction sites. Lin developed workers' behavior monitoring system on construction site (Lin et al. 2013) and Naticchia (2013) developed real-time unauthorized interference control system based on RFID

Proceedings of the 2015 Conference on Autonomous and Robotic Construction of Infrastructure, Ames, Iowa.

(Naticchia et al. 2013). As an important part of our infrastructure, highway construction projects have unique characteristics. These horizontal construction projects can extend through long distances. Hence, they need monitoring systems that can cover safety issues on these extensive construction worksites and their surrounding environments.

A proposed method to address this issue is the use of Unmanned Aerial System (UAS), which are remotely operated without an onboard operator. UASs can maximize the efficiency of safety monitoring in highway construction projects because no vertical obstacles affecting UAS operations would be present. UASs can easily monitor all site areas by circling around the site under a safety manager's control and delivering real-time images and videos. This technology has been utilized to perform monitoring or inspecting in various industries, for example, monitoring soil erosion (D'Oleire-Oltmanns et al. 2012) monitoring forest fires (Hinkley and Zajkowski 2011) and bridge inspection (Eschmann et al. 2012; Morgenthal and Hallermann 2014). In particular, Irizarry developed the concept of UAS-based safety inspection system during construction (Irizarry et al. 2012).

However, the use of UASs on construction sites is in very early stages and their impact on construction management tasks is not known and the implication of UASs use in construction is not fully understood. Although UAS is being researched in various industries around the world, very few studies on the impact of UAS applications in construction have been carried out. In order to understand the potential of this technology in construction environments, performance measurement and evaluation of UASs for tasks, such as safety monitoring, is necessary for supporting the implementation of UAS technology in all types of construction projects. This research defines critical factors influencing UAS performance through extensive literature review, surveys and interviews with construction and IT professionals. This study aims to define performance measurement factors for the performance of UAS in construction safety monitoring tasks in highway construction or other infrastructure projects. Furthermore, the main findings will be able to contribute to our understanding of the potential impact of adoption of UAS technology in the Architecture, Engineering, Construction and Operations (AECO) industry.

PROBLEM STATEMENT

Zhou (2013) comprehensively reviewed 119 published studies in terms of advanced safety management technology between 1986 and 2012 (Zhou et al. 2013). Even though the number of research focusing on IT-Based safety control systems has dramatically increased over two decades (Figure 1A), the construction accident rate has been still unstable and frequent in the AECO industry (Figure 1B). In addition, the construction injury rate is a big concern with this industry having the highest fatality ratio 21 percent from all industries in the United States (Figure 1C) (BLS 2015) Zhou concluded that future studies should pay more attention to proactive safety management systems, such as safety monitoring or information systems rather than the reactive system for achieving the goal of zero accidents on worksites (Zhou et al. 2013).

As one of the proactive safety control systems, Irizarry (2012) suggested the concept of a UAS safety inspection and monitoring system in the AECO industry. He proposed the UAS could provide aerial images as well as real-time videos from a range of locations around the jobsite to safety managers with fast access, since it was equipped with high resolution camera and Wireless system (Irizarry et al. 2012). Even though UAS research has been of increased interest to practitioners in the AECO industry, the concept's application has not been perfectly investigated. Moreover, researchers have never measured UAS's effects on various construction environments. For this reason, measurement and evaluation of the performance of UAS-based safety monitoring system is needed. In addition, many important factors associated

with UAS technology are not fully understood. Recent studies have aimed to solve existing technical problems, introduced new technology to improve the current systems, or ignored the factors influencing the performance of the systems.

A. Research Trend of Advanced Safety Control System (1986 ~ 2012)

B. Fatalities in Construction Industry (2008-2013) (BLS 2015)

C. Fatality Ratio in the U.S. Industry in 2013 (BLS 2015)

Figure 1. IT Safety Research trend and Construction Accidents

Therefore, there are gaps in most practitioners' understanding of which factors can affect the performance of UAS system. This paper will answer the research questions stemming from three main research problems and fill the aforementioned gaps (Table 1.) The goal of this study is to define critical factors that may contribute or influence the performance of UAS-based monitoring system through industry-wide surveys.

Table 1. Research Problem Statement

Research Problems	Research Questions	Research Gaps
AECO Industry is not familiar UAS	How has the UAS concept been applied in industries including AECO?	*Research Gaps are* (1) What factors can affect performance of UAS in case of safety monitoring tasks, (2) How they affect, and (3) What their impacts are on the highway construction worksite
UASs' potential applications *(i.e. Safety Monitoring task)* is not understood	How can a UAS be applied for safety monitoring or inspection in construction?	
Factors that may contribute to the performance of UAS and benefits from UAS have not been investigated	What are critical factors that may influence the performance of UAS in safety monitoring? What are potential benefits of UAS in case of safety monitoring, or the potential attributes to evaluate the performance of UAS?	

RESEARCH BACKGROUND

Safety Monitoring

Construction environments usually have low quality working-conditions as well as high accident risk potential. Safety managers are responsible for preventing construction workers from having any type of construction accident. Toole (2002) determined that most construction accidents have eight basic causes: (1) Insufficient Safety Training, (2) Weak enforcement of safety, (3) Insufficient safety equipment (4) Unsafe work method sequencing, (5) Unsafe site conditions, (6) Improper Safety equipment, (7) Poor attitude toward safety, and (8) workers' bad behavior (Toole 2002). The safety manager should pay attention to the above eight causes of fatalities on construction jobsites. Irizarry (2012) identified the three main characteristics of observation in safety inspection. First, the observation should be frequently performed. Second, the manager should be able to observe in person all designated areas and tasks on the jobsite. Third, the managers should interact with workers on site (Irizarry et al. 2012).

Lee and Kim (2009) developed a mobile safety monitoring system, which is based on hybrid sensor, in order to reduce the rate of fatal accidents on construction sites. Prabhu (2005) developed a Tablet PC application to inspect jobsites for safety issues and prevent fatalities. Leung et al (2008) developed a monitoring system based on network cameras that can be used in a web environment to observe the quality of construction work. Lin et al (2013) developed a model for tracking workers' behavior on a large-dam construction site. Naticchia (2013) reviewed previous literature and developed a monitoring system based on ZigBee technology in order to detect unauthorized worker behavior in real-time. Table 2 summarizes previous research about safety monitoring systems.

Table 2. Current IT-based safety monitoring systems

References	System Function	Main Information	Technology
(Lee et al. 2009)	Reduce dead zones of safety management where fatal accidents, especially falls	Developed and applied on the real jobsite	Hybrid Sensor
(Sunkara 2005)	Safety inspection, Fatality Prevention	Modeling, performance evaluation, case study	Tablet PC Application
(Leung et al. 2008)	Monitoring the quality of construction work	Developed the model, Pilot study	Network Camera
(Lin et al. 2013)	Workers' behavior analysis, Onsite Tracking	Modeling, Application on real site	RSSI, ZigBee
(Naticchia et al. 2013)	Real-time unauthorized interference control	Laboratory testing, Onsite test	RFID ZigBee

UAS Applications

Unmanned Aerial System (UAS)

Unmanned Systems have brought great benefits to military missions and most recently to civilian life. These systems are unmanned hardware platforms equipped to perform data collection and sometimes processing, and to operate without direct human intervention, such as

unmanned aerial vehicle, satellites, and underwater explorers. In particular, Unmanned Aircraft System (UAS) has been the focus of potential application in various industry areas in the United States in recent years. UAS, commonly known as a drone, can be defined as, *"A powered aerial vehicle that does not carry a human operator, uses aerodynamic forces to provide vehicle lift, can fly autonomously or be piloted remotely"* (Newcome 2004). The Federal Aviation Administration (FAA), the national aviation authority of the United States, has adopted the term, "UAS (Unmanned Aircraft/Aerial System)" instead of "UAV (Unmanned Aerial Vehicle)", because the concept of unmanned aircraft should have ground control station, vehicles, and other elements for its safe operation.

Federal Aviation Administration (FAA) Regulation in the U.S

Federal Aviation Administration (FAA) has authority over all commercial flight regulations in the United States National Airspace System (NAS). The FAA defines two types of small UAS operations in the United States: (1) public operations and (2) civil operations, and they managed the regulatory environments for each flight type. Therefore, familiarity with these regulations is very important if the commercial application of UAS on construction environments is to be understood.

Public operations can be defined as government-related aircraft operations to conduct public activities including military operations, law enforcement, and research and development. FAA issues Certificate of Authorization or Waiver (COA) to qualified applicants who want to use UAS for public operations in the United States. COA is a permission that UAS operators must request to use UASs for commercial applications (FAA 2015A). Then COA holders can control and operate UASs legally. Between 2006 and 2012, 791 COA applications were approved out of 897 based on analysis of FAA's released data. In addition, total 79 organizations have obtained COAs from the FAA as of February 25th, 2015 (FAA, 2015B). Civil operations can be considered any operation that cannot meet the required criteria for public operations. The FAA suggests two methods to grant an authorization for civil operations: Section 333 exemptions and Airworthiness Certificate. A total of 289 petitioners have been granted Section 333 exemptions as of May 5th, 2015 (FAA, 2015C).

UAS Applications in various industries

Unmanned Aerial Systems (UASs) were initially utilized in military missions and boarder observation in the United States (Nisser and Westin 2006). More recently, considerable other studies have also been devoted to potential applications of UASs in various industries such as agriculture, meteorological observation, forestry, archeology, and infrastructure (Table 3). In addition, federal or state agencies in the United States have been operating small UASs with the goal of law enforcement or surveillance. According to the Association for Unmanned Vehicle Systems International (AUVSI), the market for UAVs is about $11.3 billion, and the potential spending will grow to over $140 billion for the next 10 years in the United States (Jenkins and Vasigh 2013).

UAS Safety Inspection and Monitoring System

Irizarry (2012) suggested the concept of a UAS safety inspection tool and examined two feasible scenarios for UAS implementation. The UAS can fly all around the construction jobsite and provide safety managers with real time information such as work sequencing and worker behavior (Irizarry et al. 2012). A UAS can be equipped with high-resolution cameras, various sensors including a Global Positioning System (GPS). In addition, they can be operated

autonomously or semi-autonomously with pre-defined flight paths over construction sites. Figure 2 shows the general framework of UAS's application for monitoring safety issues on construction sites. First, Heuristic Evaluation (HE) was conducted to evaluate the user interface of an of-the-shelf and quad copter type UAS (Parrot AR drone). Second, a user participation experiment was designed to decide the optimal interface size among three alternatives: (1) Plain screen, (2) Phone size, and (3) Tablet PC. In this experiment, it was concluded that the combination of drone and user interface with tablet PC size display was adequate to perform safety inspection related tasks on the construction site. The results motivate the continued study of UAS technology for safety management related tasks.

Table 3. Recent UAS's application studies in various industries

Industry	References	UAS's Function
Agriculture And Forestry	(D'Oleire-Oltmanns et al. 2012)	Monitoring soil erosion
	(Hinkley and Zajkowski 2011)	Monitoring forest fires
Meteorology	(Reuder et al. 2009)	Observing atmospheric Boundary Layer
Archeology	(Rinaudo, Chiabrando, Lingua 2012)	Monitoring daily work of the excavation
	(Saleri et al. 2013)	Creating 3D models of archaeological heritages
Infrastructure	(Eschmann et al. 2012; Morgenthal and Hallermann 2014)	Bridge inspection
	(Eschmann et al. 2012)	Building and facility inspection

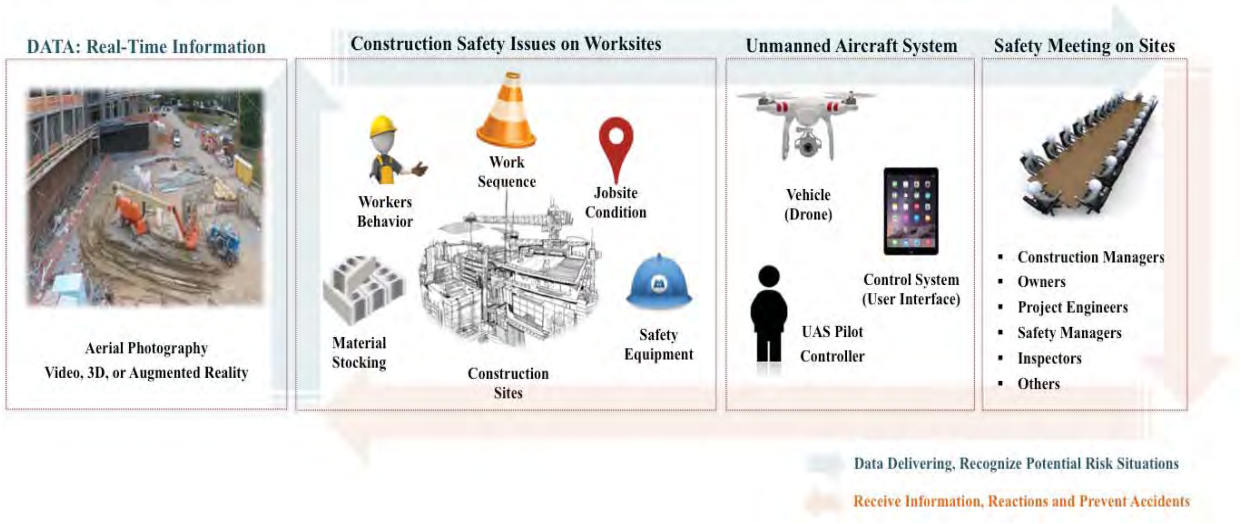

Figure 2. Concept of UAS-based safety monitoring

Critical Factors Influencing Performance

In the AECO industry, a Performance Measurement System (PMS) is an essential element of construction management. The use of a simple and well-designed PMS is essential for supporting the implementation of business strategies such as the application of drone technology for safety monitoring on the construction site (Sarhan and Fox 2013). It is very important that the factors affecting performance should be reasonably defined in order to accurately evaluate performance of a system. Nitithamyong (2006) conducted an empirical study to define potential factors influencing performance of commercial Web-Based Construction Project Management Systems (WPMSs). The author defined 42 potential factors and potential 36 measurements, which can be used for evaluating performance of the WPMS. These potential elements were further refined from previous literature reviews, interviews with professionals from 18 construction firms and the results of collected data from the questionnaire survey of 39 professionals who had practical experience in the AECO industry (Nitithamyong and Skibniewski 2006).

RESEARCH METHODOLOGY

This exploratory study aimed defining and analyzing factors that may influence the performance of a UAS-based safety monitoring system was conducted in three main phases and activities as shown in figure 3. The stages are (1) development of a conceptual factor model, (2) survey instrument, (3) analyzing and defining factors. The following sections in this chapter describe the steps of the study in more detail.

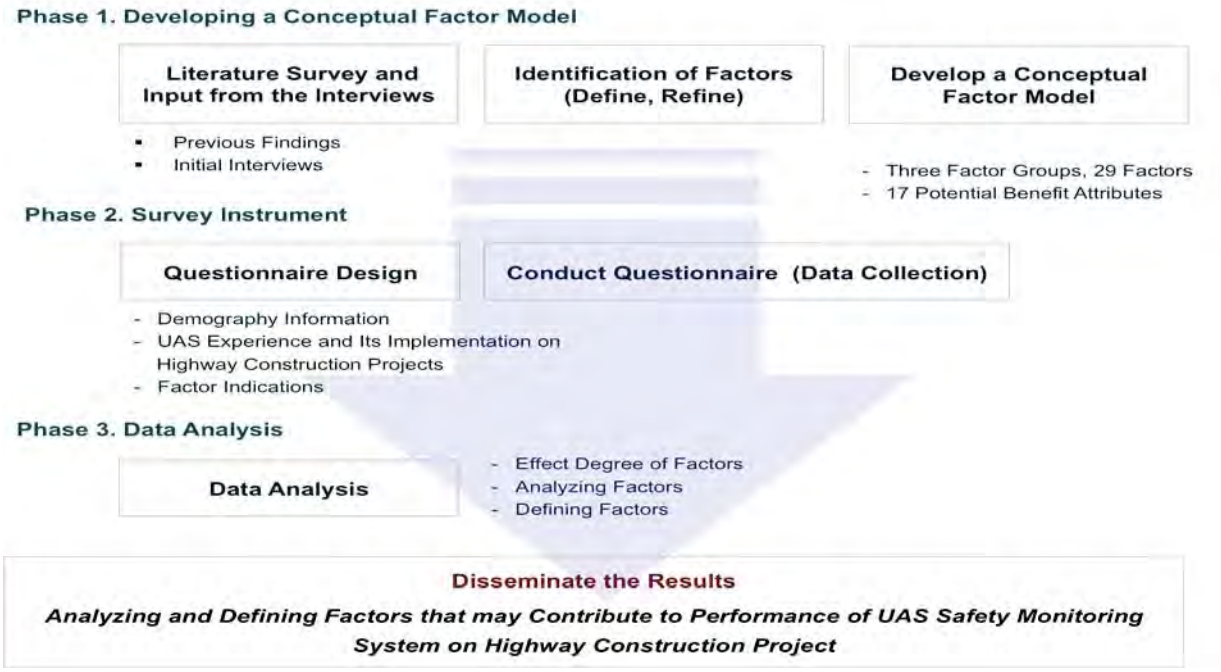

Figure 3. Research Work plan

The first phase began with a comprehensive literature review and interviews to develop an initial factor model. The UAS-based safety inspection concept was used in study (Irizarry et al. 2012), factor analysis for implementing safety management system was performed (Ismail et al. 2012), and Nitihamyong and Skibniewski (2006) method for defining success or failure factors and measures of a web-based project management system was adopted in this study. In addition,

semi-structured interviews with seven professional IT researchers and three construction project personnel were conducted. The interviewees first watched the visual assets (images and videos) obtained from a UAS at construction sites on a laptop and were introduced to the UAS safety monitoring system concept. Then they provided feedback that was used to develop the factors that may have an effect on the performance of a UAS safety monitoring system on construction environments. The interviews were conducted on November 2014.

Questionnaire Survey Instrument

The questionnaire Instrument had three parts, including demographic questions, personnel opinions on UAS and highway construction projects, and the initial set of factors. Demographic questions were asked to understand the background of survey participants. The second section required participants to describe their knowledge and experience of UAS as well as uses of a UAS safety monitoring system on highway construction projects. The respondents were also requested to indicate if the presented factors would affect the UAS's performance on highway construction projects. Questions with three choice options; Yes, No, Do not know, were used for indicating participants agreement level. Topics in the questions included UAS's system characteristics, project characteristics, project team characteristics. This questionnaire survey was reviewed by Georgia Institution of Technology's Institutional Review Board (IRB) and approved for use with human subjects. A total 15 responses have been collected in a three-week period from mid April to early May 2015.

RESULTS

Developing Conceptual Factor model

A total of 46 potential factors were derived based on the three previous studies and input from the interview with IT and construction professionals. These factors include 29 potential factors and 17 potential benefit attributes. Three main factor groups include (1) UAS system features, (2) Project Team features, and (3) Project Features that may impact the performance of UAS safety monitoring system in highway construction projects. Particular UAS systems may influence the performance of UAS, since they have some specifications like controller, battery and camera. They need to be considered in order to develop an optimal safety monitoring system. In addition, implementing such a system on construction projects requires various conditions, such as interest, training, knowledge, or experience, to be considered. This is one of the most important considerations to define factors for successful performance of UAS. All control systems for construction management require different functions, environments, and benefits on construction projects. The project has varied conditions and features so they should be considered to implement UAS and measure UAS performance. In this paper, the factor of project type and owner type are defined as highway construction project and owner as government agency respectively.

In addition, there are several other measures such as benefits of performance that should be considered when evaluating the performance of UAS-based safety monitoring systems on highway construction environments. These are anticipated impacts when the UAS safety monitoring system is implemented. Finally, a conceptual factor model was developed as described in Figure 4. Table 4 summarizes the potential factors associated with the three factor groups and Table 5 describes the potential attributes related to the benefits or performance of UAS safety monitoring system.

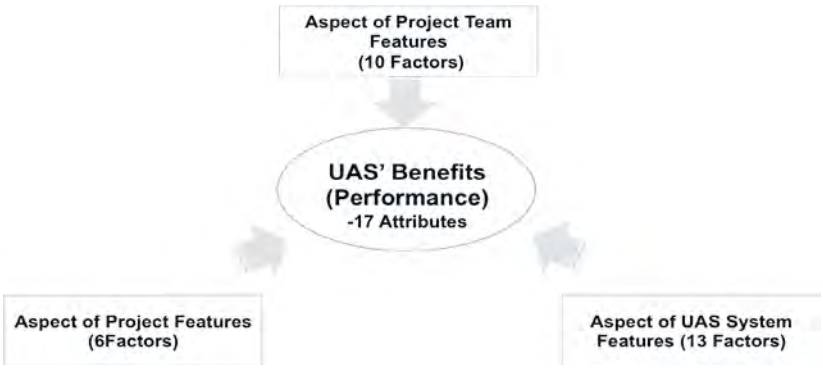

Figure 4. Conceptual Factor Model

Table 4. Potential Factors Influencing UAS Performance

Factor Group	Factor Description
UAS System Features (13)	1. Easy user interface for UAS operation
	2. Obtained quality of visual assets (photo, video)
	3. Battery life of the UAS
	4. UAS system reliability
	5. Maximum Visible Angle of the UAS Camera
	6. Autonomous flight capability
	7. Communication range for UAS control
	8. Equipped Sensors (i.e. GPS, Compass etc.)
	9. Flight Stability
	10. Features of UAS camera (i.e. Image resolution, video recording capability, infrared)
	11. Available sensors (i.e. Compass, Gyroscope, Accelerometer, etc.)
	12. Emergency response system (Failsafe for lost connection, return to ground control station, etc.)
	13. UAS system's easy upgradability without manufacturer's services
Project Features (6)	1. Project location (urban vs. rural)
	2. Project cost
	3. Project size
	4. Duration of project
	5. Complexity of the construction tasks
	6. Sub contractors trades involved
Project Team's Features (10)	1. Team's prior experience with UAS
	2. Team attitudes toward UAS in construction Projects
	3. Team's prior experience with IT-based safety system
	4. Team attitudes toward IT in construction projects
	5. User type (safety manager or hire pilot)
	6. Knowledge of UAS safety monitoring system features
	7. Adequacy of resources for UAS use as safety monitoring system (i.e. money, time, personnel, etc.)
	8. UAS control ability of users (safety managers or project managers)
	9. Adequacy of training or education for UAS use as safety monitoring system
	10. Clear method to measure the performance of UAS safety monitoring system

Questionnaire Survey Results

The targeted respondents of the survey were professionals who are involved in project or construction management and safety management (i.e. owners, construction managers, engineers, or safety managers) in the AECO industry. For three weeks, a total of 15 responses were collected to explore the factors that may impact on the UAS performance in terms of safety monitoring on highway construction environments. Of these 15 participants, six have over 20 years of experience (40%), three have worked between 11-20 years (20%), and others have experience of less than 10 years (40%) in the construction industry. The results also show they have various work positions in construction companies. There are three project managers (20%), five safety managers (33.33%), two BIM managers (13.33%), one IT director (6.67%), one scheduler (6.67%) and others including owner and risk manager (20%). Figure 5 depicts the demographic information of all respondents.

Table 5. Potential Benefit Attributes

Features	Attribute Description
Potential Performance Attributes	1. Reduce bottlenecks in communication during safety control process
	2. Effective management of construction workers' behaviors
	3. Inspection of personal protective equipment use
	4. Effective monitoring of the whole work site
	5. Effective monitoring of hard to access areas on work sites
	6. Effective monitoring of traffic and vehicles on work sites
	7. Effective monitoring of heavy or hoisting equipment on work sites
	8. Reduce time it takes to perform safety monitoring tasks
	9. Makes identification of safety issues easier
	10. Reduces number of construction injuries
	11. Reduces cost of safety management system
	12. Expedites reaction to potential hazards
	13. Improves project safety performance
	14. Improves overall project performance
	15. Enables immediate reporting of potentially dangerous situations and allows preventive measures to be applied
	16. Simplification of documentation process or reduces waste time for documentation (reduce hardcopy)
	17. Enhances and identification and actions regarding potential hazards on sites

Figure 5. Demographic Information of Respondents

The second section asked respondents to share their views about UAS on highway construction projects. All of them already had knowledge of the concept of UAS or drone and how the machine is operated. Specifically, nine (60%) had experience with UAS for hobby (11.1%), training (11.1%), or utilizing on the construction project (77.8%). They have operated and been familiar with UAS for less than two years. Figure 6 summarizes that the respondents' UAS experiences. 13 out of 15 respondents (80%) had positive opinions about the implications of UAS safety monitoring system on the highway construction project.

Almost all respondents (80%) had positive expectations of the use of a UAS safety monitoring system on highway construction environments. They mainly agreed with that a UAS would be a good fit for safety monitoring on highway construction sites since these are more horizontal and open sites, and they can extend for miles. In addition, they suggested and recommended that USAs can access areas humans sometimes cannot directly access, can monitor work flow, jobsite logistics and material stocking on the jobsite, and have the capability to reduce the costs safety monitoring. On the other hands, only two (20%) were concerned that the FAA will not allow legally the use of UAS on the construction site and the battery life of UAS would limit the effectiveness of UAS for safety monitoring tasks.

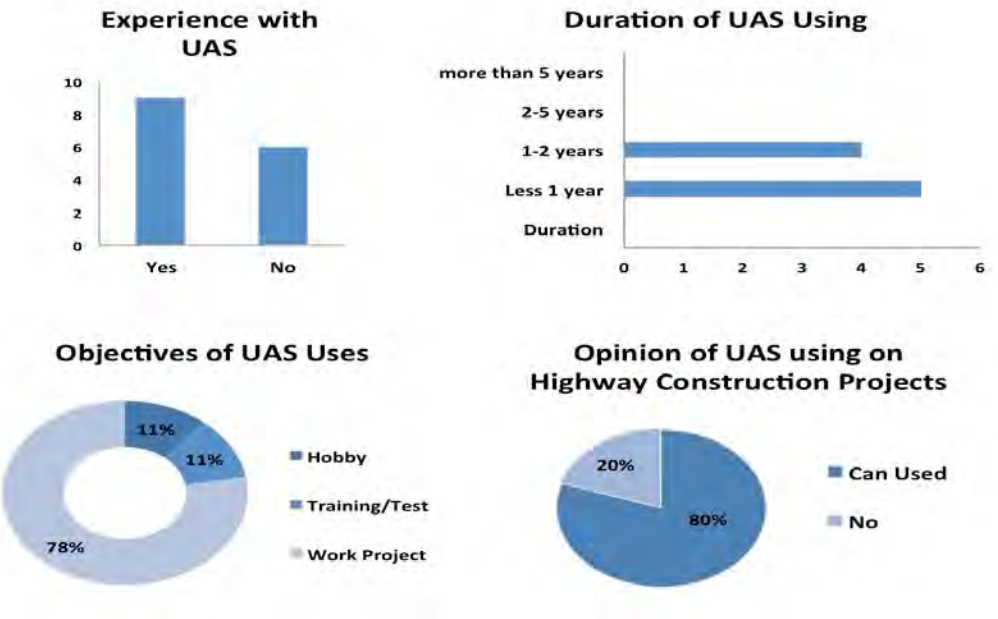

Figure 6. UAS Experience of Respondents

Since 40% of respondents had no experience with this tool, this could affect on the reliability of the result of this analysis. Therefore, this paper has only an exploratory analysis and introduces preliminary results. Continued research will include field flight test with a small UAS platform where project personnel will participate in the test and then be asked to provide their opinion about the factors and performance of UAS's applications on highway construction projects.

Exploratory Analysis of Factors

Factors that may influence the performance of UASs are derived from the extensive literature review and the interviews with industry professionals. The last section of the questionnaire survey asked the respondents to indicate whether they thought the factors would affect the

performance of a UAS-based safety monitoring system on highway construction sites. Regarding the factors influencing the performance of UASs, all of respondents agreed that the seven factors of (1) ease of user interface for UAS operation, (2) quality of visual assets, (3) UAS system reliability, (4) features of UAS camera, (5) team's prior experience with UAS, (6) adequacy of resources for UAS use as safety monitoring system, and (7) adequacy of training or education for UAS use as safety monitoring system should be considered as influencing factors on the performance of UAS applications in the case of safety monitoring system on highway construction environments.

However, more than half of respondents did not know or disagreed that two factors, such as (1) UAS system's easy upgradability without manufacturer's services and (2) sub contractors trades involved contribute to the performance of the UAS safety monitoring system on highway construction projects. In addition, one-third of the professionals did not know if duration of project, complexity of the construction tasks and user type (safety manager or hire pilot) were related to the considerations for UAS's performance for safety monitoring tasks on the jobsites or not. Since the number of response for this survey is small, these factors must be considered after collecting more data from construction and UAS practitioners. Table 6 provides details on the magnitude of the impact of the factors based on indications of responses collected from the respondents.

Regarding the benefits and performance attributes, 14 out of 15 personnel agreed that effective monitoring of the whole work areas could be achieved with a UAS safety monitoring system on highway construction projects. The apparent benefits or performance measures are (1) Effective monitoring of traffic and vehicles on sites, (2) Effective monitoring of heavy or hoisting equipment on sites, (3) Enhanced identification of actions related to potential hazards on sites with 87% of respondent in agreement. One explanation is that use of small UAS platform in highway construction sites can be a potential safety control system and contribute to the effective monitoring tasks on large worksites. However, the time it takes to perform safety monitoring and simplifying the documentation process or reducing wasted time for documentation could not be considered as benefits from utilizing a small UAS. In addition, they were doubtful that a UAS monitoring system can improve overall project performance or can reduce number of construction accidents on highway construction worksites. Table 7 illustrates more details about UAS benefits or performance measures.

A total of 29 potential factors that may influence the performance of UAS monitoring system, particularly, the case of safety condition monitoring on highway construction environments was developed. In addition, 17 expected benefits, can be used for evaluating performance of UAS safety monitoring system on jobsites, are also derived in this paper. Even though a limitation was revealed during data collection, this paper presents two main preliminary results: First, UAS system characteristics and inner team's characteristics can certainly influence the UAS performance for safety monitoring tasks on highway construction projects. That is why there were not a lot of real implications and implementations of UAS on real construction sites so the professionals mostly considered technical factors affecting UAS performance.

Second, the potential benefits from UAS applications on highway construction projects or the performance measure attributes could not be well focused. It was difficult for many survey participants to indicate definite answers. For this reason, field tests should be conducted with a UAS platform on highway construction projects, because the construction project personnel did not have experiences with UAS for safety monitoring on the jobsite. Through those tests, additional survey participants who have experience with UAS on highway construction projects could be included as well as improving the reliability of the collected data for futures studies.

Table 6. Influence of Factor

Factor Group	Factor Description	Results*		
		Yes	No	Do Not Know
UAS System Features (13)	1. Easy user interface for UAS operation	1.00	-	-
	2. Obtained quality of visual assets (photo, video)	1.00	-	-
	3. Battery life of the UAS	0.80	0.07	0.13
	4. UAS system reliability	1.00	-	-
	5. Maximum Visible Angle of the UAS Camera	0.80	-	-
	6. Autonomous flight capability	0.80	0.07	0.13
	7. Communication range for UAS control	0.87	-	0.20
	8. Equipped Sensors (i.e. GPS, Compass etc.)	0.93	-	0.07
	9. Flight Stability	0.93	-	0.07
	10. Features of UAS camera (i.e. Image resolution, video recording capability, infrared)	1.00	-	-
	11. Available sensors (i.e. Compass, Gyroscope, Accelerometer, etc.)	0.87	-	0.13
	12. Emergency response system (Failsafe for lost connection, return to ground control station, etc.)	0.87	-	0.13
	13. UAS system's easy upgradability without manufacturer's services	0.47	-	0.53
	Average:	0.87	0.01	0.12
Project Features (6)	1. Project location (urban vs. rural)	0.80	0.20	-
	2. Project cost	0.80	0.20	-
	3. Project size	0.87	0.13	-
	4. Duration of project	0.67	0.33	-
	5. Complexity of the construction tasks	0.67	0.33	-
	6. Sub contractors trades involved	0.47	0.53	-
	Average:	0.71	0.29	-
Project Team's Features (10)	1. Team's prior experience with UAS	1.00	-	-
	2. Team attitudes toward UAS in construction Projects	0.93	0.07	-
	3. Team's prior experience with IT-based safety system	0.80	0.13	-
	4. Team attitudes toward IT in construction projects	0.73	0.20	-
	5. User type (safety manager or hire pilot)	0.67	0.20	0.13
	6. Knowledge of UAS safety monitoring system features	0.87	0.07	0.07
	7. Adequacy of resources for UAS use as safety monitoring system (i.e. money, time, personnel, etc.)	1.00	-	-
	8. UAS control ability of users (safety managers or project managers)	0.87	0.07	0.07
	9. Adequacy of training or education for UAS use as safety monitoring system	1.00	-	-
	10. Clear method to measure the performance of UAS safety monitoring system	0.87	0.07	0.07
	Average:	0.87	0.08	0.05

*Converted percentage (%) to Decimal Scale

Table 7. Analysis on Potential Benefits and Performance Attributions

Descriptions	Results*		
	Yes	No	Do Not Know
1. Reduce bottlenecks in communication during safety control process	0.60	0.20	0.20
2. Effective management of construction workers' behaviors	0.53	0.07	0.40
3. Inspection of personal protective equipment use	0.73	0.27	-
4. Effective monitoring of the whole work site	0.93	0.07	-
5. Effective monitoring of hard to access areas on work sites	0.80	0.20	-
6. Effective monitoring of traffic and vehicles on work sites	0.87	0.07	0.07
7. Effective monitoring of heavy or hoisting equipment on work sites	0.87	0.07	0.07
8. Reduce time it takes to perform safety monitoring tasks	0.60	0.33	0.07
9. Makes identification of safety issues easier	0.73	0.07	0.20
10. Reduces number of construction injuries	0.60	0.07	0.33
11. Reduces cost of safety management system	0.53	0.20	0.27
12. Expedites reaction to potential hazards	0.67	0.13	0.20
13. Improves project safety performance	0.80	0.07	0.13
14. Improves overall project performance	0.53	0.13	0.33
15. Enables immediate reporting of potentially dangerous situations and allows preventive measures to be applied	0.60	0.20	0.20
16. Simplification of documentation process or reduces waste time for documentation (reduce hardcopy)	0.47	0.33	0.20
17. Enhances and identification and actions regarding potential hazards on sites	0.87	0.07	0.07
Average:	0.69	0.15	0.16

*Converted percentage (%) to Decimal-scale

CONCLUSIONS

The application of UAS in the construction industry is relatively new yet the technology can bring many benefits to industry practitioners. A UAS can be utilized as a safety monitoring system on highway construction projects when equipped with high-resolution cameras and an array of sensors including a Global Positioning System (GPS) and Gyroscope. Highway construction environments have a big advantage to fly small UAS around the jobsite since that project can extend long distances without vertical obstructs. Nevertheless, there is doubt of the effectiveness of UAS safety monitoring system implementation on highway projects because the factors influencing their performance are not fully understood. Since most practitioners are still uncertain about the benefits or performance of UAS, measuring performance and improvement of UAS implementation is very difficult or impossible at the present time.

This exploratory study has discussed the results of a questionnaire to obtain professional 's perceptions about UAS monitoring system of safety conditions on highway construction environments. The perceptions of 15 industry professionals working in the United States were collected to analyze the critical factors and performance attributes of the UAS system. As a result, 29 factors that may influence the performance of UAS safety monitoring and 17 attributes to evaluate the performance were experimentally analyzed as the initial step of this UAS research in the AECO industry. The analysis resulted in two main research findings. First, the

practitioners were only familiar with the technical elements of UAS or they just imagined or expected the relationship between their team characteristics and the UAS implementation on the project. This is why they almost did not have many experiences with UAS monitoring system on the construction environment. Second, the project personnel did not know about the performance attributes and potential benefits from UAS system well. They had difficulty in exactly indicating whether the described attributes can be benefits, or if they should be considered in evaluating the performance of UAS. Low sample size in the survey is a limitation to be considered.

This exploratory study contributes to establish the initial group of factors that may influence the performance of a UAS-based safety monitoring system in highway construction environments. In addition, as the beginnings of understanding UAS applications in the construction industry, the potential benefits of the system and performance measures were identified. It is definitely an important step to increase UAS implementation as well as clearly a guide the development UAS-based system strategies in the AECO industry.

REFERENCES

BLS. (2015). “Revisions to the 2013 Census of Fatal Occupational Injuries (CFOI) counts.” *BLS*, (August).

D’Oleire-Oltmanns, S., Marzolff, I., Peter, K. D., and Ries, J. B. (2012). “Unmanned aerial vehicle (UAV) for monitoring soil erosion in Morocco.” *Remote Sensing*, 4(11), 3390–3416.

Eschmann, C., Kuo, C., and Boller, C. (2012). “Unmanned Aircraft Systems for Remote Building Inspection and Monitoring.” *Proceedings of the 6th European Workshop on Structural Health Monitoring, July 3-6, 2012, Dresden, Germany*, 1–8.

FAA. (2015, MAY 10A). *Public Operations - Certificate of Waiver of Authorization (COA)*

FAA. (2015, MAY 10B). *Freedom of Information Act Responses*

FAA. (2015, MAY 10C). *Authorizations Granted Via Section 333 Exemptions*.

Hinkley, E. A., and Zajkowski, T. (2011). “USDA forest service–NASA: unmanned aerial systems demonstrations–pushing the leading edge in fire mapping.” *Geocarto International*, 26(2), 103–111.

Irizarry, J., Gheisari, M., and Walker, B. N. (2012). “Usability assessment of drone technology as safety inspection tools.” *Electronic Journal of Information Technology in Construction*, 17(September), 194–212.

Ismail, Z., Doostdar, S., and Harun, Z. (2012). “Factors influencing the implementation of a safety management system for construction sites.” *Safety Science*, Elsevier Ltd, 50(3), 418–423.

Jenkins, D., and Vasigh, B. (2013). “The economic impact of unmanned aircraft systems integration in the United States.” (March), 1–40.

Lee, U.-K., Kim, J.-H., Cho, H., and Kang, K.-I. (2009). “Development of a mobile safety monitoring system for construction sites.” *Automation in Construction*, Elsevier B.V., 18(3), 258–264.

Leung, S. W., Mak, S., and Lee, B. L. P. (2008). “Using a real-time integrated communication system to monitor the progress and quality of construction works.” *Automation in Construction*, 17(6), 749–757.

Lin, P., Li, Q., Fan, Q., and Gao, X. (2013). “Real-time monitoring system for workers’ behaviour analysis on a large-dam construction site.” *International Journal of Distributed Sensor Networks*, 2013.

Morgenthal, G., and Hallermann, N. (2014). “Quality assessment of Unmanned Aerial Vehicle (UAV) based visual inspection of structures.” *Advances in Structural Engineering*, 17(3), 289–302.

Naticchia, B., Vaccarini, M., and Carbonari, A. (2013). “A monitoring system for real-time interference control on large construction sites.” *Automation in Construction*, Elsevier B.V., 29, 148–160.

Newcome, L. R. (2004). *Unmanned aviation: a brief history of unmanned aerial vehicles*. Aiaa.

Nisser, T., and Westin, C. (2006). “Human factors challenges in unmanned aerial vehicles (uavs): A literature review.” *School of Aviation of the Lund University, Ljungbyhed*.

Nitithamyong, P., and Skibniewski, M. J. (2006). “Success/Failure Factors and Performance Measures of Web-Based Construction Project Management Systems: Professionals’ Viewpoint.” *Journal of Construction Engineering and Management*, 132(1), 80–87.

Reuder, J., Brisset, P., Jonassen, M., Müller, M., and Mayer, S. (2009). “The Small Unmanned Meteorological Observer SUMO: A new tool for atmospheric boundary layer research.” *Meteorologische Zeitschrift*, 18(2), 141–147.

Rinaudo, Chiabrando, Lingua, and S. (2012). “Politecnico di Torino Porto Institutional Repository.”

Saleri, R., Cappellini, V., Nony, N., Pierrot-Deseilligny, M., Bardiere, E., Campi, M., and De Luca, L. (2013). “UAV photogrammetry for archaeological survey: The Theaters area of Pompeii.” *Digital Heritage International Congress (DigitalHeritage), 2013*, 497–502.

Sarhan, S., and Fox, A. (2013). “Performance measurement in the UK construction industry and its role in supporting the application of lean construction concepts.” *Australasian Journal of Construction Economics and Building*, 13, 23–35.

Sunkara, P. (2005). “A Tablet PC Application for Construction Site Safety Inspection and Fatality Prevention.” Louisiana State University.

Toole, T. M. (2002). “Construction Site Safety Roles.” *Journal of Construction Engineering and Management*, 128(3), 203–210.

Zhou, Z., Irizarry, J., and Li, Q. (2013). “Applying advanced technology to improve safety management in the construction industry: a literature review.” *Construction Management & Economics*, 31(6), 606–622.

The Current State of 3D Printing for Use in Construction

Megan A. Kreiger
Construction Engineering Research Laboratory
U.S. Army Engineer R&D Center
2902 Newmark Dr
Champaign, IL 61822
Megan.A.Kreiger@usace.army.mil

Bruce A. MacAllister
Construction Engineering Research Laboratory
U.S. Army Engineer R&D Center
2902 Newmark Dr
Champaign, IL 61822
Bruce.A.MacAllister@usace.army.mil

Juliana M. Wilhoit
Construction Engineering Research Laboratory
U.S. Army Engineer R&D Center
2902 Newmark Dr
Champaign, IL 61822
Michael.P.Case@usace.army.mil

Michael P. Case
Construction Engineering Research Laboratory
U.S. Army Engineer R&D Center
2902 Newmark Dr
Champaign, IL 61822
Michael.P.Case@usace.army.mil

ABSTRACT

Over the past few years, 3D printing has become a household term, but in the near future this term may be used to describe method of construction of the house that you're sitting in. There are several groups working on developing printers capable of 3D printing building structures. Researchers, corporations, and makers are working and experimenting with extruding foam, mortar, concrete, and other materials to print things such as huts, castles, apartments, and Army structures. Part of this effort is being done by the Engineer Research and Development Center – Construction Engineering Research Laboratory (ERDC-CERL) in collaboration with NASA, to create structures for U.S. Army contingency bases using contour crafting. This paper provides an overview of additive manufacturing techniques applied to the construction of buildings and building components using extrudable construction materials and discusses the motivation for research in this field by ERDC-CERL. The use of 3D printing in construction of structures has the potential to change construction methods and the buildings that surround us in terms of labor requirements, logistics, energy performance, and speed.

Proceedings of the 2015 Conference on Autonomous and Robotic Construction of Infrastructure, Ames, Iowa.

Key words: 3D printing—additive manufacturing—large-scale—buildings

INTRODUCTION

Advances in building construction are a result of experience and education of accountable parties in the industry, which is preceded by a large body of research on the subject. Uncertainties that arise from the acceptance of alternative practices as well as the interdependence on professional knowledge, code regulations, and interdisciplinary relationships leads to complexities that often result in slow adoption of new technologies (Dubois and Gadde 2001; Khoshnevis 2004; Balaguer and Abderrahim 2008; Blayse and Manley 2015). Much of the focus in construction advancement in past decades has been placed on energy efficiency, fostered by related programs such as Energy Star (Energy Star 2013), LEED (U.S. Green Building Council 2015), and the development of international regulations (International Code Council 2014; International Code Council 2015). Projects have conventionally maintained the application of industry accepted construction methods associated with the use of common building materials (e.g. Concrete Masonry Units, Cast-in-place concrete, wood, and steel). However, with greater access to technology, research in automated construction processes has become increasingly popular.

Masonry construction dominates military building projects domestically and internationally. The costs associated with traditional construction techniques are ever increasing, in large part due to the high price of transporting materials to job sites and increases in labor costs. Worker productivity drives both the cost and time to completion of structures built using concrete masonry units (CMU). For example, consider a small structure measuring 16’ wide, 32’ long and 8’ tall with two doorways built using CMU. Assuming standard grouting requirements and that a mason with the assistance of one laborer lays 200 CMU blocks per work day using 8”x8”x16” blocks, the outside walls of the structure could be completed in approximately two days (Scott 2009). The outer walls of a wood framed structure of this size would take at least 1 day to complete, with a team consisting of three carpenters and one laborer in order to lift heavy sections without additional equipment (Freund 2004; “Cost to Frame Wall - Zip Code 47474” 2015). A concrete structure generally takes at least 5 days to cure before any construction or service loads can be applied, in addition to forming, rebar placement, pouring, form removal, and other requirements (Simmons 2011). These estimates include only the exterior wall structure construction time and do not include any time for framing the doorway, provisions for the roof, reinforcement, internal walls of the structure, exterior cladding or finishing. While this may be acceptable in many cases, there are situations where this process is too slow and costly.

The U.S. Army has unique requirements when constructing contingency bases in remote and potentially hostile environments. These requirements include minimizing the number of Soldiers or civilian contractors required to be on-site, logistics for shipping of construction materials (typically lumber) and energy-related fuel, and time to occupancy. As the U.S. Army reduces the size of the force, fewer personnel required for construction frees up Soldier resources from the construction itself or security duties. Today’s semi-permanent contingency bases typically use lumber-based construction, with materials often purchased and shipped over large distances. Concrete is locally available in much of the world and a capability to use cementitious or other indigenous materials without a need for form work would substantially reduce logistics for construction materials. In addition to construction materials, tents and wooden structures in contingency bases do not offer the high levels of energy efficiency found in today’s domestic and commercial markets. Energy to heat, cool, and ventilate these structures must be

transported in the form of fuel (usually JP-8), resulting in high costs, increased convoy requirements and higher exposure of personnel to attack. Well-built structures would mitigate this risk by decreasing energy requirements.

3D PRINTING

3D printing provides a potential solution to U.S. Army contingency base requirements. Although many people may associate 3D printing with plastic trinkets, biological applications, or even printing automobiles, it is capable of much more. As is common with regards to construction from sky scrapers to sports stadiums, two words often apply, “think larger.” The use of large-scale 3D printing is often overlooked, as it is a relatively new application of this technology. In the next few years this term may be associated with the buildings around us. Researchers, corporations, and hobbyists are working and experimenting with extruding foam, mortar, concrete, and other materials to print building structures, such as, huts, a castle, apartments, and Army bases or shelters.

While 3D printing or additive manufacturing (AM) technology was developed in the 1980s, the field has expanded dramatically over the past 5 years. It has had an impact on many fields and applications in ways that were previously viewed as too costly or impossible using traditional manufacturing methods.

3D printing is generally used to reduce material requirements, create custom objects, reduce labor, and for rapid prototyping. 3D printing of building structures also shares these focuses, with potential to reduce the amount of materials needed to be shipped to the build site, create unique buildings, reduce the number of laborers required, and provide a capability to print the buildings in a relatively short amount of time.

The various groups working on 3D printing buildings have different goals. Some are focused on a more experimental setup, others on creating a new form of technology by making an efficient system, and others are focused on looking for practical solutions to building construction. Different materials are used in each project. Some methods focus on the creation of molds for a building by creating a cavity to fill with an alternate material, whereas others focus on directly printing the structure with the print materials. There are also a number of projects using small-scale printers and objects (e.g. building blocks) to build large structures, but relatively few which attempt to build large sections or the entire building at one time (Williams 2015). There are multiple research projects being done by groups all over the world in an effort to effectively 3D print large-scale structures. This paper reviews and summarizes this work in the next section.

The Engineer Research and Development Center (ERDC) is investigating the use of this method for the construction of contingency base shelters. In cooperation with the University of Southern California and NASA, researchers have constructed a number of prototypes that use 3D printing technology to test robotic construction methods using locally sourced concrete materials. ERDC is currently working towards an on-site construction concrete 3D printer that will be able to print a 16’x32’x8’ structure within 24 hours. A conceptual representation of the equipment and process is shown in Figure 1.

Figure 1. Concept representation of ACES 3D printer. (ERDC 2015)

CURRENT RESEARCH

Many different methods are implored by AM technologies to construct large-scale structures including fused-filament fabrication (FFF), powder-bed and inkjet head, and extrusion printing. While many methods exist for small-scale printers, only a few are relevant to the construction industry and are described below.

Fused-Filament Fabrication

Fused filament fabrication (FFF), also known by other more proprietary terms, is the most readily available type of 3D printer in households and businesses due to its maker (a community dedicated to fabricating objects) and open-source following. It uses a filament-type material which is heated through an extruder and deposited as a string of material on the build platform. After the first layer is printed, the printer then repeats the process, building the next layer on the previous one. An example of this type of deposition process is shown in Figure 2.

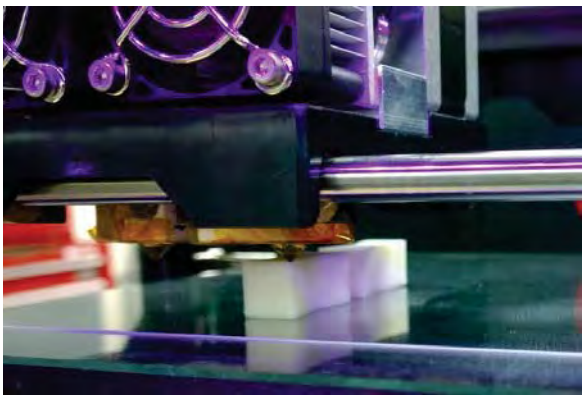

Figure 2. A small-scale fused-filament fabrication 3D printer

3D Print Canal House

A factory gantry-based FFF project was started by DUS Architects and partners in Amsterdam. The project known as the 3D Print Canal House takes the common 3D printer to the next level. The Kamermaker (Roombuilder) 3D printer builds large polymer-based components, up to 2m x

2m x 3.5m, out of polymer beads instead of the traditional spools. The components are then trucked to the site or assembled on-site. They are experimenting with multiple materials, but are focused mainly on polymer-based structures. They are also experimenting with filling their structure with lightweight foaming eco-concrete to provide structural and insulation properties. The project is expected to be completed in 2017 (DUS Architects 2015). The methods is limited to mostly polymers and materials that solidify quickly upon cooling, the major disadvantages of this method are the material limitations.

Powder-bed and Inkjet Head Printing

Powder-bed printing, also known as binder jetting, is a printer that initially spreads a thin layer of powder (e.g. sand) across the build area, then immediately dispenses a binder in the areas where the structure is desired, see Figure 3. There are other similar powder-bed processes (e.g. laser sintering) which will not be discussed in this paper. After each layer is complete, it spreads out another thin layer of powder and repeats the process. This process repeats until there is a complete structure. Once the structure has finished, the binder must be allowed to cure and then the excess material is removed. This method can print objects that would be nearly impossible using most other 3D printing methods or traditional construction, because of the support added by the unbound powder material.

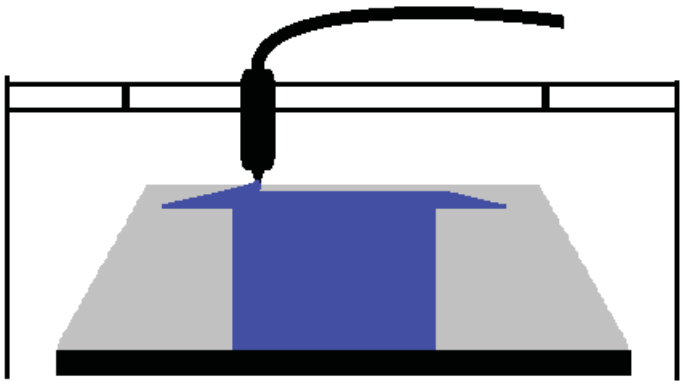

Figure 3. Basic representation of powder-bed and inkjet printing. Gray depicts unbound powder and blue is the binder combined with the powder. The sand spreading apparatus is not shown.

D-Shape

D-shape is a factory gantry-based powder-bed 3D printer built in the United Kingdom by Monolite UK Ltd. This system can print up to 6m x 6m x 6m of architectural structures and components at a time, which are then trucked to the site. It uses granular material deposition using a powder bed and inkjet method composed of sand and a binder to create structures. It works by putting down a full layer of sand, then going over the sand with the print heads while extruding a binder where the structure is desired. The layers are between 5-10mm. The structure itself takes about 24 hours to solidify, after which the excess sand must be removed to show the sandstone-like or marble-like structure underneath. Originally using epoxy or polyurethane, it now uses an organic binder to make an environmentally friendly structure. The goals of this project are to increase quality and safety, while decreasing time and costs.

D-shape won top prize in the Change the Course - New York City Waterfront Construction Competition for innovative construction ideas for waterfront infrastructure ran by the New York

City Economic Development Corporation (NYCEDC) in 2013. (D-Shape 2015; New York City Economic Development Corporation 2013) One example of the projects D-shape is working on is the Landscape house. The project is going to be printed in sections, filled with fiber-reinforced concrete, and put into place. (Crook 2013; EeStairs 2015).

While the method does provide greater freedom for architectural design, a drawback to this technique is that it requires a large amount of material to work with, as the sand or other powder has to be built up to the top of the print in the entire build area. In turn the powder which supports the structure during the curing time requires a labor intensive period of excess material removal before the print can be used.

Extrusion Printing

The extrusion print method is very similar to FFF, but uses a variety of slurry-like or clay-like materials to create a structure. This type of 3D printer extrudes a fluid-like material out of a nozzle and builds layer upon layer. The difference is that because the materials used are not based on a cooling process for solidification, the cure time is longer than in FFF. This means that there may be a wait time between layers or after a certain number of layers before proceeding with the print. It also limits the geometry of the printed structure due to the fluid-like behavior and the freshly printed state dependent on the material used for the print.

Factory delta-based clay printer:

World's Advanced Saving Project

The World's Advanced Saving Project (WASP) started in 2012, uses clay and fluid-dense materials to print moderately sized structures (World's Advanced Saving Project 2015). Able to print in materials such as ceramic and porcelain, the goal of the project is clay houses. The creations from this group have been known as "mud huts" and utilize local materials to provide long lasting low-impact structure.

On-site boom arm foam printer:

MIT (Digital Construction platform)

Massachusetts Institute of Technology (MIT) has been developing a truck-mounted boom, "Digital Construction Platform," that can be used as a 3D printer. On the boom, there is an industrial arm with a fast response time, which compensates for the long period oscillations of the boom. The combined reach of the boom and robotic arm is 80'. The current model can be used for additive or subtractive manufacturing, by extruding with foam or using an attached milling head to shape, respectively. This concept is similar to the commonly used method of insulated concrete forms (ICF), where a foam form is setup and filled with concrete. This system is complex, but provides multiple benefits including easy transportation, little to no setup time, a greater freedom of movement, and the potential to continue a print beyond the immediate print area by repositioning.

On-site swarm concrete printer:

IAAC Minibuilders

A research team at the Institute for Advanced Architecture of Catalonia (IAAC) has created a unique 3D printing system of 3 types of small robots (foundation, grip, vacuum). Each robot has

a different function, contributing to the creation of a large structure made out of concrete (“Small Robots Printing Big Structures” 2015). The first robot is a foundation robot, which follows a line to print the first 20 layers. The grip robot clamps onto the existing material and continues to print the structure. These robots are capable of printing ceilings and lintels by printing horizontally. After the structure is in place, vacuum robots are placed on the structure and print extra shells. This system is capable of very flexible shapes and is not limited by the size of the machine. A disadvantage of this system is that the building envelope is more limited in complexity and thickness.

Factory gantry-based concrete printer:

Freeform Project

At the Loughborough University in Leicestershire, U.K., a team in the Civil and Building Engineering department has been developing a factory gantry-based concrete printer with multiple industrial partners (Buswell and Austin 2015). This printer creates components by extruding concrete through a single nozzle, which is used in conjunction with a softer material to support overhangs and is later removed. The use of a foam-based support material in concrete printers provides the freedom of design that is typically associated with powder-bed print methods, while limiting the support to needed areas to reduce waste.

Winsun Co.

In China, Winsun has created a factory gantry-based concrete 3D printer for building components (Winsun 2015). The printer measures 150m long x 10m wide x 6.6m tall, uses concrete extrusion to print buildings in sections, then ships the pieces by truck, which are assembled on-site with a crane. The pieces are generally printed such that the roof is one solid piece with the walls and needs to be tilted up 90 degrees during the build for proper orientation. They have built at least 10 houses and are creating many types of smaller structures as well. Win Sun has created a couple of ‘firsts’ in the 3D printing construction world: the first full-sized printed structure with a roof and the world’s tallest 3D-printed building at 5-stories high, both from components. This follows a more traditional approach to building construction, where the pieces are shipped to the site and assembled. This method still potentially reduces waste and time, but puts the burden on the shipment of materials to the site.

On-site gantry-based concrete printer:

Backyard Castle

Andrey Rudenko and his collaborators have designed and built a gantry-based 3D printer in his backyard. This printer is mounted on rails at the build site and is capable of printing concrete structures up to 12’ tall with each layer of concrete measuring 10mm height and 30mm width. He printed a castle out of concrete with a building footprint of 3m x 5m (Krassenstein 2014; Rudenko 2015). This method utilizes on-site construction, but still requires the use of printed components. The use of on-site construction would be beneficial to construction areas that are difficult to access.

USC

One of the earliest groups to work on 3D printing of structures was the University of Southern California (USC), led by Behrokh Khoshnevis. Funded in part by the ERDC-CERL, they have been working on automated construction by contour crafting (CC) for over 10 years (Khoshnevis

2004; Kamrani and Nasr 2006). Their system is an on-site gantry which is mounted on rails at the build site. It currently has arguably the most advanced shaping and material handling system. The extruder is a multi-nozzle print head with a trowel to smooth the layers while printing. The nozzle itself is 3D printed and has an interruptible material delivery system so it can stop when needed for short amounts of time. USC was funded by NASA to investigate using the contour crafting technology to print extraterrestrial structures using lunar material (Khoshnevis 2012). The contour crafting technology has a large amount of research behind it and is potentially the most feasible for on-site construction. The multiple print heads speed up print time while still allowing complicated wall cavity geometry. This technique does come with some limitations as the design is limited to the capabilities of the multi-nozzle print head.

SHORTCOMINGS

There is a movement toward using 3D printing technology for the construction of building structures, but there are limitations that must be overcome before widespread use is possible. The current 3D printed building structures are experimental, as further characterization of print materials, clarification of construction practices and printing processes, and integration into current building code regulations is required.

Extrusion printing methods show the most promise for acceptance into the construction industry, as the materials (i.e. clay and concrete) and method of material placement (i.e. concrete pumping) are similar to those used currently in the field. With over 10 years of experience in concrete 3D printing, the work at USC provides a first stop for the current body of extrusion printing. Other technologies, while not as developed, show much promise. The Digital Construction Platform at MIT is still relatively early in its development, but shows that a simple modification to current construction technology, such as a boom crane, will allow for large print areas. It is unclear at this time whether the technology will support concrete printing or is limited to lightweight materials such as foam. The IAAC Minibuilders provide for flexibility in design and construction, but may require a change in skills and knowledge (e.g. robotic controls) that is not as readily available in on a typical construction site.

The methods implored by Win Sun, the Freeform project, and similar may be more readily accepted due to its similarity to the current precast concrete industry, requiring very little change for the construction industry as the house is built in sections using cranes. This method does require transportation of large concrete sections and the use of large machinery to lift them into place.

Other methods, such as, fused filament fabrication and powder bed printers are more familiar to those in the AM community, but may be slow to acceptance in the construction industry. The FFF method used in the 3D Print Canal House project is set to be completed in 2017, however the technology relies on quick cooling after an initial heating, which limits the materials to polymers and other rapid cooling materials. The powder bed printer by D-shape provides architectural freedom, but requires large amounts of powder material to support the print during setting, leading to material waste after curing despite the ability to recycle leftover powder.

The 3D printing industry still continues to be a novelty to the general public and applications may still be too new to be generally accepted. A great deal of work needs to be done to get this technology ready for use in construction, but when it is ready, it has potential to change the structures around us in ways never previously thought possible. 3D printing may lead to a world where construction and architectural design are not limited by conventional methods and where a unique design is merely printed under the same conditions as a basic structure would be.

FUTURE DIRECTION

Still in its infancy, the 3D printing of buildings is a growing field that still requires much research before the technology will become a viable option for the everyday job site. Further knowledge is required in the areas of materials testing and characterization, structural design requirements, the incorporation into building codes and standards, and the standardization of construction practices. Concrete materials should be characterized based on typical mix designs, required particle size based on print head diameter, rheology, and the use of indigenous materials. In an industry where uncertainties exist there is also a need for material testing standards. On the structural side, the use of reinforcement will be a major concern, whether it is discontinuous fibers, fiber meshes, or the more familiar welded wire and reinforcing bars with grouting. Another structural challenge is the printing of roofs or over voids (e.g. windows, doorways, mechanical openings), and how the voids are reinforced. On the construction side, research should be focused on general practices for applying the technology on-site (e.g. site grading requirements, construction requirements, environmental considerations, scheduling and cost considerations). Furthermore, the incorporation of the technology in building codes and standards should be the final step in acceptance.

CONCLUSION

There is a growing effort to be able to construct structures using 3D printing technology. Many projects are able to create small structures or components of structures currently, but more needs to be done regarding material behavior and applicability for building structures. Building codes will need to take into account this new technology before it can be readily used. As technology advances and research is done in the area, this field will continue to evolve and 3D printed buildings may be a possibility over the next few years.

ACKNOWLEDGMENTS

Special thanks to Eric Kreiger at Bacon Farmer Workman Engineering and Testing, Inc. for contributions to this paper. Thanks also to Jason Galtieri, and W. Jacob Wagner at ERDC-CERL for conversations and input on this paper. The authors would also like to thank Dr. Joshua Pearce at Michigan Technological University for conversations on 3D printing topics.

REFERENCES

Balaguer, Carlos, and Mohamed Abderrahim. 2008. *Trends in Robotics and Automation in Construction*. INTECH Open Access Publisher. http://cdn.intechopen.com/pdfs/5555.pdf.

Blayse, Aletha M., and Karen Manley. 2015. “Key Influences on Construction Innovation.” *Construction Innovation* 4 (3): 143–54. Accessed May 18.

Buswell, Richard, and Simon Austin. 2015. “Freeform Construction: Partners.” *Loughborough University*. http://www.freeformconstruction.com/partners.php.

“Cost to Frame Wall - Zip Code 47474.” 2015. *Homewyse*. http://www.homewyse.com/services/cost_to_frame_wall.html.

International Code Council. 2014. *2015 International Energy Conservation Code*. ICC.

Crook, Jordan. 2013. “The World’s First 3D-Printed Building Will Arrive In 2014 (And It Looks Awesome).” Blog. *TechCrunch*. January 20. http://techcrunch.com/2013/01/20/the-worlds-first-3d-printed-building-will-arrive-in-2014-and-it-looks-awesome/.

D-Shape. 2015. “The Technology.” *Monolite UK*. http://www.d-shape.com/tecnologia.htm.

Dubois, Anna, and Lars-Erik Gadde. 2001. “The Construction Industry as a Loosely Coupled System - Implications for Productivity and Innovativity.” In . Oslo, Norway. http://www.impgroup.org/uploads/papers/169.pdf.

DUS Architects. 2015. “3D Print Canal House.” Accessed May 18. http://3dprintcanalhouse.com/.
EeStairs. 2015. “EeStairs Founding Father of the Landscape House.” http://www.eestairs.com/en/743_eestairs_founding_father_of_the_landscape_house.htm .
Energy Star. 2013. “ENERGY STAR Certified Homes, Version 3 (Rev. 07) National Program Requirments.” http://www.energystar.gov/ia/partners/bldrs_lenders_raters/downloads/National_Program_Requirements.pdf.
Freund, James F. 2004. “How to Estimate the Cost of Rough Carpentry Framing.” American Society of Professional Estimators. http://www.aspenational.org/userfiles/file/Technical%20Papers/2007/TechPaper_May2007.pdf.
International Code Council. 2015. “Overview of the IgCC.” Accessed May 18. http://www.iccsafe.org/codes-tech-support/codes/2015-i-codes/igcc/.
Kamrani, Ali, and Emad Nasr. 2006. Rapid Prototyping: Theory and Practice. Springer.
Khoshnevis, Behrokh. 2004. “Automated Construction by Contour Crafting—related Robotics and Information Technologies.” *Automation in Construction*, The best of ISARC 2002, 13 (1): 5–19. doi:10.1016/j.autcon.2003.08.012.
Khoshnevis, Behrokh, A. Carlson, N. Leach, M. Thangavelu. 2012. "Contour Crafting Simulation Plan for Lunar Settlement Infrastructure Buildup." Earth and Space 2012: 1458-1467. doi:10.1061/9780784412190.155.
Krassenstein, Eddie. 2014. “Architect Plans to 3D Print a 2-Story Home in Minnesota Using a Homemade Cement Printer.” *3DPrint.com*. April 22. http://3dprint.com/2471/3d-printed-home-in-minnesota/.
New York City Economic Development Corporation. 2013. “NYCEDC Announces Three Winners of Change the Course - The NYC Waterfront Construction Competition.” *NYCEDC*. April 10. http://www.nycedc.com/press-release/nycedc-announces-three-winners-change-course-nyc-waterfront-construction-competition.
Rudenko, Andrey. 2015. “3D Concrete House Printer.” *Total Kustom*. http://totalkustom.com/home.html.
Scott, Rick. 2009. “Estimate the Cost of A Concrete Masonry Unit Wall.” *Estimating Today*, July.
Simmons, H. Leslie. 2011. *Olin’s Construction: Principles, Materials, and Methods*. John Wiley & Sons.
“Small Robots Printing Big Structures.” 2015. *Minibuilders*. http://iaac.net/printingrobots/.
U.S. Green Building Council. 2015. “Guide to LEED Certification.” *USGBC*. http://www.usgbc.org/cert-guide.
Williams, Adam. 2015. “Berkeley Researchers Pioneer New Powder-Based Concrete 3D Printing Technique.” *Gizmag*. March 12. http://www.gizmag.com/berkeley-researchers-pioneer-powder-based-concrete-3d-printing/36515/.
Winsun. 2015. Accessed May 18. http://www.yhbm.com/.
World’s Advanced Saving Project. 2015. “About Us - WASProject.” *WASP*. http://www.wasproject.it/w/en/wasp/.

Bridge Structural Condition Assessment using 3D Imaging

Simon Laflamme
Department of Civil, Construction and Environmental Engineering
Iowa State University
416A Town Engineering
Ames, IA 50011-3232
laflamme@iastate.edu

Yelda Turkan
Department of Civil, Construction and Environmental Engineering
Iowa State University
428 Town Engineering
Ames, IA 50011-3232
yturkan@iastate.edu

Liangyu Tan
Department of Civil, Construction and Environmental Engineering
Iowa State University
427 Town Engineering
Ames, IA 50011-3232
tan@iastate.edu

ABSTRACT

Objective, accurate, and fast assessment of bridge structural condition is critical to timely assess safety risks. Current practices for bridge condition assessment rely on visual observations and manual interpretation of reports and sketches prepared by inspectors in the field. Visual observation, manual reporting and interpretation has several drawbacks such as being labor intensive, subject to personal judgment and experience, and prone to error. Terrestrial laser scanners (TLS) are promising sensors to automatically identify structural condition indicators, such as cracks, displacements and deflected shapes, as they are able to provide high coverage and accuracy at long ranges. However, there is limited research conducted on employing TLS to detect cracks for bridge condition assessment, which mainly focused on manual detection and measurements of cracks, displacements or shape deflections from the laser scan point clouds. TLS is an advance 3D imaging technology that is used to rapidly measure the 3D coordinates of densely scanned points within a scene. The data gathered by a TLS is provided in the form of 3D point clouds with color and intensity data often associated with each point within the cloud. This paper proposes a novel adaptive wavelet neural network (WNN) based approach to automatically detect concrete cracks from TLS point clouds for bridge structural condition assessment. The adaptive WNN is designed to self-organize, self-adapt, and sequentially learn a compact reconstruction of the 3D point cloud. The architecture of the network is based on a single-layer neural network consisting of Mexican hat wavelet functions. The approach was tested on a cracked concrete specimen. The preliminary experimental results show that the proposed approach is promising as it enables detecting concrete cracks accurately from TLS point clouds. Using the proposed method for crack detection would enable automatic and remote assessment of bridge condition. This would, in

Proceedings of the 2015 Conference on Autonomous and Robotic Construction of Infrastructure, Ames, Iowa.

turn, result in reducing costs associated with infrastructure management, and improving the overall quality of our infrastructure by enhancing maintenance operations.

Key words: laser scanning—bridge condition assessment—crack detection—wavelets—neural networks

INTRODUCTION

The majority of bridge condition assessments in the U.S. are conducted by visual inspection, during which a printed checklist is filled by trained inspectors. An inspector must correctly identify the type and location of each element being inspected, document its distress, manually record this information in the field and then transcribe that information to the bridge evaluation database after arriving back at his/her office. This is a complex and time-consuming set of responsibilities which are prone to error.

Terrestrial laser scanners (TLS) are promising sensors for documenting as-built condition of infrastructure (Hajian and Brandow, 2012), and they have already been utilized by a number of state DOTs for this purpose at the project planning phase. Furthermore, TLS technology has been shown to be effective identifying structural condition indicators, such as cracks, displacements and deflected shapes (Park et al. 2007; Olsen et al. 2009; Werner and Morris, 2010; Meral 2011; Wood et al. 2012), as they are able to provide high coverage and accuracy at long ranges. However, there is limited research conducted on employing TLS to detect cracks for bridge condition assessment, which mainly focused on manual detection and measurements of cracks, displacements or shape deflections from the laser scan point clouds (Chen 2012; Chen et al. 2014; Olsen et al. 2013).

The research presented in this paper attempts to automatically detect cracks from TLS point clouds (Olsen et al. 2009; Anil et al. 2013; Adhikari et al. 2013; Mosalam et al. 2013) for bridge structural condition assessment. TLS is an advance imaging technology that is used to rapidly measure the 3D coordinates of densely scanned points within a scene (Fig. 1(a)). The data gathered by a TLS is provided in the form of 3D point clouds with color and intensity data often associated with each point within the cloud. Point cloud data can be analyzed using computer vision algorithms (Fig. 1(b)) to detect structural conditions (Fig 1(c)).

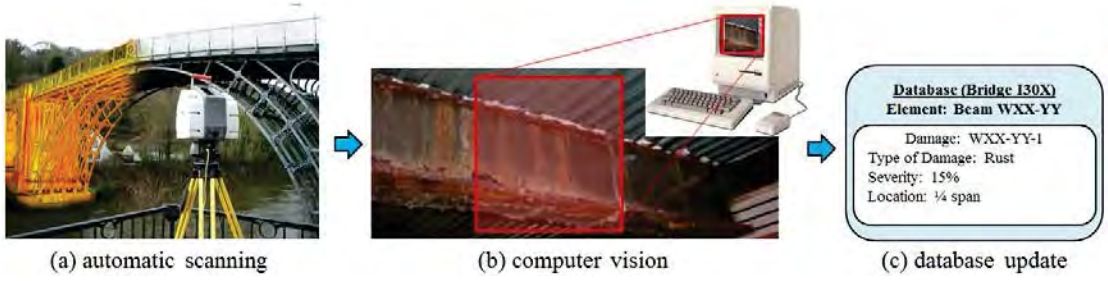

Figure 1. Research Vision

In its raw format, TLS point cloud data contains significant number of data points that is unstructured, densely and non-uniformly distributed (Meng et al. 2013). Therefore, in machine learning community, substantial effort has been put in reconstructing 3D shapes from point

clouds. Popular reconstruction methods include the utilization of Splines (Gálvez & Iglesias 2012) and partial differential equations (PDE) (Wang et al. 2012), seen as an improvement over Splines in terms of numbers of parameters. Neural networks have also been proposed, and demonstrated as superior to PDE-based methods in (Barhak & Fisher 2001).

The overarching goal of this research is to detect 3D shapes from point clouds real-time while scanning on-site. However, there exist critical challenges in designing a shape reconstruction algorithm for real-time adaptive scanning, namely:

- The algorithm must adapt sequentially to enable adaptive scanning.
- The representations must be compact to reduce demand on memory. A compact representation can also facilitate queries over a large database, particularly useful in extracting prior information in the case of sequential training.
- The number of parameters must remain low to accelerate computational speed. A high number of parameters would result in a substantial lag in the parameterization process.
- The algorithm must be robust with respect to noise in data, which can be substantial with TLS-based technologies.

Neural networks have been proposed as candidates for providing robust and compact representations. In particular, Radial Basis Functions (RBF) neural networks have been applied to the problem of shape reconstruction (Bellocchio et al. 2013). Compared against traditional types of neural networks, they provide a better approximation, convergence speed, optimality in solution and excellent localization (Suresh et al. 2008). Furthermore, they can be trained faster when modeling nonlinear representations in the function space (Howlett 2001). Recent work has been published in utilizing sequential RBF networks for reconstructing surfaces from point clouds (Meng et al. 2013). A self-organizing mapping (SOM) (Kohonen 2001) architecture was used to optimize node placement, and the algorithm provided good accuracy with minimum number of nodes.

The authors have developed a sequential adaptive RBF neural network for real-time learning of nonlinear dynamics (Laflamme & Connor 2009), and returned similar conclusions where the network showed better performance with respect to traditional neural networks. They also designed wavelet neural networks (WNN) for similar applications in (Laflamme et al. 2011, Laflamme et al. 2012). WNN are also capable of universal approximation, as shown in (Zhang & Benveniste 1992). This particular neural network has also been demonstrated as capable to learn dynamics on-the-spot, without prior knowledge of the underlying dynamics and architecture of the input space.

The study presented in this paper proposes a novel adaptive wavelet neural network (WNN) based approach to automatically detect concrete cracks from TLS point clouds for bridge structural condition assessment. The adaptive WNN is designed to self-organize, self-adapt, and sequentially learn a compact reconstruction of the 3D point cloud. The approach was tested on a cracked concrete specimen, and it successfully reconstructed 3D laser scan data points as wavelet functions in a more compact format, where the concrete crack was easily identified. This is a significant improvement over previous TLS based crack detection methods as it does not require a priori knowledge about the crack or the 3D shape of the object being scanned. It also enables to process 3D point cloud data faster and detect cracks automatically. Furthermore, since it is designed to self-organize, self-adapt and sequentially learn a compact reconstruction of the 3D point cloud, it can easily be adapted for real-time scanning in the field, which will be investigated in the future using the adaptive WNN approach presented in this paper.

BACKGROUND

Terrestrial Laser Scanning (TLS) Technology

Terrestrial Laser Scanning (TLS) – also known as Light Detection and Ranging (LiDAR) – enables direct acquisition of 3D coordinates from the surface of a target object or scene that are visible from the laser scanner's viewpoint (Alba et al. 2011; Vosselman and Maas 2013; Xiong et al. 2013). TLS is based on either time-of-flight (TOF) or phase-based technology to collect range (x, y, z) and intensity data of objects in a scene. The two technologies differ in calculating the range, while both acquire each range point in the equipment's spherical coordinate frame by mounting a laser on a pan-and-tilt unit that provides the spherical angular coordinates of the point. TOF scanners emit a pulse of laser light to the surface of the target object or scene and calculate the distance to the surface by recording the round trip time of the laser light pulse. Phase based scanners measure phase shift in a continuously emitted and returned sinusoidal wave. Both types of TLS achieve similar point measurement accuracies. They differ in scanning speed and maximum scanning range. Typically, phase-based TLS achieve faster data acquisition (up to one million points per second), while TOF-based TLS enables collecting data from longer ranges (up to a kilometre).

TLS implementation in the AEC-FM Industry

Laser scanning technology enables capturing comprehensive and very accurate three-dimensional (3D) data for an entire construction scene using only a few scans (Cheok et al. 2002). Among other 3D sensing technologies, laser scanning is the best adapted technology for capturing the 3D status of construction projects and condition of infrastructure accurately and efficiently. In a study by Greaves and Jenkins (2007), it is shown that the 3D laser scanning hardware, software, and services market has grown exponentially in the last decade, and the Architecture, Engineering, Construction and Facilities Management (AEC-FM) industry is one of its major customers. This shows that owners, decision makers and contractors are aware of the potential of using this technology for capturing the 3D as-built status of construction projects and condition of infrastructure. However, laser scanners' current adoption rate is very low despite their tremendous benefits. The major reasons are related to the big size of data they produce and the long data processing time required.

Laser scanners can output extremely high resolution models, but at a much larger file size and processing time (Boehler and Marbs, 2003). Despite the remarkable accuracy and benefits, laser scanners' current adoption rate in the AEC-FM industry is still low, mainly because of the data acquisition and processing time and data storage issues. Full laser scanning requires significant amount of time. Depending on the size of the site, it can take days for large scale high-resolution shots. Accordingly, resulting data file sizes are typically very large (e.g., a single high resolution scan file size could be a couple of gigabytes or much larger). Therefore, data storage and processing are the two biggest factors for the low adoption rates of laser scanners in the AEC-FM industry.

Thus, there is a need for advanced algorithms that enable automated 3D shape detection from low resolution point clouds during data collection. This would improve project productivity as well as safety by reducing the amount of time spent on-site. Importantly, practical applications of the developed algorithms to field laser scanners will be straightforward since commercially available laser scanners on the market are generally programmable (Trimble Inc. 2015).

RESEARCH METHODOLOGY: ADAPTIVE WAVELET NETWORK

An adaptive wavelet neural network (WNN) has been designed to sequentially learn a compact reconstruction of the 3D point cloud. The architecture of the WNN is based on a single-layer neural network, as illustrated in Fig. 2, consisting of h *Mexican Hat* wavelets centered at μ_i, with a bandwidth σ_i where each function (or node) ϕ_i can be written as below:

$$\phi_i(\zeta) = \left(1 - \frac{\|\zeta - \mu\|^2}{\sigma^2}\right) e^{-\frac{\|\zeta-\mu\|^2}{\sigma^2}} \quad \text{for } i = 1,2,\dots,h \tag{1}$$

The wavelet network maps the z_j coordinate of point $\zeta_j = [x_j, y_j]$ using the following function:

$$\tilde{z}_j = \sum_{i=1}^{h} \gamma_i \phi_i(x_j, y_j) \tag{2}$$

where γ_i are function weights, and the tilde denotes an estimation.

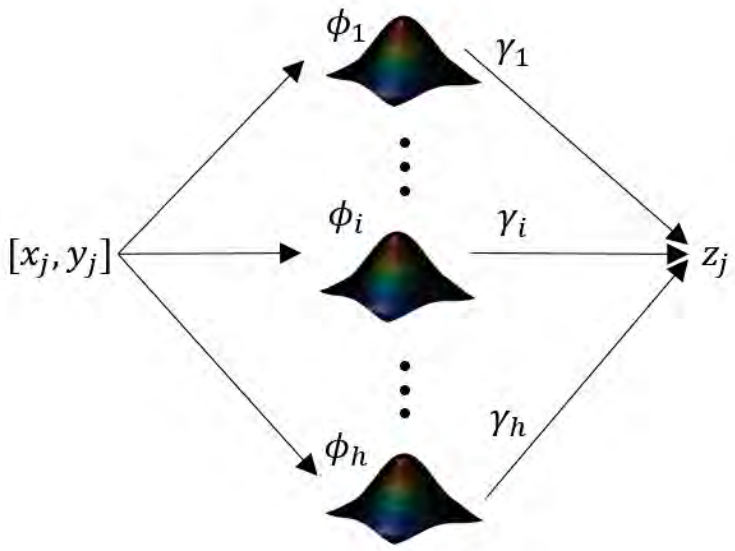

Figure 2. Single-layer architecture of the wavelet network

The network is self-organizing, self-adaptive, and sequential. The self-organizing feature consists of the capability to add functions at sparse locations. This is done following Kohonen's Self-Organizing Mapping Theory (Kohonen 2001). The self-adaptive feature consists of adapting the network parameters $\boldsymbol{\sigma}$ and $\boldsymbol{\gamma}$ to learn the compact representation. Lastly, the sequential feature refers to the capability of the network to learn at representation while scanning is occurring, in a sequential way, in opposition to a batch process. This sequential capability would be used to interact with the 3D scanner in real-time.

The wavelet network algorithm is as follows. First, a new point $\boldsymbol{\zeta_j}$ is queried from the scanner, along with its associated $\boldsymbol{z_j}$**.** The shortest Euclidean distance is computed between the location

of the new point $\boldsymbol{\zeta_j}$ and the center of the existing functions $\boldsymbol{\mu_i}$ for $\boldsymbol{i = 1, 2, \dots, h}$.If the shortest distance is greater than a user-defined threshold $\boldsymbol{\lambda}$, a new function is added at $\boldsymbol{\mu_{h+1} = \zeta_j}$ and the number of functions increases by 1. Note that this threshold decreases with decreasing bandwidth $\boldsymbol{\sigma_i}$, which allows the creation of denser regions where the network resolution is higher. The weight of the new function is taken as $\boldsymbol{\gamma_{h+1} = z_j}$. Second, if no new function is added, the estimate $\tilde{\boldsymbol{z}}_{\boldsymbol{j}}$ is compared against the value $\boldsymbol{z_j}$, and the network error $\boldsymbol{e = \tilde{z}_j - z_j}$ is computed. Third, the network parameters $\boldsymbol{\sigma_i}$ and $\boldsymbol{\gamma_i}$ are adapted using the backpropagation method (Laflamme *et al.* 2012):

$$\dot{\xi} = -\Gamma_{\xi} \left(\frac{\delta z}{\delta \xi} \right) e \tag{3}$$

where $\boldsymbol{\xi = [\sigma, \gamma]}$, and $\boldsymbol{\Gamma_{\xi}}$ are positive constants representing the learning rate of the network.

EXPERIMENTS AND PRELIMINARY RESULTS

The adaptive wavelet network has been validated on a cracked concrete specimen. The specimen was scanned using a Trimble TX5 phase-based TLS on a region limited to 50 by 65 mm^2 to focus the study on the algorithm itself. A total of 8170 points have been generated. The specimen is shown in Fig. 3, along with a zoom on the limited region (Fig. 3(b)). Fig. 3 (b) shows the crack that runs through the region with a wider region (along the first 35.1 mm from the bottom), and a smaller damage geometry along 9.8 mm and after.

Fig. 4 shows a typical fitting result obtained using 59 nodes. The compact representation provides a good fit of the 3D point cloud, and includes the damage feature. A study was conducted on the accuracy of the representation as a function of the number of nodes in the network, by changing the parameter λ while keeping all other network parameters constant. The accuracy was measured in terms of the root means square (RMS) error. Fig. 5 is a plot of the RMS error as a function of the number of nodes. It also shows the relative computing time versus the network size. In this case, there is a region in which the algorithm provides an optimal representation in term of RMS error. The decrease in performance for a higher number of nodes can be attributed to the network parameters that become mistuned. In particular, when more nodes are allowed in the network and the initial bandwidth is large, one would expect a relatively higher training period to obtain an acceptable level of accuracy. The relative computing time changes linearly with the number of nodes in the network.

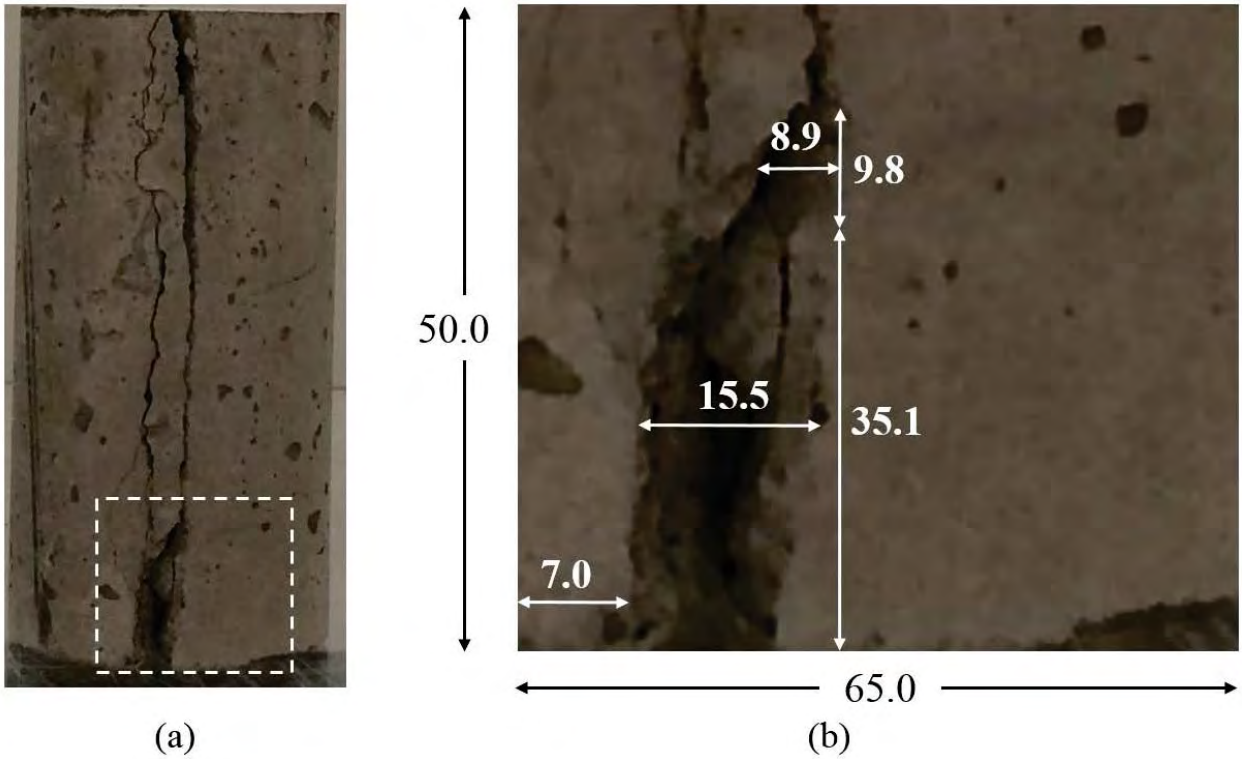

Figure 3. (a) Specimen (scanned region shown by the dashed rectangle); and (b) zoom on the scanned region (distances in mm).

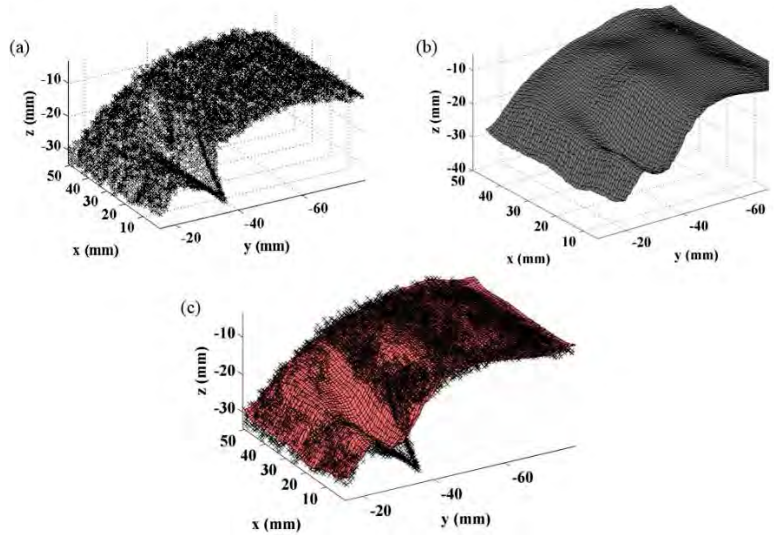

Figure 4. (a) Point cloud; (b) Compact representation; and (c) Overlap of point cloud and representation.

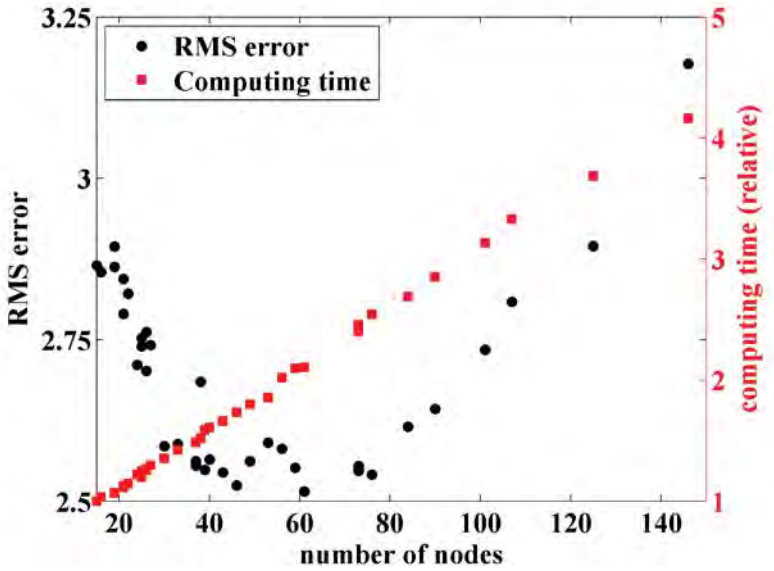

Figure 5. RMS error and relative computing time versus wavelet network size.

While the wavelet network provides an accurate representation of the 3D point cloud, it should be also capable of extracting key features, such as damage. With this particular example, an attempt was made to automatically localize the damage and determine its severity. The strategy consists of identifying regions of wavelets (or nodes) of lower bandwidths, which would indicate a region of higher resolution, thus the location of a more complex feature (a crack, in this case). Fig. 6(a) is a wavelet resolution map, which is obtained by computing the average wavelet bandwidth within a region of the representation. Dark blue areas indicate a high resolution region, while dark red areas represent low resolution regions. The damage is approximately localized using this strategy. Next, the crack length and width were estimated by evaluating the maximum distances along the x- and y-axes within a group of wavelets of low bandwidth. Fig. 6(b) is a plot of the computed crack length and width as a function of the number of nodes. The approximate crack length is more accurately determined for networks created with a large number of nodes, but yet yields to an acceptable approximation. The estimated crack width increases with increasing number of nodes. This is explained by the presence of a high resolution region around the coordinate [-20, 20], shown in Fig. 6(a), that is perceived as a crack. A representation created with a large number of functions may over-fit the 3D point cloud.

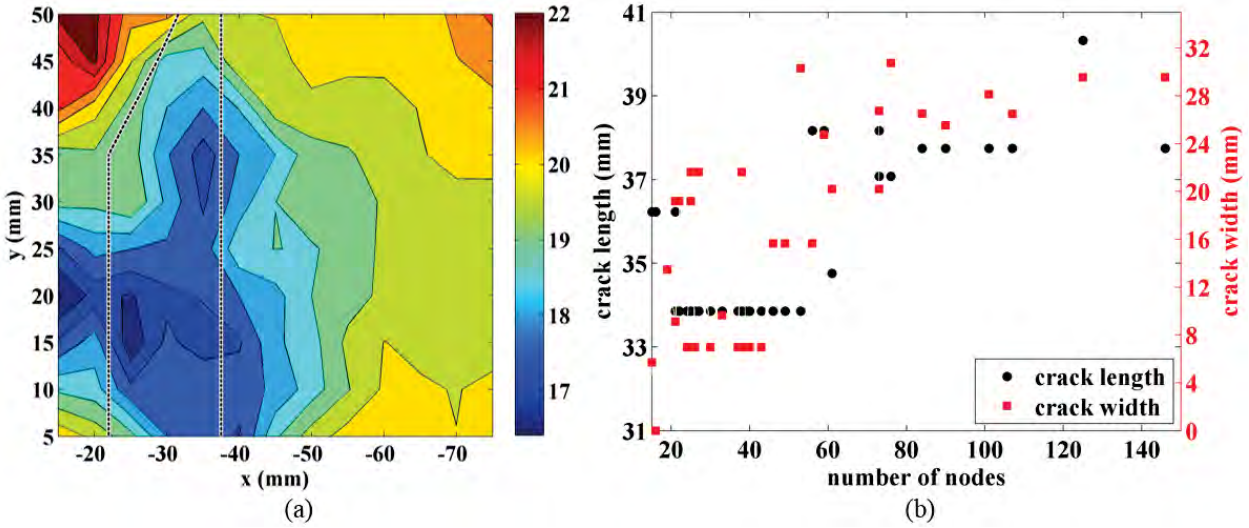

Figure 6. (a) Wavelet resolution map showing the average wavelet bandwidths for a representation using 59 nodes (the approximate crack region is shown within the black-dashed region); and (b) Identified crack length and width based on wavelet resolutions.

CONCLUSIONS

A strategy to sequentially construct a compact representation of a 3D point cloud has been presented. The representation is wavelet network capable of self-organization, self-adaptation, and sequential learning. It can be utilized to transform thousands of 3D point cloud data obtained from a TLS or LiDAR into a small set of functions. The proposed wavelet network has been demonstrated on a cracked cylindrical specimen. It was shown that the algorithm was capable of replacing a set of 8170 3D coordinates into a set of 59 functions while preserving the key features of the scan data, which included a crack. By looking at local regions of high-resolution wavelets, it is possible to localize these features, and estimate their geometry. While the promise of automatic damage detection has been demonstrated, the development of more complex algorithms in future work could lead to more accurate numerical localization and estimation of damage.

ACKNOWLEDGMENTS

This research is funded by Midwest Transportation Center (Award# 011296-00014). The authors would like to thank Ahmad Abu-Hawash, Justin Spencer, and Michael Todsen from Iowa DOT for their continuous support by providing us with data, and for sharing their expertise and experience during this project. Any opinions, findings, conclusions, or recommendations expressed in this paper are those of the authors and do not necessarily reflect the views of Midwest Transportation Center or Iowa DOT.

REFERENCES

Alba M.I., Barazzetti L., Scaioni M. Rosina E., and Previtali M. Mapping infrared data on terrestrial laser scanning 3D models of buildings, *Remote Sensing*, 3(9): 1847–1870, 2011.

Anil E.B., Akinci B., Garrett J.H., Kurc O. (2013). Characterization of laser scanners for detecting cracks for post-earthquake damage inspection. *Proceedings of the International Symposium on Automation and Robotics in Construction and Mining*, IAARC, pp 313-320.

Adhikari, R. S., Zhu, Z., Moselhi, O., & Bagchi, A. (2013). Automated Bridge Condition Assessment with Hybrid Sensing. *Proceedings of the International Symposium on Automation and Robotics in Construction and Mining*, IAARC, pp.1263-1270.

Barhak, J., & Fischer, A. (2001). Parameterization and reconstruction from 3D scattered points based on neural network and PDE techniques. *Visualization and Computer Graphics, IEEE Transactions on*, *7*(1), 1-16.

Bellocchio, F., Borghese, N. A., Ferrari, S., & Piuri, V. (2013). Hierarchical Radial Basis Functions Networks. In *3D Surface Reconstruction* (pp. 77-110). Springer, New York.

Boehler W., Marbs A. (2003). Investigating laser scanner accuracy. Institute for spatial information and surveying technology. University of Applied Sciences, Mainz, Germany.

Chen S. (2012). Laser Scanning Technology for Bridge Monitoring, Laser Scanner Technology, Dr. J. Apolinar Munoz Rodriguez (Ed.), ISBN: 978-953-51-0280-9, InTech

Chen, S. E., Liu, W., Bian, H., & Smith, B. (2014). 3D LiDAR Scans for Bridge Damage Evaluations. *Bridges*, *10*, 9780784412640-052.

Cheok G.S., Leigh S., Rukhin A. (2002). Calibration experiments of a Laser Scanner. *Building and Fire Research Laboratory, National Institute of Standards and Technology*, Gaithersburg, MD, USA.

Gálvez, A., & Iglesias, A. (2012). Particle swarm optimization for non-uniform rational B-spline surface reconstruction from clouds of 3D data points. *Information Sciences*, *192*, 174-192.

Greaves T., Jenkins B. (2007). 3D laser scanning market red hot: 2006 industry revenues $253 million, %43 growth, *SPAR Point Research*, LLC 5 (7).

Hajian, H., Brandow, G. (2012). As-Built Documentation of Structural Components for Reinforced Concrete Construction Quality Control with 3D Laser Scanning. *Proceedings of the 2012 ASCE International Conference on Computing in Civil Engineering*. ASCE Publications, pp.253-260.

Howlett, R. J., & Jain, L. C. (Eds.). (2001). *Radial basis function networks 1: recent developments in theory and applications* (Vol. 66). Springer.

Kohonen, T. (2001). *Self-organizing maps* (Vol. 30). Springer Science & Business Media.

Laflamme, S., & Connor, J. J. (2009, March). Application of self-tuning Gaussian networks for control of civil structures equipped with magnetorheological dampers. In *SPIE Smart Structures and Materials+ Nondestructive Evaluation and Health Monitoring* (pp. 72880M-72880M). International Society for Optics and Photonics.

Laflamme, S., Slotine, J. J. E., & Connor, J. J. (2011). Wavelet network for semi-active control. *Journal of Engineering Mechanics*, *137*(7), 462-474.

Laflamme, S., Slotine, J. E., & Connor, J. J. (2012). Self-organizing input space for control of structures. *Smart Materials and Structures*, *21*(11), 115015.

Meng, Q., Li, B., Holstein, H., & Liu, Y. (2013). Parameterization of point-cloud freeform surfaces using adaptive sequential learning RBFnetworks. *Pattern Recognition*, *46*(8), 2361-2375.

Meral C. (2011). Evaluation of Laser Scanning Technology for Bridge Inspection, MS Thesis, Civil Engineering Department, Drexel University

Mosalam, K. M., Takhirov, S. M., & Park, S. (2014). Applications of laser scanning to structures in laboratory tests and field surveys. *Structural Control and Health Monitoring*, *21*(1), 115-134.

Olsen, M. J., Kuester, F., Chang, B. J., & Hutchinson, T. C. (2009). Terrestrial laser scanning-based structural damage assessment. *Journal of Computing in Civil Engineering*, *24*(3), 264-272.

Olsen, M. J., Chen, Z., Hutchinson, T., & Kuester, F. (2013). Optical techniques for multiscale damage assessment. *Geomatics, Natural Hazards and Risk*, *4*(1), 49-70.

Park, H. S., Lee, H. M., Adeli, H., & Lee, I. (2007). A New Approach For Health Monitoring Of Structures: Terrestrial Laser Scanning. *Computer aided civil and infrastructure engineering*, *22*, 19–30.

Suresh, S., Narasimhan, S., & Sundararajan, N. (2008). Adaptive control of nonlinear smart base-isolated buildings using Gaussian kernel functions. *Structural Control and Health Monitoring*, *15*(4), 585-603.

Trimble Inc. Trimble TX5 3D Laser Scanner User Guide. Online: http://mep.trimble.com/sites/mep.trimble.com/files/Trimble%20TX5%20User%20Guide.pdf

Trimble Inc. Trimble TX5 Automation Interface User Guide. Online: http://mep.trimble.com/sites/mep.trimble.com/files/marketing_material/Trimble_TX5_Automation_Interface.pdf

Wang, C., Shi, Z., Li, L., & Niu, X. (2012). Adaptive Parameterization and Reconstruction of 3D Face Images using Partial Differential Equations. *IJACT: International Journal of Advancements in Computing Technology*, *4*(5), 214-221.

Werner T., Morris D. (2010). 3D Laser Scanning for Masonry Arch Bridges. *Proceedings of FIG Congress, Facing the Challenges – Building the Capacity*.

Wood, R. L., Hutchinson, T. C., Wittich, C. E., & Kuester, F. (2012). Characterizing Cracks in the Frescoes of Sala degli Elementi within Florence's Palazzo Vecchio. In *Progress in Cultural Heritage Preservation* (pp. 776-783). Springer Berlin Heidelberg.

Vosselman G. and Maas H.-G. *Airborne and Terrestrial Laser Scanning*, first ed. Whittles Publishing, Dunbeath, UK, 2010.

Xiong X., Adan A., Akinci B., and Huber D. Automatic creation of semantically rich 3D building models from laser scanner data, *Automat. Constr.*, 31: 325–337, 2013.

Zhang, Q., & Benveniste, A. (1992). Wavelet networks. *Neural Networks, IEEE Transactions on*, *3*(6), 889-898.

Bluetooth Low Energy Sensing Technology for Proximity Construction Applications

JeeWoong Park
School of Civil and Environmental Engineering,
Georgia Institute of Technology,
790 Atlantic Dr. N.W.,
Atlanta, GA 30332-0355, United States,
jpark463@gatech.edu

Dr. Yong Cho
School of Civil and Environmental Engineering,
Georgia Institute of Technology,
790 Atlantic Dr. N.W.,
Atlanta, GA 30332-0355, United States,
yong.cho@ce.gatech.edu

Willy Suryanto
School of Civil and Environmental Engineering,
Georgia Institute of Technology,
790 Atlantic Dr. N.W.,
Atlanta, GA 30332-0355, United States,
wsuryanto3@gatech.edu

ABSTRACT

Safety is considered one of the most importance components that need to be successfully addressed during construction. However, dynamic nature and limited work space of roadway work zones create highly occupied working environments. This may further result in hazardous proximity situations among ground workers and construction equipment. In fact, historical incident statistics prove that the current safety practice has not been effective and there is a need for improvement in proving more protective working environments. This study aims at developing a technically and economically feasible mobile proximity sensing and alert technology and assessing it with various simulation tests. Experimental trials tested the sensing and alert capability of the technology against its accuracy and reliability by simulating interactions between equipment and a ground worker. Experimental results showed that the developed mobile technology offers not only adequate alerts to the tested person in proximity hazardous situations but also other advantages over the commercial products that may play an important role in overcoming the obstacles for rapid deployment of new technology in construction segments.

Key words: Bluetooth low energy—construction safety—construction equipment—iBeacon—proximity sensing

Proceedings of the 2015 Conference on Autonomous and Robotic Construction of Infrastructure, Ames, Iowa.

INTRODUCTION

With the development of wireless technology in the last decade, mobile devices have become an essential component in our daily life being used for multiple purposes. The advancement in the wireless technology enabled most of the recently produced cars equipped with a Bluetooth technology. The driver is then able to communicate with his/ her mobile device via a Bluetooth enabled car, triggering phone calls listening to music and radio without having to making physical contacts with the device. This has turned our daily activity of driving a car into a much safer experience, allowing the driver to better focus on the road. According to (Statista, 2015), the population of smartphone users have rapidly been increasing and the expected number of population in the U.S. is 183 million, which is more than a half U.S. population (See Figure 1).

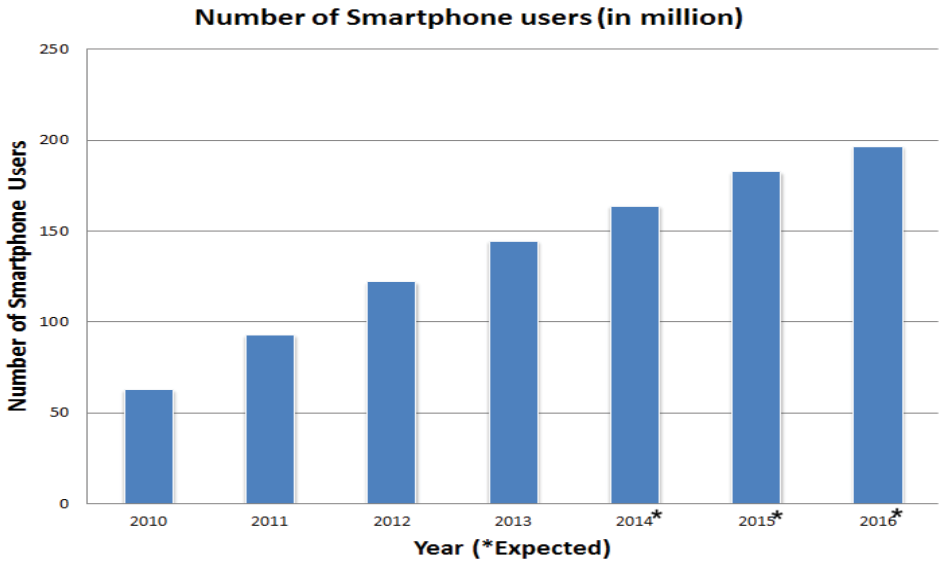

Figure 1. The number of smart phone users in the U.S.

Safety is one of the most importance components that need to be successfully addressed during construction. However, dynamic nature and limited work space of roadway work zones create highly occupied working environments. This may further result in hazardous proximity situations among ground workers and construction equipment. 962 deaths of workers were recorded at a road construction sites from 2003 to 2010. In addition, about 30% of deaths related to construction 2012 were resulted from being struck by a vehicle. These historical incident data prove that the current safety practice has not been effective and there is a need for improvement in proving more protective working environments. Recent industrial (ENR, 2015) efforts have been found with deploying cameras and motion sensors near the blind spots of a piece of equipment. Various proximity sensing devices have been discussed and evaluated by (Ruff, 2007), (Begley, 2006), (Marks and Teizer, 2012) and (Larsson, 2003). Tested and evaluated systems in the past research require external hardware, such as camera, laser scanner, tripod, power supply lines, heavy antenna, or tags. These are the major components of each of the systems to achieve communication between a hazardous source and an object that is potentially in a dangerous zone. While being major components, these requirements are barriers that limit the systems' feasibility and practicality in dynamic construction applications. In addition to the infrastructure requirement, there are other parameters that are crucial for assessing a system's feasibility and practicality, including detection area, cost, maintenance, accuracy, precision, consistency, alert method, adaptability, required power sources, ease of

use, ease of deployment. Benefits and limitations of other proximity sensing systems were discussed in (Castleford et al., 2001; Goodrum et al., 2006; Marks and Teizer, 2013)

Although smart devices are already pervasive and embedded into our society, their potential uses in construction industry have not been discussed and minimal research and experimentation have not been conducted with utilizing smart devices, despite the efforts made with other technologies in the last decade. This study proposes a wireless proximity sensing technology that utilizes Bluetooth transmitters and mobile devices to create a proximity sensing and warning system. The authors consider that several characteristics of smart devices, such as pervasiveness, availability, and familiarity to end users, are the key factors to realize a feasible and practical technology. In the following sections, an extensive overview of the proposed system will be discussed, and experimental validation and conclusion will follow.

OBJECTIVE

In adopting a proximity sensing and alerting system, several factors play an important role for a system to be feasible and pragmatic. They include detection area, cost, maintenance, accuracy, precision, consistency, alert method, size of infrastructure, adaptability, required power sources, ease of use, ease of deployment, and others. The main objective of this study is to develop and validate a proximity sensing system that is economically and technically feasible and practical. The system should provide minimal infrastructure, adaptability with calibrating ability, intensifying alerts to reflect the degree of dangerousness, and real-time alerts to pedestrian workers and equipment operators during hazardous proximity situations. Widely available smart devices and low-cost Bluetooth transmitters are utilized to create a proximity sensing and alert system. Through field experimentations, their performance have been tested and assessed in various aspects.

PROPOSED PROXIMITY SENSING SYSTEM

The proposed proximity sensing system is based on Bluetooth based wireless sensing technology (iBeacon technology). This system offers various promising characteristics, including rapid connectivity, ease of deployment, low-cost hardware, minimal infrastructure and ease of integration with other systems. These characteristics are especially beneficial when considering adoption into construction industry. The system provides intensifying alerts upon creation of hazardous incidents to mitigate potential risks that will otherwise be posed upon workers and equipment. The system is composed of major components to create a basic proximity sensing and alert system, and of auxiliary components to support the system in different aspects.

System Major Components

The developed system is composed of three main hardware components, including 1) signal transmitters (Bluetooth transmitter), 2) personnel receivers (Bluetooth enabled mobile device), 3) equipment operator's receiver (Bluetooth enabled mobile device), and the software component which provides an user interface and application function on which the system operates. A signal transmitter (beacon) is called Equipment Protection Unit (EPU) that transmits Bluetooth signal using Bluetooth Low Energy (BLE). Beacons are to create detection area from a hazard source to protect workers. Figure 2 describes an example of beacon deployments on a piece of construction equipment and a worker operating nearby. To create a symmetrical detected area, several beacons are attached symmetrically around a piece of construction equipment. A worker on the right of Figure 2 is equipped with a Bluetooth enabled mobile device, which is also called Pedestrian worker's Personal Protection Unit (PPU). This PPU provides intensifying sound alerts and vibration upon breach into a hazardous zone defined

based on a piece of equipment considered. An equipment operator is also equipped with a Bluetooth enabled mobile device, which is also called Equipment operator's Personal Protection Unit (PPU). When a potential hazardous incident is created, this PPU provides intensifying alerts and the direction of the incident with respect to the equipment.

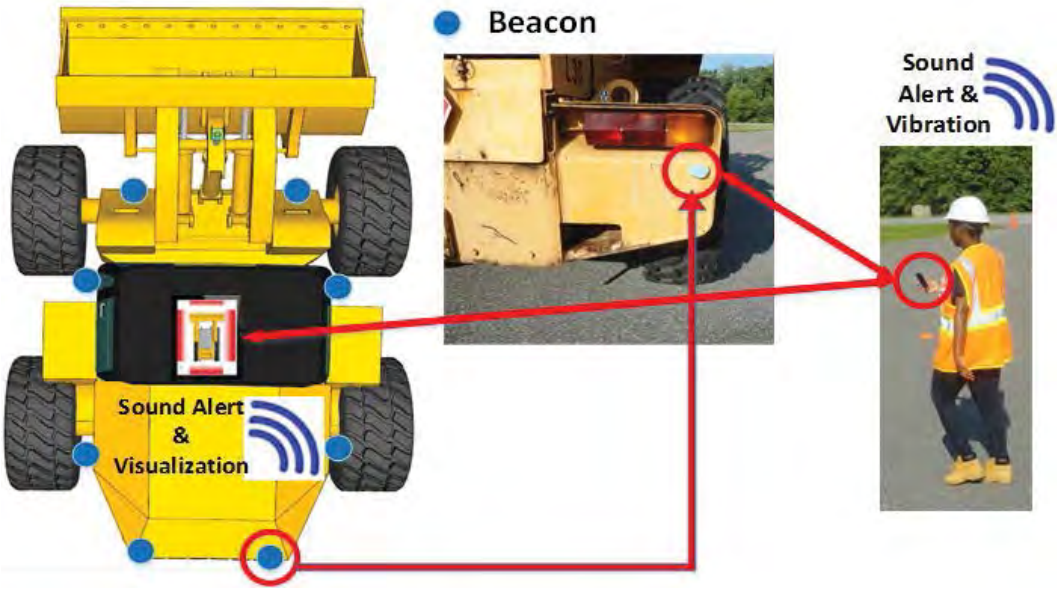

Figure 2. Major components of the proposed system

System Auxiliary Components

The proposed system is also composed of several auxiliary components to reinforce the communication and alert system especially when operating in a harsh working environment and to provide more features and opportunities for post safety analysis. Additional Bluetooth enabled devices including a smartwatch and an earpiece can be incorporated into the existing system for enhanced vibratory and sound alerts. Also, a cloud server is configured for the proposed system to gather data that indicate a potentially created hazardous situation. Whenever hazard incident is created, the system can send to a cloud server the creation of the incident for post safety analysis.

System Component Communication Flow

Previous sections described the roles of each of the components. This section explains the system work flow and details in each of the flow steps. Figure 3 shows a flow chart for one cycle of communication of the system. This flowchart illustrates one cycle of the system communication. After each cycle the flowchart points to "Keep Monitoring", which basically indicates that cycles are repeating. Each cycle starts with communication of beacons from a hazardous source (e.g., a piece of equipment) and a mobile device (e.g., a protected worker). Based on the user's distance set-up, the system determines if dangerous zone has been breached by either the piece of construction equipment or the worker during the dynamic interaction of the two. When it is determined to be breached, the system proceeds with

prevention actions to provide an additional chance for the worker and equipment to escape from the scene. The prevention actions immediately take place without time delay from the hazard situation detection by the system. Audible alerts and vibration get triggered to the worker's PPU, while audible alerts and visualization of the direction of the hazard situation with respect to the equipment are provided to the equipment operator via his/ her PPU. In addition, the system support cloud based data collection to allow for post analysis.

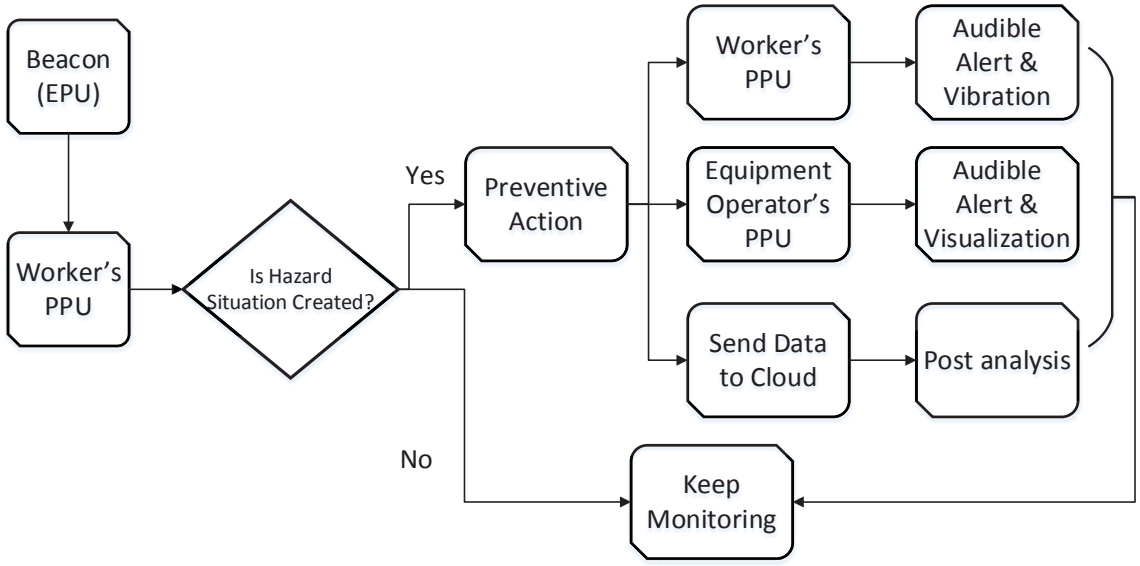

Figure 3. Communication flow for one cycle

Methods

The proposed system is a Bluetooth based system whose communication among devices is accomplished by radio signal transmission. The transmitted radio signal is recorded and the recorded Received Signal Strength (RSS) estimates the approximate horizontal distance between the beacons and receiver. The user can perform calibration to set his/ her desired distance range at which the system initiates alerts. This calibrated range is then trisected to provide intensifying alerts to indicate the degree of dangerousness of a created hazardous situation. Upon the creation of the hazardous situation, the worker's PPU immediately turns to a beacon to send out signals to the nearby operator's PPU. With this signal, alerts and visualization can be realized on the equipment operator's PPU.

System Deployment and Calibration

The key aspect in system deployment is to acquire a symmetrical coverage centered from a piece of construction equipment. To improve the quality of symmetrical coverage, multiple Bluetooth signal transmitters are deployed around the equipment. This deployment allows the communication to reply more on beacons that experience the least amount of multipath effects and signal degradation. In addition, to reduce the amount of signal interference, care should be taken when placing beacons on a piece of equipment so that the best line of sight is obtained.

Calibration is desired for two major reasons. First, the RSS is dependent on environmental conditions. For different equipment and environmental conditions, there is no guarantee for the

radio communication to be in the same quality. Second, each user's may have a different desired coverage range. Per user's need for coverage range, by collecting RSS at a desired distance for each of the beacons, calibration is performed.

FIELD VALIDATION

To validate the proposed proximity sensing and alert system, a set of experimental trials were designed and conducted to evaluate the system. To assess the system reliability and effectiveness, (1) trials were performed at eight different angles centered from a piece of equipment and (2) two different pieces of equipment were tested, such as a wheel loader and a dump truck. The design of experimental simulation is to emulate real-time construction roadway work zone operations. Presented material in this paper is mobile workers and static equipment situation. Figure 4 shows the test bed and approach angles for worker and equipment interaction simulations during testing. A worker equipped with a worker's PPU approaches to a piece of construction equipment and the alert distance (at which breach into hazard zone is detected) was recorded for each of the trials. For each angle of the eight angles, 20 trials were made for statistical data collection.

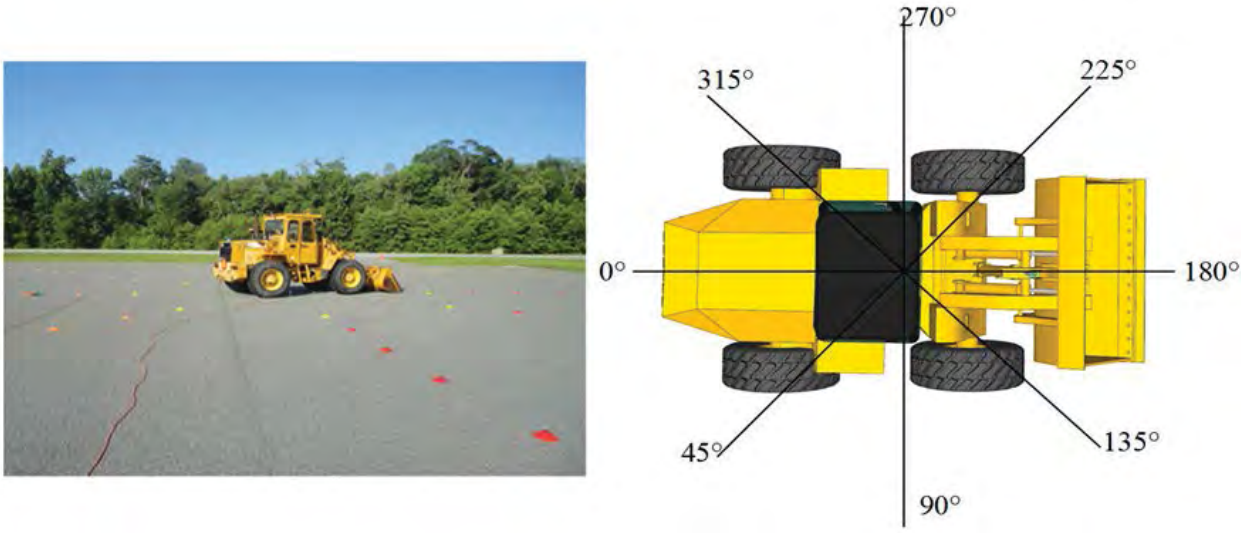

Figure 4. Test bed and approach angles during trial simulations

For these two different sets of trials, calibration was only performed for the trial with wheel loader. The purpose of this was to observe the difference in RSS behavior, thus difference in alert distance accuracy, in different environmental conditions and to confirm the needs of calibration. In the wheel loader trials, the alert distance was set to 12 meters, and the same setup was used for the truck trials. Statistically analyzed data for two complete sets of trials are tabulated in Table 1, and Figure 5 shows plots for the sets of trials. In the simulation with the wheel loader, the overall average alert distances did not deviate significantly from the set distance of 12 meters except at 135°. This drop needs be investigated considering various factors, such as battery, interference with the surroundings, or potential mal-functions of transmitter. As seen in both Table 1 and Figure 5, overall average alert distances for the dump

truck simulation are, however, greater than those for the wheel loader simulation. This shows that the importance of calibration to obtain a desired distance. In this case, the RSS was more powerful with the truck simulation, and proper calibration should be able to manage this difference to set the alert distance as desired by the worker. Other than the average alert distance, the two simulations behaved similarly.

Table 1. Statistical analysis of alert distance and standard deviation

Approach angle	Wheel loader		Dump truck	
	Average (m)	Std (m)	Average(m)	Std (m)
0°	15.3	2.7	16.8	3.4
45°	12.2	3.0	17.1	2.5
90°	12.4	3.6	22.6	2.8
135°	5.3	1.8	19.2	1.9
180°	12.4	3.9	17.1	1.6
225°	13.0	3.6	18.8	1.7
270°	15.2	1.0	16.2	1.4
315°	17.3	1.0	12.5	2.9

*std is standard deviation.

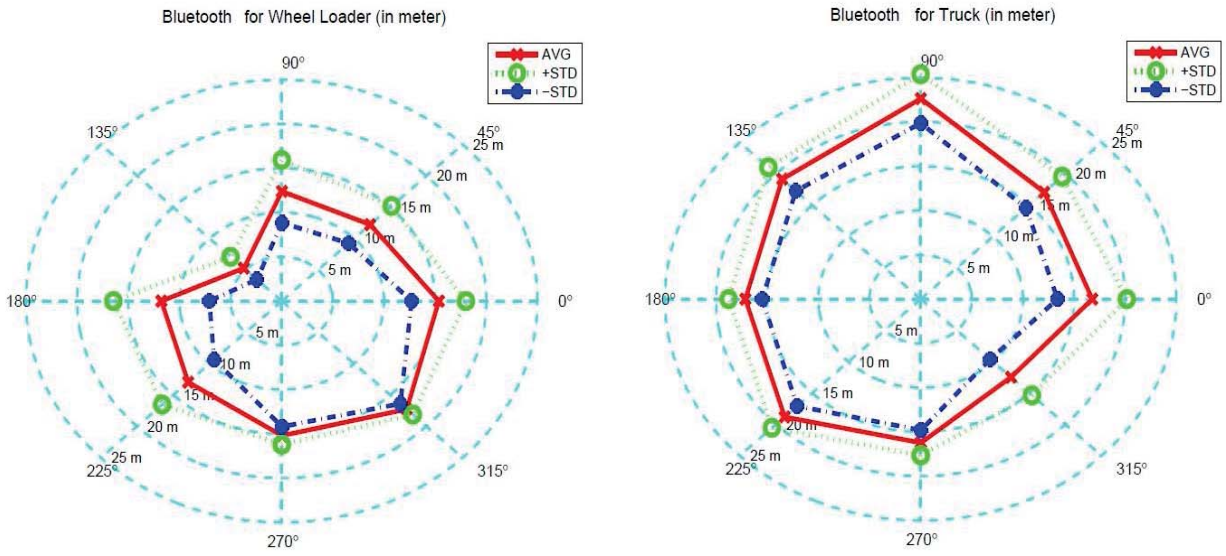

Figure 5. Field trials with a wheel loader (left) and a dump truck (right)

Table 2 displays another statistical result showing recall values. Different values of distance at failure were used to compute recall values as the definition of distance at failure may be different depending on the application. As Table 2 is read, one should keep in mind that the average alert distances of the two simulations (wheel loader and dump truck) were different, and therefore, their direct comparisons should not be made. For the entire trials, the system performed with less than 3% recall rates for less than five meters distance at failure. Five meter distance boundary seems reasonable as alerts are simultaneously provided to both the

pedestrian worker and equipment operator allowing them to stop operations and take a proper action for avoidance of collision. However, if the lower distance boundary (distance at failure) is required as high as nine meters, one should consider having a higher desired distance, in this case higher than 12 meters.

Table 2. Statistical analysis of recall rates

Distance at failure (m)	Number of false negative			Recall rate
	Wheel Loader (out of 160)	Truck (out of 160)	Total (out of 320)	
3	3	0	3	0.9%
5	8	0	8	2.5%
7	25	0	25	7.8%
9	32	2	34	10.6%

CONCLUSION

This study aims at developing a technically and economically feasible mobile proximity sensing and alert technology and assessing it with various simulation tests. In order to overcome the barrier of deployment costs, a cost effective system was developed. This system is based on Bluetooth technology, which is already widely available in most of the recent smart devices. Also, the system offers minimal infrastructure, ease of deployment, calibration functionality and adaptability, compared with other similar proximity sensing and alert systems. Experimental trials were designed and performed to evaluate the proposed proximity sensing and alert system for its capability to offer real-time situational awareness via alerts to pedestrian workers and equipment operators working in proximity hazardous situations. Results of the simulated tests showed that this system was acceptable in providing pedestrian workers and equipment operators multiple forms of alerts. Upon the detection of a potential hazardous situation, immediate alerts were provided to both the pedestrian worker and the equipment operator. This can help to minimize the proximity related accidents by providing an additional chance of time and space for the workers to escape from the hazardous scenes.

REFERENCES

Begley, R. (2006). "Development of Autonomous Railcar Tracking Technology Using Railroad Industry Radio Frequencies". *Research Opportunities in Radio Frequency Identification Transportation Applications*, 59–60. Retrieved from http://citeseerx.ist.psu.edu/viewdoc/download?doi=10.1.1.125.4645&rep=rep1&type=pdf#page=67

Castleford, D., Nirmalathas, A., Novak, D., and Tucker, R. S. (2001). "Optical crosstalk in fiber-radio WDM networks". *IEEE Transactions on Microwave Theory and Techniques*, *49*(10), 2030–2035. doi:10.1109/22.954826

ENR. (2015). "More Blind-Spot Sensors Make Jobsites Safer". Retrieved April 9, 2015, from http://enr.construction.com/products/equipment/2015/0216-65279more-blind-spot-sensors-make-jobsites-safer.asp

Goodrum, P. M., McLaren, M. A., and Durfee, A. (2006). "The application of active radio frequency identification technology for tool tracking on construction job sites". *Automation in Construction*, *15*(3), 292–302. doi:10.1016/j.autcon.2005.06.004

Larsson, T. (2003). "Industrial forklift trucks: Dynamic stability and the design of safe logistics". *Safety Science Monitor*, *7*(1), 1–14. Retrieved from http://www.diva-portal.org/smash/record.jsf?pid=diva2:430110

Marks, E., and Teizer, J. (2013). "Method for testing proximity detection and alert technology for safe construction equipment operation". *Construction Management and Economics*, *31*, 1–11. doi:10.1080/01446193.2013.783705

Marks, E., and Teizer, J. (2012). "Proximity Sensing and Warning Technology for Heavy Construction Equipment Operation" (pp. 981–990). Construction Research Congress. doi:10.1061/9780784412329.146

Ruff, T. (2007). "*Recommendations for evaluating and implementing proximity warning systems on surface mining equipment*". Retrieved from http://stacks.cdc.gov/view/cdc/8494/Print

Statista. (2015). "Smartphone users in the U.S. 2010-2018 | Forecast". Retrieved from http://www.statista.com/statistics/201182/forecast-of-smartphone-users-in-the-us/

A Design Framework for Off-road Equipment Automation

Brian L. Steward
Department of Agricultural and Biosystems Engineering
Iowa State University
2325 Elings Hall
Ames, Iowa 50011
bsteward@iastate.edu

Lie Tang
Department of Agricultural and Biosystems Engineering
Iowa State University
2325 Elings Hall
Ames, Iowa 50011
lietang@iastate.edu

Shufeng Han
John Deere Intelligent Solutions Group
4140 114th Street
Urbandale, IA 50322
hanshufeng@johndeere.com

ABSTRACT

Design frameworks can be helpful in the development of complex systems needed to automate machines. Designing autonomous off-road machinery requires having the means for managing the complexity of multiple interacting systems. A design framework, consisting of four technical layers, is presented. These layers are (1) machine architecture, (2) machine awareness, (3) machine control, and (4) machine behavior. Examples of technology advanced in development efforts of autonomous, robotic platforms for agricultural applications are provided. Linkages were made to applications in the construction machinery sector. Similarities between agricultural and construction automation exist in each of the technical layers.

Key words: automation—design framework—perception—machine localization—machine behavior

INTRODUCTION AND BACKGROUND

Developing autonomous or robotic construction machinery systems can be inspired by similar technological developments in other sectors. In agriculture, for example, automated agricultural machinery technology has been under development for almost 50 years. In the 1970s, electronics for monitoring and control were introduced to agricultural machines, particularly for controlling the chemical application rate of agricultural sprayers and monitoring the consistent drop of seeds in a planter. The most significant advance toward agricultural machine autonomy started in the 1990s when precision agriculture became the key driver for integrating more sensors and controls into agricultural machinery.

Proceedings of the 2015 Conference on Autonomous and Robotic Construction of Infrastructure, Ames, Iowa.

Precision agriculture is a management strategy to reduce the management scale from field scale to sub-field scales – on a meter-by-meter scale or in management zones with similar soils or topography. Precision agriculture is an approach to intensively managing spatial and temporal variability of agricultural fields. It is enabled by automation technologies, but there are many examples around the world where precision agriculture management is practiced under low technology conditions.

In the large scale agricultural practices of North America, Europe, and Australia, among others, automated operation of agricultural machines has been relied upon to achieve the goal of precision agriculture. As an example, variable-rate application of chemical inputs, one of the major precision agriculture practices, needs the application rate to be changed on-the-go and sometimes within every square meter of a field. Manual operation and control of the machine is infeasible under large field conditions. Thus automatic rate control has been implemented on these machines.

However, while many agricultural machinery operations have some automation technology embedded in them, there are few examples of autonomous or robotics machines in agriculture. Based on the experience of the industry with automation technology, the vision of autonomous and robotic systems has developed nevertheless. The use of small field robots is desirable for many precision agriculture practices, such as soil sampling, crop scouting, site-specific weed control, and selective harvesting. Robotic applications are not only desirable, but are also more economically feasible than conventional systems for some agriculture applications (Pedersen et al., 2006).

There are several underlying motivations to move to more autonomous and robotic agricultural field operations. First in many cases, automated processes can achieve a greater precision in meeting performance specifications than can humans. An automatically guided tractor, for example, can be driven through a field with smaller deviations from a straight line resulting in lower overlapped application of inputs and fewer skipped areas which were not properly treated. Automation thus leads to greater input efficiency. The availability and cost of labor can be prohibitive in agriculture particularly because of the timeliness requirements of agricultural processes such as planting and harvesting. Agricultural automation can extend the productivity of human labor by working in collaboration with humans in a co-robotic fashion. Recent increases in agricultural productivity have been achieved through increasing equipment size. Many agricultural machines are now facing limits to larger sizes, and increased size also leads to soil compaction which has a negative impact on crop yield. Autonomous field robots have potential to address productivity barriers and reduced soil compaction at the same time through small vehicle platforms operating in a fleet to accomplish the needed work rates. Such small vehicles also have the potential to reduce energy inputs (Toledo et al., 2014).

While there are many differences between the agricultural machinery and construction machinery sectors, there are also several similarities. Similarities between the two sectors include machinery interaction with media such as soil or biomaterials with uncertain physical parameters that are spatially and temporally varying. Both sectors need to lower costs and improve input efficiency, as well as improve performance and productivity. Additionally, in both cases, human operators interact with the machines, and other people work in close proximity to the machines, so safety is of primary importance. Construction and agriculture both seek to minimalize environmental impact while developing an infrastructure that meets human needs.

A main goal of agricultural automation then is to increase food production for a growing world population. Many estimate that food production will need to double by 2050 to keep up with the demand driven by growing population and affluence. These production increases must occur while also minimizing negative environmental impacts. In the automation of earthmoving and road construction machines, as specific examples of construction machinery automation, the goals are different, but bear some similarity to those of agricultural automation. Construction automation goals include improved productivity particularly in the earthmoving and material transport applications (Singh, 2002, 1997). Efficiency is also an important goal. Process and quality control of a construction process is an important goal as in the applications of roller-integrated compaction measurements (Vennapusa et al., 2009) or concrete paving (Castro-Lacouture et al., 2007). Safety of construction workers is also an important goal (Shi et al., 2005; Dumpert, 2004).

The goal of this paper is to present a design framework developed for autonomous or robotic machines in agriculture that it might inspire similar thinking about robotic construction machines, particularly those used for road construction or earthmoving.

DESIGN FRAMEWORK FOR AUTONOMOUS MACHINES

Machine autonomy is the capability of a machine to achieve operational goals independent of human operation or intervention in an uncertain environment. Thus autonomy requires a much higher level of complexity and artificial intelligence than observed in machines that are simply automated. To manage this complexity and to understand where various research and development projects fit in the context of building autonomous machines, a design framework has been developed to categorize the required technologies for robotic agricultural machines (Han et al., 2015). This design framework is general enough to be applied to autonomous construction machines as well. The framework consists of four different technology layers naturally dependent on one another (Figure 1). These layers are, starting from the bottom: (1) machine architecture, (2) machine awareness, (3) machine control, and (4) machine behavior. Each layer is described below with applications from the agricultural machinery area. Possible extensions to construction robots are provided.

Machine Architecture

In autonomous systems engineering, an architecture is a means for managing complexity. Autonomous and robotic machines of necessity are complex systems comprised of various components and sub-systems; many of which are complex systems themselves. Since individual humans and teams are limited in their time and resources, as well as their ability to keep track of details, they need a way to manage system complexity during development. The principle of abstracting complexity through encapsulation of components and using clearly defined interfaces to the components is generally what is meant by the phrase “robotic system or software architecture.”

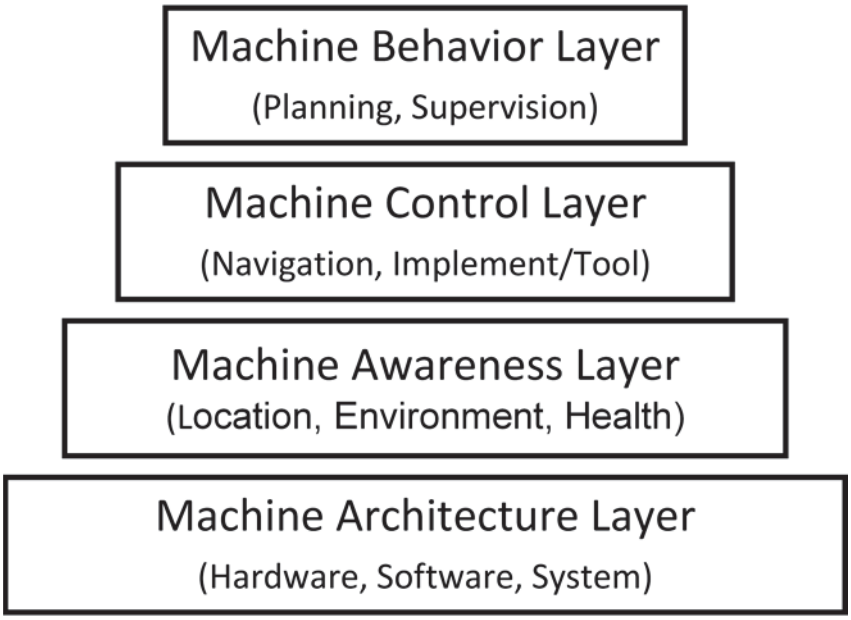

Figure 1. A four-layer design framework for autonomous machines.

Autonomous robots require, to varying degrees, architecture for both hardware and software. Just thinking about the components required for a particular robotic application and how those components are connected to one another and are interacting with one another is a simple example of system architecture. Potential is excellent for leveraging the work across research teams through system architectures that can be shared. These architectures can be proprietary so that development teams can internally manage complexity. Architectures can also be open and public to facilitate more rapid development across development teams, as well as to facilitate the interconnectivity of components and sub-systems available on the market.

At the lowest level, an autonomous construction machine is composed of hardware and software components required for the machine's function. These components include the mechanical parts and assemblies making up the machine along with a prime mover and drive train needed to control and apply power to meet the operational goals of the machine. For machine automation and eventual autonomy, these hardware components also include the electronic, sensing, and actuation components required to automate machine functions. A machine's system architecture, consisting of both hardware and software, must be in place to build the higher level layers needed for autonomy. Since the machine must interact with the physical world, a physical hardware architecture must be in place. For an autonomous construction robot, the hardware must enable mobility within the job site, as well as provide the capability to perform operations in an automated manner. The hardware architecture must be mechatronic – an integration of mechanical, electrical and electronic, fluid power, and computational systems – to provide the functionality required to support autonomous operations. The necessary interconnections between systems are needed to communicate both data and power. Other hardware that must be present are the sensors which transduce physical into electrical signals and actuators which provide force and motion to interact with the soils or other materials.

Complementary to the hardware architecture, software and communications architectures must also be in place so that the development of higher level layer technology can be built on pre-

established software components enabling communication and reusing lower level computational solutions. While different architectures may focus on different aspects of robotic systems, they tend to provide means for (1) modularizing tasks for processes that are important to a functioning robot, (2) defining messaging systems and protocols for inter-process communication, and (3) defining operations that must occur across distributed processes. Several illustrative robotic system architectures portray key features of architectural thinking that is needed for autonomous machines.

Kramer and Scheutz (2007) surveyed nine open source robotic development environments, or system architectures, for mobile robots, and evaluated their usability and impact on robotics development. Jenson et al. (2014) surveyed available robotic system architectures including CARMEN, CLARAty, Microsoft Robotics Developer Studio, Orca, Orocos, Player, and ROS. They also found examples of lesser known architectures which may be more relevant to agricultural robots, including Agriture, Agroamara, AMOR, Mobotware, SAFAR, and Stanley. Of these, four architectures, CARMEN, Agroamara, Mobotware, and SAFAR, had field trials for agricultural applications. However, open source availability was limited and only Mobotware had been recently updated.

In early efforts to promote architectural thinking about agricultural robots, Blackmore et al. (2002) proposed a conceptual system architecture for autonomous tractors that consisted of a set of objects or agents which have well defined narrow interfaces between them. The two types of agents are processes and databases. A process carries out tasks to achieve a goal. Nine processes were defined and described: Coordinator, Supervisor, Mode Changer, Route Plan Generator, Detailed Route Plan Generator, Multiple Object Tracking, Object Classifier, Self-Awareness, and Hardware Abstraction Layer (Figure 2). Three databases were defined (Tractor, Implement, and GIS) and are used to store and retrieve data about the machine and its operational context. This type of architectural thinking could be applied to construction robots as a means for determining the structure required for construction robots.

The Joint Architecture for Unmanned Ground Systems (JAUGS) has seen some implementations in agriculture including an autonomous orchard tractor and an autonomous utility vehicle (Torrie et al., 2002). JAUGS was primarily a standard messaging architecture to enable components to communicate to one another in a standard manner. Later, JAUGS was changed to JAUS (Joint Architecture for Unmanned Systems) to be more generally applied to all types of unmanned vehicles and became a Society of Automotive Engineers standard. The standard has two parts; the Domain Model which describes the goals for JAUS, and the Reference Architecture which specifies an architecture framework, a message format, and a standard message set (Rowe and Wagner, 2008).

The Robotics Operating System (ROS; Open Source Robotics Foundation) is a general open-source robotic operating system not specific to any application domain. It provides an interface for passing messages between processes running on different host computing platforms that make up the computer hardware architecture of a robot. ROS also provides a broad set of libraries and tools useful for robotics development. Libraries include (1) standard robot message definitions, (2) the transform library for managing coordinate transform data, (3) a robot description language for describing and modelling a robot, (4) means for collecting diagnostics about the state of the robot and (5) packages for common robotics problem such as pose estimation, localization, and mobile navigation (ROS.org, 2015; Quigley et al., 2009). ROS has applicability to autonomous construction machines. It has been used as a part of larger system architectures for agricultural machines.

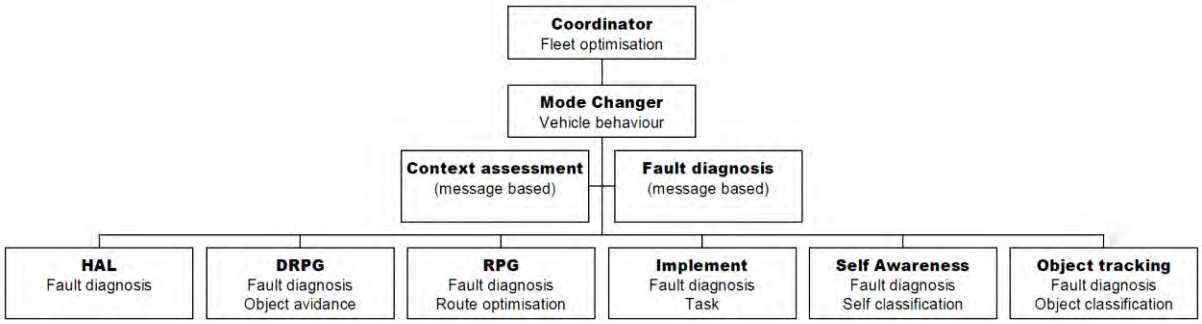

Figure 2. A conceptual system architecture consisting of ten encapsulated processes, databases and inter-process messaging for an autonomous tractor (Blackmore et al., 2002).

FroboMind is a robotic software systems architecture intended to assist in the development of field robots for precision agriculture tasks (Jenson et al., 2014; Figure 3). FroboMind has a four part structure, which from lowest to highest levels include: operating system, middleware, architecture, and components. The Linux operating system Ubuntu was chosen because of its large distribution and long-term support. ROS was used for the middleware to define the internal communication structure between processes. The FroboMind architecture level consists of four modules, which are perception (sensing and processing), decision making (mission planning and behavior), action (executing and controlling), and safety modules. The component level consists of software components implemented as ROS packages. FroboMind is open source and has been used in the development of several agricultural robots. It is not a hard real-time system, but its "soft" real-time performance appears to be sufficient for agricultural robotics applications, and would likely be satisfactory for construction applications. While FroboMind was designed for field robots doing precision agriculture tasks to enable field experiments and more efficient reuse of existing work across projects, it could also provide an architecture for construction robots.

Robotic software system architectures provide the means for handling complexity through well-defined processes and messaging, as well as higher level features, all of which are needed for construction robots. These architectures also promote reusability, which enables research and development teams to build on one another's work and move toward more autonomy in construction machines.

Machine Awareness

The next design framework layer, machine awareness, is built on the machine architecture layer which contains the transducers that convert machine and environment signals into electrical signals. Machine awareness, conversion of sensor signals into knowledge about machine state and work environment, is fundamental to producing autonomous machine behavior. Autonomous machines must have awareness of their state and location, the work environment including objects to be avoided and the shape of the terrain, and properties of the material that the machine is processing. In addition, they must have machine health awareness. This machine awareness layer mainly consists of localization and perception technologies.

For off-highway applications in agriculture and construction, localization is often accomplished through a global navigation satellite system (GNSS) with inertial sensors. However, many applications require the machine to follow some local path or more efficiently move within a job

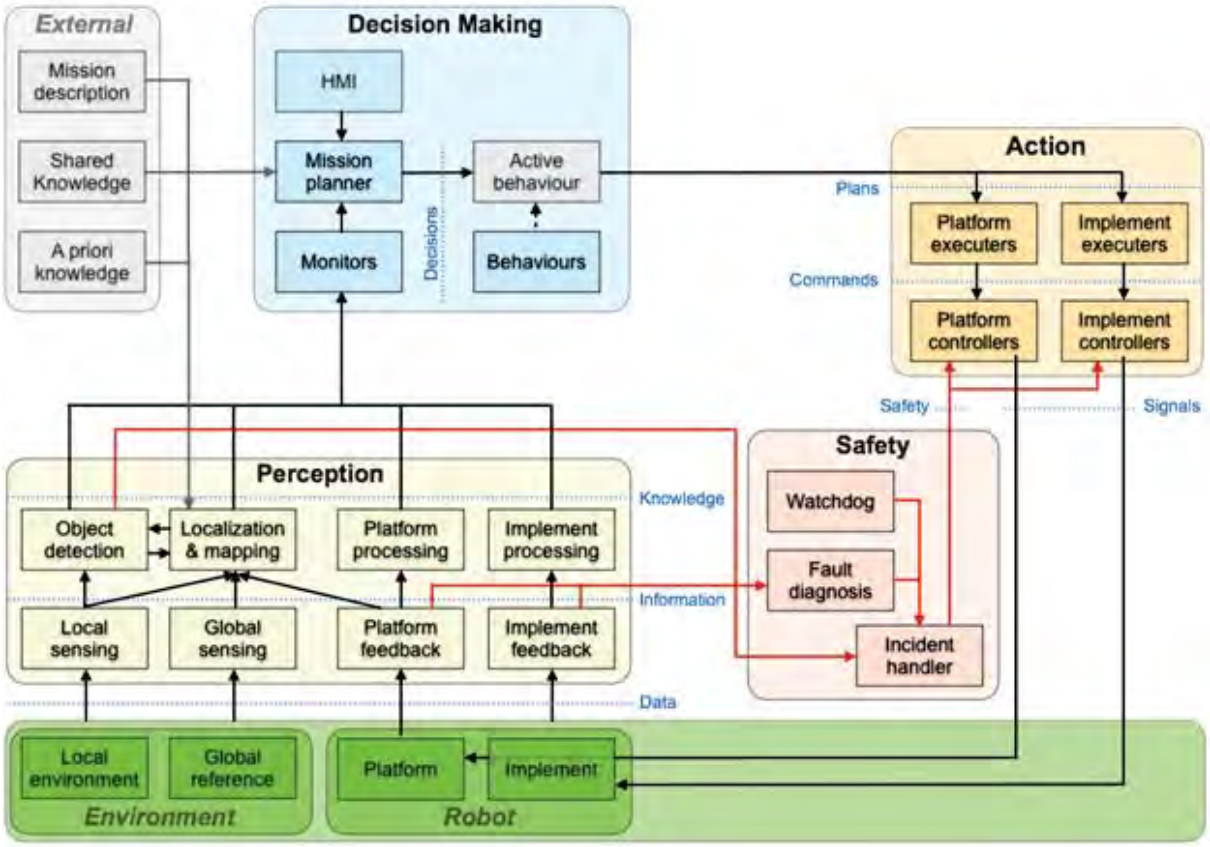

Figure 3. The FroboMind architecture level consists of perception, decision making, and action modules along with a separate safety module (Source: Jensen et al., 2014).

site. In these cases, machine localization using relative position sensors has advantages. Included in this localization sub-layer are sensor fusion methods enabling more robust localization through complementary sensors. Sensor fusion can extend localization when one of the sensor signals is lost and can improve localization accuracy when various error sources exist from any single sensor in the system.

Before a machine can be classified as autonomous, it must perceive its environment to carry out its tasks effectively and safely. A primary goal of machine perception is machine safeguarding to ensure safe operation of the machine. Obstacle detection, recognition, and avoidance are typical steps in machine safeguarding. Perception algorithms and strategies are built on top of the perception sensors in the hardware architecture to achieve safeguarding functions.

Both agricultural and construction machines need to perceive features of the environment with which they are interacting. Agricultural machines need to interact with the crop, soil and field topography to accomplish field operations. Construction machines also need to interact with the soil and job site terrain. For autonomous operation, machine perception systems are needed with the following capabilities: localization to determine where the machine is relative to the world coordinate systems, object recognition of obstacles around the machine, navigation and collision avoidance so that the machine can safely interact with its environment, and learning and inference so that the perception system can solve new problems. Han et al. (2015)

reviewed perception sensors used for navigation and obstacle detection in autonomous agricultural vehicles. Sensor technologies that have been investigated for this application include vision sensors which are used to capture two-dimensional scene information, as well as stereo vision and active 3D camera that add range information. Laser, Ladar, Lidar, Radar sensors as well as ultrasonic sensors have been used for range detection and 3D reconstruction of the scene. Many of these same sensors have been used for construction automation for object detection, pile shape estimation, elevation measurement across terrains (Singh, 1997, 2002). Sensors for the physical properties of soils have application in both agricultural and construction domains (Rossel et al., 2011).

With any machine, failures or breakdowns will occur. Thus, the condition of the machine must be monitored, and machine health awareness is needed to achieve machine autonomy. In a human-operated machine, the operator is not only controlling the operation of the machine, but is also monitoring the machine through visual, audio, or vibration cues to ensure that the machine is functioning correctly. As machinery is automated, machine condition monitoring, along with fault detection and diagnosis, also must be automated, although it can still have some reliance on human intervention when a human operator is present. For driverless, autonomous machines, machine intelligence to monitor machine health must be in place to produce machine health awareness with no human assistance – a very big requirement for the development of these machines. Machine health awareness requires a high degree of intelligence, perhaps higher than all other requirements for an autonomous machine.

Central to health awareness are technologies often referred to as condition monitoring systems or fault detection and diagnostic systems. Condition monitoring is typically part of an overall maintenance strategy for a process, machine or machine system, which will involve a human manager. It uses signals from a machine acquired with sensors to provide some indication of the condition of machine components. Based on these signals and their changes over time, with some signal processing and pattern recognition analysis, managers can make decisions about what maintenance interventions should be taken and when they should be scheduled.

Implementing a machine health awareness system for an autonomous machine requires several layers of technology, which can be structured in a format similar to the design framework presented above (Figure 4). For machine health awareness, there first must be a hardware layer consisting of sensors that are measuring physical signals known to be related to machine component condition. Several sensing modes have been used for condition monitoring and will be described below. Secondly, the signals from the sensors must be preprocessed to remove abnormal signals and then processed to extract the features that are correlated to machine component conditions. Next, fault detection applies automatic pattern recognition processes to determine if a fault has occurred in the system. Generally this step involves finding deviations from patterns associated with normal operation. Once a fault has been detected, it must be diagnosed to identify what the fault is and what might have caused it.

The last layer might be the most important for an autonomous machine, i.e., to decide what action should be taken next and then execute it. Several possible actions can be taken when a fault occurs, including: (1) initiate a graceful shutdown and remain at current position, (2) stop operations and move to a designated location for maintenance, (3) stop operations, alert remote human supervisor for further instructions, or (4) continue operations, and send a warning message to human supervisor. Blackmore et al. (2002) identified six safety modes similar to those listed above.

Many sensing modes for machine condition monitoring exist (Khodabakhshian, 2013). Temperature measurement can be used to detect increased friction in bearings that are moving into a failure mode. Dynamic monitoring of vibration signals or acoustic signals associated with rotating machines can find vibration signatures related to wear and machine life. Monitoring internal wear debris or particle contamination of lubricants is another approach. While light blockage particle sensors are available, they are typically not applied directly to off-road machines because of cost and robustness limitations. Typically, oil is sampled from the machine being monitored and analyzed in a laboratory setting, which does not lend itself to autonomous machine health awareness. However, dielectric spectroscopic sensing technology for oil contaminants shows promise for an on-line sensor to be used continuously during machine operation (Kshetri et al., 2013), and could be applied to autonomous machines. Finally, monitoring machine performance variables, such as power consumption or hydraulic pressure, and searching for anomalies in those dynamic variables shows promise as a condition monitoring approach. Craessarts et al. (2010) took this approach applying self-organizing maps and neural networks to detect failures on a New Holland combine harvester.

The application of these technologies to both autonomous agricultural and construction machines has limitations. Vibration analysis, for example, is more easily applied to rotating machinery and is not as suitable to machines involving lateral motion or limited rotational motion. Others are also better suited for more controlled machine operating environments found in factories rather than in fields or job sites. While some off-highway machine monitoring technologies exist, little has been done to more broadly monitor agricultural machine health.

Machine Control

Once an autonomous machine has awareness of its location, environment, and health, the machine control layer must next be in place. For agricultural applications, machine control is necessary to navigate the vehicle through the field and to control the implements accomplishing field operations. In construction applications, the vehicle must be navigated along paths in the job site and control the soil engaging tools such as buckets or blades or the construction process such as compacting soil or paving. Agricultural examples of machine control are presented below to provide insight in how this domain has developed machine control leading toward machine autonomy.

Navigation control of agricultural machines is highly developed and has progressed through several generations of automatic guidance technologies as applied to conventional agricultural vehicles and implements. However, for smaller, next-generation field robots, research questions exist since robotic vehicle platforms may provide additional degrees of mobility freedom, through independent four wheel steering (4WS) and four wheel drive (4WD), that can be utilized for novel navigation control strategies.

The main goal of navigation controls is to automatically guide or steer a vehicle along a path and to minimize the error between the actual trajectory that the vehicle takes and the desired path. Automatic guidance of mobile agricultural field equipment improves the productivity of many field operations by improving field efficiency and reducing operator fatigue. The idea of automatically guiding vehicles is by no means new, and relevant literature can be found from several decades back (Parish and Goering, 1970; Grovum and Zoerb, 1970; Smith et al., 1985). The launching of the Global Position System (GPS) in the early 1990's led to research

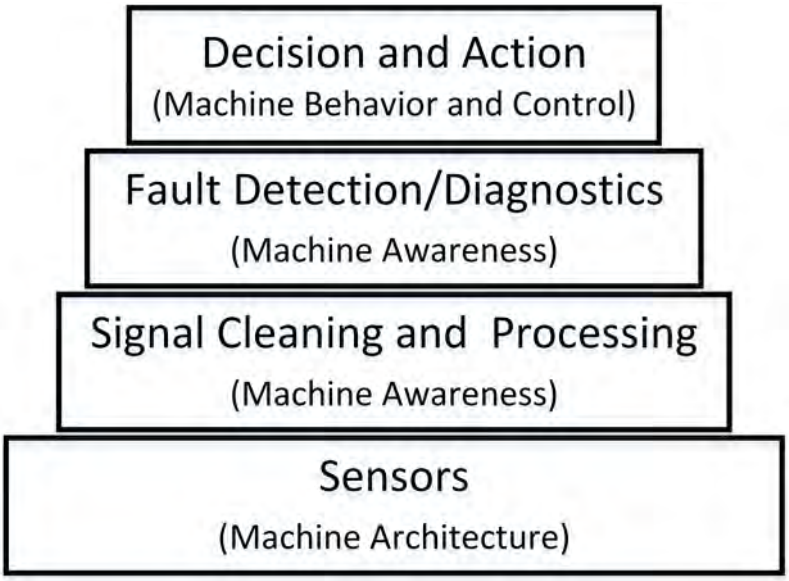

Figure 4. Machine health awareness requires several layers of technology.

investigating the use of GPS as a positioning system for automatic guidance (Larsen et al., 1994; Elkaim et al., 1997; Griepentrog et al., 2006; Burks et al., 2013). Commercialization of GPS-based automatic guidance occurred in the first decade of this century, and was adopted very quickly to become one of the most highly adopted precision agriculture automation technologies.

Agricultural robotic vehicles operate under environmental uncertainties and time-varying parameters. External factors such as soil conditions also affect vehicle dynamic characteristics. Both unpredictable internal perturbations and external disturbances create a great challenge. In their early work to develop a self-tuning navigation controller for farm tractors, Noh and Erbach (1993) used a variable forgetting factor in an adaptive steering controller based upon a minimum variance control strategy to cope with nonlinear time-varying dynamics. More recently, Gomez-Gil et al. (2011) developed two control laws: one for tracking straight lines and the other for tracking circular arcs. These control laws were shown to have global asymptotic stability with no singularity points.

Four-wheel-steering and four-wheel-drive designs provide maneuverability and traction control advantages to a field robot. Tu (2013) reported on the development of a 4WD/4WS vehicle and developed a sliding mode control-based robust navigation controller. Sliding mode control has robustness to parameter perturbations and external disturbances, making it suitable for off-road environments. Errors of 0.08 m and 0.13 m were observed for straight-line and curved trajectory tracking, respectively, in field tests (Figure 5).

Navigation control for the guidance of construction equipment has different requirements. Often 3D control is required. For grading, the blade height is controlled along with the path of the vehicle. However, there may be good cross-collaboration between agriculture and construction motivated by the example of the agricultural robotics research community. Here, the vision of autonomous systems opened up investigations into new machine forms which are feasible if a human operator is no longer required. With the new machine forms come new navigation control strategies. While this process may play out differently in the construction domain,

autonomy does open the machine form design space to the consideration of new forms that are no longer designed around an operator.

Implement control has also been implemented commercially for various agricultural machine operations. For example, in the case of liquid chemical application, chemical application rate control was first developed and commercialized in the late 1970s, upon which variable rate application systems were developed in the 1990s. Since that time, more and more aspects of machine operations have been automatically controlled.

Implement control is also available so that the burden on the operator to control implement settings can be moved to automatic control. This reduces stress and fatigue on the operator and gives the operator freedom to take on more of a supervisory role of the overall machinery system. In addition, implement control often leads to the reduction of errors in the field operation such as turning on or off the seeding at the wrong location and overlap of adjacent swaths or skips in chemical application. There are many implement control examples for field crop machines.

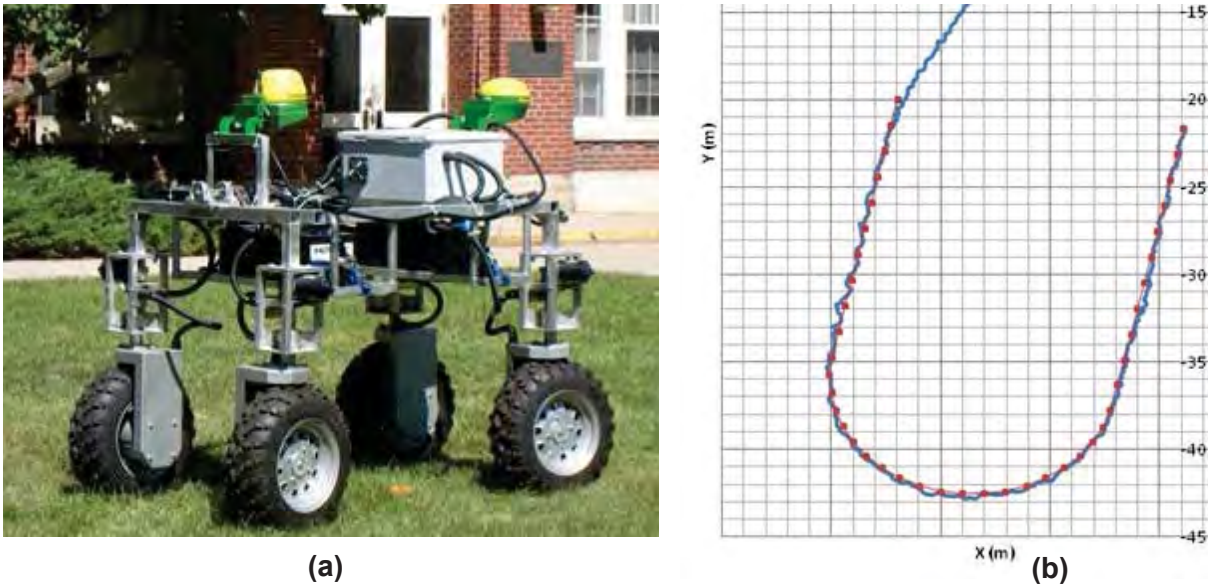

Figure 5. Robust navigation control of a small four-wheel drive/steer agricultural robot (a) tracking over a U-shaped path (b) (Source: Tu, 2013).

A widely adopted control system application in precision agriculture is automatic section-control, which ranks second only to automatic guidance technology in terms of its commercial success. To implement section control, the width of a field sprayer boom is divided into multiple sections, with individual sections controlled in an on/off fashion. Boom section control can enable more efficient spraying by reducing pass-to-pass overlap as well as preventing application to off-target areas. Each section is controlled independently of the rest of the system – based on the section's location within the field or canopy. These systems rely on a task computer to control the desired state of each section based on the section's location within the field, taken from accompanying sensors and/or on-board maps. A main benefit of using the boom section-control technology for a sprayer is the reduction in the of chemical application overlap. The savings realized through the adoption of section-control technology is mainly based on the number of control sections and the field shape (Luck et al., 2011).

The path to agricultural machine autonomy has occurred in a series of implement control technologies assisting human operators to accomplish a field operation with great work quality or higher productivity with lower operator fatigue. Similar applications can also be found in construction machines such as machine control for intelligent compaction.

Machine Behavior

Machine behavior is the highest layer of the design framework and includes mission planning and machine supervision. For a robot to be autonomous, it must exhibit behaviors similar to those observed of humans. Some of these behaviors include planning by determining the best plan of action to achieve a particular goal and supervision by monitoring the work environment and making modifications to the planned actions based on new information.

Blackmore et al. (2007) promoted a structure for defining the behaviors field robots need to perform agricultural operations autonomously. At the highest level, a field operation is the action that a robot will carry out to meet the needs of a crops' cultural practices. Within an operation, certain tasks must be carried out – either deterministic or reactive. Deterministic tasks can be planned before the operation starts, are goal-oriented to achieve the objective of the operation, and can be optimized to best draw on the resources available. Reactive tasks are foreseen responses to uncertain situations that may occur during the operation. They are captured in terms of behaviors that the robot should do in response to new situations. For example, when an unknown obstacle is perceived in the current path of the robot, the robot should behave according to the type of obstacle. If a tree is perceived in the path, the robot could alter its path to go around it. If an animal is detected in the path, the robot might wait until it moves away, or produce stimuli to scare the animal away, or stop and seek guidance from a human supervisor. An example deterministic task is field coverage where the robot covers a field by navigating through a predetermined coverage path. Several examples of autonomous machine behavior research in the agricultural domain are presented below.

Optimal Path Planning

For agricultural field operations, the goal is to cover the entire field with that operation, such as tillage or planting. Determining the best path direction is the main goal of coverage path planning. Whole fields can usually be covered by straight parallel paths with alternating directions parallel to the optimal coverage path direction for each given field. Several approaches to optimal path direction discovery have been investigated. The time and travel over field surfaces associated with field operations should be minimized within constraints associated with machine characteristics, field topography, and field operation-specifics characteristics. To achieve these goals, optimized coverage path planning algorithms are needed for both planar surfaces and fields with three dimensional terrain features.

Optimized Coverage Path Planning on Planar Surfaces

Research has been done on coverage path planning of planar surfaces, but results have some limitations in being applied to agricultural fields. Following the longest edge of the field is a simple strategy, but it is only suitable for fields with simple convex shapes such as a rectangles. Fabret et al. (2001) framed the coverage path planning problem as a Traveling Salesman Problem (TSP), and first chose a "steering edge" that provided the direction to guide successive swaths. In the field headland, characteristic points were then collected. Those points were connected by lines in the steering direction via an associated graph constructed by a TSP solver.

Field boundary irregularities must be considered for general coverage path planning solutions. Field decomposition has potential to further improve the efficiency of field operations before

determining the best path directions in fields, particularly those with irregular field boundaries. The trapezoidal decomposition method has been investigated as an approach to field decomposition (Berg et al., 1999; Choset et al., 1997). Oksanen and Visala (2009) explored greedy search algorithms to find coverage paths of planar (2D) field surfaces. Their search algorithm iteratively found the optimal trapezoidal field decomposition and path direction using a split and merge strategy.

Jin and Tang (2010) developed an algorithm that optimally decomposed planar fields and planned optimized operational patterns (Figure 6). Their algorithm used a geometric model which represented the coverage path planning problem. Their algorithm produced better solutions than farmers' solutions and showed good potential to improve field equipment efficiency on planar fields.

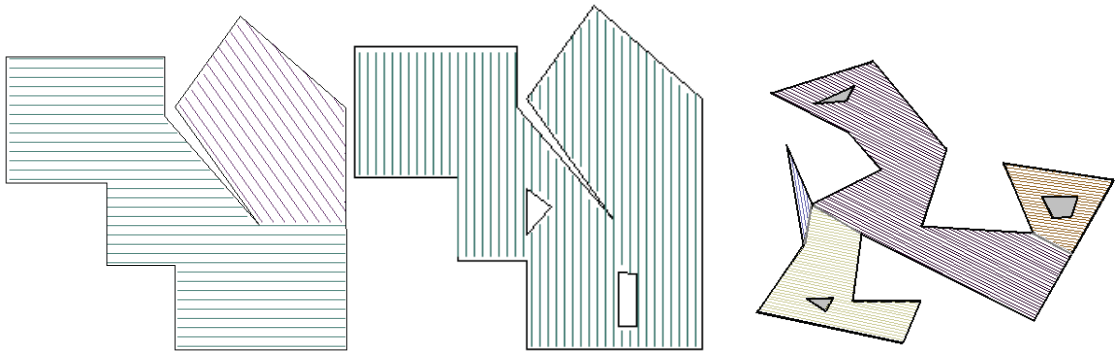

Figure 6. Example results from an optimized coverage path planning algorithm for planar field surface. The inner polygons indicate non-traversable obstacles (Jin and Tang, 2006, 2010).

Optimized Coverage Path Planning on 3D Terrain

More factors must be considered when optimizing the coverage path over terrain with three-dimensional (3D) topographic features. The main factors are headland turning, soil erosion, and skipped area. Jin and Tang (2011) approached the problem by first developing an analytical 3D terrain model with B-Splines surface fits to facilitate the computation of various path costs. Then they analyzed different coverage costs on 3D terrains and developed methods to quantify soil erosion and curving path costs of particular coverage path solutions. Similar to the planar field approaches, they developed a terrain decomposition and classification algorithm to divide a field into sub-regions with similar field attributes and comparatively smooth boundaries. The most appropriate path direction of each region minimized coverage cost. A "Seed Curve" search algorithm was successfully developed and applied to several practical farm fields with various topographic features (Figure 7).

Optimized Vehicle Routing

After optimal field decomposition and coverage path planning, the vehicle route, which is the sequence of an agricultural vehicle following individual paths, can be further optimized to minimize the distance traveled in headland turning and improve field efficiency when performing an agricultural operation. Bochtis et al. (2009) developed a mission planner based on an algorithmic approach where field coverage planning was transformed and formulated, as a vehicle routing problem (VRP), which was formulated as an integer programming problem. Through this approach, non-working travel distance was reduced by up to 50% compared to the conventional non-optimized method. They also incorporated different operational requirements

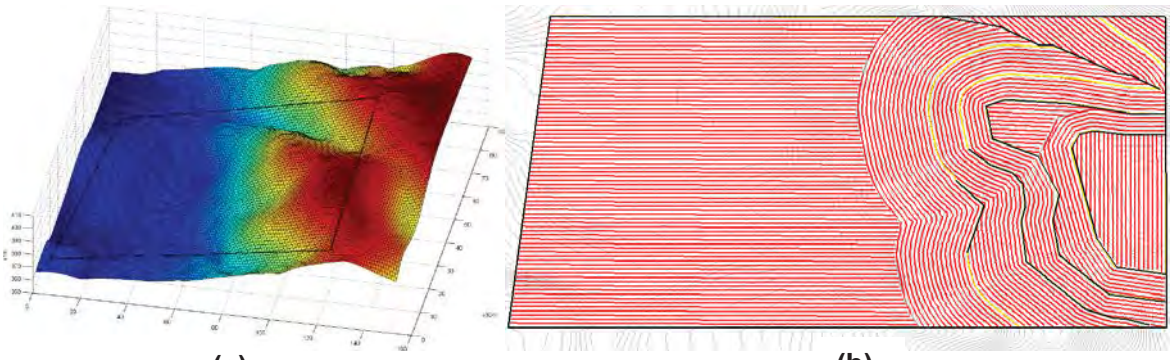

(a) (b)

Figure 7. Elevation model for a field where terraces and valleys exist (a) along with the results (b) of a path planning algorithm designed for optimized coverage of a 3D terrain (Jin and Tang, 2011).

and produced a different field pattern for each particular operation, which were optimal in non-working travel distance (Figure 8).

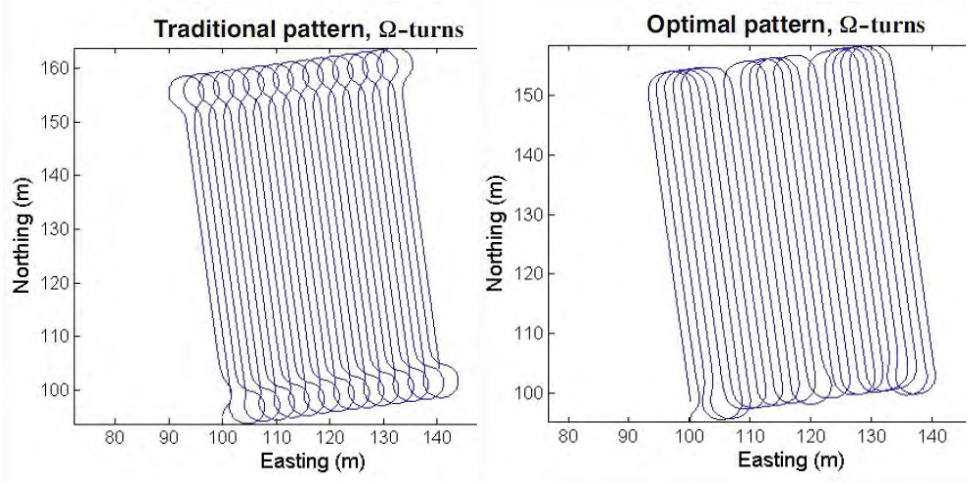

(a) (b)

Figure 8. Differences between traditional turning pattern (a) and optimized turning pattern (b) from an optimized vehicle routing algorithm for a mowing operation (Bochtis et al., 2009).

CONCLUSIONS

A design framework for autonomous machines was presented in this paper. While the framework has emerged from the agricultural domain, its generality allows a broader application to other domains. The layers of machine architecture, awareness, control, and behavior will need to be developed for autonomous machines in any domain.

ACKNOWLEDGMENTS

This research was supported by Hatch Act and State of Iowa funds, and this paper is a paper of the Iowa Agriculture and Home Economics Experiment Station, Ames, Iowa.

REFERENCES

Berg, M. D., M. V. Kreveld, M. Overmars and O. Schwarzkopf (2000). *Computational Geometry. 2nd ed*. Springer, New York, NY, USA.

Blackmore, B. S., S. Fountas, and H. Have (2002). Proposed system architecture to enable behavioral control of an autonomous tractor. In: Zhang, Q. (ed.), *Automation Technology for Off-Road Equipment: Proceedings of the 2002 Conference,* ASAE, St. Joseph, Mich,, USA.

Blackmore, B. S., S. Fountas, S. Vougioukas, L. Tang, C. G. Sørensen, and R. Jørgensen (2007). Decomposition of Agricultural Tasks into Robotic Behaviours. *Agricultural Engineering International: the CIGR Ejournal*, 9.

Bochtis, D. D., S. G. Vougioukas, and H. W. Griepentrog (2009). A mission planner for an autonomous tractor. *Transactions of the ASABE*, 52: 1429-1440.

Burks, T., D. Bulanon, K. S. You, Z. Ni, and A. Sundararajan. (2013). Orchard and vineyard production automation. In: Zhang, Q. and F.J. Pierce (eds), *Agricultural Automation: Fundamentals and Practices*, CRC Press, Boca Raton, FL, USA. pp. 149-204.

Choset, H. and P. Pignon (1997). Coverage path planning: the boustrophedon cellular decomposition. In: *Proceedings of International Conference on Field and Service Robotics,* Canberra, Australia.

Craessaerts, G., J. De Baerdemaeker, and W. Saeys (2010). Fault diagnostic systems for agricultural machinery. *Biosystems Engineering*, 106: 26-36.

Dumpert, J. (2004). *Hardware and software design for a system of autonomous highway safety markers* (Doctoral dissertation, University of Nebraska).

Elkaim, G., M. O'Conner, T. Bell, and B. Parkinson (1997). System Identification and Robust Control of Farm Vehicles Using CDGPS. *Proceedings of ION GPS,* 10:1415-1426.

Fabret, S., P. Soueres, M. Taix and L. Cordessed (2001). Farmwork path planning for field coverage with minimum overlapping. In: *Proceedings of 2001 8th IEEE International Conference*, IEEE, Piscataway, New Jersey, USA.

Gomez-Gil, J., J. C. Ryu, S. Alonso-Garcia and S. K. Agrawal (2011). Development and validation of globally asymptotically stable control laws for automatic tractor guidance. *Applied Engineering in Agriculture*, 27: 1099-1108.

Griepentrog, H. W., B.S. Blackmore, and S. G. Vougioukas (2006). Positioning and Navigation. In: Axel Munack (ed), *CIGR Handbook of Agricultural Engineering, Vol. VI Information Technology*, ASABE, St. Joseph, Mich. USA. pp. 195-204.

Grovum, M. A. and G. C. Zoerb (1970). An automatic guidance system for farm tractors. *Transactions of the ASAE* 13: 565 -576.

Han, S., Steward, B. L., and L. Tang. (2015). Intelligent Agricultural Machinery and Field Robots. In Precision Agriculture Technology for Crop Farming, ed. Zhang, Q. CRC Press.

Jin, J. and L. Tang (2010). Optimal coverage path planning for arable farming on 2D surfaces, *Transactions of the ASABE*, 53: 283-295.

Jin, J. and L. Tang (2011). Coverage path planning on three-dimensional terrain for arable farming. *Journal of Field Robotics*, 28: 424-440.

Jensen, K., M. Larsen, S. H. Nielsen, L. B. Larsen, K. S. Olsen, and R. N. Jørgensen (2014). Towards an open software platform for field robots in precision agriculture. *Robotics,* 3: 207-234.

Khodabakhshian, R. (2013). Maintenance management of tractors and agricultural machinery: Preventive maintenance systems. *Agricultural Engineering International: CIGR Journal*, 15: 147-159.

Kramer, J., and M. Scheutz (2007). Development environments for autonomous mobile robots: A survey. *Autonomous Robots*, 22: 101-132.

Kshetri, S., B. L. Steward, and S. J. Birrell (2014). Dielectric Spectroscopic Sensor for Particle Contaminant Detection in Hydraulic Fluids. *ASABE Paper Number 1914249,* ASABE, St. Joseph, Mich. USA.

Larson, W. E., G. A. Nielsen, and D. A. Tyler (1994). Precision navigation with GPS. *Computers and Electronics in Agriculture,* 11: 85-95.

Luck, J.D., R.S. Zandonadi, and S.A. Shearer (2011b). A case study to evaluate field shape factors for estimating overlap errors with manual and automatic section control. *Transactions of the ASABE* 54: 1237-1243.

Noh, K-M. and D. C. Erbach. (1993). Self-tuning controller for farm tractor guidance. *Transactions of the ASAE* 36: 1583-1594.

Oksanen, T., and A. Visala. (2009). Coverage path planning algorithms for agricultural field machines. *Journal of Field Robotics*, 26: 651-668.

Parish, R. L., and C. E. Goering (1970). Developing an automatic steering system for a hydrostatic vehicle. *Transactions of the ASAE*, 13: 523–527.

Pedersen, S. M., S. Fountas, H. Have, and B. S. Blackmore (2006). Agricultural robots – system analysis and economic feasibility. *Precision Agriculture*, 7:295-308.

Quigley, M., K. Conley, B.Gerkey, J. Faust, T. Foote, J. Leibs, R. Wheeler, and A.Y. Ng (2009). ROS: an open-source Robot Operating System. In: *ICRA Workshop on Open Source Software*, 3: 5.

ROS (2015). *ROS Core Components*. Accessed at www.ros.org/core-components. Retrieved on January 1, 2015.

Rossel, R. V., Adamchuk, V. I., Sudduth, K. A., McKenzie, N. J., & Lobsey, C. (2011). Proximal soil sensing: an effective approach for soil measurements in space and time. *Advances in Agronomy*, 113: 237-282.

Rowe S. and C. Wagner (2008). *An Introduction to the Joint Architecture for Unmanned Systems (JAUS)*. Technical Report. Cybernet Systems Corporation, Ann Arbor, Mich. USA. Accessed at www.openskies.net/papers/07F-SIW-089%20Introduction%20to%20JAUS.pdf. Retreived on Jan. 31, 2015.

Toledo, O. M., B. L. Steward, L. Tang, and J. Gai (2014). Techno-economic analysis of future precision field robots. *ASABE Paper No. 141903313,* ASABE, St. Joseph, Mich. USA.

Tu, X. (2013). *Robust Navigation Control and Headland Turning Optimization of agricultural vehicles.* Graduate Theses and Dissertation. Iowa State University, Ames, Iowa, USA.

Singh, S. (1997). The State of the Art in Automation of Earthmoving. *ASCE Journal of Aerospace Engineering*, 10: 179-188.

Singh, S. (2002). State of the art in automation of earthmoving, 2002. Proceedings of the Workshop on Advanced Geomechatronics.

Shi, J., Goddard, S., Lal, A., Dumpert, J., & Farritor, S. (2005). Global Control of Robotic Highway Safety Markers: A Real-time Solution. *Real-Time Systems*, 29, 183-204.

Smith, L. A., R. L. Schafer, and R. E. Young (1985). Control algorithms for tractor-implement guidance. *Transactions of the ASAE* 28: 415-419.

Torrie, M. W., D. L. Cripps, and J. P. Swensen. (2002). Joint Architecture for Unmanned Ground Systems (JAUGS) Applied to Autonomous Agricultural Vehicles. In Zhang, Q. (ed.), *Automation Technology for Off-Road Equipment: Proceedings of the 2002 Conference,* ASAE, St. Joseph, Mich,, USA. pp. 1-12

Discrete Element Modelling (DEM) For Earthmoving Equipment Design and Analysis: Opportunities and Challenges

Mehari Tekeste, Assistant Professor
Department of Agricultural and Biosystems Engineering
Iowa State University
2356 Elings Hall
Ames, Iowa, 50011
mtekeste@iastate.edu

ABSTRACT

Simulation of granular materials (soil, rocks) interaction with earthmoving machines provides opportunities to accelerate new equipment design and improve efficiency of earthmoving machine performances. Discrete Element Modelling (DEM) has a strong potential to model soil and rocks bulk behavior in response to forces applied through interaction with machinery. Numerical representation of granular materials and methodology to validate and verify constitutive micro-mechanical models in DEM will be presented. In addition, how DEM codes can be integrated to CAE tools such as multibody dynamics will also be discussed. A case study of tillage bar-soil interaction was modeled in EDEM to predict tillage draft force and soil failure zone in front of tool moving at 2.68-m/sec and depth of 102-mm. The draft force and soil failure zone was predicted at 10% and 20% error from laboratory measured data.

Key words: soil (geomaterials)—discrete element modelling—off-road machinery—calibration

BACKGROUND: SIMULATION BASED DESIGN USING DISCRETE ELEMENT MODELLING

Earthmoving machinery product development and verification tests involve interaction of machine equipment with granular materials (soil, biomass and rock). The geomaterial properties and their conditions impact the equipment performance in terms of productivity, efficiency and durability. The traditional and iterative product development cycle of “Design--Physically build prototype--Field test” is laborious, costly and time demanding. Virtual engineering tools have potential to accelerate product design engineering and reduce field testing. Automation of earthmoving system modelling architect (Cannon and Singh, 2002) will need a geomaterial-tool interaction model component to simulate earthmoving equipment trajectory motion. Simulation of soil-tool interaction is essential for virtual earth-moving product development and automation of earth moving operations.

Simulation based tools consist of generating CAD geometry surface mesh, pre-processing, material model, solver, post-processing and data analytics for engineering decision support. Modelling geomaterial - tool interaction will require versatile material models, quick and easy testing methods to generate data for model parameters calibration and numerical tool to solve geomaterial-tool interaction responses. Generally there are two broad categories of geomaterial-tool interaction problems 1) load loosening processes for instance in tillage tools, soil flow from bulldozer blades, soil fill in loader buckets; and 2) load bearing process in soil to vehicle tractive devices interactions where soil supports vehicle loads and helps generate

Proceedings of the 2015 Conference on Autonomous and Robotic Construction of Infrastructure, Ames, Iowa.

traction. The desired engineering objectives are generally to reduce energy expenditure during cutting and tillage processes, maximize soil fill on buckets, easy soil flow from crawler blades, maximize traction and optimal soil density for growing crops.

Discrete Element Modelling (DEM) has the potential to simulate soil-tool interaction and could also be integrated in co-simulation with other systems modelling tools such as Finite Element Analysis (FEA), Multi-Body Dynamics (MBD) and Computational Fluid Dynamics (CFD). DEM formulation comprises numerical representation of the particle shape and size, assembly of particles, constitutive micro-mechanics contact laws that defines force vs. displacement relationships; and every time step contact detection and explicit numerical integration governed by Newton's law of motion (Cundall and Strack, 1997). Details in contact laws and their formulation are available in literature (Walton and Braun, 1986; Luding, 2008; Cleary, 2010; EDEM, 2011). The DEM contact laws originated based on Hertizian contact theory and now there are advanced contact models that defines the relationship between forces and displacement using material normal and tangential stiffness, coulomb friction coefficient, damping coefficient, rolling resistance coefficient, cohesion/adhesion and bond parameters.

Researchers have shown the predictive capability of DEM to model behaviour of granular materials since late 70's after Cundall and Strack (1979). Some of the works related to earthmoving include DEM modelling of wide cutting blade to soil interaction on scaled experimental box to predict forces on crawler blades and soil flow in front of the cutting blade (Shmulevich et al., 2007); simulation of hydraulic excavator digging process using confining stress dependent DEM cohesive soil model (Obermayr et al., 2014); and DEM modelling of soft ground cutterhead (4.2-m in diameter) predicting torque performance for different Tunnel Boring Machine (TBM) cutterhead designs (Mongillo and Alsaleh, 2011).

OPPORTUNITIES AND CHALLENGES FOR USE OF DEM IN EARTHMOVING INDUSTRY

In theory DEM, a particle based modelling technique, is able to simulate particles interaction with earth moving equipment and makes it ideal fit to integrate the tool into the engineering work flow for product design and performance. DEM has shown to be a proven research and development tool in manufacturing and process industry (Favier, 2011) especially where particles are non-cohesive, resemble to spherical shape and the size of engineering problem are manageable using desktop multi-core computers. With the continuous increase in computing power and efficiency in parallel computing, DEM has started to become a useful tool for large scale applications in mining and construction industries (Cleary, 2010; Mongillo and Alsaleh, 2011).

This paper illustrates potential opportunities and challenges with DEM for earthmoving machine virtual protyping construction equipment and automation process. The discussion in this paper may apply to the interactions of crawler blade (over 3-m X 3-m blade width X blade height for instance John Deere 1050K and CAT D9), bucket (with loader capacity over 6 M^3 (Yd^3) for instance John Deere 844 and CAT 980) and ripper tine with geomaterials ranging from clay-sized (less than 0.002-mm) to gravel (75-mm).

The challenges with utilizing DEM arise from the difficulty with particle based approximation of geomaterial and its dynamic behaviour. Geomaterials have spatial-temporal variations in conditions (wet to dry), wide range of particle sizes (clay to gravel size) and their response to loading have stochastic bulk response behaviour. Approximation of these realistic geomaterial type, size and conditions using DEM spheres and solving bulk geomaterial to large size

machine interaction using micro-mechanics contact laws are either computationally prohibitive or impossible to fit within reasonable engineering work flow. DEM based engineering analysis in earth moving industry thus demands a methodology that is adaptive towards the desired systems engineering, existing DEM code requirement and simulation process that will provide industry value added results.

DEM USE FOR ENGINEERING DESIGN ANALYSIS

DEM simulation work flow for simple geometry motion, granular shape close to spheres and small number of particles is fairly straight forward. For large scale industrial applications that require DEM integrated into earth moving product development cycle and transient coupling with other methods such as FEA, MBD and CFD for systems modelling, DEM simulation work flow can be looked as a component of system engineering. The system layers proposed in Figure-1 may apply to earth moving simulation based design and automation. This may capture the requirements from the application, simulation and granular mechanics know-how to systematically define DEM shape and size approximation, calibrate DEM particle model and simulation of application with reduced uncertainty and controlled variance for design and system optimization.

(1) Defining systems requirement and setup for material model calibration • Design and systems application requirements • Material boundary condition • Experimental test development • Upscale benchmark test development
(2) Material model calibration and simplification for application simulation • Material model properties fit for the defined requirement • DEM advance physics and co-simulation • Computing efficiency (upscaling, simplification of geometry boundary)
(3) Application product simulation • Accelerate virtual product development • Accelerate computing within defined accuracy • Data analytics and optimization

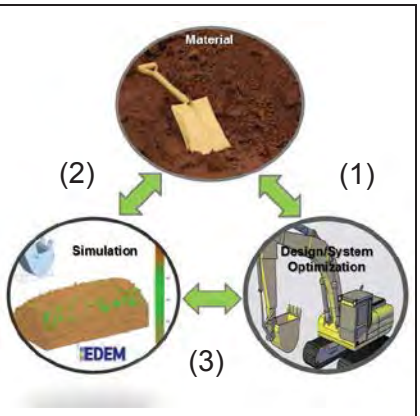

Figure 1. DEM for simulation in systems engineering

DEM Material Properties Development

The major steps in DEM particle model development consists 1) define the shape and particle size representation; 2) identify micro-mechanics contact model that captures the expected geomaterial behaviour (elastic, plastic, cohesive and non-cohesive); and 3) determine the material model properties.

Shape and Particle Size Approximation

Shape and particle size approximation have strong influence on the dynamics of granular system and computational effort. The shape of DEM assembly of particles affect packing of particles (void ratio), shear strength, angle of repose and discharge from hoppers and relative particle velocity on conveying (Cleary, 2010; Lu et al., 2015).

In DEM codes particle shape is approximated using spheres, glued (clumped) spheres and non-spherical particles (for instance polyhedron, ellipsoids). Spherical DEM particle representation

has benefit in terms of relatively easier contact detection algorithm, simpler overlap based force-displacement calculation and reduced computational effort. According to Cleary (2010), the computational cost with superquadrices was 2 to 3 times compared with spheres. Commercial DEM codes such as EDEM from DEM solutions UK and Particle Flow Code (*PFC*) from Itasca Consulting Group, Inc have overlap spherical capability and rolling resistance DEM models to numerically reproduce mechanical interlocking effect on dynamics of granular systems. Lee et al. (2012) used non-spherical primitive shape from polyhedral DEM code. Hohner et al. (2015) studied various non-spherical particle shape approximation types (polyhedra, multi-sphere cluster, superellipsoids) on hopper discharge and found out that shear strength of the particle bed and discharge from hopper were affected by sphericity and aspect ratio but less on fine scale resolutions of shape surface approximation. The choice of spherical or non-spherical shape approximation depends on user know how on engineering problem, dimensional measured properties of the geomaterial, bulk material behaviours, affordable computational effort and availability of shape library in the DEM code. For most of natural geomaterials (cohesive and non-cohesive soils) expect gravel, measurement of geometric shape parameters such as sphericity, angularity, aspect ratio and surface roughness are difficult to obtain and easily reproduce in DEM primitive shapes. For non-spherical and angular materials that exhibit mechanical interlocking and affect their initial packing density, it is important to make significant effort to use non-spherical DEM shape approximation using clumped sphere, non-spherical primitive shapes or rolling resistance contact models.

Similar to shape representations, particle size approximation to real geomaterial size distribution also influences DEM bulk material response behaviour and computation effort. The smallest DEM particle size derives the explicit time step value for DEM calculation. Geomaterial DEM modelling, it is computationally prohibitive to match equivalent clay, silt and sand size fractions.

DEM particle size scaling is thus necessary and can be done using linear scaling factor of DEM mean particle size, particle size distribution or ratio number of particle to geometry (wall) dimension. Lee et al. (2012) applied DEM particle size scaling by a factor of 10 times larger than the experimentally measured sub-angular uniformly graded fine sand distribution and normalized by D_{50}. DEM simulation of triaxial compression with polyhedral particle shape, Lee et al. (2012) successfully reproduced initial packing density and stress-strain of undrained triaxial compression sand soil test.

Limited studies are available that investigate various DEM shape approximations and particle scaling methodology and how they relate to achieve the desired quality of dynamics of bulk material response behaviour and computational effort. Similarly studies are needed on upscaling methodology from small size simulation used for calibration of DEM model parameters, shape and size to simulation of large size earth moving applications.

Experimental test and calibration methodology

Simulation of bulk (macro) geomaterial behaviour interaction with equipment using DEM assembly of spherical or non-spherical particles and micro-mechanics laws can only be achieved through calibration of the DEM parameters with measured response variables. Methodology to generate DEM material properties fit for the approximation of bulk material response to equipment interaction within relatively short time is often more relevant than to measure individual granular particle to particle or particle to geometry model parameters. As shown in Figure -1, the steps for system requirement and material properties development will help to identify experimental tests and measured response variables for model calibration.

Soil mechanical properties (stress-strain, angle of internal friction, cohesion) obtained from geotechnical ASTM standard tests (tri-axial, shear and others) can be good candidates. Other experimental tests that reflect in-situ geomaterial behaviour and allow to measure multiple dependent variables such as angle of repose, deformation, torque and forces will provide enhanced accuracy for wider granular dynamics behaviour.

DEM calibration process involves first reproducing initial packing density (void ratio) of particle assembly with estimated initial model parameters. DEM virtual experiments are then conducted taking the model parameters as independent variables and response properties similar to the experimental test as dependent variables. Besides to the material model parameters (stiffness and coefficients), shape and size parameters can be added as independent variables during calibration process. Reducing the number of model parameters for calibration is always helpful. For instance in quasi-static engineering systems, determination of coefficient of restitution may be less important than shear stiffness and friction coefficients. In dynamic system application for instance in grind milling and transfer chutes where system performance is dependent on collision energy losses characterization, coefficient of restitution is important. Sensitivity and optimization scheme will then be deployed to generate calibrated DEM particle model and properties to be used for application simulation.

Simulation of Application

Upscaling and computational accuracy

The main engineering value from DEM modelling is obtained from simulation of industrial application using the calibrated DEM particle model. Depending on the simulation domain of industrial application, the particle size or distribution used in the calibration process may need scaling before using it for application simulation. Upscaling DEM particle model into large size simulation will need know-how on particle: geometry system similarity and scale-invariance of contact models (Feng et al., 2009). Interpretation of DEM results from virtual equipment design changes may not necessarily eliminate the uncertainty/stochastic natural geomaterial behaviour and their associated equipment performance. Having DEM results with acceptable variance and showed value-added trends of improved performance from virtual equipment changes can be considered successful outcome.

Some engineering design and analysis may require coupling with CFD, FEM and MBD. For earth-moving application, coupling of DEM with MBD and FEM will be more applicable to transfer transient loads from geomaterials into rigid or flexible multibody mechanical or hydraulic driven systems for equipment (excavator buckets, blade) kinematics motion control and structural stress analysis. DEM coupling with other tools will involve surface element position mapping, interpolation and synchronization of sampling time (Favier, 2011) that will affect the stability and accuracy. For automation of earth-moving operation with soil-tool interaction in the

loop with actuator-control algorithms for equipment trajectory as proposed in Cannon and Singh (2000) can be implemented using DEM coupling technique.

Predicting Tillage Force

Simple tillage-soil interaction was modelled in EDEM Academic (EDEM, 2011) to predict forces and soil failure. EDEM model was developed with Hertz-Mindlin (with no slip) contact model to replicate the tillage tool bar from linear soil bin test in Becker (2008). The test parameters from Becker (2008) are shown in Table-1.

Table 1. Tool dimension and test parameters (Becker, 2008)

Parameters	Dimension Value
Geometer	42
Width (mm)	50.8
Length (mm)	203.2
Thickness (mm)	12.7
Tool depth (mm)	102
Tool velocity (mm/sec)	268
Density (kg/m^3)	1760
Moisture content (%, d.b.)	9.15

Initial Feasibility Simulation using 5-mm and 10-mm particle size

Assembly of single sphere particle and two sizes (5-mm and 10-mm particle diameter) in simulation soil box (length = 790-mm, width = 265-mm; and depth = 408-mm) in EDEM 2.7. The total number in the soil box were 274494 and 36432 with 5-mm and 10-mm, respectively. Baseline properties shown in Table-2 were used for DEM parameters of particle size sensitive. Steel geometry was used for the tool and the soil box. The values for coefficient of static friction was estimated from angle of internal friction coefficient of soil composition and bulk density reported in Becker (2008). The soil-tool interaction parameter was assumed as 10% lower than the soil:soil interaction. The other interaction parameters were best guess and quick sensitivity EDEM runs (not reported). Particle were generated using EDEM factory creator filling the soil box and compressed at 0.02m/sec to obtain stable and maximum bulk density. The bulk density after relaxed DEM soil particle assembly for 5-mm and 10-mm was 1700 kg/m^3 (3% lower than the measured bulk density). Simulation was run for 0.19-sec with time step of 1.0e-06 sec using 12- CPU cores. Output variables tool forces (horizontal and vertical) and velocity to predict soil failure zone in front of tillage tool were sampled at 0.01-sec interval.

Table 2. Base line DEM properties for Hertz-Mendlin (No Slip) (EDEM, 2011)

Poisson's ratio	0.3
Shear modulus (Pa)	1e+06
Density (kg/m^3)	2650
Soil:Soil Interaction	
Coefficient of restitution	0.01
Coefficient of static friction	0.36
Coefficient of rolling friction	0.4
Soil:Steel Interaction	
Coefficient of restitution	0.01
Coefficient of static friction	0.33
Coefficient of rolling friction	0.2

The predicted horizontal (draft) force from 10-mm DEM particle was higher and closer to the lab measured (Becker, 2008) draft forces (Mean = 416 N and Standard deviation = 36.9 N) than the 5-mm DEM particle. DEM elapsed computational time with 5-mm was 1.5 times greater than 10-mm particle size. Thus to understand the sensitivity of Hertz-Mendlin contact model parameters to predict force and soil failure flow, 10-mm particle size DEM model was used.

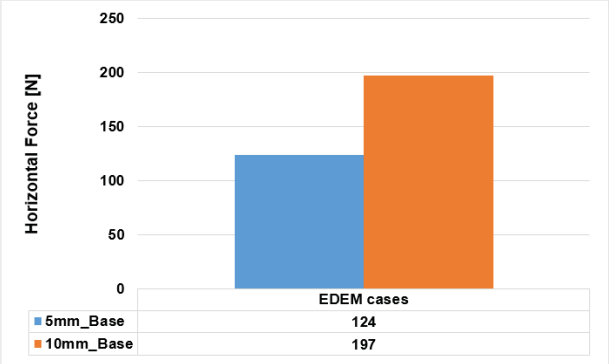

Figure 2. DEM predicted Horizontal (draft) force for the rigid flat bar for 5-mm and 10-mm. The lab measured draft force was 416 N (Standard deviation = 36.9 N).

Sensitivity of Forces and Soil Failure to DEM model parameters

For the sensitivity study of soil:soil and soil:steel interaction parameters, four EDEM runs represented as base line; HH = High:High; MM= Medium:Medium; and ML = Medium:Low (Table-3) were simulated. The material parameters of density, poisson's ratio and shear modulus; and coefficient of restitution for the soil:soil and soil:steel were kept constant. Assumption was made the change in coefficient of restitution may not influence the soil flow in front of tool traveling at 2.68 m/sec.

Table 3. DEM parameters used for sensitivity study (Base line was considered as lowest value; HH = High High; MM= Medium Medium; and ML = Medium Low showed ranking for soil:soil and soil:steel interaction ranges).

	Sensitivity Classes for EDEM runs			
DEM Parameters	Base	HH	MM	ML
Soil:soil Coefficient of static friction	0.36	0.90	0.60	0.60
Soil:soil Coefficient of rolling friction	0.40	0.90	0.60	0.60
Soil:steel Coefficient of static friction	0.33	0.90	0.60	0.30
Soil:steel Coefficient of rolling friction	0.20	0.90	0.60	0.30

The results for predicting horizontal force (draft) and soil failure from tool bar interaction with soil are shown in Figure 3. Medium Low (ML) values DEM interaction parameters showed good prediction (10% error) in horizontal force compared to the lab measured value. The soil failure zone infront of the tool were better predicted with the base line properties at 20% error. The DEM parameters providing better estimate for force prediction and soil flow are in different ranges especially on the soil:soil particle interaction parameters. Further study is needed to optimize DEM parameters for two conflicting objective functions. The shear modulus may affect the force prediction and should be considered in next optimization steps.

With the sensitivity study of DEM tool-soil interactions, bulk tool-soil interaction response variables from simple tests can be used to obtain better estimate range of combination of DEM parameters. The simple test used in this experiment captures soil response behaviour similar to cultivator sweep (shovel) interaction for tillage operations.

This exercises demonstrates implementation of the value of adaptive system approach and know-how of the engineering problem for calibration DEM parameters instead of depending on individual DEM parameters measurement.

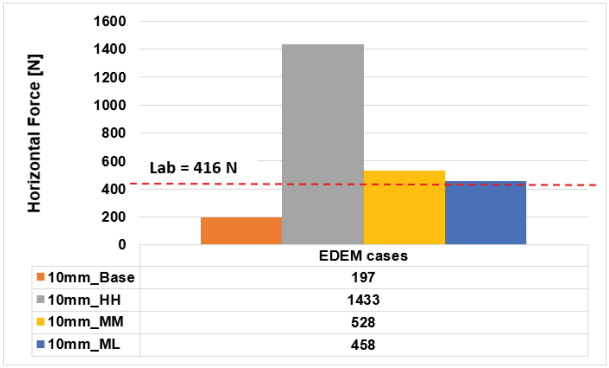

(A) DEM predicted Horizontal (draft) force

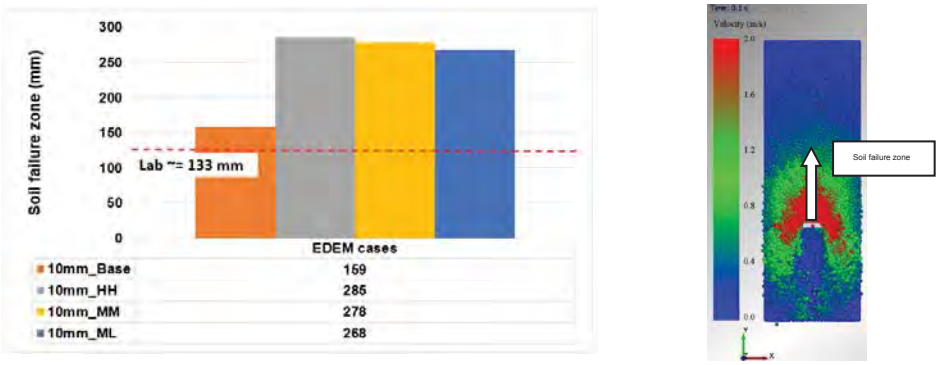

(B) DEM predicted soil failure zone

Figure 3. DEM predicted Horizontal (draft) force and soil failure zone from sensitivity model parameters of 10-mm particle. The lab measured draft force was 416 N (Standard deviation = 36.9 N) and soil failure zone was 133-mm.

CONCLUSION AND FUTURE STUDIES

- DEM based simulation of earth-moving equipment interaction with goematerials has strong potential for off-road machinery industry to support virtual prototyping in design and process improvements.

- Effective utilization of DEM for earth-moving requires adaptive system approach to improve the inherent limitations of DEM in terms of trade-off in shape approximation and particle size definitions versus real geomaterials; calibration methodology from micro-

mechanics to macro-experimental mechanical behaviour; and scaling principles in mechanical, geometry and particle size from simple tests to application simulation sizes.

- Simulation of tillage bar-soil interaction was run in EDEM and showed the sensitivity of Hertz-Mendlin contact model parameters for predicting horizontal tillage tool force and soil failure zones. This demonstrates the value of adaptive system approach in utilizing DEM model for tool-soil interaction problems.

- Future research studies are needed on “realistic” geomaterial shape approximate vs. accuracy of dynamic granular behaviour, development of material tests fit for DEM calibration purposes, robust calibration and optimization methodology for shape, particle size and material models; and methods to evaluate application simulation output uncertainty and variance for earth-moving virtual product development.

REFERENCES

Barker, M.E. (2008). Predicting loads on ground engaging tillage tools using computational fluid dynamics. PhD. Dissertation. Iowa State University.

Cannon, H. and S. Singh (2000). Models for Automated Earthmoving, In P. Corke and J. Trevelyan, Editors, Experimental Robotics VI, Lecture Notes in Control and Information Sciences, Springer Verlag, Sydney. 183-192.

Cleary, P.W. (2010). DEM prediction of industrial and geophysical particle flows. Particuology 10:106-118.

Cundall, P.A. and O.D.L. Strack (1979). A discrete numerical model for granular assemblies. Geotechnique 29:47-65.

EDEM (2011). EDEM theory reference guide. Edinburgh, UK: DEM Solutions.

Feng Y.T., K. Han, D.R.J. Owen and J. Loughran (2009). On upscaling of discrete element models: similarity principles", Engineering Computations. 26 (6): 599 - 609

John Favier (2011). Using DEM for Engineering Design and Analysis: Opportunities and Challenges. 6th International Conference on Discrete Element Modelling (DEM 6) Proceeding. Golden, Colorda, USA. Pp 36-4.

Hohner D, S. Wirtz and V. Sherer (2015). A study on the influence of particle shape on the mechanical interactions of granular media in a hopper using the Discrete Element Method. Powder Technology 278: 286-305.

Itasca Consulting Group, Inc. (2015). PFC (Particle Flow Code in 2 and 3 Dimensions), Version 5.0, Documentation Set. Minneapolis: ICG.

Lee, S. J., Y.M.A. Hashash and E.G. Nezami (2012). Simulation of triaxial compression tests with polyhedral discrete elements. Computers and Geotechnics 43: 92-100.

Luding S (2008). Cohesive, frictional powders: contact models for tension. Granular Matter 10: 235-246.

Mongillo, G and M. Alsaleh (2011). Discrete Element Method to Predict Soft Ground Cutterhead performance. In *Rapid Excavation and Tunneling Conference Proceedings*, 1058-1067. R. Steve and R. Victor. Society for Mining, Metallurgy & Exploration, Inc. (SME) 12999 East Adam Aircraft Circle, Englewood, Colorado 80112.

Obermayr M, C. Vrettos, P. Eberhard and T. Dauwel (2014). A discrete element model and its experimental validation for the prediction of draft forces in cohesive soil. Journal of Terramechanics 53: 93-104.

Shmulevich I., Z. Asaf and D. Rubinstein (2007). Interaction between soil and a wide cutting blade using the discrete element method. Soil & Tillage Research 97: 37-50.

Walton, O.R. and R.L. Braun (1986). Stress Calculations for assemblies of inelastic spheres in uniform shear. Acta Mechanica (63):73-86.

Impacts of Automated Machine Guidance on Earthwork Operations

Pavana K. R. Vennapusa, David J. White, Charles T. Jahren
Center for Earthworks Engineering Research
Department of Civil, Construction, and Environmental Engineering
Iowa State University, Ames, Iowa
Email: pavanv@iastate.edu; djwhite @iastate.edu; cjahren@iastate.edu

ABSTRACT

Use of automated machine guidance (AMG) that links sophisticated design software with construction equipment to direct the operations of construction machinery with a high level of precision, has the potential to improve the overall quality, safety, and efficiency of transportation construction. Many highway agencies are currently moving towards standardizing the various aspects involved in AMG with developing the design files to implementing them during construction. In this paper, two aspects of AMG and their impacts on earthwork operations are discussed. The first aspect deals with the estimation of earthwork quantities and its impact on productivity on costs. The second aspect deals with the factors contributing to the overall accuracy of AMG. These two aspects are discussed in this paper using survey responses from various AMG users (contractors, agencies, software developers, and equipment manufacturers) and some experimental test results. Both these aspects are critical to understand during implementation of AMG as these have productivity and cost implications to the users.

Keywords: automated construction—earthwork quantities—accuracy—specifications—GPS—AMG

INTRODUCTION

Currently, highway agencies are improving electronic design processes that support construction with automated machine guidance (AMG) and deliver higher quality products to the public. Equipment providers are rapidly advancing software tools and machines systems to increase automation in the design and construction process. Motivation to more widely adopt AMG processes therefore exists. However, the framework for adoption of AMG into the complex framework of design to construction has not been fully developed. Technical, equipment, software, data exchange, liability/legal, training, and other barriers, limits progress with AMG implementation into construction projects. To address these issues, a national level study was initiated by the Transportation Research Board as the National Cooperative Highway Research Program (NCHRP) 10-77 study.

In this paper, two specific aspects of AMG that directly influences the earthwork operations are discussed. The first aspect deals with earthwork quantity estimation using AMG. The second aspect deals with accuracy of AMG and the various factors that contribute to errors in the AMG process. Both these aspects are critical to understand in a practical perspective as these have productivity and cost implications to the contractors and agencies. In the following, each of these aspects are separately discussed by presenting results of a national survey conducted with over 500 participants from agencies, contractors, equipment vendors, software vendors, and some experimental tests conducted by the authors. Survey results of selected questions are presented herein for brevity, and all results are available in White et al. (2015).

Proceedings of the 2015 Conference on Autonomous and Robotic Construction of Infrastructure, Ames, Iowa.

EARTHWORK QUANTITY ESTIMATION

Earthwork pay items are historically objects of great dispute between agencies and contractors. Proper use of digital information for AMG will likely result in less confusion and more accuracy than traditional methods of earthwork pay item quantification and payment. According to the survey responses (see White et al. 2015), a majority of the survey responding contractors currently use DTMs for estimating quantities, means and methods, constructability, quantity of the progress of work, and payment. Earthwork pay quantification from AMG must include mechanisms that all parties in the contract (both the agency-owner and the contractor) can trust. The efficient use of digital information in AMG applications typically involves creation of a digital terrain model (DTM) during initial planning, which is then passed to the design phase for addition of design data in a 3D model. This facilitates efficient computation and measurement of earthwork quantities for use during the procurement phase (bidding). Finally, the construction phase involves verification of project as-built quantities.

Impact of AMG on Productivity Gain and Cost Savings

Figure 1 presents responses from contractors and vendors on the impact of AMG on productivity gain and project cost savings. A majority of the equipment vendors indicated potential productivity gain of about 40% and potential cost savings of about 25 to 40% using AMG. On the other hand, a majority of the contractors indicated potential productivity gain of about 10 to 25% and potential cost savings of about 10 to 25% using AMG. Productivity gain and cost savings reported in the literature on earthwork construction projects using AMG is also presented in Figure 1 (Jonasson et al., 2002; Aðalsteinsson, 2008; Forrestel, 2007; Higgins, 2009; Caterpillar, 2006).

Jonasson et al. (2002) reported productivity gain and cost savings information for a fine grading project using a motorgrader with different position measurement technologies (i.e., ultrasonic's, 2D and 3D lasers, and GPS). The productivity gain ranged from about 20 to 100% and cost savings ranged from about 15 to 40%, depending on the position measurement technology used. The cost savings were due to a reduction in surveying support and grade checking, an increase in operational efficiency, and a decrease in number of passes. Their study indicated that the 3D laser systems required a direct line of sight to the equipment while the GPS systems did not, which resulted in a small increase in fleet productivity and a decrease in unit cost using GPS guidance systems over 3D laser systems.

Aðalsteinsson (2008) reported results from a field demonstration project conducted using an excavator to excavate a trench with 1650 cubic yards of sandy gravel material. In his study, the AMG approach showed a productivity gain of about 25% over a no AMG approach. Caterpillar (2006) reported results from a field demonstration project conducted in Spain by constructing two 80 m identical roads: one road with AMG on construction equipment and the other with similar equipment but using conventional methods and no AMG. AMG was used for bulk earth moving and fine grading work. An overall productivity increase of about 101%, fuel cost savings of about 43%, and increased consistencies in grade tolerances were reported for this project.

The results from these field case studies and survey responses indicate that the productivity gain and cost savings using AMG on earthwork projects can vary significantly (with productivity gains in the range of 5% to 270% and cost savings in the range of 10% to 70%). This variation is most likely because of various contributing factors, such as project conditions, materials, application, equipment used, position measurement technologies used, and operator experience.

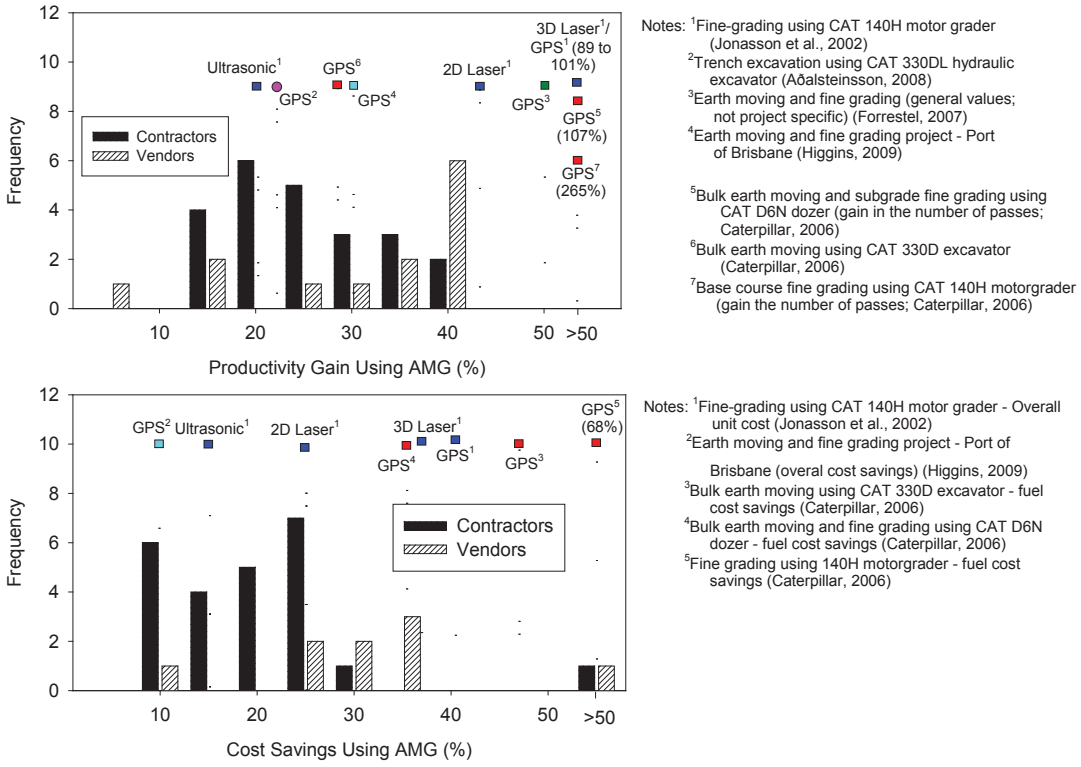

Figure 1. Survey Responses by Contractors and Vendors and Productivity Gain and Potential Cost Savings using AMG, and Data obtained from Field Case Studies

Earthwork Quantity Computation and Measurement

Accuracy of DTMs

Survey results reported by White et al. (2015) indicated that a majority (> 70%) of contractors, software/hardware vendors, and agencies who responded believe that the number of elevation data points used in creating the DTM is an important factor in the accuracy of the DTM. Evaluating the accuracy of DTMs by comparing them to the actual surface is a challenging and expensive task.

Various interpolation methods are available in the literature for generating contour grid data for DTMs, which include: (a) inverse distance to power; (b) Kriging; (c) local polynomial; (d) minimum curvature; (e) nearest neighbor; and (f) triangulated irregular network (TIN). To study the influence of the number of data points, three different data sets, with 78, 38, and 11 data points, were captured over a 540 m^2 area. The area consisted of a sloping terrain with an elevation difference of about 3.5 m over 60 m length. DTMs were generated using the six different interpolation methods described above. DTMs generated from 78 data points are presented in Figure 2.

The accuracy of each DTM that used 78 data points was evaluated using a cross-validation technique. This technique involved taking out a known data point from the data set, estimating the point using the model, and comparing the estimated value with the actual one. This process was repeated for all 78 data points. An absolute mean error (calculated as the average of absolute value of the difference between the actual and the estimate value) was then calculated for each interpolation method, as summarized in Table 1.

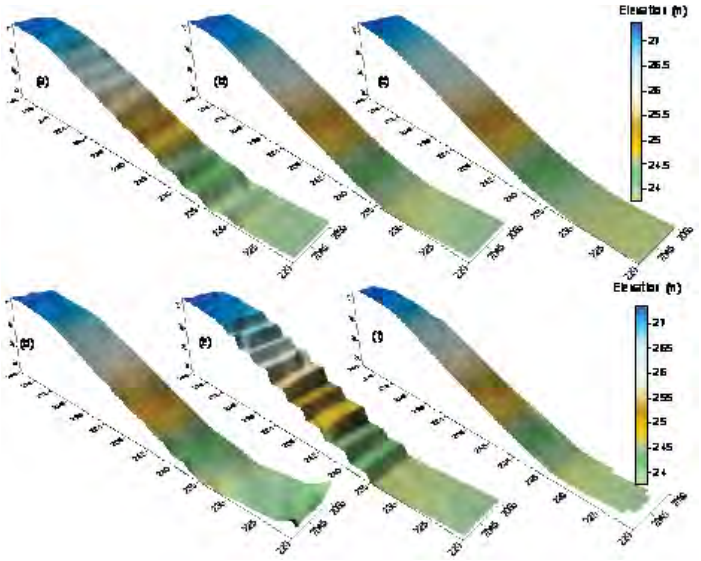

Figure 2. DTMs of a 540m^2 area using 78 elevation data points using different interpolation methods: (a) inverse distance to a power; (b) kriging; (c) local polynomial; (d) minimum curvature; (e) nearest neighbor; (f) TIN

Table 1. Absolute mean error of estimated elevation data based on cross-validation process using different interpolation methods

Data Interpolation Method	Estimated Elevation Absolute Mean Error (mm)
Inverse distance to power	100
Kriging	20
Local polynomial	70
Minimum curvature	50
Nearest neighbor	40
Triangulated irregular network (TIN)	30

For this data set, results indicated that the Kriging method is the most accurate method with 0.02 m absolute mean error. The TIN method showed a slightly higher absolute mean value of 0.03 m. The grid generated using the Kriging method with 78 data points was then considered as a “true” representative surface, and it was used as a comparison to the grid data generated using the other interpolation methods, as summarized in Table 2. The Kriging method produced absolute mean error of 0.02 m using 38 data points and 0.05 m using 11 data points. The TIN method produced slightly higher absolute mean error values. Minimum curvature, local polynomial, and inverse distance to power methods produced greater absolute mean error values, compared to the TIN method. The nearest neighbor method could not replicate the surface terrain, as it doesn’t interpolate the data, which is clearly a limitation of the method.

It is important that existing surfaces are portrayed as accurately as possible, so the model can be passed ahead to the design, estimation, bidding, and construction phases of the project with high fidelity. A proper understanding of the factors that influence the accuracy of the DTM is important to understand and must be addressed during the model development phase.

Table 2. Absolute mean error of estimated elevation data by comparing Kriged DTM with 79 points with different interpolation methods

	Estimated Elevation Absolute Mean Error (m)		
Data Interpolation Method	**79 Data Points**	**38 Data Points**	**11 Data Points**
Inverse distance to power	0.06	0.10	0.11
Kriging	0.00	0.02	0.05
Local polynomial	0.06	0.07	0.07
Minimum curvature	0.03	0.04	0.09
Nearest neighbor	0.06	0.12	0.24
Triangulated irregular network (TIN)	0.01	0.04	0.06

Computation of Earthwork Quantities

Earthwork quantities are traditionally computed using the average-end-area method, which is based on averaging the areas of two consecutive cross-sections and multiplying the average by the distance between them (Burch, 2007). A polar planimeter is typically used by surveyors to measure the area by tracking the boundaries.

Using DTM, the surface-surface method can be used to compute quantities, by overlapping the existing terrain and the design DTM surfaces. The U.S. Army Corps of Engineers (2004) provides a detailed explanation of the surface-surface quantity estimation method using TIN surfaces. Many software applications (including Microstation and Autodesk) now have the capability to easily compute quantities using the surface-surface method. The accuracy of the generated DTM, as described above, plays a significant role in the estimated earthwork quantities. Soil shrink-swell factors also affect to the overall quantity estimation, which are dependent on the soil type, so they must be selected appropriately (Burch, 2007).

Vonderohe et al. (2010) reported that differences between average-end-area and surface-surface increases as the cross-section levels increase, although the relationship is not linear. As the cross-section intervals decrease, the computations become theoretically the same. The differences are observed to be as great as 5% when 100 ft cross-section intervals are used with the average-end-area method. Such differences can contribute to significant cost discrepancies for large projects. The advantage of using DTMs is that earthwork quantities can be computed “on the fly,” as the model is being developed, and also during construction. Various layers and volumes that represent various bid items and various costs can be collected and categorized during the design process. Designed surfaces are accurately portrayed and can be passed ahead in the AMG process with high fidelity.

Model Enhancement for Construction Purposes

Model enhancement might be necessary during the development process for certain aspects, such as providing offsets between pavements and subgrades, delineating areas where equipment operation is excluded, and correcting inconsistencies that are not problematic for design models but are for AMG. The benefits of this work phase are that the constructor may discover possible design improvements or design errors in the model, which can end up saving time and money during construction. The constructor may develop a better understanding of how to construct the project as the design model is enhanced. The constructor could improve

construction productivity and safety by adding exclusion zones for equipment and methods to track equipment usage during construction.

Model Conversion to AMG Format

It may be possible to develop automatic load counts and infer earthwork or pavement volume or tonnages moved by equipment using onboard weight detection. A data collection method could be developed to infer current elevations of partially-completed projects by knowing current equipment elevations. This information may be used to monitor current earthwork volumes for partial payment.

Model Conversion to QA/QC Format

QA/QC personnel can potentially use DTM and the final design model to automatically locate test locations and display results. Elevations of existing surfaces can be obtained quickly and modeled in 3D to estimate current earthwork and pavement volumes or tonnages for partial payments. Quality information is processed along with volume information to ensure that partial payments are made for earthwork or pavement that meets quality requirements.

Limitations

The limitations in all of the above, however, include potentially higher up-front costs for software, hardware, and highly-trained personnel, and the possible inability to make gut-level checks for some types of design errors. Downstream personnel may be critical of design personnel for alternative designs that were not used and documented in unused parts of the model. Designers may consider inspection of the details of the design process by downstream personnel to be too invasive of their professional autonomy.

ACCURACY OF AMG PROCESS DURING CONSTRUCTION

The accuracy of the AMG process during construction is primarily influenced by three variables: (a) position measurement technology; (2) construction processes; and (c) human errors.

Survey responses from surveyors and planners indicated total station surveying (robotic and conventional) is considered more accurate than GPS and photogrammetric surveying. Manufacturers and researchers have published the precision and accuracy values of various position measurement technologies in the technical literature (Peyret et al., 2000; Retsher, 2002; Barnes et al., 2003; Mautz, 2008; and Trimble, 2008).

It does not appear that the effect of construction process and human errors has ever been thoroughly studied or quantified. Most contractors, vendors, and agency personnel who responded to the survey questions reported that these variables play a major role in the overall accuracy of the AMG process.

Position Measurement Technologies

Table 3 provides a summary of accuracy, coverage range, measurement principle, and relative cost of different position measurement technologies that are typically used in construction applications. The laser or ultrasonic technologies offer higher vertical (elevation) accuracies than GPS and have shown success in achieving tighter tolerances on some fine grading projects (Daoud, 1999). However, laser or ultrasonic technologies have some practical limitations with use in rain, dust, wind, and snow, and need frequent charging of deep cell

batteries (Cable et al., 2009). These technologies also require a direct line of sight between the control station and the receiver on the equipment, which is why they have not been used on heavy earth moving equipment, other than motor graders (Jonasson et al., 2000).

GPS-based technologies can overcome the limitations stated above with laser and ultrasonic technologies, but they don't offer high vertical accuracy. Peyret et al. (2000) noted that RTK GPS systems normally have vertical accuracy (±2 cm) or twice the horizontal accuracy (±1 cm). A vertical accuracy level of ±2 cm is not sufficient for applications such as paving or fine grading. Another common problem reported with GPS-based technologies is limited availability of satellites (and, consequently, poor signal attenuation) when operating close to structures, trees, or underground environments. Currently, the U.S. Air Force is committed to maintaining availability of 24 operational GPS satellites, 95% of the time (U.S. Air Force 2014) and is projecting for increased number of satellites in the future. The relative gain in accuracy from an increased number of satellites may be marginal (Hein et al. 2007), however, AMG users can expect to increase the chances of having the minimum number of satellites required to achieve a certain amount of accuracy because of the new additional satellites.

Recent advancements with use of HA-NDGPS with initiatives from FHWA, globally positioned GDGPS and IGS technologies is providing opportunities to achieve cm level accuracy without significant on-site investment. U.S. Air Force is currently in the process of developing and launching a next-generation GPS satellite (GPS III) which will be available for all military and civilian applications with improved accuracies (U.S. Air Force 2014).

GPS with laser or ultrasonic augmentation offers improved vertical accuracies (2 to 6 mm) (Trimble, 2008). From recent field studies on concrete paving projects in Iowa, Cable et al. (2009) found that laser-augmented GPS measurements are somewhat capable of guiding the paver and controlling elevation to achieve a reasonable profile for low-volume roads, but recommended that improvements (or fine tuning) in software is required to better control the elevation that will result in smoother surface profiles.

Construction Process and Human Errors

The overall accuracy of the AMG process includes these construction process parameters: (a) speed of operation; (b) direction of travel; (c) terrain; and (d) material type and support conditions (uniformity). These parameters have not been thoroughly studied or documented in the technical literature and they are application-specific or machine-specific. A statistical approach to quantify the influence of these factors on the overall accuracy of the AMG process is presented in White et al. (2015).

The level of impact for each of these factors differs with the application type. Speed of operation affects AMG accuracy and overall project costs. Increasing speed decreases the ability of machines to react to error signals and, consequently, reduces the accuracy of the measurement. However, productivity declines as speed declines, impacting project costs. The effect of speed of operation is clearly interlinked with the abilities of the position measurement technology feedback response time. The terrain on a job site can have an impact. Although not critical for paving and fine grading applications, terrain can be critical for general earthwork and excavation applications.

The type of material and support conditions under the equipment (whether stable or unstable, uniform or non-uniform) impacts the overall accuracy. Unstable or non-uniform support

conditions under the equipment make it more difficult to maintain control relative to the reference. This factor can play a critical role in paving and fine grading applications, and may not be as critical for general earthwork and excavation applications.

Table 3. Summary of Different Position Measurement Technologies

System	Accuracy	Range	User Cost	Reference
Conventional GPS (no corrections)	Variable, > 5 m	Global	Low	DoD, 2008
Assisted GPS (via mobile phones)	Variable, 2 to 10 m	Global	Low	Mautz, 2008
GPS integrated with INS	Variable	Global	Variable	Mautz, 2008
Wide Area Augmentation System (WASS) or Satellite Based Augmentation System (SBAS)	1.6 to 3.2 m horizontal and 4 to 6 m vertical	Global	Low	FAA, 2008
Nationwide differential GPS (NDGPS)	1 m within 150 km of the broadcast site	Global	Low	ARINC Inc., 2008
HA–NDGPS	10 cm horizontal and 20 cm vertical	Global	Low – currently in development	FRP, 2012
Global DGPS	10 cm horizontal	Global	Low	NASA, 2014
International GNSS Service (IGS)	<10 cm horizontal and vertical	Global	Low	Moore, 2007
RTK GPS	cm	Global	Moderate to high	Mautz, 2008
Locata (pseudolites)	6 mm	2 to 3 km	High	Barnes et al., 2003
Laser- augmented GPS	3 to 6 mm	300 m/line of site radius of laser source	Moderate to high	Trimble, 2008
Laser	±2 mm		Low to moderate	Retscher, 2002
Robotic total station	±2 mm	700 m/line of site radius of source	High	Retscher, 2002
Ultrasonic	±1 mm	Immediate reference	Low to moderate	Trimble, 2008
Ultrasonic augmented GPS	±1 mm	Immediate reference	Moderate to high	Trimble, 2008
Infrared laser	0.1 to 0.2 mm	2 to 80 m	High	Kraut-Schneider, 2006

SUMMARY OF KEY FINDINGS

Impacts of AMG on Earthwork Quantities

- Earthwork pay quantification from AMG must include mechanisms that all parties to the contract (both the agency-owner and the contractor) can trust.
- The accuracy of the generated DTM plays a significant role in the estimated earthwork quantities. Experimental test results documented herein indicated that the interpolation model and the number of data points both affect the accuracy of the DTM.
- Model enhancement might be necessary during the development process for certain aspects, such as providing offsets between pavements and subgrades, delineating areas

where equipment operation is excluded, and correcting inconsistencies that are not problematic for design models but are for AMG.

- The results from case studies described in the literature and survey responses indicate that the productivity gain and cost savings using AMG on earthwork projects can vary significantly because of various contributing factors, such as project conditions, materials, application, equipment used, position measurement technologies used, and operator experience.
- It is important that existing surfaces are portrayed as accurately as possible, so the model can be passed ahead to the design, estimation, bidding, and construction phases of the project with high fidelity. A proper understanding of the factors that influence the accuracy of the DTM is important to understand and must be addressed when developing the model.

Accuracy of AMG Process

- AMG component accuracies is an issue that affects various stages of the process including: Initial data collection for developing existing surface terrains; development of DTM and EED, AMG processes, procedures, and end-user competencies, QA/QC reported practices, heavy and fine grading equipment operations, and paving equipment operations.
- A common problem reported with GPS-based technologies is limited availability of satellites (and, consequently, poor signal attenuation) when operating close to structures, trees, or underground environments. Currently, the U.S. Air Force is committed to maintaining availability of 24 operational GPS satellites, 95% of the time and is projecting for increased number of satellites in the future. While the relative gain in accuracy from an increased number of satellites may be marginal (Hein et al., 2007), AMG users can expect to increase the chances of having the minimum number of satellites required to achieve a certain amount of accuracy because of the new additional satellites.
- The overall accuracy of the AMG process includes various construction process parameters: speed of operation, material type and support conditions (uniformity), and terrain. These parameters have not been thoroughly studied or documented in the technical literature and they are application-specific or machine-specific.

REFERENCES

ARINC Inc. (2014). *NDGPS Assessment Report,* Final Report, Prepared by ARINC Inc. for Operations Research and Development, Federal Highway Administration, McLean, VA.

Aðalsteinsson, D.H. (2008). *GPS Machine Guidance in Construction Equipment*, BSc. Final Project Report, School of Science and Engineering, Háskólinn Í Reykjavík University, Iceland.

Barnes J., Rizos, C., Wang, J., Small, D., Voigt, G., Gambale, N. (2003). "LocataNet: A New Pseudolite-Based Positioning Technology for High Precision Indoor and Outdoor Positioning." *Proceedings of the 16th International Technology meeting of the Satellite Division of the U.S. Institute of Navigation,* Portland, OR.

Burch, D. (2007). *Estimating Excavation,* Craftsman Book Company, Carlsbad, CA.

Cable, J.K., Jaselskis, E.J., Walters, R.C., Li, L., and C.R. Bauer. (2009), "Stringless Portland Cement Concrete Paving." *Journal of Constr. Engrg. and Mgmt.,* 135(11), p.1253-1260.

Caterpillar. (2006). *Road Construction Production Study,* Malaga Demonstration and Learning Center, Spain <http://www.trimble-productivity.com/media/pdf/ProductivityReport CATRoadConstruction2006.pdf> (accessed June 2010).

Daoud, H. (1999). "Laser Technology Applied to Earthworks.'' *16th IAARC/ IFAC/IEEE International Symposium on Automation and Robotics in Construction*, Universidad Carlos III de, Madrid, Madrid, Spain, Proceedings C. Balaguer, ed., p. 33–40.

DoD. (2008). *Global Positioning System Standard Positioning Service Performance Standard*, 4th Edition, Published by the Positioning, Navigation, and Timing Executive Committee, Department of Defense, Washington, D.C.
FAA (2008). *Global Positioning System Wide Area Augmentation System (WAAS) Performance Standard*, 1st Edition, Published by the Federal Aviation Administration, Washington, D.C.
Forrestel, R. (2007). "3D Models for Machine Guidance Systems," Presented at the 2007 Highway Engineering Exchange Program International Conference (IHEEP), Albany, NY.
FRP (2012). *2012 Federal Radionavigation Plan,* Published by the Department of Defense, Department of Homeland Security, and the Department of Transportation, National Technical Information Service, Springfield, VA.
Hein, G., Rodriguez, J., Wallner, T., Eissfeller, B., and P. Hartl. (2007). "Envisioning a Future GNSS System of Systems—Part 2." *Inside GNSS,* 2(2), p. 64–72.
Higgins, M. (2009). "Positioning Infrastructures for Sustainable Land Governance," *Presented at the FIG-World Bank Conference*, Washington, D.C.
Jonasson, S., Dunston, P.S., Ahmed, K., and J. Hamilton. (2000). "Factors in Productivity and Unit Cost for Advanced Machine Guidance." *Journal of Construction Engineering and Management*, 128(5), p. 367-374.
Kraut-Schneider, R. (2006), *Untersuchungen zur Leistungsfähirkeit des Messystems Indoor GPS*, Diploma Thesis, University of Applied Sciences Karlsruhe, Baden-Wuttemberg, Germany.
Mautz, R. (2008). "Combination of Indoor and Outdoor Positioning." *1st International Conference on Machine Control and Guidance*, Zurich, Switzerland.
Moore, A. W. (2007). "Innovation: The international GNSS service – Any questions?", *GPS World*, 58-64.
NASA (2014). *The Global Differential GPS System*, Jet Propulsion Laboratory at the California Institute of Technology, National Aeronautics and Space Administration (NASA), Pasadena, CA. <http://www.gdgps.net/> (Accessed December 2014)
Peyret, F. Betaille, D., and Hintzy, G. (2000). "High-precision applications of GPS in the field of real-time equipment positioning." Autom. Constr., 9(3), 299-314.
Retscher, G. (2002). "Multi-sensor systems for machine guidance and control." FIGXXII Intl. Congress Meeting, April 19-26, Washington, D.C.
Trimble (2008). *Trimble construction solutions for heavy and highway*. http://www.trimble-productivity.com/media/pdf/trimbleHeavyHighwaysSolutions.pdf (accessed May 11, 2010).
U.S. Air Force (2014). *Space Segment – Constellation Arrangement*, National Coordination Office for space-Based Positioning, Navigation, and Timing, U.S. Air Force, Washington, D.C. <http://www.gps.gov/systems/gps/space/> (accessed December 2014).
U.S. Army Corps of Engineers (2004). *Engineering and Design Hydrographic Surveying: EM 1110-2-1003*, Department of the Army, U.S. Army Corps of Engineers, Washington, D.C.
Vonderohe, A, Hintz, C., and A. Hanna, (2010). *3D Design Terrain Models for Construction Plans and Control of Highway Construction Equipment*, CFIRE 02-05, National Center for Freight & Infrastructure Research & Education, Madison, WI.
White, D.J., Jahrent, C., Vennapusa, P., Westort, C., Alhasan, A., Turkan, Y., Guo, F., Hannon, J., Sulbaran, T., and Dubree, A. (2015). *Use of the Automated Machine Guidance (AMG) within the Transportation Industry,* NCHRP 10-77 Draft Final Report, National Cooperative Highway Research Program, Washington, D.C. (in review).

Robotic Hybrid Data Collection System Development for Efficient and Safe Heavy Equipment Operation

Chao Wang, Ph.D.
School of Civil and Environmental Engineering
Georgia Institute of Technology
790 Atlantic Dr.
Atlanta, GA, 30332
cwang2@gatech.edu

Yong K. Cho, Ph.D.
School of Civil and Environmental Engineering
Georgia Institute of Technology
790 Atlantic Dr.
Atlanta, GA, 30332
yong.cho@ce.gatech.edu

ABSTRACT

This paper introduces a framework of automatic object recognition and rapid surface modeling to aid the heavy equipment operation in rapidly perceiving 3D working environment at dynamic construction sites. A custom-designed data acquisition system was employed in this study to rapidly recognize the selected target objects in a 3D space by dynamically separating target object's point cloud data from a background scene for a quick computing process. A smart scanning method was also applied to only update the target object's point cloud data while keeping the previously scanned static work environments. Then the target's point cloud data was rapidly converted into a 3D surface model using the concave hull surface modeling algorithm after a process of data filtering and downsizing to increase the model accuracy and data processing speed. The performance of the proposed framework was tested at a steel frame building construction site. The generated surface model and the point cloud of static surroundings were wirelessly presented to a remote operator. The field test results show that the proposed rapid target surface modeling method would significantly improve productivity and safety in heavy construction equipment operations by distinguishing a dynamic target object from a surrounding static environment in 3D views in near real time.

Key words: segmentation—object recognition—point cloud—laser scanner—site development

INTRODUCTION

Visibility-related accidents can be easily caused by the interactions between workers, equipment, and materials. This problem can lead to serious collisions without pro-active warnings. There have been a number of advances in vision-aid techniques because lacking full visibility is a major contributing factor in accidents at construction sites. 3D spatial modeling can help to optimize equipment control [1,24], significantly improve safety [2-3], monitor construction progress [4], and enhance a remote operator's spatial perception of the workspace [5-8]. However, the rapid processing of tens of thousand bits of range data in real time is still an unsolved problem requiring further investigation [9]. Unstructured work areas like construction

Proceedings of the 2015 Conference on Autonomous and Robotic Construction of Infrastructure, Ames, Iowa.

sites are difficult to graphically visualize because they highly involve unpredictable activities and change rapidly. Construction site operations require real-time or near real-time information about the surrounding work environment, which further complicates graphical modeling and updating.

One commonly used method to obtain the 3D position of an object is based on 3D laser scanning technology [7,10-11]; this method, however, has some limitations, such as low data collection speed and low object recognition rates [12]. It has always been a challenge to recognize specific objects from a 3D point cloud in unstructured construction environments because it is difficult to rapidly extract the target area from background scattered noises in a large and complex 3D point cloud.

While rapid workspace modeling is essential to effectively control construction equipment [13], few approaches have been accepted by the construction industry due to the difficulty of addressing all the challenges of current construction material handling tasks with the current sensor technologies. Thus, an innovation in rapid 3D spatial information is necessary to meet the challenges. The main objective of this paper was to validate a 3D visualization framework to collect and process dynamic spatial information rapidly at a construction job site for safe and effective construction equipment operations. Multi-video camera integrated vision-based object recognition and tracking method has been developed, based on which, a smart laser scanning method was proposed to reduce data size and scanning time.

LITERATURE REVEW

For the operator to monitor blind spots of the workspace from the cab, a vision-based system using a single or multiple cameras is an inexpensive option [14]. Brilakis et al. [15] introduced 2D vision-based methods that recognize new overlapping feature points and track them in the subsequent video stream. To acquire a precise 3D position of objects with additional depth information, generally two or more cameras generate a stereo view after calibration with known intrinsic parameters. Park et al. [16] achieved more accurate 3D locations of tracking objects by projecting the centroids of the tracked entities from two cameras to 3D coordinates. Notwithstanding the recent advances, there are some known drawbacks of vision-based techniques in tracking moving equipment at the sites: 1) additional infrastructure is needed to install and maintain cameras; 2) fixed camera locations have limited view angles and resolutions, and 3) the results are sensitive to lighting conditions [17].

Laser scanners have been extensively utilized to automatically obtain the “as-is” condition of the existing buildings [18]; they also can be used to classify and capture a complex heavy equipment operation as it happens or to provide automated feedback to those who are conducting the operations [7,17,19]. Teizer et al. presented a methodology for real-time 3D modeling using Flash LADAR which has a limited measurement range and low accuracy for outdoor use [3]. Lee et al. proposed an automated lifting-path tracking system on a tower crane to receive and record data from a laser device [13]. Bosche and Hass registered 3D static CAD objects to laser-scanned point cloud data [20], which can be utilized to efficiently assess construction processes. However, most of the algorithms were developed mainly to recognize and register static objects’ models to point clouds. Few applications have demonstrated the technical feasibility of registering dynamic models to point clouds in real or near real time.

In the authors’ previous studies [17], a model-based automatic object recognition and registration method, Project-Recognize-Project (PRP), was introduced to register the CAD models with the corresponding point cloud of the recognized objects through comparing the recognized point cloud of the objects with existing CAD models in a database (shown in Figure 1). While the PRP approach provides very detailed, accurate solid models in a point cloud, the

limitation of this method is that it only works for the objects which have corresponding models in the database. In this study, a non-model based, surface modeling method is introduced to automatically recognize and visualize dynamic objects on construction sites.

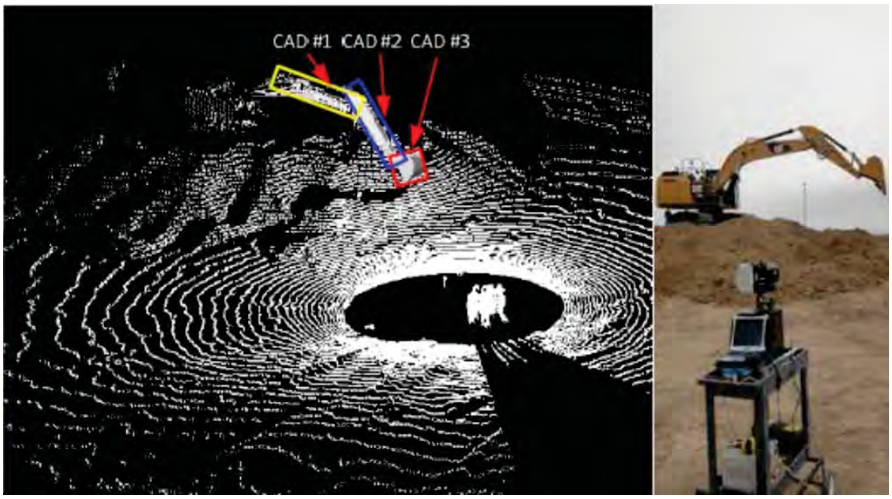

Figure 1. Model-based object recognition and registration [17]

FRAMEWORK OF THE PROPOSED METHODOLOGY

In Figure 2, the framework of the proposed rapid surface modeling method is illustrated. The developed data acquisition system is composed of two 2D line laser scanners (80 meter working ranges at 100Hz scan speed, up to 2.5 sec / 360º scan, 190º for vertical line), a digital camera and three video cameras with a resolution of 0.25 degrees in a vertical direction and 0.0072 degrees in a horizontal direction. In this system, multiple degree-of-freedom (DOF) kinematic problems were solved based on the mechanical installation, and 3D point cloud data and digital image streams can be collected simultaneously. Utilizing this form of flexible design together with Time-of-flight (TOF) laser scanner working type, higher scanning resolution and faster scanning rate were obtained, which is more suitable for the complicated dynamic construction environments.

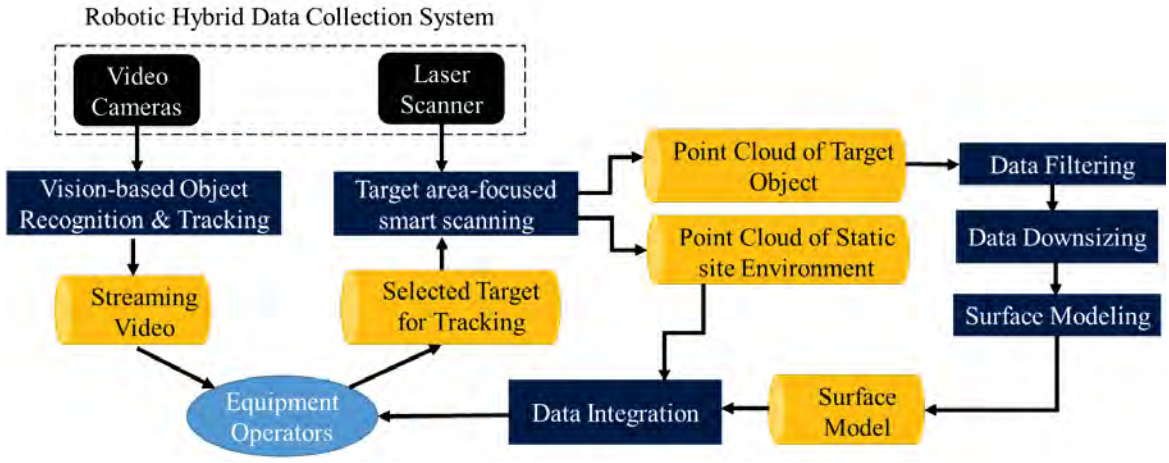

Figure 2. The framework of the proposed method

Working together with the laser scanner system, the digital video cameras were employed to capture real time image streams in the jobsite for the operators. Then, the operators can select

the target objects in the image streams by drawing a bounding box through the developed graphical user interface. Using a robust local feature detector, Speeded Up Robust Features (SURF) [21], image-based target object recognition and tracking algorithms were implemented.

Taking the bounding box area as an input, smart scanning and visualization processes were immediately applied to separately collect and update the data of the target object and the static site environment. The major two steps of the smart scanning method are: (1) a static jobsite environment is scanned by the laser system with a very high resolution. Those collected site data are stored in the memory; and (2) from the second scanning round, only the point clouds in the dynamic target area specified by the equipment operator are updated separately. In this process, the size of point cloud data obtained from complex, large construction sites and the updating time can be significantly reduced.

Table 1. Data size of each step of the proposed methodology

		Number of points
Raw data		24,330
Filtered data		24,276
Downsized data	**Leaf size = 50 * Resolution***	108
	Leaf size = 10 * Resolution	1,730
	Leaf size = 5 * Resolution	4,674
	Leaf size = Resolution	22,138

*Resolution = 0.06 m.

Surface modeling of point clouds can be more advantageous for the equipment operators over the point-cloud-only visualization because a surface model of target object can be better distinguished from a complex point-cloud environment. The concave hull approach is one of the most widely used surface modeling methods creating a polygon that represents the area occupied by a set of points. A concave hull better details the shape of the point cloud than the convex hull does. A concave hull of a set of surfaces is the enclosing concave surfaces with smallest volume. There are several existing concave hull calculation algorithms [22], however the efficiency of these algorithms decreases significantly because of high computing queries for the large size of point cloud data like the ones obtained from construction jobsites.

The raw data size of point cloud data collected from a construction jobsite is quite a large and as a result, it is challenging to process and visualize these data in real or near real time. In this study, as shown in Figure 1, the smart scanning technology was employed at the very beginning of the surface modeling phase in order to significantly reduce the data size of the point clouds and the surface modeling time. In addition, outliers of the point data were statistically identified and removed to improve concave hull model accuracy. Then, a data filtering and downsizing process was conducted to further decrease the number of points. The goal of data downsizing is to increase the data processing speed by reducing the amount of overly dense data being processed.

EXPERIMENTS AND RESULTS

Validation of the proposed methodology was implemented on a crawler crane at a building construction site. The data acquisition system was mounted on a mobile cart, and set up in the working area of the equipment, especially in its blind spots. It firstly scanned the whole jobsite and kept the point cloud data in the database; then smart scanning and visualization were fulfilled based on the selected tracking objects. All tests were benchmarked on an Intel Core i5

CPU with 4GB RAM on a 64 bit Windows mobile computer. It should be noted that the required resolution, registration accuracy, and scan rate for successful surface modeling vary based on the scan range, ambient lighting conditions, properties of the target (e.g., shape, color, reflectivity, and moving speed), and the number of mounted 2D laser scanner. In this study, all data were collected from the system with two 2D laser scanners, and the maximum scan speed of which is 227,500 points/sec. The scan speed could be doubled if four 2D laser scanners were equipped [17].

Table 2. Processing time of each step of the proposed methodology

		Data Downsizing Leaf Size (m)			
		3	0.6	0.3	0.06
Data Filtering Time (sec.)		0.176	0.176	0.176	0.176
Data Downsizing Time (sec.)		0.004	0.005	0.006	0.008
Surface Modeling Time (sec.)	α = 1.0 * Leaf Size	0.189	0.302	0.446	1.354
	α = 1.5 * Leaf Size	0.188	0.254	0.410	1.363
	α = 2.0 * Leaf Size	0.188	0.255	0.410	1.371
	α = 2.5 * Leaf Size	0.188	0.253	0.408	1.366
	α = 3.0 * Leaf Size	0.188	0.254	0.408	1.365
	α = 3.5 * Leaf Size	0.184	0.255	0.407	1.370
	α = 4.0 * Leaf Size	0.183	0.254	0.405	1.370
	α = 4.5 * Leaf Size	0.184	0.253	0.406	1.373

The whole crane was chosen as a tracking target to track. The collected raw data includes 24,330 points, and its resolution is 0.06 m. The leaf size applied for data downsizing was 0.3 m, which also applied five times of the resolution. The data size decreased to 24,276 and 4,674 correspondingly after data filtering and downsizing (Table 1). Then, 8 different α values were assigned to the proposed surface modeling algorithm. Table 2 shows the processing time under different data downsizing scales and the size of the concave hull segments. Finally, the result with α = 1.0 * leaf size was taken as the output shown to the operator. The total processing time can be found in Table 3, and it is less than 0.5 seconds. Figure 3 displays a pre-scanned point clouds of site scene and a scene with a crane model embedded which is continuously updated at each scan.

Table 3. Total processing time

Process	Time (sec.)
Data filtering	0.104
Data downsizing*	0.009
Surface modeling**	0.223
Total processing time	0.336

*Leaf size = 0.3 m, **α = 1.0 * leaf size

CONCLUSION AND FUTURE STUDY

In this study, a specially designed data capturing system was utilized to collect point cloud data from multiple laser scanners; while multiple video camera arrays were used to rapidly recognize and track the selected dynamic construction equipment objects including a backhoe loader and a crane. The validation of the proposed method was implemented at a real world construction jobsite. The concave hull of the crawler crane was generated in less than 0.5 seconds, and then the data were smoothly transferred to the operator in a cabin. The test results indicate that the

proposed rapid workspace modeling approach can improve the heavy equipment operations by distinguishing surface-modeled dynamic target objects from the point cloud of existing static environment in 3D views in near real time.

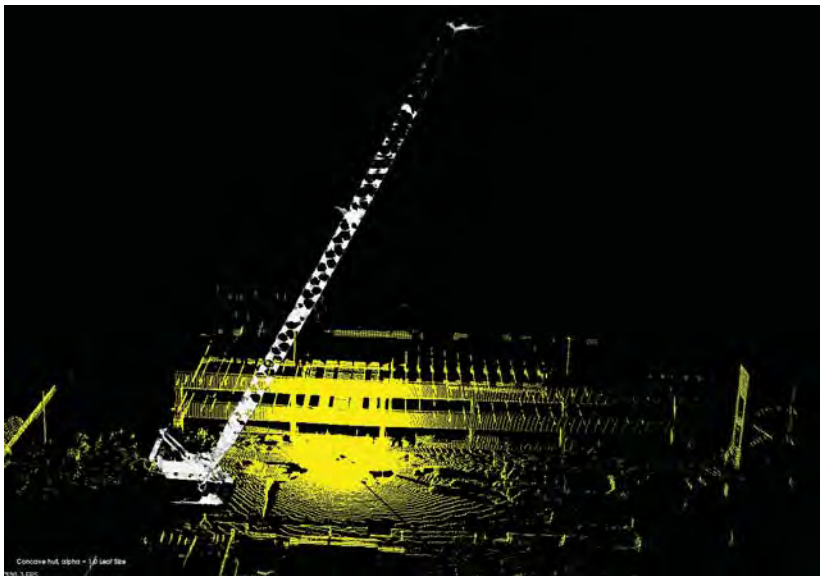

Figure 3. A crane model embedded in the site environment

While the surface modeling time is sufficiently fast enough for real-time operation, the data collection time should be carefully configured based on the types of equipment (e.g., size and moving speed), distance, ambient lighting, and reflectivity.

For future work, the research will continue to improve the resolution of laser scanner data while reducing data collection time. With an increase in scanning speed, the scanned resolution is lowered accordingly. To resolve this issue, a smart scanning approach with differentiated scan speeds will be further developed, to allow faster rotations for the areas to be skipped, and slow the scan speed for the target areas. Improving surface modeling speed using a higher performance computer and surface model quality will be another future research focus.

ACKNOWLEDGMENTS

This material is based upon work supported by the National Science Foundation (Award #: CMMI-1055788). Any opinions, findings, and conclusions or recommendations expressed in this material are those of the authors and do not necessarily reflect the views of the NSF.

REFERENCES

[1] H. Son, C. Kim, K. Choi, Rapid 3D object detection and modeling using range data from 3D range imaging camera for heavy equipment operation, Automation in Construction 19(7) (2010) 898-906.
[2] J. Teizer, B. S. Allread, C. E. Fullerton, J. Hinze, Autonomous pro-active real-time construction worker and equipment operator proximity safety alert system, Automation in Construction 19(5) (2010) 630-640.
[3] J. Teizer, C. H. Caldas, C. T. Haas, Real-Time Three-Dimensional Occupancy Grid Modeling for the Detection and Tracking of Construction Resources, ASCE Journal of Construction Engineering and Management 133(11) (2007) 880-888.
[4] H. Son, C. Kim, 3D structural component recognition and modeling method using color and 3D data for construction progress monitoring, Automation in Construction 19(7) (2010) 844-854.

[5] Y. Cho, C. Haas, K. Liapi, S. Sreenivasan, A framework for rapid local area modeling for construction automation, Automation in Construction 11(6) (2002) 629-641.
[6] Y. Cho, C. Haas, S. Sreenivasan, K. Liapi, Error Analysis and Correction for Large Scale Manipulators in Construction, ASCE Journal of Construction Engineering and Management 130 (1) (2004) 50-58.
[7] Y. Cho, C. Wang, P. Tang, C. Haas, Target-focused local workspace modeling for construction automation applications, ASCE Journal of Computing in Civil Engineering 26(5) (2012) 661-670.
[8] Y. Cho, C. Haas, Rapid Geometric Modeling for Unstructured Construction Workspaces, Journal of Computer-Aided Civil and Infrastructure Engineering 18 (2003) 242-253.
[9] J. Gong, C. H. Caldas, Data processing for real-time construction site spatial modeling, Automation in Construction 17(5) (2008) 526-535.
[10] P. Tang, D. Huber, B. Akinci, R. Lipman, Automatic reconstruction of as-build building information models from laser-scanned point clouds: A review of related techniques, Automation in Construction 19 (2010) 829-843.
[11] D. Huber, B. Akinci, P. Tang, A. Adan, Using laser scanner for modeling and analysis in architecture, engineering and construction, Proceedings of the Conference on Information Sciences and Systems (CISS) (2010) Princeton, NJ.
[12] C. Kim, J. Lee, M. Cho, C. Kim, Fully automated registration of 3D CAD model with point cloud from construction site, 28th International Symposium on Automation and Robotics in Construction, Seoul, Korea, (2011) 917-922.
[13] G. Lee, H. Kim, C. Lee, S. Ham, S. Yun, H. Cho, B. Kim, G. Kim, K. Kim, A laser-technology-based lifting-path tracking system for a robotic tower crane, Automation in Construction 18(7) (2009) 865-874.
[14] T. M. Ruff, Recommendations for evaluating & implementing proximity warning systems on surface mining equipment, Research Report to the National Institute for Occupational Safety and Health, Centers for Disease Control, (2007) < http://www.cdc.gov/niosh/mining/works/coversheet202.html >.
[15] I. Brilakis, M. Park, G. Jog, Automated vision tracking of project related entities, Advanced Engineering Informatics 25 (2011) 713-724.
[16] M. Park, C. Koch, I. Brilakis, Three-dimensional tracking of construction resources using an on-site camera system, J. Comput. Civ. Eng. 26(4) (2012) 541-549.
[17] Y. Cho, M. Gai. Projection-Recognition-Projection (PRP) Method for Rapid Object Recognition and Registration from a 3D Point Cloud, ASCE Journal of Computing in Civil Engineering (2014) doi: 10.1061/(ASCE) CP.1943-5487.0000332 (in press).
[18] C. Wang, Y. Cho, M. Gai, As-is 3D Thermal Modeling for Existing Building Envelopes Using a Hybrid LIDAR System, ASCE Journal of Computing in Civil Engineering 27(6) (2013) 645–656.
[19] Y. Arayici, An approach for real world data modeling with the 3D terrestrial laser scanner for built environment, Automation in Construction 16 (6) (2007) 816–829.
[20] F. Bosche, C. T. Haas, Automated retrieval of 3D CAD model objects in construction range images, Automation in Construction 17(4) (2008) 499-512.
[21] H. Bay, T. Tuytelaars, L. V. Gool, SURF: Speeded up robust features, Computer Vision–ECCV (2008) 404-417.
[22] P. Zhou, Computational Geometry: Analysis and Design on the Algorithms, second edition, Tsinghua University press, Beijing, 2005.
[23] C. Kim, C. Haas, K. Liapi, C. Caldas, Human-Assisted Obstacle Avoidance System Using 3D Workspace Modeling for Construction Equipment Operation, ASCE J. Comp. in Civ. Engrg. 20(3) (2006) 177-186.

Designing Digital Topography: Opportunities for Greater Efficiency with a Primitives and Operators Approach

Caroline Westort
Department of Landscape Architecture
Iowa State University
156 College of Design
Ames, IA 50010
cwestort@iastate.edu

ABSTRACT

This paper focuses on characterizing *proposed* human-built topographic forms and describing them parametrically. Two basic approaches exist for characterizing shape algorithmically: *parametric* descriptions, which describe discrete geometries, and *non-parametric methods*, which for the most part work on fields. This paper offers a brief overview of the range of parametric modeling options for topography, a set of criteria that need to be fulfilled for any successful landform design system, and a *primitives* and *operators* approach that offers some specific advantages in the AMG context.

Key words: DTM—design—landform

INTRODUCTION

Reshaping land to meet societal needs is a complex, disruptive, time consuming, and costly effort. Industry increasingly relies on Digital Terrain Models (DTMs) as the principle medium for landform design and the basis for autonomous construction machinery (AMG). However, controlling DTM geometry remains a non-trivial algorithmic problem. At the project concept stage and later during construction, existing 3D manipulation methods are cumbersome and unwieldy, adding to downtime, guesswork and inefficiencies in the field.

Landform Design

Landform as a creative, expressive medium

Landforms may be used as design elements unto themselves, and also to organize and establish the base upon which other elements may be composed on a site. Landscape architects and engineers think of topography in both functional quantitative and spatial qualitative terms [1-3]. Through use of slope, elevation change, convex and concave re-grading, both subtle and dramatic meanings can be achieved [4].

Landscape designers use a variety of abstractions which help to organize or synthesize their design of landform, including 'signatures' of contour lines in plan [2, 4, 5]; compositions of regular geometric solids [6] and flat planes with break lines and transitions [5]; and processes of land formation: erosion, deposition, scraping and piling, etc. [7, 8]. The topographic condition of a site is therefore regarded as an essentially plastic one.

Proceedings of the 2015 Conference on Autonomous and Robotic Construction of Infrastructure, Ames, Iowa.

Through 3D modeling, rendering and visualization, designers try out an assortment of design alternatives on a topographic surface. Through manipulation of 3D models or images design alternatives are seen, changed, and analyzed [9]. For environmental designers, visualization works in close concert with manipulation and quantitative and qualitative analysis. The editing and analysis tasks can be more closely integrated in the digital medium, as shown in Figure 2.

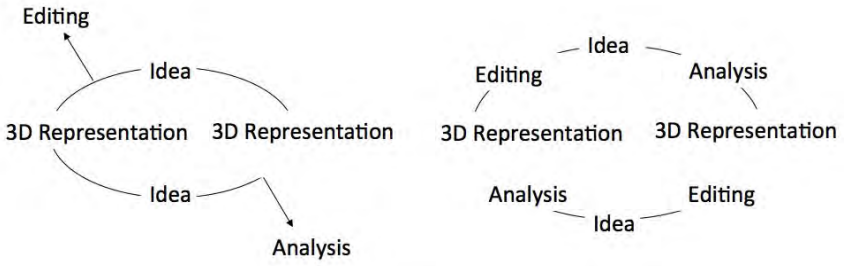

Figure 2: Iterative design loop for topography that shows how digital methods can integrate editing and analysis tasks more tightly in the iterative life cycle of a design project.

Digital landform representation

Landform is challenging to represent in any medium [10] especially computationally where large scales, fuzzy edges, continuous surfaces, and huge datasets pose particular challenges [11-14]. **Digital Terrain** in this project is defined as the elevation of the earth's surface above some reference geoid. Over the last few decades ever-larger quantities of terrain data with higher accuracy in (x, y) and z have become available to represent existing earth surface geometry. **Digital Terrain Models** (DTMs) are an important class of surface models [14] increasingly becoming the principle medium for landform design and construction [15, 16, 19].

Automated Machine Guidance

Dramatic advances with AMG in recent decades allow a remotely operated bulldozer to construct a landform from a precise 3D DTM [16-19-30]. Landscape architects and civil engineers work from existing site survey DTMs to propose and revise many drafts of proposed topographic surface geometry both on paper and with software to produce a final landform design, called a *grading plan* by landscape architects [2], or *the design* in the engineering domain [25]. Designers typically hand-off a grading plan to the earthworks contractor only once so the final construction is often the first and only full-scale built realization of a design that the team encounters. However, a lot can happen to the design once it is taken into the field and construction begins. *Site conditions, equipment incompatibilities, weather factors, personnel skill, preference and taste issues* are categories of unforeseen factors that can significantly impact a design once construction gets underway. Thus DTMs often require editing during construction to avoid downtime in the system and guesswork in the field [19, 20, 21, 25, 30].

Control criteria for DTM geometry over the lifecycle of a grading project

Controlling DTM geometry remains a non-trivial algorithmic problem [31, 32]. Methods for changing DTM geometry are cumbersome and unwieldy [34], thereby limiting the ability to creatively explore, modify, and optimize topographic form. These shortcomings yield serious inefficiencies throughout the lifecycle of a project and result in a need for improved tools for landform design that fulfill the following **criteria**:

3D
Local geometric control
Ease of handling
Quick response time
Quantitative accuracy

What is generally missing is the ability to iteratively revise, update, edit, modify, manipulate – i.e., “sculpt” DTMs, both *before* and *during* the construction phase as a way to insure quality design.

Approaches to DTM Manipulation

3D model manipulation strategies for topography have evolved chiefly in the CAD and geographic information system (GIS) digital domains [10], with the former focusing primarily on the parameterization of objects, the latter on combinations of spatial attribute information with digital terrain models in several representations (TINS, DTMs, contours, e.g., see [34]) The simplest and most common of these is the regular tessellation, mesh, displaced as a raster array. Large raster arrays are reasonable to use for representation of arbitrarily shaped “natural” existing features such as the earth’s surface, but the manipulation tools available make them neither an efficient nor expressive medium for design.

Geographic information systems (GIS) have evolved to handle the large datasets characteristic of landscape, but have mostly focused on the display and analysis of elevation data, rather than on active tools for manipulating landform. Figure 3 shows the manipulation scopes of action available in many GISs which allow only either global or ‘local’ changes to a model: a local change is a change that happens to a single vertex, a global change is one that affects the entire topographic dataset, e.g., scale changes, which exaggerate the Z value [35].

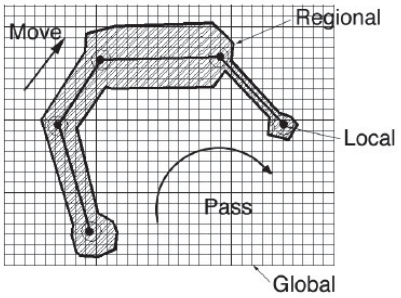

Figure 3: Local, regional, global scopes of action.

While some operations exist to limit the scope of activity to a mask of pixels or a specific polygon, these techniques are not especially useful for landform design. An example of a DTM editor developed to resolve artifacts resulting from elevation data interpolation has been an interesting approach [36]. As have algorithms for compression [37-42], line of site, shortest path, drainage [43], multiple observers[40], local maxima and minima, and drainage patterns[44] and siting from first principles. These approaches, while promising, have focused on data extraction and algorithmic techniques acting on geospatial data for *existing landform geometry* of a digital terrain surface, rather than *proposed* geometry – the target concern here.

A key advantage of digital/virtual methods is the ability to directly manipulate a 3D representation [45-49]. The following list, adapted from [50] and [51] summarizes some of the 3D topographic modeling tools available in current industry-standard CAD software packages:

Data Structures

Contours—Landform design using 2D CAD systems relies heavily upon the representation of 3D form as contour lines; an abstraction well suited to representation, but notoriously cumbersome for design. It is also a data structure with key disadvantages: Oversampling along, and under-sampling between lines. Manipulating contour lines effectively with CAD systems remains a daunting challenge, requiring spline curves and geometric constraints that have nowhere yet been satisfactorily packed for—much less mastered by—designers from any discipline.

B-Rep—Boundary Representations—The surface of an object is described as a description stored as a list of vertices, lines joining the vertices, and list of faces. These include Bezuer-spline curves (B-splines), Non-uniform rational basis spline (NURB) surfaces

Primitives—A set of simple, generic, 3D models (cube, sphere, cylinder, cone, torus, wedge, lane and others). These primitives can be scaled, translated, and rotated within the application, often both interactively (such as with a mouse), and by numerical input.

CSG—Constructive Solid Geometry—An object is represented as a combination of simple primitives such as cues, spheres, and cylinders. These basic solids are used as building blocks for more complex objects by means of a system that uses Boolean combinations (union, intersection, and difference) to describe the logical operations of adding two objects, subtracting one from another, or designing the overlap between two objects.

Voxels—Volume/Solid Modeling. Spatial occupancy enumeration divides – dimensional space into cubic units called voxels, or a 3D pixels.

Operators:

Swept Forms—a 2-dimensional (XY) section ‘swept’ along a third (Z) dimension.

Extrusion—a template is swept in a direction orthogonal to the plane in which it lies.

Surface of Revolution—a 2D template, closed or open, rotated about an axis.

Skin—the ability to construct a ‘skeleton’ of a form and then wrap a surface skin around it to create an object

Patches—same as skin except using boundaries as the skeleton.

Curved Patches—while popular remain too computationally intensive to be justified or affordable for most landform design.

Primitives

What is called for is a specification of landform primitives—mound, swale, plane, for example – that carry their own parametric definitions and constraints, and so enable ‘regional’ changes, between local and global in their scope, in which slopes, radii and other dimensions may be user-specified and propagated (Figure 3). Geometric modeling with pure Euclidean shape primitives such as cones and cylinders is promising [8], but by itself is too limited for most landform design, which more often than not involves the design of a continuous surface rather

than of a solid. While some efforts for landscape are promising [51, 53] no unifying ontology, or organizing Landscape Information Model (LIM) currently exists.

A wide variety of disciplines and scales use a range of terms and parameters to describe discrete topographic shape, and they vary qualitatively and quantitatively. Moreover, landform shapes are frequently described in terms of an underlying DTM Data structure. I.e., there are contour line specific forms, or signatures, TIN specific data structures. A sampling of this diversity includes:

- *Geomorphological forms*, landforms produced by the earth's natural processes (e.g. drumlins, eskers, moraines, saddles, valleys, cliffs, glacial forms) [7, 8, 54-58]

- *Domain-specific forms, e.g.,* Contour line signatures [3-5], American Disabilities Act design specifications [59].

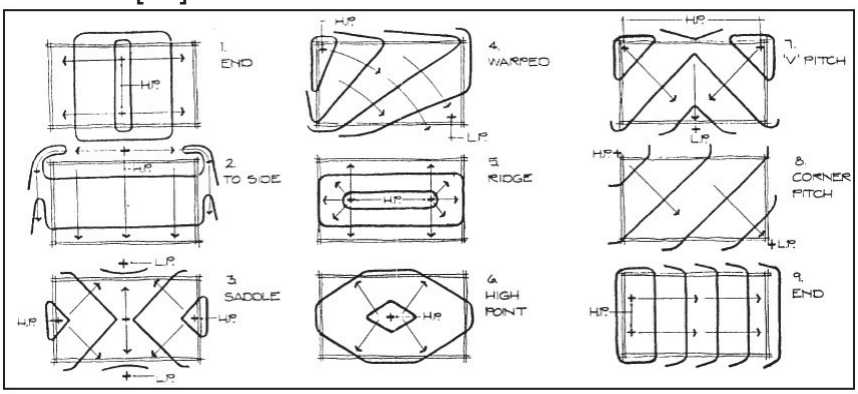

Figure 4: Contour line signatures.[60]

- *Project-type specific* (e.g., roadways, levees, sand dunes, water management, golf courses, battlefields, gaming environments, American Disabilities Act (ADA) compliant features)

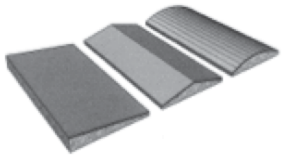

Figure 5: Road profile primitive forms [5]

- *Individual Project specific forms*, A particular project may standardize its own set of topographic forms for re-use throughout a project.[61]

- *Tool-based forms*, shovels, rakes, particle guns.

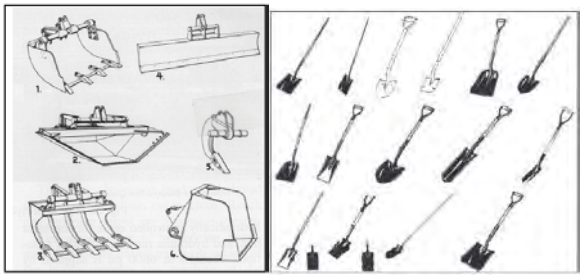

Figure 6: Example tool-based specific forms.[62]

Operators

Defining a universal set of geometric parameters for landform, coupled to a way to combine the primitives together, would contribute to dramatically improved geometric control over a DTM surface. Specification of a set of operations, such as cutting or filling tools, with parametrically defined shape characteristics (such as angles of slope, depth of fill, etc.) to be performed along a path. This set of operations is then swept along the path, either over an existing base terrain, or on a blank surface, and the result is a terrain geometry, which has the desired shape.

Conceptual framework for a primitives and operators approach

A simple and useful way to generalize all topographic forms as four generic shapes derivable from either a point- or line-based feature. General concavity or convexity are subsequent shape descriptors.

Mounds – point-based convex surface
Craters – point based concave surface
Berms – line-based concave surface
Swales – line based convex surface.

Figure 7 shows this initial set, with their blade and path shapes abstracted and combined using a sweep (extrude) algorithm.

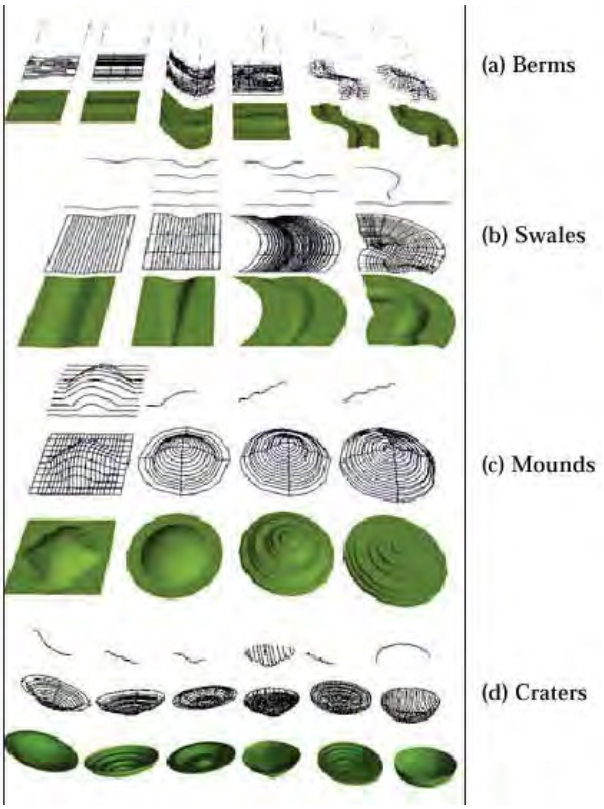

Figure 7: Generic subset of topographic primitives, abstracted as blades and paths shapes

Operators to generate these sorts of geometries as part of a continuous surface were then prorammed as a plug-in software to AutoCAD. Figures 8 and 9 show these initial results.

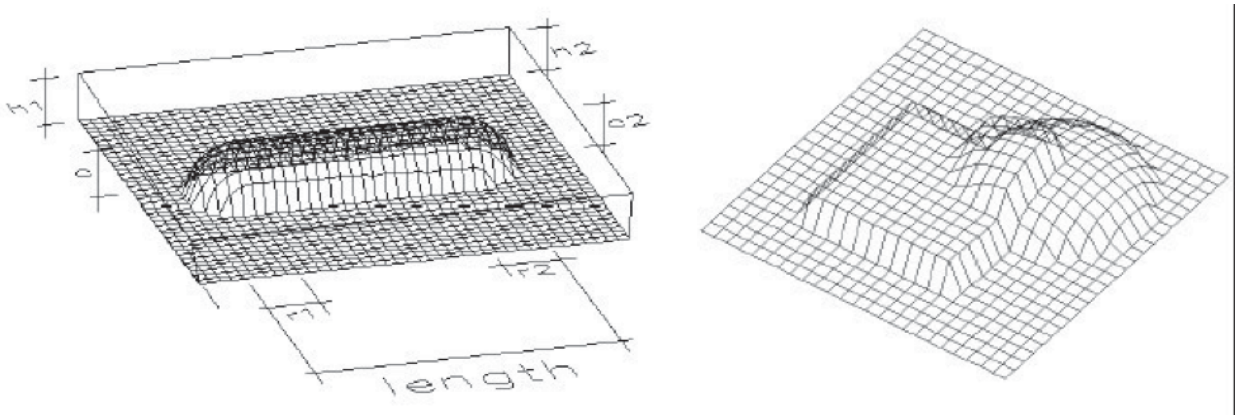

Figure 8. A parameterized berm primitive left.

Figure 9. Boolean combination operators on mound primitives on the right

A stand-alone prototype software was then generated as a generic sculpting tool definition, Figure 9.T his implementation kept geometric change parameters separate from any underlying DTM data structure description, Figure 10.

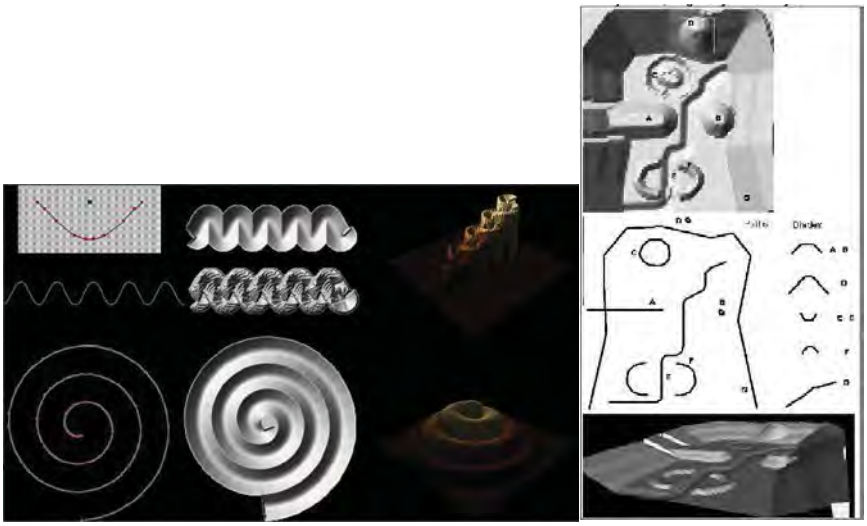

Figure 9: Left Topographic surface sculpting generic tool.[50]

Figure 10: Right Blade and path abstractions as alternative descriptions[63]

Summary & Discussion

A set of blades and path primitives describe proposed topographic form such that the following criteria for a digital terrain design system are fulfilled: 3D, local geometric control, ease of handling, quick response time, quantitative accuracy. A primitives and operators formalism represents an intermediate internal data structure that is independent of the underlying DTM data structure, and therefore would represent an exciting opportunity for increased efficiency in the AMG context.

The following are some outstanding challenges that would need to be resolved for this to happen:

Challenge 1: Primitive shapes can have a wide range of relationships with one another. In the case of a primitive blade shape that is extruded along a primitive path shape, what is the desired relationship, symmetrical, static, dynamic with other primitive models. How to provide interactive handles to the user for setting and varying these shape parameters.

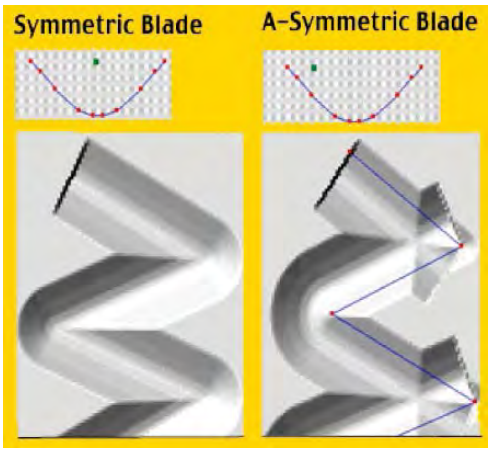

Figure 11: Symmetrical versus A-Symmetrical blade and path relationships [65]

Challenge 2: Should the relationship between primitives simulate real world on-the-ground tool behavior or physical phenomena? E.g. shovels, bulldozers, graders, rakes, etc.? What soil-type, moisture content is assumed? Gravity? Since final DTM geometry is the priority, and simulation of the manipulation process itself is of secondary importance, those geometry determining "real-world" parameters which affect final landform shape will be prioritized.

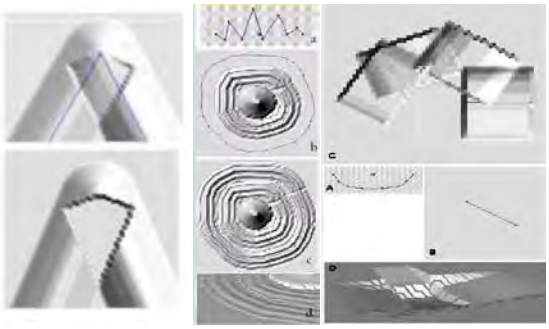

Figure 12: Left, corner and overlap options.

Figure 13: Middle, rake simulation blade

Figure 14: Right, shovel simulation blade

Challenge 3: Embedding into the underlying terrain – how does the blade-path complex embed in the underlying DTM surface? Is it an absolute or relative relationship? How are these relationships parameterized to optimize interactive user control.

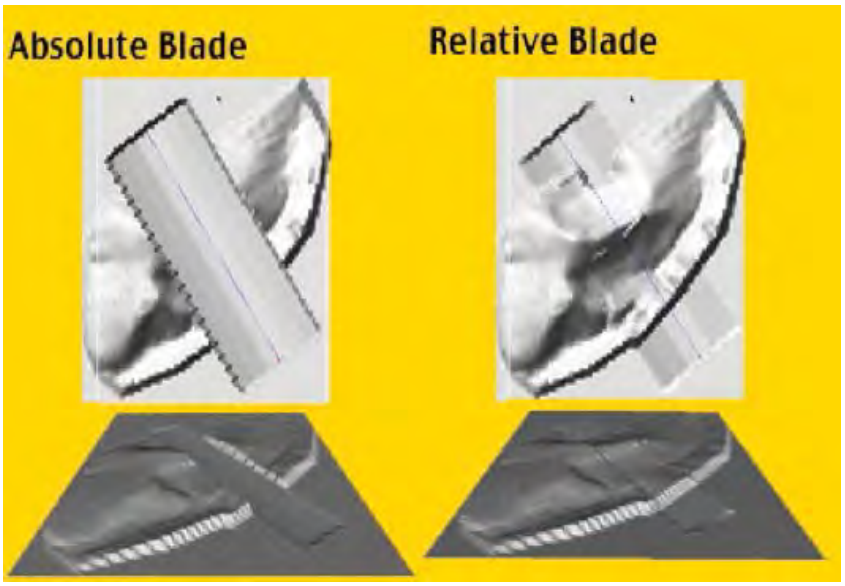

Figure 15: Absolute versus relative relationship of the blade-path-relationship with the underlying terrain data.

REFERENCES CITED

1. J. Beardsley and N. Grubb, *Earthworks and beyond: contemporary art in the landscape*: Abbeville Press, 1989.
2. S. Strom, K. Nathan, and J. Woland, *Site engineering for landscape architects*: John Wiley & Sons, 2013.
3. H. C. Landphair and F. Klatt, "Landscape architecture construction," 1979.
4. R. K. Untermann, "Grade easy: an introductory course in the principles and practi ces of grading and drainage," 1973.
5. P. Petschek, *Grading for landscape architects and architects*: Walter de Gruyter, 2008.
6. M. Ferraro and R. Mallary, "ECOSITE: A Program for Computer-Aided Landform Design," *Proceedings ACM/SIGGRAPH (NY 1977)*.
7. R. J. Chorley, R. P. Beckinsale, and A. J. Dunn, *History of the Study of Landforms: Or The Development of Geomorphology: The Life and Work of William Morris Davis* vol. 2: Psychology Press, 1973.
8. B. Etzelmüller and J. R. Sulebak, "Developments in the use of digital elevation models in periglacial geomorphology and glaciology," *Physische Geographie,* vol. 41, pp. 35-58, 2000.
9. J. Corner, "Representation and landscape: drawing and making in the landscape medium," *Word & Image,* vol. 8, pp. 243-275, 1992.
10. S. M. Ervin, "Digital Terrain Models," *Landscape Architecture, Magazine,* January, 1994 1994.
11. W. R. Franklin, "Towards a mathematics of terrain."
12. W. R. Franklin, M. Inanc, and Z. Xie, "Two novel surface representation techniques," *AutoCarto Vancouver, Washington,* 2006.
13. W. R. Franklin, Z. Xie, E. Lau, and Y. Li, "Algorithms for terrain and bathymetric sensor data."
14. R. Weibel and M. Heller, *Digital terrain modelling*: Oxford University Press, 1993.
15. B. Alsobrooks, "Introduction of 3D Technology & Machine Control Systems," ed.

16. A. Vonderohe, "Status and Plans for Implementing 3D Technologies for Design and Construction in WisDOT," Construction and Materials Support Center University of Wisconsin – Madison Department of Civil and Environmental Engineering WisDOT Project ID: 0657-45-11, 2009/05//undefined 2009.
17. C. Zhang, A. Hammad, and H. Bahnassi, "Collaborative Multi-Agent Systems for Construction Equipment Based on Real-Time Field Data Capturing," *Journal of Information Technology in Construction,* vol. 14, pp. 204-228, 2009/06//undefined 2009.
18. A. Zogheib, "Autonomous Navigation Tool for Real & Virtual Field Robots," in *1st International Conference on Machine Control & Guidance 2008*, 2008, pp. 1-11.
19. C. D. O. TRANSPORTATION, "Digital Design Environment Guide," Newington, CTOctobor 2007.
20. F. D. o. T. F. E. C. S. O. (ECSO), "Multi-Line Earthwork for Designers," F. D. o. T. F. E. C. S. O. (ECSO), Ed., ed, 2007, p. 72.
21. T. Hampton. (2005, 2005) 3D Grade Control Puts Designers Right in the Operator's Seat. *Enigineering News Record*. Available: http://www.dot.state.mn.us/caes/files/pdf/enr_3d_grade_control_10_05.pdf
22. J. J. Hannon, "NCHRP Synthesis 372 Emerging Technologies for Construction Delivery," Transportation Research Board 978-0-309-09791-8, 2007 2007.
23. J. J. Hannon, *NCHRP Synthesis 385 Information Technology for Efficient Project Delivery*: Transportation Research Board, 2008.
24. J. J. Hannon and D. Townes, "GPS Utilization Challenges in Transportation Construction Project Delivery," in *The construction and building research conference of the Royal Institution of Chartered Surveyors*, Georgia Tech, Atlanta USA, 2007, p. 15.
25. T. Hoeft, "Improving Construction Efficiencies Through 3D Electronic Design," C. Jarhen, Ed., ed, 2009, p. 1.
26. D. Kratt, "Design Memorandum NO. 18-05-Electronic Files Submittal with the Final Contract Plans," ed, 2005.
27. M. Leja and R. Buckley, "Cross-Section Preparation and Delivery Memorandum," ed: California Department of Transportaion, 2004.
28. A. Z. Sampaio, A. R. Gomes, and J. Prata, "Virtual Environment in Civil Engineering: Construction and Maintenance of Buildings," in *ADVCOMP 2011, The Fifth International Conference on Advanced Engineering Computing and Applications in Sciences*, 2011, pp. 13-20.
29. D. Sheldon and C. Mason, "A Proposal for Statewide CAD Standards in Iowa," Howard R. Green Company2009/04//undefined 2009.
30. P. Söderström and T. Olofsson, "Virtual Road Construction – a Conceptual Model," in *W78 Conference*, Maribor, Slovenia, 2007, pp. 255-261.
31. X. Wang, M. J. Kim, P. E. D. Love, and S.-C. Kang, "Augmented Reality in built environment: Classification and implications for future research*," *Automation in Construction,* vol. 32, pp. 1-13, July 2013 2013.
32. S. Andrews and S. Geiger, "Unlocking Design Data," presented at the 19th Annual AGC/DOT Technical Conference, New York, 2005.
33. F. Vahdatikhaki, A. Hammad, and S. Setayeshgar, "Real-time simulation of earthmoving projects using automated machine guidance," in *The 30th ISARC*, Montréal, Canada, 2013, pp. 718-730.
34. R. Laurini and D. Thompson, *Fundamentals of spatial information systems*: Academic press, 1992.
35. S. M. Ervin and C. Y. Westort, "Procedural Terrain; A Virtual Bulldozer," in *Proceedings CAAD-Futures, International Conference on Computer Aided Architectural Design*, 1995.

36. H. Bär, "Interaktive Bearbeitung von Geländeoberflächen-Konzepte, Methoden, Versuche," 1996.
37. *Representing landscapes : a visual collection of landscape architectural drawings / edited by Nadia Amoroso*. Abingdon, Oxon ; New York: Abingdon, Oxon ; New York : Routledge, 2012.
38. B. Cutler, W. R. Franklin, and T. Zimmie, "Fundamental Terrain Representations and Operations: Validation of Erosion Models for Levee Overtopping," in *NSF Engineering Research and Innovation Conference*, Honolulu, 2009.
39. R. Fabio, "From point cloud to surface: the modeling and visualization problem," *International Archives of Photogrammetry, Remote Sensing and Spatial Information Sciences,* vol. 34, p. W10, 2003.
40. W. R. Franklin, M. Inanc, Z. Xie, D. M. Tracy, B. Cutler, and M. V. Andrade, "Smugglers and border guards: the GeoStar project at RPI," in *Proceedings of the 15th annual ACM international symposium on Advances in geographic information systems*, 2007, p. 30.
41. M. Inanc, *Compressing terrain elevation datasets*: ProQuest, 2008.
42. M. Metz, H. Mitasova, and R. Harmon, "Efficient extraction of drainage networks from massive, radar-based elevation models with least cost path search," *Hydrology and Earth System Sciences,* vol. 15, pp. 667-678, 2011.
43. M. V. Andrade, S. V. Magalhaes, M. A. Magalhães, W. R. Franklin, and B. M. Cutler, "Efficient viewshed computation on terrain in external memory," *GeoInformatica,* vol. 15, pp. 381-397, 2011.
44. T.-Y. Lau and W. R. Franklin, "COMPLETING RIVER NETWORKS WITH ONLY PARTIAL RIVER OBSERVATIONS VIA HYDROLOGY-AWARE ODETLAP."
45. W. J. Mitchell, "A computational view of design creativity," *Modeling Creativity and Knowledge-Base Creative Design,* pp. 25-42, 1993.
46. W. J. Mitchell, *The logic of architecture: Design, computation, and cognition*: MIT press, 1990.
47. W. J. Mitchell, *Computer-aided architectural design*: John Wiley & Sons, Inc., 1977.
48. W. J. Mitchell, *Digital design media*: John Wiley & Sons, 1995.
49. M. McCullough, W. J. Mitchell, and P. Purcell, *The electronic design studio: architectural knowledge and media in the computer era*: MIT Press, 1990.
50. S. M. Ervin, *Landscape modeling : digital techniques for landscape visualization / Stephen M. Ervin, Hope H. Hasbrouck*. New York: New York : McGraw-Hill, 2001.
51. S. Mealing, *Mac 3D: Three-dimensional Modelling and Rendering on the Macintosh*: Intellect Books, 1994.
52. M. Flaxman, "Fundamentals of Geodesign," *Proceedings Digital Landscape Architecture, Buhmann/Pietsch/Kretzel (Eds.): Peer Reviewed Proceedings Digital Landscape Architecture, Anhalt University of Applied Science, Germany,* 2010.
53. S. Ervin, "A system for GeoDesign," *Proceedings Digital Landscape Architecture, Anhalt University of Applied Science, Germany,* 2011.
54. T. R. Allen, "Digital terrain visualization and virtual globes for teaching geomorphology," *Journal of Geography,* vol. 106, pp. 253-266, 2008.
55. D. G. Brown, D. P. Lusch, and K. A. Duda, "Supervised classification of types of glaciated landscapes using digital elevation data," *Geomorphology,* vol. 21, pp. 233-250, 1998.
56. R. Dikau, "The application of a digital relief model to landform analysis in geomorphology, Raper J., Three Dimensional Applications in Geographical Information Systems, 1989, 51-77," ed: Taylor and Francis, London.
57. R. Dikau, "The application of a digital relief model to landform analysis in geomorphology," *Three dimensional applications in geographical information systems,* pp. 51-77, 1989.

58. J. P. Wilson, "Digital terrain modeling," *Geomorphology,* vol. 137, pp. 107-121, 2012.
59. R. L. Mace, "Universal design in housing," *Assistive Technology,* vol. 10, pp. 21-28, 1998.
60. C. W. Harris and N. T. Dines, "Time-saver standards for landscape architecture," *McGraw-Hili Book Company. New York,* 1988.
61. P. Gryboś, M. Kaletowska, U. Litwin, J. M. Pijanowski, A. Szeptalin, and M. Zygmunt, "Data preparation for the purposes of 3D visualization," *Geomatics, Landmanagement and Landscape,* pp. 19-29, 2013.
62. H. L. Nichols, *Moving the earth : the workbook of excavation / Herbert L. Nichols, Jr., David A. Day*. New York: New York : McGraw-Hill, 2010.
63. C. Y. Westort, "Methods for Sculpting Digital Topographic Surfaces," University of Zurich, 1998.
64. C. Y. WESTORT, "An Explosion Tool for DTM Sculpting," *Trends in Landscape Modeling: Proceedings at Anhalt University of Applied Sciences 2003,* p. 35, 2003.
65. C. Y. Westort, "Corner, End, and Overlap “Extrusion Junctures”: Parameters for Geometric Control," in *Digital Earth Moving*, ed New York: Springer, 2001, pp. 78-86.
66. C. Y. Westort, *Digital Earth Moving: First International Symposium, DEM 2001, Manno, Switzerland, September 5-7, 2001. Proceedings* vol. 1. New York: Springer, 2001.
67. M. D. Johnson, E. C. Holley, F. P. Morgeson, D. LaBonar, and A. Stetzer, "Outcomes of Absence Control Initiatives A Quasi-Experimental Investigation Into the Effects of Policy and Perceptions," *Journal of Management,* vol. 40, pp. 1075-1097, 2014.
68. D. Gergle and D. S. Tan, "Experimental Research in HCI," in *Ways of Knowing in HCI*, ed: Springer, 2014, pp. 191-227.

Applicability and Limitations of 3D Printing for Civil Structures

Mostafa Yossef
Department of Civil, Construction and Environmental Engineering
Iowa State University
Ames, Iowa, 50011
myossef@iastate.edu

An Chen
Department of Civil, Construction and Environmental Engineering
Iowa State University
Ames, Iowa, 50011
achen@iastate.edu

ABSTRACT

Three Dimensional Printing (3DP) is a manufacturing process that builds layers to create a three-dimensional solid object from a digital model. It allows for mass customization and complex shapes that cannot be produced in other ways, eliminates the need for tool production and its associated labor, and reduces waste stream. Because of these advantages, 3DP has been increasingly used in different areas, including medical, automotive, aerospace, etc. This automated and accelerated process is also promising for civil structures, including building and bridges, which require extensive labor. If successful, it is expected that 3D structural printing can significantly reduce the construction time and cost. However, unlike applications in other areas, civil structures are typically in large scale, with length or height spanning hundreds of feet. They are subjected to complex loadings, including gravity, live, wind, seismic, etc. Therefore, it is challenging to develop suitable printing tools and materials. As a result, although there are limited 3D printed buildings, 3DP of civil structures is still at a primitive stage. This papers aims to explore the applicability of 3DP for civil structures. The first part is devoted to a review of 3DP in different areas, including 3D printed buildings. Based on the state of art, the weakness and opportunities of 3DP are identified. Finally, future directions for 3DP in civil structures are discussed.

Key words: 3D Printing—review—civil structures—applicability—limitations

INTRODUCTION

Three Dimensional Printing (3DP) was evolved from automated production, which started in the early twentieth century. It was first applied in manufacturing and automotive industries. Recently, its applications were expanded to other industries, including medical, aerospace, construction, etc. This automated and accelerated process is also promising for civil structures, including building and bridges, which require extensive labor. However, many factors have limited its further development. As a result, although there are limited application of 3DP in civil construction, 3DP of civil structures is still at a primitive stage. This paper first reviews the latest development of 3DP in construction and other areas. It then identifies the limiting factors and challenges of 3DP. Finally, future directions of 3DP in civil engineering are discussed.

Proceedings of the 2015 Conference on Autonomous and Robotic Construction of Infrastructure, Ames, Iowa.

BRIEF HISTORY OF 3D PRINTING

According to 3DPI (2014), 3DP started in the late 1980's. It was known as Rapid Prototyping (RP) technology developed by Kodama in Japan. Six years later, Charles Hull invented Stereo Lithography Apparatus (SLA). In 1987, SLA-1 was introduced as the first commercial RP system. In 1989, a patent for Selective Laser Sintering (SLS) was issued for Carl Deckard at University of Texas. Through the 1990's until early 2000's, SLS has been developed to focus on industrial applications such as casting. New terminology, Casting and Rapid Manufacturing (RM), was introduced for such applications. In 2005, the terminology evolved to include all processes under Additive Manufacturing (AM). The term *Additive Manufacturing* (AM) is defined by ASTM as "a process of joining materials to make objects from 3D model data, usually layer upon layer" (ASTM Standard 2012). Unlike *Subtractive* term which means machining away the material from a block to form the required object. Casting or shaping the material in a mold is often called *Formative* process. Table 1 shows a summary of different techniques used in AM (Buswell et al. 2007).

Table 1 –Summary of AM techniques (Buswell et al. 2007)

Process	Description
Stereolithography (SLA)	Liquid photopolymer resin is held in a tank. A flat bed is immersed to a depth equivalent to one layer. Lasers are used to activate the resin and cause it to solidify. The bed is lowered and the next layer is built.
Fused Deposition Modelling (FDM)	Extrudes a narrow bead of hot plastic, which is selectively deposited where it fuses to the existing structure and hardens as it cools.
Selective Laser Sintering (SLS)	Utilises a laser to partially melt successive layers of powder. One layer of powder is deposited over the bed area and the laser targets the areas that are required to be solid in the final component.
3D Printing (3DP)	Based on inkjet printer technology. The inkjet selectively deposits a liquid binder onto a bed of powder. The binder effectively 'glues' the powder together.

3DP is based on AM process. It is a process where a 3D model is created using Computer Aided Drafting (CAD) software. The model is then transferred to the 3D printer as a standard data known as stereolithography language (STL), where the model is converted into layers that can be applied consecutively. Each layer is formed where the printer head deposits an activating agent, and premixes it with a power material. The layers are bonded together consecutively to form the 3D object. In 2009, the first commercial 3D printer was offered for sale. In 2012, an alternative 3D printer was introduced at entry level of the market with affordable price.

APPLICATIONS OF 3D PRINTING

3DP has been increasing used in different areas. Architectural modelling is one of the major areas that uses 3DP for developing prototypes that facilitate the communication between the architect and customer. Architect can print now complex structures and color it as well for better representation (Gibson et al. 2002). In medical area, 3DP is used to create high quality bone

transplant, modelling of damaged bones for better fracture analysis (James et al. 1998; Murray et al. 2008). 3PD can also be used to print complex shapes, such as human tissue or artificial blood vessels that are used in coronary bypass surgery (Wong and Hernandez 2012). Dentists are using 3DP to create a plaster model of the mouth or to replace patient's teeth (van Noort 2012). In aerospace industry, 3DP is used to print airfoils (Thomas et al. 1996). In automotive field, Song et al. (2002) used RP technology to manufacture the die of an automobile deck part.

3DP FOR CIVIL STRUCTURES

Warszawski and Navon (1998) pointed out the following problems concerning construction industry: low labor efficiency compared with automated machines, high accident rate, low quality work due to insufficient skilled workforce, and difficulty of applying control of construction site. Applying automation or 3DP can overcome these problems.

Automation in construction industry started in terms of robotics [Gambao et al. (2000); Kuntze et al. (1995); Lorenc et al. (2000); Williams et al. (2004)]. Buswell et al. (2007), (2008) conducted a review over RM technologies for construction, based on which they developed a Freeform Construction method. The term of Freeform Construction was defined for methods that deliver large-scale components for construction without the need of formworks using AM. They concluded that Freeform Construction could reduce the construction cost and provide freedom of selecting desired geometry with better performance than traditional method. Lim et al. (2009) stated that Freeform Construction methods are currently limited to CC (US); Concrete Printing (UK); and D-shape (Italy).

Khoshnevis (1998) introduced the Contour Crafting (CC) which later become an effective method of printing 3D houses. Khoshnevis (2004) defined CC as "*an additive fabrication technology that uses computer control to exploit the superior surface-forming capability of troweling to create smooth and accurate planar and free-form surface"*. The idea of CC was to use two trowels to form a solid planar surface for external edges. Filler material such as concrete can then be poured to fill the extruded area. They demonstrated that CC can be used in building structures as shown in Figure 1, where a nozzle is supported by a gantry system which moves in two parallel lanes. The nozzle is capable of full 6-axis positioning and can extrude both sides and filler material. CC nozzle can also be used for forming paint-ready surface, placing reinforcement before pouring concrete, plastering and tiling, plumbing and installing electrical modules and communication line wiring.

Zhang and Khoshnevis (2013) developed an optimized method for CC machine to efficiently construct complicated large-scale structures. Extensive research was done to avoid collision between multiple nozzles. Three approaches were compared, namely: path cycling, buffer zone path cycling and auxiliary buffer zone. The results indicated that the path cycling and buffer zone cycling provided the maximum optimization. They concluded that using CC method is significantly faster than traditional methods and implementation to multi-story building is possible by climbing as shown in Figure 3.

According to Roodman and Lenssen (1995), the construction industry consume more than 40% of all raw materials globally. CC can reduce the material waste from 7 tons to almost none for a single-family home. And the speed of the construction can be increased to one day per house. Although the ability of using this method in luxury structures or complex structures is still limited, implementation of CC can help with fast construction of low income housing and emergency shelter.

Despite the many advantages of CC, Lim et al. (2009) listed some limitations of CC as follows. The mold is not disposed and becomes a part of the wall. CC method requires excessive steps including molding, installing reinforcement, and placing concrete to build layers up to 20 mm high. These limitations encouraged them to develop another Freeform Construction method called Concrete Printing. Similar to 3DP idea, the concrete printing machine has a frame of 5.4m x 4.4 m (footprint) x 5.4 m (height) and a printing head moving on a mobile beam. A 9 mm nozzle is supported with the printing head to provide the material extrusion. Later, Le et al. (2012) conducted experimental program to figure out the optimum mix design of a high-performance fiber-reinforced fine-aggregate concrete for printing concrete.

The 3D printed houses can provide a cheap and efficient homes of low-income families. The printed houses consist of different printed parts assembled together to form the house. It can take less than 24 hour to build one house. However, no details are provided about 3DP of wiring, plumbing and HVAC, etc.

The latest development of 3DP was from WinSun, a Chinese company. They printed five-story apartment block using 3DP as shown in Figure 4 (Charron 2015). They stated that the houses were in full compliance with relevant national standards, which overcomes one of the main issues that face 3D printed houses. WinSun also printed a decorated house as shown in Figure 5.

3DP can also be used for non-conventional structures. DUS, a Dutch architecture company used 3DP to design facades integrated with solar panels, where the angle of the solar panel could be optimized automatically for any location. This can eliminate the need of manufacturing a mold for every different location (Jordan et al. 2015).

Other automation effort was done by the industry sector. For example, Shimizu Corporation in Japan developed an automated system that included erection and welding of steel-frames, laying concrete floor planks, installation of exterior and interior wall panels, and installation of various other units (Yamazaki and Maeda 1998).

Lim et al. (2012) compared CC, D-shape, and Concrete Printing. They concluded that Concrete Printing could optimize strength prior to manufacturing, which resulted in less material. It could also create complex concrete shapes without the need of labor-intensive molding as shown in Figure 2.

CHALLENGES OF 3DP FOR CIVIL STRUCTURES

As described above, 3DP allows for mass production, uses less labor, increases the construction speed and produces less waste compared to traditional construction methods. 3D printed structure is a layered structure, which is not new in civil engineering. Concrete Masonry Unit (CMU) structure is a typical layered structure, where the CMU units are installed by pieces and bonded together with mortar. The author of this paper has designed CMU buildings up to 13 stories and 125 feet high. The integrity of 3D printed structure is better than CMU structure. Therefore, 3D printed structure should be able to exceed the height of CMU structure. However, the tallest building that has been printed so far was the 5-story apartment building. Khoshnevis (2004) and Buswell et al. (2007) stated multiple issues that slowed down the growth of automation industry in construction. It can be summarized as follows:

- automated fabrication is often not suitable for large scale products and conventional design approaches;

- smaller ratio of automated products in comparison with other industries;
- only limited material can be used by automated machines;
- expensive automated machines tend to be unfeasible economically; and
- managerial issues and the increasing pressure towards environmental issues of construction materials in developing countries (Guthrie et al. 1999).

CONCLUSIONS AND FUTURE DIRECTIONS OF 3DP FOR CIVIL STRUCTURES

It can be shown from this paper that the application of 3D printing in civil engineering is promising. It can not only help to improve communication among designers by creating prototypes of the desired projects, but also be used in high-stress performance testing and end-user applications. Considering the limitations described above, in the authors' opinion, the following directions of 3DP for civil structures deserve further attention.

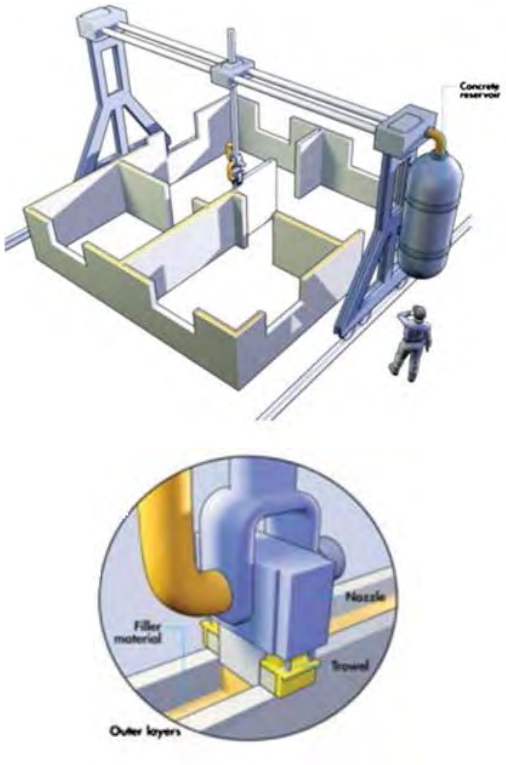

Figure 1 - Schematic view of construction of conventional buildings using CC (Zhang and Khoshnevis 2013)

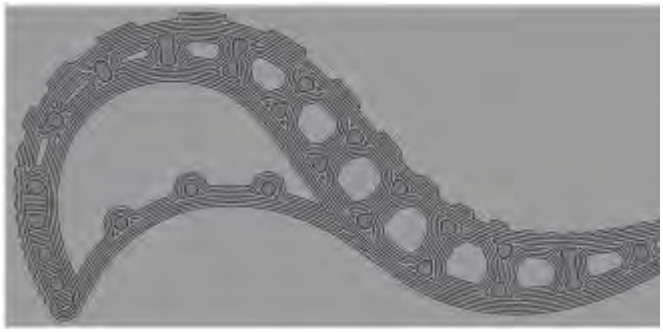

(A)

(B)

Figure 2 – Complex Concrete Printing Product (a) 3D Model (Lim et al. 2012), (b) During printing (Le et al. 2012)

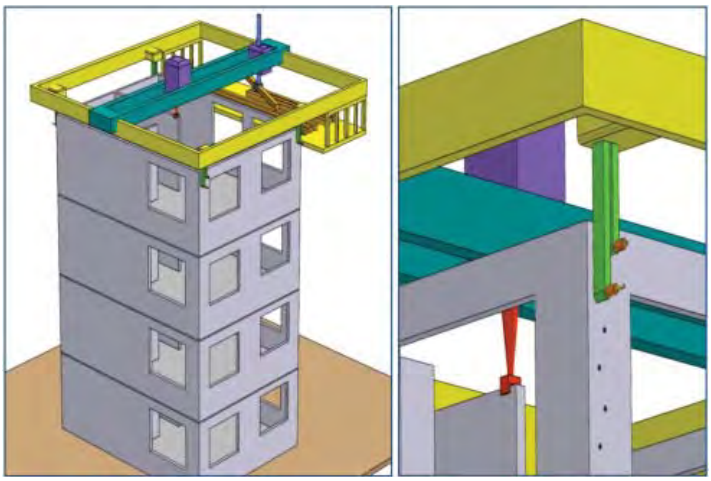

Figure 3 – Construction of multi-story buildings using Contour Crafting method (Zhang and Khoshnevis 2013)

Figure 4 – A 3D printed five-story apartment block (Charron 2015)

Figure 5 – A Decorated 3D printed house (Charron 2015)

Construction components of significant size are heavy, typically being up to 5 tons. Suitable equipment needs to be developed in order to lift and move heavy component. However, before suitable equipment can be developed for large scale structure, in-situ deposit approach, i.e., printing lighter parts on site followed by assembly would be an alternative option.

3DP can be especially useful for structures with complex shapes. For example, rubber can be used to print shock absorbers in a large scale which can help in reducing the seismic effects on buildings. A prototype is shown in Figure 6.

3DP can also open up a frontier to use new materials. These new materials need to satisfy specific requirements from 3DP. For example, they need to have proper curing time since the lower layer needs to support the upper layer. The bonding between different layers should be strong. These materials also require extensive testing to determine their mechanical properties, including the properties of the materials, inter- and intra-layers.

Figure 6 - 3D Printed Rubber Shock Absorber (http://3dprinting.co.uk/)

Jordan et al. (2015) stated that automated industry will take over the constructions process. This requires revising building codes to ensure that additive machines are operating within limits and meet performance criteria. For example, the 3D printed structure should be able to take complex loads, including gravity, live, wind, seismic, etc., and satisfy the performance requirements, such as fire, smoke and toxicity. In addition to that, current safety factors are high due to the consideration of human mistakes. Such factors can be lowered in case of using automated machines instead of human workforce.

Development of a complete process from the parametric design until printing the building is needed to control the whole process and eliminate any wasted time during printing. Khoshnevis (2004) proposed a planning system that shows each component of future automated system. Figure 7 shows a brief explanation for the proposed plan.

Further research is also needed in connections for 3D printed structures, where few studies are available. These include, but not limited to, beam-column, column-footing, wall connections, etc.

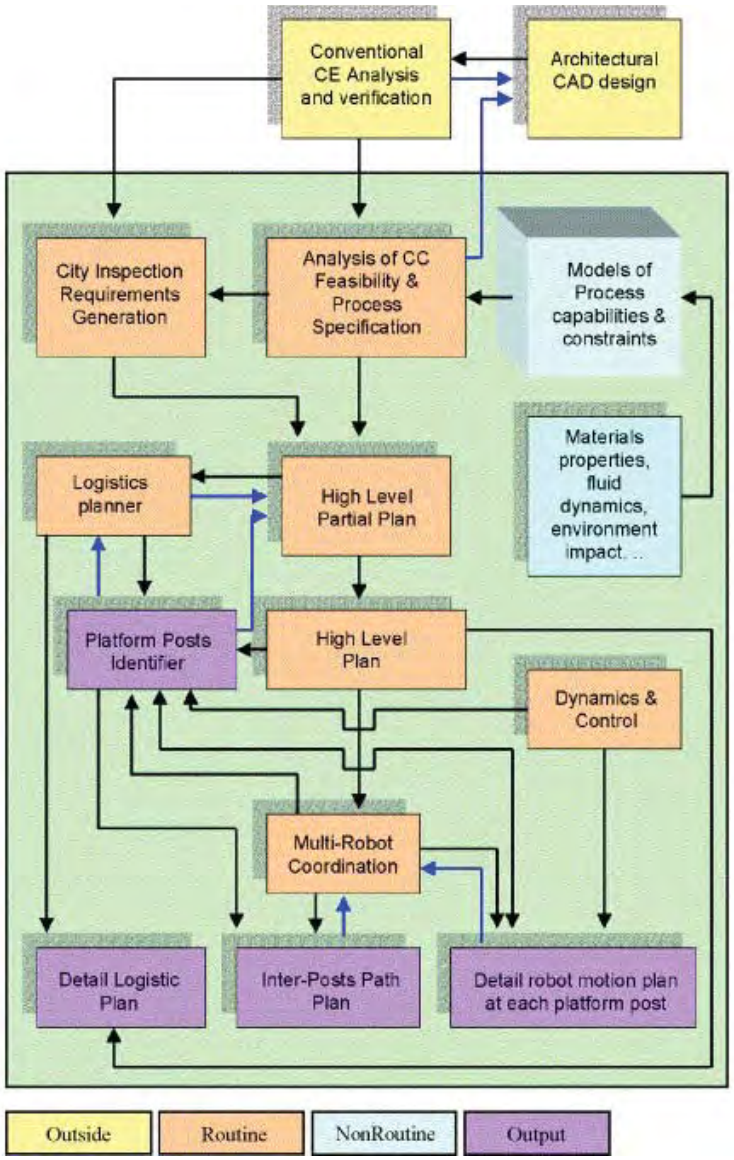

Figure 7 – Components of future automated construction (Khoshnevis 2004)

REFERENCES

3DPI. (2014). "3D Printing History: The Free Beginner's Guide." *3D Printing Industry*, <http://3dprintingindustry.com/wp-content/uploads/2014/07/3D-Printing-Guide.pdf> (May 18, 2015).

ASTM. (2012). "F2792. 2012 Standard terminology for additive manufacturing technologies." *West Conshohocken, PA: ASTM International. www.astm.org.*

Buswell, R. A., Soar, R. C., Gibb, A. G. F., and Thorpe, A. (2007). “Freeform Construction: Mega-scale Rapid Manufacturing for construction.” *Automation in Construction*, 16(2), 224–231.

Buswell, R. A., Thorpe, A., Soar, R. C., and Gibb, A. G. F. (2008). “Design, data and process issues for mega-scale rapid manufacturing machines used for construction.” *Automation in Construction*, 17(8), 923–929.

Charron, K. (2015). “WinSun China builds world’s first 3D printed villa and tallest 3D printed apartment building.” *3ders.org*, <http://www.3ders.org/articles/20150118-winsun-builds-world-first-3d-printed-villa-and-tallest-3d-printed-building-in-china.html> (May 18, 2015).

Gambao, E., Balaguer, C., and Gebhart, F. (2000). “Robot assembly system for computer-integrated construction.” *Automation in Construction*, 9(5-6), 479–487.

Gibson, I., Kvan, T., and Wai Ming, L. (2002). “Rapid prototyping for architectural models.” *Rapid Prototyping Journal*, MCB UP Ltd, 8(2), 91–95.

Guthrie, P., Coventry, S., Woolveridge, C., Hillier, S., and Collins, R. (1999). “The reclaimed and recycled construction materials handbook.” *CIRIA, London, UK*.

James, W. J., Slabbekoorn, M. A., Edgin, W. A., and Hardin, C. K. (1998). “Correction of congenital malar hypoplasia using stereolithography for presurgical planning.” *Journal of Oral and Maxillofacial Surgery*, 56(4), 512–517.

Jordan, B., Dini, E., Heinsman, H., Reichental, A., and Tibbits, S. (2015). “The Promise of 3D Printing.” *Thornton Tomasetti*, <http://www.thorntontomasetti.com/the_promise_of_3d_printing/> (May 18, 2015).

Khoshnevis, B. (1998). “Innovative rapid prototyping process makes large sized, smooth surfaced complex shapes in a wide variety of materials.” *Materials Technology*, 13(2), 52–63.

Khoshnevis, B. (2004). “Automated construction by contour crafting—related robotics and information technologies.” *Automation in Construction*, 13(1), 5–19.

Kuntze, H.-B., Hirsch, U., Jacubasch, A., Eberle, F., and Göller, B. (1995). “On the dynamic control of a hydraulic large range robot for construction applications.” *Automation in Construction*, 4(1), 61–73.

Le, T. T., Austin, S. A., Lim, S., Buswell, R. A., Gibb, A. G. F., and Thorpe, T. (2012). “Mix design and fresh properties for high-performance printing concrete.” *Materials and Structures*, 45(8), 1221–1232.

Lim, S., Buswell, R. A., Le, T. T., Austin, S. A., Gibb, A. G. F., and Thorpe, T. (2012). “Developments in construction-scale additive manufacturing processes.” *Automation in Construction*, 21, 262–268.

Lim, S., Le, T., Webster, J., Buswell, R., Austin, S., Gibb, A., and Thorpe, T. (2009). “Fabricating construction components using layer manufacturing technology.” *Global Innovation in Construction Conference*, Loughborough University.

Lorenc, S. J., Handlon, B. E., and Bernold, L. E. (2000). “Development of a robotic bridge maintenance system.” *Automation in Construction*, 9(3), 251–258.

Murray, D. J., Edwards, G., Mainprize, J. G., and Antonyshyn, O. (2008). “Optimizing craniofacial osteotomies: applications of haptic and rapid prototyping technology.” *Journal of oral and maxillofacial surgery : official journal of the American Association of Oral and Maxillofacial Surgeons*, 66(8), 1766–72.

Van Noort, R. (2012). “The future of dental devices is digital.” *Dental materials : official publication of the Academy of Dental Materials*, 28(1), 3–12.

Roodman, D. M., and Lenssen, N. (1995). *A Building Revolution: How Ecology and Health Concerns Are Transforming Construction*. *Worldwatch Institute*.

Song, Y., Yan, Y., Zhang, R., Xu, D., and Wang, F. (2002). “Manufacture of the die of an automobile deck part based on rapid prototyping and rapid tooling technology.” *Journal of Materials Processing Technology*, 120(1-3), 237–242.

Thomas, C. L., Gaffney, T. M., Kaza, S., and Lee, C. H. (1996). “Rapid prototyping of large scale aerospace structures.” *1996 IEEE Aerospace Applications Conference. Proceedings*, IEEE, 219–230.

Warszawski, A., and Navon, R. (1998). “Implementation of Robotics in Building: Current Status and Future Prospects.” *Journal of Construction Engineering and Management*, American Society of Civil Engineers, 124(1), 31–41.

Williams, R. L., Albus, J. S., and Bostelman, R. V. (2004). “Self-contained automated construction deposition system.” *Automation in Construction*, 13(3), 393–407.

Wong, K. V., and Hernandez, A. (2012). “A Review of Additive Manufacturing.” *ISRN Mechanical Engineering*, 2012, 1–10.

Yamazaki, Y., and Maeda, J. (1998). “The SMART system: an integrated application of automation and information technology in production process.” *Computers in Industry*, 35(1), 87–99.

Zhang, J., and Khoshnevis, B. (2013). “Optimal machine operation planning for construction by Contour Crafting.” *Automation in Construction*, 29, 50–67.

Time-Optimal Path Planning for Automated Grain Carts

Mengzhe Zhang
Department of Mechanical Engineering
Iowa State University
2025 Black Engineering
Ames, 50011
mengzhez@iastate.edu

Sourabh Bhattacharya
Department of Mechanical Engineering
Iowa State University
2025 Black Engineering
Ames, 50011
sbhattac@iastate.edu

ABSTRACT

In this paper, we address a motion planning problem for an autonomous agricultural vehicle modeled as tractor-trailer system. We first present a numerical approach and a primitive-based approach for computing the time-optimal path based on given static initial and goal configurations. In the former approach, we define a value function for the entire state space. The value function is consistent with the time to reach goal configuration, and it is finally used to compute the optimal trajectory. In the latter approach, based on the regular and singular primitives, we present an algorithm to construct such primitives and derive the final path. Subsequently, we extend the results and present a dynamic motion planning strategy to accommodate the case of mobile target configuration. Finally, simulation results are provided to validate the feasibility and effectiveness of these techniques.

Key words: motion planning—autonomous—agricultural vehicle

INTRODUCTION

Logistics problem can be described as the management of resources in order to meet specific requirements, or customers. The resources to be dealt with include physical items such as materials and tools, as well as abstract items such as information and energy. Logistics problem can be embodied in many aspects, such as business, economics and agriculture. In this paper, we address the problem of logistics in path planning for agricultural vehicles.

Currently, crop-harvesting is usually performed by agricultural machines called combines (combine harvesters). Due to the limited capacities of the combines, a grain cart is involved for transporting the grains from combines to the depot. If there are sufficient number of grain carts, each combine can go alongside with a grain cart for unloading. However, if the number of combines exceeds the number of grain carts, a single grain cart has to serve multiple combines. Based on the fact that the grain cart is a tractor-trailer system, we explore the problem of time-optimal path planning for an autonomous grain cart to move from one combine to the next combine.

Proceedings of the 2015 Conference on Autonomous and Robotic Construction of Infrastructure, Ames, Iowa.

There have been some efforts in the past to address the problem of harvesting in large-scale farming scenarios. In (Fokkens and Puylaert 1981), a linear programming model for harvesting operations is presented. The model gives the management results of harvesting operations at the large scale grain farm. In (Foulds and Wilson 2005) and (Basnet and Foulds 2006), researchers analyze the scheduling problem of farm-to-farm harvesting operations for hay and rape seed. These works mainly focus on scheduling harvesting operations from farm to farm. In contradistinction, our research focuses on the motion planning for an unloading vehicle in a single field.

Recently, path planning of agricultural machines has received some attention in the research community. In (Makino, Yokoi, and Kakazu 1999), authors develop a motion planning system, which integrates global and local motion planning components. In (Ferentinos, Arvanitis, and Sigrimis 2002), authors propose two heuristic optimization techniques in motion planning for autonomous agricultural vehicles. In (Ali and Van Oudheusden 2009), authors address the motion planning of one combine by using integer linear programming formulation. In (Oksanen and Visala 2009), coverage path planning problem is considered. The presented algorithms not only aim to find an efficient route, but also ensure the coverage of the whole field. In (Hameed, Bochtis, and Sørensen 2013), a coverage planning approach is proposed with the consideration of the presence of obstacles. However, compared with our research, the aforementioned works do not consider the problem of path planning on unloading vehicles and do not model the vehicle as a tractor-trailer system.

There has been some previous research to plan optimal trajectories for tractor-trailer model which are prevalent in farming applications. In (Divelbiss and Wen 1994), authors present an algorithm to find a feasible path which satisfies the given non-holonomic constraints. In (Divelbiss and Wen 1997), authors propose a trajectory tracking strategy which controls a tractor-trailer system moving along a path generated off-line. In (Hao, Laxton, Benson, and Agrawal 2004), researchers present a differential flatness−based formation following for a tractor-cart moving along with a combine harvester. In (Astolfi, Bolzern, and Locatelli 2004), an application of using Lyapunov technique is proposed to design the control laws for tractor-trailer model to follow a prescribed path. Researchers introduce the notion of equivalent size and propose an approach for path planning based on genetic algorithm in (Liu, Lu, Yang, and Chen 2008). In (Yu and Hung 2012), the tractor-trailer model is regarded as a Dubins vehicle, which can only move with constant speed and turn with upper bounded curvature. The proposed algorithm is used to find the shortest path in Dubins Traveling Salesman Problem with Neighborhoods (Isaacs, Klein, and Hespanha 2011). In (Chyba and Sekhavat 1999) and (Chitsaz 2013), authors introduce the notion of regular primitive and singular primitive which are local time-optimal.

The contribution of this paper can be summarized as follows. First, according to the mathematical model of grain cart, we present a numerical approach, as well as a primitive-based approach to find the time-optimal solution to the path planning problem in different situations. To tackle the case of moving target configuration, we further propose a two-stage motion planning strategy, taking advantage of the previous results. Finally, feasibility and effectiveness of presented techniques are demonstrated by simulations.

The rest of the paper is organized as follows. In Section II, we present the mathematical models for both combine and grain cart. In Section III, we present our previous work on the scheduling of agricultural operations. Based on the scheduling scheme, we formulate the path planning problem for grain cart in Section IV. In Section V, we present a numerical approach to obtain the

time-optimal path between two given configurations. In Section VI, a primitive-based approach is considered to solve the problem. In Section VII, we address the dynamic case by proposing a two-stage motion planning strategy. In Section VIII, simulation results are presented. In Section IX, we conclude with some future work.

MATHEMATICAL MODELING

In this section, we describe the mathematical models for the combine harvester and the grain cart.

Combine Harvester

Combine harvester is the machine for harvesting crops, for example, wheat, oats, rye, barley corn, soybeans and flax. Figure 1 shows a combine at work. In this active mode, the header cuts the crop and feeds it into threshing cylinder. Grain and chaff are separated from the straw when crop goes through the concaved grates. The grain, after being sieved, will be stored in the on-board tank temporarily, and the waste straw is ejected. We use C to denote the maximum capacity of on-board tank.

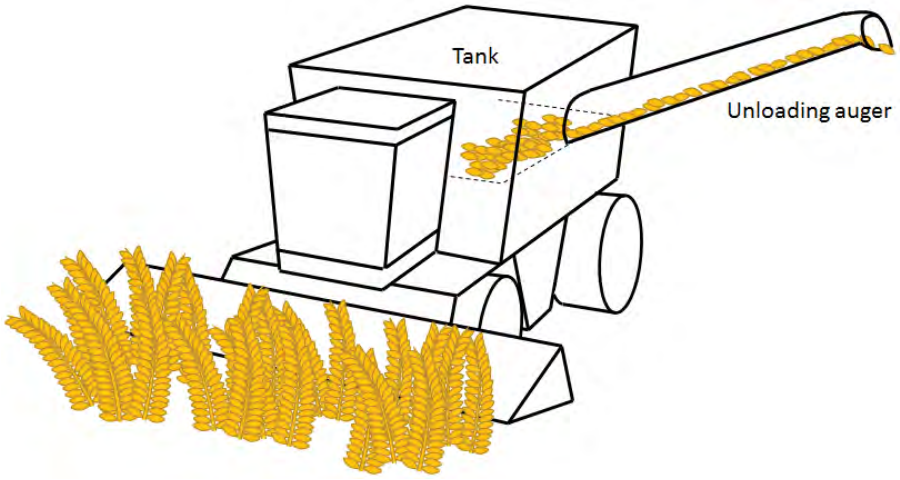

Figure 1. Combine harvester

Threshing grain loss is an important issue for combine harvester. For any combine, the quantity of threshing grain loss greatly depends on the forward speed of the harvester. In (Flufy and Stone 1983), authors show that automatic control has a better performance than manual control on the threshing grain loss. The forward speed is controlled to give a level of crop feed according to the required threshing grain loss. In this paper, we simplify the model and assume that all the combines posses identical constant speed, denoted as v_{ch}.

Since the tank does not hold a large capacity, modern combine usually has an unloading auger for removing the grains from the tank to other vehicles. For most of the combines, the auger is mounted on the left side, as shown in Figure 1. At this point, a vehicle has to be on the left side of the combine to empty the tank. Here we denote the unloading rate of the tank using auger as r_u. So when a combine proceeds with the harvesting and the unloading operations simultaneously, the unloading rate is $r_u - r_f \ \ (r_u > r_f)$.

Grain Cart

A grain cart, also known as chaser bin, is a trailer towed by a tractor. In this paper, we use term grain cart to represent the system including both the tractor and the trailer. Figure 2(a) shows the appearance of a grain cart. Because of the larger capacity, one can use it to collect grains from multiple combines so that the combines could work without interruption.

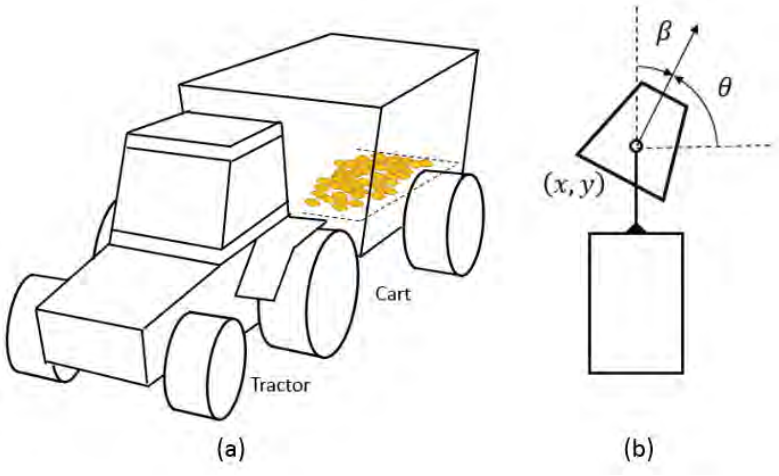

Figure 2. Grain cart

Figure 2(b) shows a grain cart. We model the grain cart as a trailer attached to a car-like robot. The robot is hitched by the trailer at the center. The equations of motion for the grain cart are as follows.

$$\dot{q} = \begin{pmatrix} \dot{x} \\ \dot{y} \\ \dot{\theta} \\ \dot{\beta} \end{pmatrix} = \begin{pmatrix} v\cos\theta \\ v\sin\theta \\ \omega \\ -v\sin\beta + \omega \end{pmatrix}$$

where $q = (x, y, \theta, \beta) \in \mathbb{R}^2 \times S^1 \times S^1$ is the configuration, $u = (v, \omega) \in U = [-1, 1]^2$ is the control. In the configuration q, (x, y) is the coordinate of robot's center, θ is the robot's orientation, β is the angle between trailer orientation, and the robot orientation. v and ω denote the speed and angular velocity of the robot, respectively (Chyba and Sekhavat 1999) (Chitsaz 2013).

PREVIOUS WORK

In previous work, we addressed the logistics scheduling problem of grain cart during harvesting operation. A scheduling scheme was proposed for an arbitrary number of combines with a single grain cart. Based on the mathematical models and proposed scheme, the grain cart could serve multiple combines without stopping harvesting operation. In the scheme, the grain cart was scheduled to serve the combines sequentially, so that it needed to move along a trajectory from one combine to the next combine. Figure 3 shows an example of the path planning. Based on the scheduling scheme of N-combine case, we have obtained

$$\Delta T \leq \frac{(r_u - r_f)C - (N-1)r_f C}{r_f (r_u - r_f)(2N-2)} \tag{1}$$

where ΔT denotes the travel time for the grain cart to switch. Since the travel time is constrained, in this paper we focus on finding the time-optimal solution to the path planning problem. In the next section, we provide an elaborated problem description.

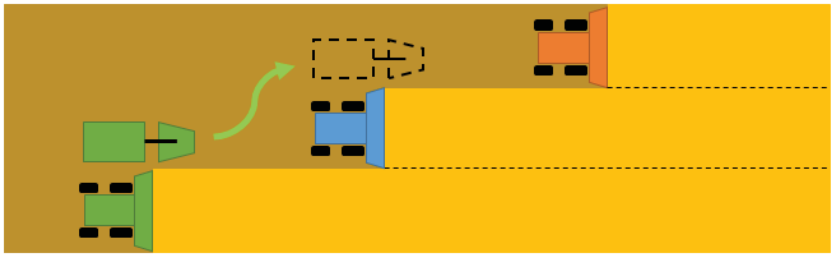

Figure 3. Path planning of the grain cart

PROBLEM DESCRIPTION

In this section, we formulate the problem. Consider a grain cart moving from one combine to the next combine, we would like to find the time-optimal solution for the grain cart to perform the path planning. In other words, given initial configuration, denoted as q_i and goal configuration, denoted as q_g, we intend to compute the path from q_i to q_g minimizing the total travel time. In the following sections, we first consider the case when initial and final configurations are static, following which, we extend the result to a dynamic target configuration case.

NUMERICAL APPROACH

In this section, we present a numerical approach to solve the navigation problem between two given static configurations. Before computing the trajectory, we first define a value function and establish Hamilton-Jacobi equation based on tractor-trailer model. Then we present an update scheme for computing the value function. Finally, the trajectory is computed using the obtained results.

Hamilton-Jacobi Equation

Denote the set of admissible path from the configuration q_i as $\mathrm{A}_{x_i, y_i, \theta_i, \beta_i}$. Given a goal configuration q_g, we define the corresponding value function $u : q \to \mathbb{R}^+ \cup \{0\}$ as follows (Takei, Tsai, Shen, and Landa 2010).

$$u(q(T)) = \inf\{T : q(t) \in \mathrm{A}_{x_i, y_i, \theta_i, \beta_i}, q(T) = q_g\} \tag{2}$$

The value function can be regarded as the optimal cost-to-go for the tractor-trailer model with certain constraints, an initial configuration and a final configuration. By applying dynamic programming principle for (2), we have

$$u(q(t)) = \inf\{u(q(t+\Delta t)) + \Delta t : q(t) \in \mathsf{A}_{x_i, y_i, \theta_i, \beta_i}\} \tag{3}$$

Dividing the terms by Δt and taking $\Delta t \to 0$, we are able to derive

$$-1 = \inf\{\bigtriangledown u \cdot \dot{q} : | v | = 1, | \omega | \le 1\} \tag{4}$$

With the equations of motion of the grain cart, *Hamilton-Jacobi-Bellman equation* is obtained as follows.

$$-1 = \cos(\theta)\frac{\partial u}{\partial x} + \sin(\theta)\frac{\partial u}{\partial y} - \sin(\beta)\frac{\partial u}{\partial \beta} + \inf_{|\omega| \le 1}\{\dot{\theta}(\frac{\partial u}{\partial \theta} + \frac{\partial u}{\partial \beta})\} \tag{5}$$

The last term in (5) can be eliminated by applying bang-bang principle $w = \pm 1$. Since q_i is the goal configuration which has no cost-to-go, we have $u(q_g) = 0$. For the points located in the obstacle or outside the space, we define the cost-to-go to be infinity. In the next section, we present an update scheme for the defined value function.

Update Scheme

In order to find the time-optimal path satisfying (5), we apply fast sweeping method and propose an update scheme for the value function $u(q)$ in the entire space. The basic idea is to employ the fact that the value function has zero cost-to-go at the goal configuration, and to compute the value function from the nodes close to the goal configuration, to the nodes at farther positions.

With this in mind, we first set up a four dimensional uniform Cartesian grid with refinement $(h_x, h_y, h_\theta, h_\beta)$. Let $u_{a,b,c,d} = u(q_{a,b,c,d}) = u(ah_x, bh_y, ch_\theta, dh_\beta)$ be the approximation of the solution on the grid nodes. Moreover, we discretize ω in the range of $[-1,1]$ and further define $u^*_{a,b,c,d}$ as follows.

$$u^*_{a,b,c,d} = \min_{\omega_i \in [-1,1]}\{u(q_{a,b,c,d} + \dot{q}\Delta t)\} + \Delta t \tag{6}$$

where $\dot{q} = (\cos(ch_\theta), \sin(ch_\theta), \omega_i, -\sin(dh_\beta) + \omega_i))^T$, ω_i is the *i*th element in the discretization and Δt is the length of time step. For the value of $u(q_{a,b,c,d} + \dot{q}\Delta t)$, we take the value directly if it is lying on the presented grid, otherwise it is approximated by taking the average value of the adjacent nodes.

Finally, the update scheme can be described in the following way.

$$u^{n+1}_{a,b,c,d} = \min\{u^n_{a,b,c,d}, u^{*n}_{a,b,c,d}\} \tag{7}$$

where the superscripts denote the iteration. We set up the termination condition of the computation as follows.

$$(\| u^{n+1}_{a,b,c,d} - u^{n}_{a,b,c,d} \|_2)^2 < \text{ò} \tag{8}$$

where $\text{ò} > 0$ is an arbitrary number.

Computing Trajectory

By using the obtained value function, we are able to derive the time-optimal path from any initial configuration q_i to the goal configuration q_g. According to (5), the control law can be summarized as follows.

$$\begin{aligned} \dot{x} &= \cos\theta \\ \dot{y} &= \sin\theta \\ \dot{\theta} &= -sgn(\frac{\partial u}{\partial \theta} + \frac{\partial u}{\partial \beta}) \\ \dot{\beta} &= -\sin\beta + \dot{\theta}. \end{aligned} \tag{9}$$

Note that the partial derivative in (9) is obtained by applying central difference approximation. In the computation of trajectory, the values of u which are not on the grid are computed using a nearest-neighbor interpolation.

The numerical approach computes the time-optimal trajectory efficiently if the corresponding value function is provided. The main time consumption is in computing the value function of the final configuration. But in real implementation, one can compute the value function beforehand. Therefore, the time cost will not influence the real-time operation on path planning. In the next section, we consider another approach to address the situation when we do not have such value function.

PRIMITIVE-BASED APPROACH

Related Work

Based on the model presented in Section II, the time-optimal trajectory satisfies Pontryagin Maximum Principle. In (Chitsaz 2013), authors define adjoint variables $\lambda = (\lambda_x, \lambda_y, \lambda_\theta, \lambda_\beta)$ and the Hamiltonian as follows.

$$H(q, \lambda, u) = \lambda_x \dot{x} + \lambda_y \dot{y} + \lambda_\theta \dot{\theta} + \lambda_\beta \dot{\beta} = v(\lambda_x \cos\theta + \lambda_y \sin\theta - \lambda_\beta \sin\beta) + \omega(\lambda_\theta + \lambda_\beta) \tag{10}$$

Additionally, the switching functions are defined as

$$\begin{aligned} \phi_v &= \lambda_x \cos\theta + \lambda_y \sin\theta - \lambda_\beta \sin\beta \\ \phi_\omega &= \lambda_\theta + \lambda_\beta \end{aligned} \tag{11}$$

Depending on ϕ_v and ϕ_ω, the optimal trajectory, which is called *extremal*, consists of two categories, namely, *regular* and *singular*. On one hand, an extremal is called regular if the times

at which $\phi_v = 0$ or $\phi_\omega = 0$ have zero measure. On the other hand, an extremal is called *abnormal* if it has both $\phi_v \equiv 0$ and $\phi_\omega \equiv 0$. A singular is an extremal which contains a positive measure along which $\phi_v \equiv 0$ or $\phi_\omega \equiv 0$. The subtrajectories of a regular and a singular extremal are called *regular primitive* and *singular primitive*, respectively.

In the regular primitive, $\phi_v \neq 0$ and $\phi_\omega \neq 0$. Based on the state equations, a regular primitive satisfies

$$\begin{aligned} \theta(t) &= \omega t + \theta(t_0) \\ x(t) &= x(t_0) + (v/\omega)(\sin(\theta) - \sin(\theta(t_0))) \\ y(t) &= y(t_0) - (v/\omega)(\cos(\theta) - \cos(\theta(t_0))) \\ \beta(t) &= 2(v/\omega)\arctan(\frac{t - 2v + K_1}{t + K_1}) \\ K_1 &= \frac{2}{v - \omega\tan(\beta(t_0)/2)} \end{aligned} \tag{12}$$

where t_0 is the starting time instant and t is the passing time.

In singular primitive, we have either $\phi_v \equiv 0$ or $\phi_\omega \equiv 0$. Here since the grain cart has a constant forward speed, we only consider the case of $\phi_\omega \equiv 0$. It has been proved by (Chitsaz 2013) that if a ϕ_ω-singular primitive contains a straight line segment, either the entire primitive is a straight line segment, or

$$\begin{aligned} \alpha(t) &= \pm 2\beta(t) \\ \omega(t) = d &= \pm 2\sin(\beta(t)) \\ -\frac{\pi}{6} \le \beta(t) \le \frac{\pi}{6} \; or \; \frac{5\pi}{6} &\le \beta(t) \le \frac{7\pi}{6} \end{aligned} \tag{13}$$

in which α denotes the angle between the robot orientation and the line, d denotes the distance between robot's center and the line. The path for the latter case is called a *merging curve*.

Path Planning of Grain Cart

In our case, when the grain cart finishes unloading one combine, it should follow a path to the second combine, and move parallel to it. This implies that the final path is supposed to end with a singular primitive, denoted as S_g. Considering the fact that a merging curve has the constraints (13), we propose a combination of the path containing two regular primitives and two ϕ_ω-singular primitives, as shown in Figure 4. The grain cart initially proceeds with a regular primitive R_1. S_1 is a singular primitive connecting to R_1. R_2 and S_g are the following regular primitive and goal singular primitive, respectively.

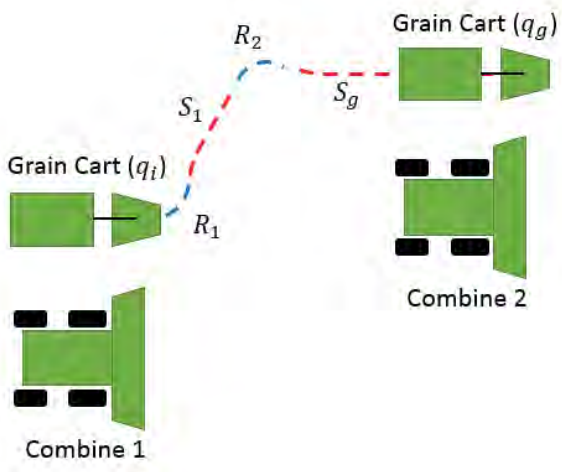

Figure 4. The path consists of 2 singular primitives (red lines) and 2 regular primitives (blue lines)

In order to minimize the travel time for the grain cart, we consider using straight lines instead of merging curves for ϕ_ω-singular primitives. Furthermore, since q_i and q_g has the same θ, it is apparent that R_1 and R_2 should have the same length, and the same central angle γ as well. Therefore, with a given γ, the slope of S_1 can be computed. Since q_i and q_g are known, the entire path can be derived. To minimize the travel time, we change the central angle corresponding to the regular primitives, and take the trajectory with minimum time in all feasible trajectories as the final path. The complete algorithm can be found in the following algorithm.

Trajectory computation using primitive-based approach:

Declare γ to be the central angle of regular primitives, $T_f = \infty$ to be the travel time of final path, P_f to be the final path

For $\gamma = 0 \to \pi$

Compute the path P_γ starting from q_i

If P_γ reaches q_g

If travel time of $P_\gamma < T_f$

$T_f =$ Travel time of P_γ, $P_f = P_\gamma$

End if

End if

End for

DYNAMIC MOTION PLANNING

In this section, we consider the case when the target configuration is dynamic. To accommodate this situation, we present a motion planning strategy that consists of two successive stages. In

the first stage, we estimate a fixed goal configuration and perform the static path planning using aforementioned approaches. In the second stage, we apply a PID control for the grain cart to move synchronizing with the combine. Next, we elaborate both stages in detail.

Since the target configuration is mobile, we consider q_g as a function of time, i.e. $q_g(t) = (x_g(t), y_g(t), \theta_g(t), \beta_g(t))^T$. Figure 5 indicates the basic idea of the estimation on the static goal configuration. In the figure, t_0 denotes the starting time. Thus $q_g(t_0)$ could be considered as the goal configuration at the beginning. At this point, we attempt to find a ΔT satisfying the ideal case that the grain cart can successfully reach the desired goal configuration $q_g(t_0 + \Delta T)$. With this in mind, we approximate the ΔT by using a lower bound on the length of the path, which is $v\Delta T$, as shown in Figure 5. Based on geometry, the approximated ΔT could be solved using the following equation.

$$(x_g(t_0) - x_i + v_{ch}\Delta T)^2 + (y_g(t_0) - y_i)^2 = (v\Delta T)^2$$
$$\Delta T = \frac{\sqrt{d_1^2 v^2 + d_2^2 (v^2 - v_{ch}^2)} + d_1 v_{ch}}{v^2 - v_{ch}^2} \tag{14}$$

where $d_1 = x_g(t_0) - x_i$ and $d_2 = y_g(t_0) - y_i$.

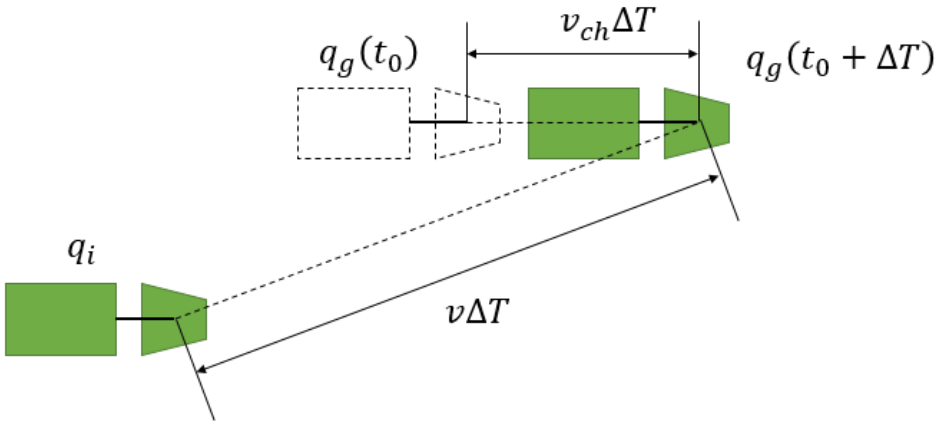

Figure 5. Dynamic motion planning

We let q_i and $q_g(t_0 + \Delta T)$ to be the initial and goal configuration in performing static path planning. Due to the fact that $v\Delta T$ is the lower bound on the path length for a non-holonomic vehicle, the grain cart will lag behind the combine when it reaches the goal configuration. Therefore, in the second stage, we apply a PID feedback control for grain cart to catch up with the combine. Figure 6 shows the block diagram for the presented control system. Position of the combine is considered to be the reference input. PID control is applied to the control of the grain cart's speed.

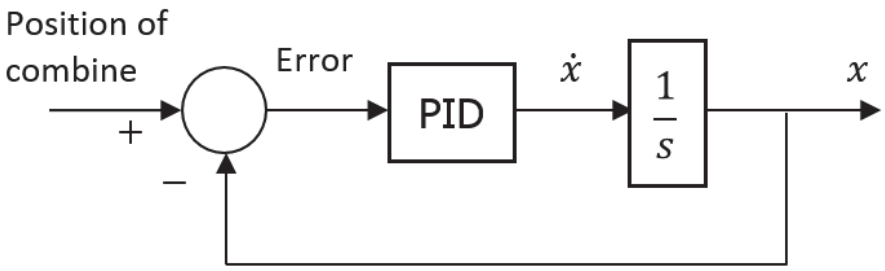

Figure 6. Block diagram for PID control system

SIMULATION

In this section, we present simulation results for the aforementioned techniques.

Figure 7 illustrates the paths obtained using numerical approach and primitive-based approach. Because of the fact that the tractor-trailer model has four state variables, it is hard to visualize the variations of all these variables. For this reason, in the simulation we only show the path of (x, y), which represents the physical location of grain cart in the environment. A colored arrow is added to show the final orientation. In this simulation, initial and goal configuration are set to be $q_i = (1,1,0,0)^T$ and $q_g = (4,4,0,0)^T$, respectively. For numerical approach, Table 1 lists all the refinement parameters in the computation of value function. In both approaches, the path computation terminates when the state of the grain cart reaches a small range of the goal configuration.

Table 1. Refinement parameters

Name	Value
h_x	0.2
h_y	0.2
h_θ	0.251 (radium)
h_β	0.251 (radium)
Δt	0.05
ò	0.005

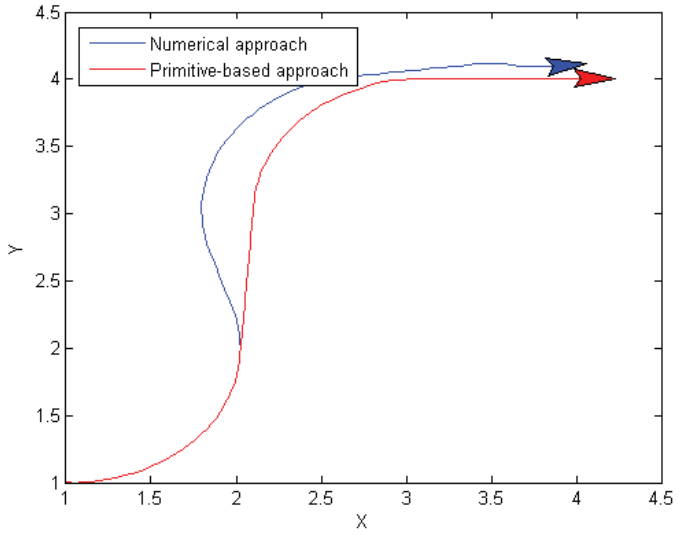

Figure 7. Simulation results with given initial and final configurations

Simulation results show that both paths finally reach the goal configuration which validates the proposed approaches. In the numerical approach, the path could be affected by the error of using inappropriate refinement parameters. With proper refinement parameters, the path could be more accurate, but it will lead to higher time consumption in the computation of value function.

In the second simulation, we compare the performance of using two proposed approaches. We keep $y_i = y_g - 4$ and plot the travel time with respect to the distance ratio $\frac{x_g - x_i}{y_g - y_i}$, as shown in Figure 8. The results show that with a given ratio, travel time of the two approaches are very close. Since the numerical approach provides us the time-optimal solution, it can be seen that the primitive-based approach also has a good performance. Note that in some cases, the performance of primitive-based approach is better because of the effect of the error in numerical approach.

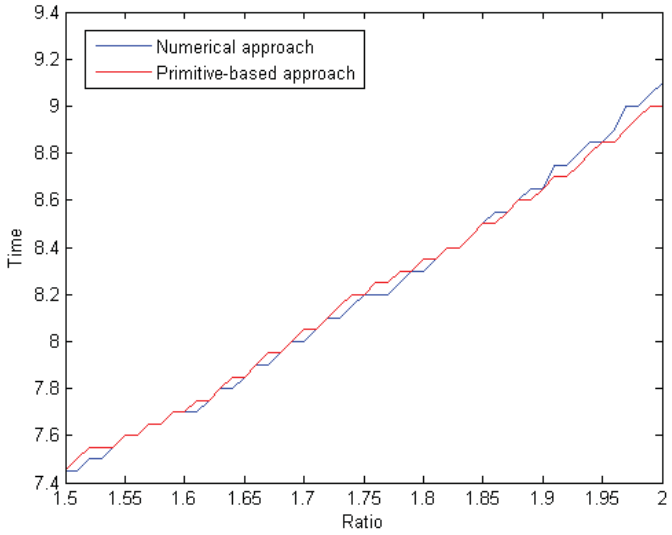

Figure 8. Travel time of using two approaches

Figure 9 illustrates the last simulation, which is an implementation of using dynamic motion planning. In this simulation, initial configuration of grain cart and initial position of combine are set to be $(1,5,0,0)^T$ and $(5,9)$, respectively. The speed of combine $v_{ch} = 0.4$, whereas the speed of grain cart v has the maximum 1. The simulation shows the paths of grain cart in both stages, which demonstrate the feasibility of the proposed dynamic motion planning strategy.

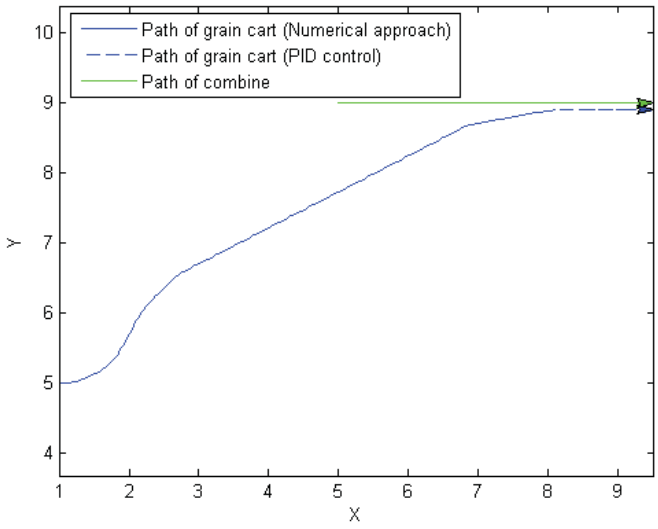

Figure 9. Dynamic motion planning

CONCLUSION

In this paper, we addressed the problem of finding the time-optimal path for the grain cart to navigate from one combine to the adjacent combine. Firstly, a numerical approach for computing the path based on given static initial and final configuration was presented.

According to the tractor-trailer model, we presented an update scheme for computing the value function corresponding to the entire state space. Finally, the trajectory could be computed with the help of this value function. Subsequently, we presented a primitive-based approach to obtain the solution. The path was considered to be constructed by regular and singular primitives that have local time optimality. Furthermore, we studied the case when target configuration was dynamic, and presented a motion planning strategy adopting the results from aforementioned approaches. Finally, simulation results were provided for these techniques. For the future work, we will consider a case of multiple grain carts, and try to coordinate grain carts so that the harvesting efficiency could be further improved.

REFERENCES

O. Ali and D. Van Oudheusden, "Logistics planning for agricultural vehicles," in *Industrial Engineering and Engineering Management, 2009. IEEM 2009. IEEE International Conference on*, pp. 311--314, Dec 2009.

A. Astolfi, P. Bolzern, and A. Locatelli, "Path-tracking of a tractor-trailer vehicle along rectilinear and circular paths: a lyapunov-based approach," *Robotics and Automation, IEEE Transactions on*, vol. 20, pp. 154--160, Feb 2004.

C. B. Basnet, L. R. Foulds, and J. M. Wilson, "Scheduling contractors' farm-to-farm crop harvesting operations," *International Transactions in Operational Research*, vol. 13, no. 1, pp. 1--15, 2006.

H. Chitsaz, "On time-optimal trajectories for a car-like robot with one trailer," *CoRR*, pp. --1--1, 2013.

M. Chyba and S. Sekhavat, "Time optimal paths for a mobile robot with one trailer," in *Intelligent Robots and Systems, 1999. IROS '99. Proceedings. 1999 IEEE/RSJ International Conference on*, vol. 3, pp. 1669--1674 vol.3, 1999.

A. Divelbiss and J. Wen, "Nonholonomic path planning with inequality," in *Robotics and Automation, 1994. Proceedings., 1994 IEEE International Conference on*, pp. 52--57 vol.1, May 1994.

A. Divelbiss and J. Wen, "Trajectory tracking control of a car-trailer system," *Control Systems Technology, IEEE Transactions on*, vol. 5, pp. 269--278, May 1997.

K. Ferentinos, K. Arvanitis, and N. Sigrimis, "Heuristic optimization methods for motion planning of autonomous agricultural vehicles," *Journal of Optimization*, vol. 23, no. 2, pp. 155--170, 2002.

Y. Hao, B. Laxton, E. R. Benson, and S. K. Agrawal, "Differential flatness-based formation following of a simulated autonomous small grain harvesting system," *Transactions of the ASABE*, vol. 47, no. 3, pp. 933--941, 2004.

M. L. Flufy and G. Stone, "Speed control of a combine harvester to maintain a specific level of measured threshing grain loss," *Journal of Agricultural Engineering Research*, vol. 28, no. 6, pp. 537 -- 543, 1983.

B. Fokkens and M. Puylaert, “A linear programming model for daily harvesting operations at the large-scale grain farm of the ijsselmeerpolders development authority,” *The Journal of the Operational Research Society*, vol.32, no. 7, pp. pp. 535--547, 1981.

L. Foulds and J. Wilson, “Scheduling operations for the harvesting of renewable resources,” *Journal of Food Engineering*, vol. 70, no. 3, pp. 281 -- 292, 2005. Operational Research and Food Logistics.

I. Hameed, D. Bochtis, and C. Sørensen, “An optimized field coverage planning approach for navigation of agricultural robots in fields involving obstacle areas,” *International Journal of Advanced Robotic Systems*, vol. 10, no. 231, pp. 1--9, 2013.

J. Isaacs, D. Klein, and J. Hespanha, “Algorithms for the traveling salesman problem with neighborhoods involving a dubins vehicle,” in *American Control Conference (ACC), 2011*, pp. 1704--1709, June 2011.

Z. Liu, Q. Lu, P. Yang, and L. Chen, “Path planning for tractor-trailer mobile robot system based on equivalent size,” in *Intelligent Control and Automation, 2008. WCICA 2008. 7th World Congress on*, pp. 5744--5749, June 2008.

T. Makino, H. Yokoi, and Y. Kakazu, “Development of a motion planning system for an agricultural mobile robot,” in *SICE Annual, 1999. 38th Annual Conference Proceedings of the*, pp. 959--962, Aug 1999.

T. Oksanen and A. Visala, “Coverage path planning algorithms for agricultural field machines,” *Journal of Field Robotics*, vol. 26, no. 8, pp. 651--668, 2009.

R. Takei, R. Tsai, H. Shen, and Y. Landa, “A practical path-planning algorithm for a simple car: a hamilton-jacobi approach,” in *American Control Conference (ACC), 2010*, pp. 6175--6180, June 2010.

X. Yu and J. Hung, “Optimal path planning for an autonomous robot-trailer system,” in *IECON 2012 - 38th Annual Conference on IEEE Industrial Electronics Society*, pp. 2762--2767, Oct 2012.